AD NUMBER

ADB261754

NEW LIMITATION CHANGE

TO

Approved for public release, distribution unlimited

FROM

Distribution authorized to U.S. Gov't. agencies only; Proprietary Information; Jun 2000. Other requests shall be referred to U.S. Army Medical Research and Materiel Command, 504 Scott Street, Fort Detrick, MD 21702-5012

AUTHORITY

USAMRMC ltr, 1 Apr 2003

AD_____

Award Number: DAMD17-96-C-6065

TITLE: Characterization and Modulation of Proteins Involved in
       Sulfur Mustard Vesication

PRINCIPAL INVESTIGATOR: Dean S. Rosenthal, Ph.D.

CONTRACTING ORGANIZATION: Georgetown University Medical Center
                          Washington, DC   20007

REPORT DATE: June 2000

TYPE OF REPORT: Final

PREPARED FOR: U.S. Army Medical Research and Materiel Command
                Fort Detrick, Maryland   21702-5012

1

NOTICE

USING GOVERNMENT DRAWINGS, SPECIFICATIONS, OR OTHER DATA INCLUDED IN THIS DOCUMENT FOR ANY PURPOSE OTHER THAN GOVERNMENT PROCUREMENT DOES NOT IN ANY WAY OBLIGATE THE U.S. GOVERNMENT. THE FACT THAT THE GOVERNMENT FORMULATED OR SUPPLIED THE DRAWINGS, SPECIFICATIONS, OR OTHER DATA DOES NOT LICENSE THE HOLDER OR ANY OTHER PERSON OR CORPORATION; OR CONVEY ANY RIGHTS OR PERMISSION TO MANUFACTURE, USE, OR SELL ANY PATENTED INVENTION THAT MAY RELATE TO THEM.

LIMITED RIGHTS LEGEND

Award Number: DAMD17-96-C-6065
Organization: Georgetown University Medical Center
Location of Limited Rights Data (Pages):

Those portions of the technical data contained in this report marked as limited rights data shall not, without the written permission of the above contractor, be (a) released or disclosed outside the government, (b) used by the Government for manufacture or, in the case of computer software documentation, for preparing the same or similar computer software, or (c) used by a party other than the Government, except that the Government may release or disclose technical data to persons outside the Government, or permit the use of technical data by such persons, if (i) such release, disclosure, or use is necessary for emergency repair or overhaul or (ii) is a release or disclosure of technical data (other than detailed manufacturing or process data) to, or use of such data by, a foreign government that is in the interest of the Government and is required for evaluational or informational purposes, provided in either case that such release, disclosure or use is made subject to a prohibition that the person to whom the data is released or disclosed may not further use, release or disclose such data, and the contractor or subcontractor or subcontractor asserting the restriction is notified of such release, disclosure or use. This legend, together with the indications of the portions of this data which are subject to such limitations, shall be included on any reproduction hereof which includes any part of the portions subject to such limitations.

THIS TECHNICAL REPORT HAS BEEN REVIEWED AND IS APPROVED FOR PUBLICATION.

_____   _____

_____   _____

REPORT DOCUMENTATION PAGE

Form Approved
OMB No. 074-0188

1. AGENCY USE ONLY (Leave blank)	2. REPORT DATE June 2000	3. REPORT TYPE AND DATES COVERED Final (16 Sep 96 - 15 May 00)

4. TITLE AND SUBTITLE	5. FUNDING NUMBERS
Characterization and Modulation of Proteins Involved in Sulfur Mustard Vesication	DAMD17-96-C-6065

6. AUTHOR(S)
Dean S. Rosenthal, Ph.D.

7. PERFORMING ORGANIZATION NAME(S) AND ADDRESS(ES)	8. PERFORMING ORGANIZATION REPORT NUMBER
Georgetown University Medical Center Washington, DC 20007 E-MAIL: drosen@bc.georgetown.edu	

9. SPONSORING / MONITORING AGENCY NAME(S) AND ADDRESS(ES)	10. SPONSORING / MONITORING AGENCY REPORT NUMBER
U.S. Army Medical Research and Materiel Command Fort Detrick, Maryland 21702-5012	

11. SUPPLEMENTARY NOTES
Report contains color graphics.

12a. DISTRIBUTION / AVAILABILITY STATEMENT	12b. DISTRIBUTION CODE
Distribution authorized to U.S. Government agencies only (proprietary information, Jun 00). Other requests for this document shall be referred to U.S. Army Medical Research and Materiel Command, 504 Scott Street, Fort Detrick, Maryland 21702-5012.	

13. ABSTRACT *(Maximum 200 Words)* Sulfur mustard (SM) causes blisters in the skin through a series of cellular changes that we are beginning to identify. Recently, using chemical inhibitors, we found a major role for Ca^{2+} and calmodulin in the induction of differentiation in human keratinocytes in response to SM. We also obtained the unexpected results that SM induces markers of apoptosis, and that this process also proceeds via a Ca^{2+}-calmodulin-dependent pathway. We have extended these studies to show that expression of calmodulin antisense RNA blocks the differentiation and apoptotic response of keratinocytes to SM. In addition, using a dominant-negative inhibitor (FADD-DN), we have found that SM-induced apoptosis is also mediated by a FADD-dependent pathway, which induces caspase activation. The involvement of such varied molecules as Ca^{2+}, calmodulin, and FADD suggests a complex network involved in SM-induced differentiation and apoptosis. However, in our studies to date, we have found that blocking any one of these upstream signals can inhibit terminal differentiation or apoptosis, indicating that these molecular pathways are potential targets for therapeutic intervention. Immortalized keratinocytes stably transfected with FADD-DN form normal epidermis on athymic mice, but have an altered response to SM. We are also currently utilizing retroviral expression vectors expressing calmodulin antisense RNA to modulate the expression of calmodulin, and thus the differentiation and apoptotic pathways in primary keratinocytes and grafted epidermis to alter SM toxicity.

14. SUBJECT TERMS			15. NUMBER OF PAGES 160
Mustard, Chemical Defense			16. PRICE CODE

17. SECURITY CLASSIFICATION OF REPORT	18. SECURITY CLASSIFICATION OF THIS PAGE	19. SECURITY CLASSIFICATION OF ABSTRACT	20. LIMITATION OF ABSTRACT
Unclassified	Unclassified	Unclassified	Unlimited

Standard Form 298 (Rev. 2-89)
Prescribed by ANSI Std. Z39-18
298-102

FOREWORD

Opinions, interpretations, conclusions and recommendations are those of the author and are not necessarily endorsed by the U.S. Army.

___✓___ Where copyrighted material is quoted, permission has been obtained to use such material.

___✓___ Where material from documents designated for limited distribution is quoted, permission has been obtained to use the material.

___✓___ Citations of commercial organizations and trade names in this report do not constitute an official Department of Army endorsement or approval of the products or services of these organizations.

N/A In conducting research using animals, the investigator(s) adhered to the "Guide for the Care and Use of Laboratory Animals," prepared by the Committee on Care and use of Laboratory Animals of the Institute of Laboratory Resources, national Research Council (NIH Publication No. 86-23, Revised 1985).

N/A For the protection of human subjects, the investigator(s) adhered to policies of applicable Federal Law 45 CFR 46.

N/A In conducting research utilizing recombinant DNA technology, the investigator(s) adhered to current guidelines promulgated by the National Institutes of Health.

N/A In the conduct of research utilizing recombinant DNA, the investigator(s) adhered to the NIH Guidelines for Research Involving Recombinant DNA Molecules.

N/A In the conduct of research involving hazardous organisms, the investigator(s) adhered to the CDC-NIH Guide for Biosafety in Microbiological and Biomedical Laboratories.

_____ 10/27/00
PI - Signature   Date

3

Table of Contents

INTRODUCTION

Sulfur mustard (SM) is a highly reactive compound that causes blisters in the skin through a series of changes that we are beginning to identify. Studies have shown that SM induces the death and detachment of the basal cells of the epidermis from the basal lamina (Rosenthal et al., 1997). Much of the evidence points to a major role for calcium and calmodulin in this response. For several years, I have been involved in studies demonstrating that Ca^{2+} plays an important role in the maintenance and homeostasis of the skin. A number of laboratories, including our own, have shown that terminal differentiation can be induced in both murine and human keratinocytes via the elevation of intracellular Ca^{2+} (Hennings et al., 1980) (Stanley and Yuspa, 1983) (Rosenthal et al., 1991). My interest in the potential role of SM in the induction of markers of keratinocyte differentiation began with the observations of two groups of investigators headed by Dr. William Smith and Dr. Radharaman Ray (presently collaborators) at USAMRICD, who found that changes in Ca^{2+} homeostasis could be observed in keratinocytes exposed to SM (Ray et al., 1993) (Ray et al., 1995) (Mol and Smith, 1996). Ca^{2+} -buffering experiments have supported the role of Ca^{2+} in the etiology of SM-induced cytotoxicity (Ray et al., 1996). While Ca^{2+} plays pleiotropic roles in a number of different cell types, earlier studies by myself as well as other groups showed that keratinocytes are exquisitely sensitive to changes in the intracellular levels of Ca^{2+}. We thus performed a series of experiments showing that SM induces Ca^{2+}/calmodulin- dependent differentiation in keratinocytes. An unexpected outcome of these experiments was the observation that SM also induced Ca^{2+}/calmodulin-dependent apoptosis. Thus, both differentiation and apoptosis could account for the basal cell toxicity observed *in vivo* in response to SM.

We tested, and are continuing to test this hypothesis by genetic and molecular methods to experimentally modulate the effects of calcium and subsequent vesication response through the use of stable genetically modified human keratinocytes that express antisense transcripts to calmodulin. As a first step towards this goal, we utilized cultured keratinocytes as well as a graft system to define the expression of normal differentiation-specific markers in the epidermis, to examine how marker expression is modified upon exposure to SM. During the first year of the contract, in collaboration with Drs. William Smith and Radharaman Ray at USAMRICD, I examined whether markers of differentiation and apoptosis are induced or altered by SM. I found that SM in fact induced both the terminal differentiation response as well as an apoptotic response in keratinocytes (Rosenthal et al., 1998; Stöppler et al., 1998). Secondly, we successfully interfered with the pathway leading to the alteration of these markers. Utilizing both chemical inhibitors and antisense oligonucleotides, we determined that Ca^{2+} and calmodulin are important to both responses, and that these two related processes may in part play a role in SM toxicity. During the second year of the contract, we made a number of other significant advances towards the understanding of the mechanisms involved in the response to SM. We characterized the molecular ordering of events responsible for SM-induced apoptosis, with

respect to the activation of proapoptotic proteins. We determined that a Fas/TNF receptor pathway was responsible for **SM**-induced apoptosis, and directly blocked this pathway by using a dominant-negative inhibitor of FADD. In the last year of the contract, we have continued to generate calmodulin antisense constructs and have packaged these constructs into retroviral vectors and used them to infect primary and immortalized cells. Finally, we have performed grafting experiments utilizing these calmodulin and FADD constructs to examine the role of these proteins in the vesication response to **SM**.

BODY

Original Hypothesis

SM causes blisters in the skin through a series of cellular changes leading to terminal differentiation and cell death. Much of the evidence points to a major role for calcium and calmodulin in this response. Blocking the calmodulin response will prevent terminal differentiation, cell death, and **SM** vesication

Statement of work

C.2.1 Task 1: Immortalized human keratinocytes will be used in the performance of exploratory studies to test the hypothesis that the expression of terminal differentiation markers can be altered in grafted animals after the topical application of **SM**

1) Indirect immunofluorescence will primarily be used to examine the expression of basal keratinocyte markers involved in cell attachment to the basal lamina.

2) Proteins showing marked changes will be examined by *in situ* hybridization to determine with the changes are based on transcriptional or posttranscriptional events.

C.2.2 Task 2: Experiments using inhibitors and/or modulators of calmodulin (CAM), intracellular free calcium increase, and glutathione to determine whether the changes in c.2.1 can be attenuated will be initiated.

C.2.3 Tasks 3 and 4: Experiments in C.2.1 and C.2.2 will be completed by examining marker expression, at successive time points, in non-transfected keratinocytes after the application of **SM** or agents dynamics/metabolism.

Research Accomplishments: Part I

CALMODULIN AND P53 ARE TARGETS FOR MODULATING SM-INDUCED APOPTOSIS.

To determine if **SM** altered keratin expression, NHEK were exposed to 100 µM **SM**, fixed after 24 h, and then subjected to FACS analysis, using the broad-range-reactive cytokeratin (CK) antibody as a tag. Following **SM** exposure, the number of CK+ cells increased significantly (data not shown). Since the CK antibody recognizes the suprabasal keratin K10, we were curious to determine if **SM** altered the expression of any differentiation-specific proteins. Immunoblot analysis with specific antisera revealed that both K1 and K10 were induced in the presence of 100 µM **SM** (**Fig.** 1A). We also examined the expression of involucrin, a precursor protein that becomes crosslinked in the fully differentiated cornified envelope (Rosenthal et al., 1997). In extracts derived from untreated cells, involucrin migrated as a 68 kDa monomer form. Following 24 h exposure to **SM**, the staining pattern shifted to higher molecular weight forms (**Fig.** 1B), suggesting that the protein is cross-linked in response to **SM**. In more recent studies (Rosenthal et al., 2000), we have shown by RT-PCR that **SM** induces K1 at the RNA level (**Fig.** 2)

We next examined the levels of fibronectin expressed in NHEK following **SM** treatment, for two reasons. First, fibronectin is expressed in basal cells, but is suppressed in suprabasal cells *in vivo*, and in response to differentiating agents *in vitro* (Adams and Watt, 1990; Nicholson and Watt, 1991). In turn, contact with fibronectin also inhibits keratinocyte differentiation (Staiano-Coico and Higgins, 1992; Drozdoff and Pledger, 1993; Watt et al., 1993). Secondly, fibronectin is a major component of the basal lamina, and forms an attachment site for the alpha 5 beta 1 integrin of the basal cells (Adams and Watt, 1990). Thus, suppression of this protein by **SM** could in part explain detachment of basal cells from the basal lamina during vesication *in vivo*. Fibronectin is produced in keratinocytes (as well as fibroblasts), in two isoforms. Both the 220 kDa and 94 kDa forms of fibronectin were reduced with time after **SM** exposure. In contrast, untreated NHEK showed no decrease in the levels of fibronectin (**Fig.** 1C).

SM induces p53 and suppresses Bcl-2

To examine possible mechanisms by which **SM** altered the differentiation response, we initially examined the expression of p53, which plays important roles in both the differentiation and apoptotic responses in keratinocytes. FACS analysis showed a significant increase in the

protein levels of p53 24 h after exposure to 100 μM **SM**, while immunoblot analysis (**Fig.** 3A) shows that this increase in p53 levels occurs within 2 h.

The *bcl*-2 gene product inhibits both keratinocyte differentiation and apoptosis. Bcl-2 levels are high in basal keratinocytes and are reduced in the differentiating layers of the epidermis (Hockenberry et al., 1991). Furthermore, expression of *bcl*-2 antisense RNA can lower endogenous levels of Bcl-2 and induce markers of terminal differentiation in mouse keratinocytes (Marthinuss et al., 1995). Following **SM** treatment, there is a significant decrease in Bcl-2 protein levels in NHEK as determined by immunoblot analysis (**Fig.** 3B).

Newly discovered caspase-mediated cleavage of epidermal keratins during SM-induced differentiation and apoptosis.

In order to study the differentiation response to **SM**, we originally focused on the suprabasal-specific keratins, K1 and K10, which are tightly regulated at the level of transcription in keratinocytes both *in vitro* and *in vivo*. However, we found that many changes may occur at the post-translational level, including a putative caspase-mediated breakdown of keratin K1 that occurs during apoptosis. Thus, we continued to employ Western analysis, as well as immunofluorescent analysis to examine the changes in these gene products in the second year. When we recently used a different polyclonal antibody directed against the C-terminus of K1, and treated cells with higher concentrations of **SM**, we discovered an apparent cleavage product of K1. The size of this product maps near a perfect consensus sequence for a site of cleavage by caspase-6 (**Fig.** 4). Moreover, point mutations near this region of K1 give rise to a genetic **blistering disorder,** epidermolytic hyperkeratosis (McLean et al., 1994). Thus, it is of interest to determine if K1 can be cleaved by caspase-6 following treatment with **SM**. We are performing the same experiments in the presence of the caspase-6 inhibitor, VEID-CHO. Inhibition of the cleavage product in the presence of the inhibitor would strongly suggest that K1 is in fact the substrate for caspase-6, and that K1 is a target during keratinocyte apoptosis.

Inhibitors of CaM block markers of differentiation

Since previous studies have shown that **SM** can induce an increase in intracellular free Ca^{2+} (Ca_i) (Ray et al., 1995) and we have observed that a rise in Ca_i is associated with the normal terminal differentiation response of keratinocytes (Rosenthal et al., 1991; Rosenthal et al., 1991; Yuspa et al., 1989), the expression of these markers suggested a role for Ca^{2+} in the **SM** response that was observed. Furthermore, we have shown that the K1 gene contains specific Ca^{2+}-inducible enhancer sequences located 3' to the gene (Huff et al., 1993) and expression of K1 (and other differentiation-specific genes) can be blocked by the Ca_i chelator BAPTA (Li et al., 1995). BAPTA also enhances the survival of keratinocytes in the presence of **SM** (Ray et al., 1996). We therefore pre-incubated keratinocytes with 20 μM BAPTA-AM for 30 min prior

to SM treatment. When NHEK were subsequently treated for 24 h with 100 μM SM, keratin K1 was suppressed (**Fig. 5A**). Although BAPTA treatment suppressed total protein synthesis by 50% after 24 h (not shown), this effect was not enough to account for the complete suppression of K1. Ca^{2+} may induce differentiation via its role in the activation of protein kinase C (Dlugosz and Yuspa, 1993). In addition, Ca^{2+}-calmodulin complexes are also generated which modulate this protein kinase C response (Chakravarthy et al., 1995). We therefore determined whether the calmodulin inhibitor W-7 could alter the differentiation response to SM. **Figure 5A** shows that a 30 min pre-treatment with W-7 prior to exposure to 100 μM SM inhibited the expression of K1. Protein calibration prior to gel-loading, followed by Ponceau-S-staining of the immunoblot (**Fig. 5B**), eliminated the possibility of loading artifact, indicating that SM induces the expression of this differentiation-specific marker via a Ca^{2+}-calmodulin-dependent pathway. The suppression of SM induction of K1 by inhibitors of CaM, as well as by inhibitors of CaM kinase II, was also observed at the RNA level (**Fig. 2**). Interestingly, calmodulin itself was transiently down-regulated by SM (**Fig. 5C**).

We also performed a time course (see **Tasks 3 and 4**), followed by Western analysis using antibodies specific for the suprabasal keratins K1 and K10, which are the major differentiation-specific proteins expressed in keratinocytes. Both K1 and K10 are weakly induced by 10 μM SM, and strongly induced in the presence of 100 μM SM, between 8 and 24 h following treatment (**Fig. 1**). We also examined the expression of other markers of differentiation including involucrin, a precursor protein that becomes crosslinked in the fully differentiated cornified envelope (Yaffe et al., 1993) (Robinson et al., 1996) (Steinert and Marekov, 1997). In untreated cells, involucrin was expressed at low levels, and was restricted to a 68 kDa monomer form. Following exposure to either 10 μM (not shown) or 100 μM SM, the level of involucrin increased; more importantly, the staining pattern shifted to heterogeneous higher molecular weight forms by 24 h, suggesting that the protein is cross-linked in response to SM.

<u>SM induces apoptosis via caspase activation</u>.

The striking increase in p53 levels and decrease in Bcl-2 levels suggested that in addition to modulating differentiation, SM may induce apoptosis as well. Recent evidence has revealed that Bcl-2 can complex with both the *Caenorhabditis elegans* death proteins 3 and 4 (Ced-3 and Ced-4) (Chinnaiyan et al., 1997). p53 has been shown to antagonize this activity of Bcl-2, perhaps via the induction of Bax, since p53 has been shown to induce *bax* gene transcription via p53 response elements within the *bax* promoter (Miyashita et al., 1995). Importantly, p53 has been shown to upregulate Fas ligand and receptor, a potential mechanism for apoptosis that was tested below. Thus, we assayed for markers of apoptosis following SM treatment. A hallmark of apoptosis in a number of cell types is the appearance of nucleosome sized ladders due to the presence of a Ca^{2+}/Mg^{2+}-dependent endonuclease that is induced in apoptotic cells, another

direct role for Ca^{2+} in apoptosis. At 300 μM **SM**, both Nco (immortalized keratinocytes) and NHEK (primary keratinocytes) showed nucleosome-sized ladders analyzed by agarose gel electrophoresis.

We have recently determined that the activation of PARP plays a role in the etiology of apoptosis in osteosarcoma cells induced to undergo programmed cell death, in which poly(ADP-ribosyl)ation corresponds with the early reversible stages of apoptosis (Simbulan-Rosenthal et al., 1998, Rosenthal et al., 1997). Antisera specific for PAR did in fact detect a strong band at 116 kDa in extracts of primary keratinocytes treated with all concentrations of **SM** tested, whereas no such band was present in extracts of control keratinocytes, indicating **SM** induces DNA strand breaks and PARP is activated. After this time point, the level of poly(ADP-ribose) decreases precipitously, similar to our previous observations using osteosarcoma cells induced to undergo apoptosis (Rosenthal et al., 1997). The expression of PAR early in apoptosis was also used as an *in vivo* marker of apoptosis as described below.

We previously determined that this characteristic rise and rapid decline in poly(ADP-ribose) levels could be attributed to the proteolytic cleavage of PARP into the characteristic 89 kDa and 24 kDa fragments, the latter of which contains the Zn^{2+} finger region and DNA binding domain (DBD). We therefore performed Western analysis to monitor the cleavage of PARP using an antibody that recognizes both the full length 116 kDa protein as well as the 89 kDa fragments of PARP. A significant conversion of full-length PARP to the 89 kDa fragment was observed following 300 μM **SM** treatment . In order to monitor the *in vivo* cleavage of PARP in the graft system, we used the antibody against the DBD of PARP.

A sensitive technique to verify that **SM** induces apoptosis is to determine the activation of caspase-3 from its precursor (pro-caspase-3; CPP32) via the use of *in vitro* translated PARP. We therefore used a combination transcription/ translation system to radiolabel full length PARP, which was subsequently incubated with extracts derived from keratinocytes treated with **SM** at different concentrations and time points. **Figure 6** (top) shows that PARP cleavage activity is clearly seen in NHEK (primary keratinocytes) in 300 μM **SM** after 24 h, as evidenced by the strong appearance of the 24 kDa and 89 kDa cleavage products. In Nco (immortalized keratinocytes), caspase-3 activity similarly increased with increasing concentrations of **SM**. Quantitative phosphorimage analysis (**Fig. 6**, bottom) shows the relative PARP cleavage activities that result from the treatment of NHEK or Nco with different concentrations of **SM** for 24 h. The high level of PARP-cleavage activity observed in 300 μM **SM** is indicative that this vesicant is also a strong inducer of apoptosis in both primary and immortalized keratinocytes, and that apoptosis is occurring via a caspase 3-like pathway.

We next further verified that **SM** induces apoptosis by determining whether the observed caspase-3 activity *in vitro* could be associated with the processing of pro-caspase-3/CPP32 into its active protease form. During apoptosis, procaspase-3/CPP32 is processed into 17 kDa and 12 kDa peptides, with the removal of a pro-peptide sequence from the N-terminus. The 17 kDa and

12 kDa fragments then form the active proteolytic heterodimer. Using an antibody that recognizes both the active (p17) and inactive (CPP32) forms of caspase-3, a slightly smaller form of CPP32 was observed 24 h after the cells were exposed to 100 μM **SM**, equivalent in size to CPP32 minus the pro-peptide sequence, suggesting that processing of the N-terminus of the precursor protein was occurring (not shown). To confirm this, the same extracts were analyzed utilizing an antibody that is specific for the pro-sequence that is removed when caspase-3 is processed into its active form. The disappearance of the slightly smaller MW band previously observed at 24 h in 100 μM **SM**, indicates that this band is missing the propeptide sequence, and is thus the result of CPP32 N-terminal processing. Following treatment with 300 μM **SM**, NHEK showed complete processing of a portion of CPP32 into the active p17 form (**Fig**. 7B). A small amount of the partially processed p20, which represents p17 + the N terminal pro-sequence, is also observed. Thus, in both 100 μM and 300 μM **SM**, markers of apoptosis are induced, although complete activation of caspase-3, PARP cleavage, and DNA fragmentation are only observed at the higher dose of **SM**.

A Ca^{2+} Calmodulin-Dependent Pathway for SM-Induced Apoptosis

To determine if **SM**-induced apoptosis was proceeding via Ca^{2+} -calmodulin dependent pathways, BAPTA and W-7 were utilized as pre-treatment agents. BAPTA had a small effect on *in vitro* PARP-cleavage activity, while greater suppression was observed following W-7 pre treatment (**Fig**. 7A). These agents also suppressed the level of DNA fragmentation.

We next determined whether this W-7-sensitive repression was related to the processing of CPP32 into its active form. In control NHEK, one of the two subunits of the active form of apopain, p17, can clearly be detected 24 h following treatment with 300 μM **SM**. However, p17 is completely suppressed by 50 μM W-7 (**Fig**. 7B). Thus, **SM** induces apoptosis via a calmodulin-dependent pathway that involves the activation of caspase-3.

We utilized the CaM antagonists W-7 or W-13 as pre-treatment agents, as well as the structurally similar, but inactive control compound W-12, to abrogate any CaM-response pathways for **SM**-induced apoptosis. W-7 and W-13, but not W-12, suppressed caspase-3 activity. We also determined whether this W-7- and W-13-sensitive repression was related to the processing of procaspase-3 into its active form. In control NHEK (untreated and W-12-treated), one of the two subunits of the active form of caspase-3, p17, can clearly be detected 24 h following treatment with **SM**. In the presence of W-7, or W-13, p17 is markedly reduced in NHEK (not shown).

The roles of CaM target proteins were also examined. Pretreatment of keratinocytes with KN62 or KN93, inhibitors of CaM kinase II (CaMKII), which has been implicated in apoptosis, did not prevent apoptosis or the activation of caspase-3 at 24 h, although suppression was observed at earlier time points (not shown). Similarly, pretreatment of keratinocytes with Cyclosporin A, an inhibitor of calcineurin, partially inhibited **SM**-induced apoptosis within 24 h,

while at 48 h, caspase-3 activity was completely suppressed (not shown). These results indicate that **SM** induces apoptosis via a CaM-dependent pathway that involves the activation of procaspase-3. Calcineurin and CaMKII play partial roles, suggesting that additional CaM-regulated proteins may be important in the induction of apoptosis by **SM**. Similarly, nuclear fragmentation (as determined by agarose gel electrophoresis, as well as internucleosomal fragmentation, determined by Hoechst staining, were inhibited by W-7).

To adopt a more specific approach we determined which of the calmodulin genes was expressed in keratinocytes. PCR analysis indicated that CaM I was the major gene expressed in both primary and immortalized keratinocytes (**Fig. 8**).

Additionally, CaM I antisense retrovirus suppressed the **SM** induction of K1 (below). Our studies thus show that CaM plays a role in the expression of K1 in response to **SM**. In addition, our initial inhibitor studies suggest that CaM KII or calcineurin may mediate the effects of CaM. RT-PCR analysis reveals that this regulation of K1 is at the level of mRNA, and appears to involve CaM kinase II, since K1 mRNA induction by **SM** is suppressed by KN62 (**Fig**. 2).

Stöppler, H., Stöppler, M. C., Johnson, E., Simbulan-Rosenthal, C. M. G., Iyer, S., Smulson, M. E., **Rosenthal, D. S.***, and Schlegel, R. The human papillomavirus 16 (HPV-16) E7 protein sensitizes primary human keratinocytes to apoptosis. *Oncogene* **17**: 1207-1214 (1998).
*corresponding author

We observed striking changes in the differentiation of primary and immortalized keratinocytes in response to **SM** (see above). In repeated experiments, markers of differentiation were induced, including K1, K10 and the crosslinking of involucrin, and the expression of fibronectin was suppressed in both a dose- and time-dependent fashion. An unexpected outcome of these experiments was the observation of the induction of significant apoptosis in primary and immortalized human epidermal cells by **SM**. Further study of the apoptotic response was performed for two major reasons: 1) Both differentiation and apoptosis are strongly induced in keratinocytes in response to **SM**, and both of these responses could contribute to basal cell death and vesication. 2) Keratinocyte differentiation and apoptosis share many similar features. For example, low levels of Bcl-2 and high levels of p53 are markers of both differentiation and apoptosis. Since these two processes may share common pathways, a single compound might act as a dual inhibitor of differentiation and apoptosis, and have important therapeutic potential. This is apparently the case for the calmodulin inhibitor W-7, which I showed to inhibit both the apoptotic and differentiation responses in keratinocytes exposed to SM.

The fact that p53 is induced in keratinocytes in response to **SM**, along with the important role that p53 may play in apoptosis, lead me to investigate the potential role of p53 in the etiology of apoptosis induced by **SM**.

We infected primary keratinocytes with retroviral constructs containing either the E6, or E7, or E6 +E7 genes of HPV18. These same retroviral vectors were also utilized for the expression of calmodulin antisense RNA described below. E6 is known to bind to and degrade p53, while E7 has been shown to upregulate the p53 gene. When cells were infected with E7 alone, p53 levels were increased (**Fig**. 9, top), indicating that E7 was expressed and functioning. E7-expressing keratinocytes were also more susceptible to **SM**-induced apoptosis (**Fig**. 9, bottom), as well as apoptosis induced by TNFα. E6 expression inhibited p53, and did not alter the apoptotic response of keratinocytes to **SM** compared to NHEK controls. On the other hand, cells expressing both E6 and E7 had a lower index of apoptosis than cells expressing only E7, indicating that E6 partially prevented E7-induced **SM**-susceptibility.

Thus, p53 partially mediates **SM** induced apoptosis. Recent evidence suggest that p53 may function via upregulation of Bax, a pro-apoptotic member of the Bcl-2 family, as well as Fas. The role of these proteins (e.g. Bad) in the apoptotic response in cultured keratinocytes is addressed below.

Simbulan-Rosenthal, C. M., **Rosenthal, D. S.**, Smulson, M. E. Poly(ADP-ribosyl)ation of p53 during apoptosis in human osteosarcoma cells. *Cancer Res.* **59**: 2190-2194 (1999).

The previous two studies showed that both calmodulin and p53 play important roles in the differentiation and apoptotic responses of keratinocytes to **SM**. Since p53 is rapidly induced in response to **SM** as well as many other apoptosis-inducing agents, we wished to determine the mechanism for the increase in p53 levels. I showed that the intracellular p53 concentration is dramatically increased within 2 h of SM treatment, further evidence that apoptosis occurs early and is the primary response of keratinocytes to SM. (Rosenthal et al., 1998). Other studies have shown that p53 levels peak within 1 h of γ-irradiation before returning to control values, about the same time required for the completion of repair of DNA damage. Another early event following DNA damage in response to exposure of cells to such agents as γ-irradiation, free radicals, or **SM** and other alkylating agents, is the poly(ADP-ribosyl)ation of various proteins that are localized predominantly adjacent to the DNA strand breaks. It was recently shown that p53 is poly(ADP-ribosyl)ated *in vitro* by purified poly(ADP-ribose) polymerase (PARP), and that binding to a specific p53 consensus sequence prevents its covalent modification (Wesierska-Gadek et al., 1996b).

To clarify the role of PARP in the accumulation of p53 induced by DNA damaging agents such as **SM**, we established and characterized a Burkitt's lymphoma cell line that both undergoes this response and contains a stably integrated PARP antisense construct under the

control of a glucocorticoid-responsive promoter (pMAMneo). I have successfully used this antisense construct to reduce levels of both PARP and calmodulin in keratinocytes. We have now shown that p53 undergoes modification by poly(ADP-ribosyl)ation *in vivo*, and have further explored how this modification is altered during apoptosis.

Control cells showed a marked increase in p53 concentration 30 min after γ-irradiation, peaked at 2 h, and returned to control values by 4 h. The p53 concentration in cells depleted of PARP also increased after γ-irradiation. However, whereas the magnitude of the maximal increase was similar in induced and uninduced cells, the p53 concentration peaked later, at 4 h, and remained elevated for 6 to 12 h after γ-irradiation in the induced cells. Thus, depletion of PARP did not affect the magnitude of the p53 response, but rather prolonged the accumulation of this protein, presumably by a direct or indirect effect on its synthesis or degradation.

Poly(ADP-ribosyl)ation of p53 at the early stages of apoptosis in human osteosarcoma cells.

To confirm whether p53 undergoes poly(ADP-ribosyl)ation during apoptosis in human osteosarcoma cells, extracts were prepared from osteosarcoma cells at various times during spontaneous apoptosis and subjected to immunoprecipitation with an anti-p53 mAb. The immunoprecipitated proteins (mainly p53 and its binding partners) were then subjected to immunoblot analysis with mAb to PAR. This approach revealed marked poly(ADP-ribosyl)ation of p53 at the early stages of apoptosis (**Fig.** 10A), coincident with the burst of PAR synthesis during this stage. The extent of poly(ADP-ribosyl)ation of p53 declined thereafter at the onset of caspase-3 (PARP cleavage) activity. Reprobing of the blot with polyclonal antibodies to p53 confirmed that the modified protein was indeed p53 (**Fig.** 10B). On the other hand, no nonspecific binding of p53 was apparent when immunoprecipitation was performed with control antibodies (pre-immune serum, "C") or with protein A-Sepharose beads ('B") alone. The observation that p53 is specifically poly(ADP-ribosylated) during the early stages of spontaneous apoptosis in human osteosarcoma cells suggests that this specific post-translational modification may have a role in regulating its activities during the cell death cascade.

THE ROLE OF THE FAS RECEPTOR AND CASPASE PATHWAY IN THE MEDIATION OF APOPTOSIS INDUCED BY SM AND OTHER AGENTS

Fas is a cell-surface receptor found or induced in most cell types, including keratinocytes (**Fig.** 21), that mediates some forms of apoptosis. Upon activation by its specific ligand (Fas L), or by agonist antibody, Fas forms a homotrimeric complex, which in turn recruits the Fas

Associated Death Domain protein (FADD) to the membrane-bound complex. In turn, it appears that one or more of the "upstream caspases" (caspase-8, -9 and/or -10) localize to the Fas-FADD complex, and become activated autocatalytically. In our study, we showed that following exposure to Fas antibody, caspase-8 is activated, which in turn causes the activation of the "executioner caspases" 3, 6, and 7. It appears that the activation of caspase-3 is sufficient for cell death by apoptosis to occur, since ectopic expression of this protein results in rapid cell death. Since caspases appear to play a central role in apoptosis, we chose caspase assays as one of the markers for apoptosis. In this study, we have further shown that caspase 8 functions to ensure apoptosis by increasing the intracellular concentration of the sphingolipid, ceramide, and that a further metabolite of ceramide, sphingosine 1-phosphate, can inhibit apoptosis induced by both anti-Fas antibody, as well as by ceramide. Further, we have observed that the levels of sphingosine 1- phosphate are regulated by calmodulin, and are elevated in differentiating keratinocytes, further supporting the notion of an overlap in regulation of keratinocyte differentiation and apoptosis pathways (**Fig.** 11).

Rosenthal, D. S., Ding, R., Simbulan-Rosenthal, C. M. G., Vaillancourt, J. P., and Nicholson, D. W. Intact cell evidence for the early synthesis, and subsequent late apopain-mediated suppression of poly(ADP-ribose) during apoptosis. *Experimental Cell Research 232*: 313-321 (1997).

We first showed that an early response to **SM** was the synthesis of PAR in the reconstituted epidermis. At that time, we believed that this was merely a response to non-specific DNA breaks induced by the alkylating effect of **SM** (Rosenthal et al., 1995). However, further studies with a well-defined apoptotic system, showed that this burst of PAR activity was in fact characteristic of early apoptosis. In this 1997 study we used a human osteosarcoma cell line that undergoes a "slow," spontaneous apoptotic death. On reaching confluency, these cells undergo the morphological and biochemical changes characteristic of apoptosis. The cells achieve confluency after ~6 days under our culture conditions. Internucleosomal DNA cleavage became evident around day 7 and increased until day 10, at which time virtually all of the cells have completed the death program. Cells from these same cultures were incubated for up to 10 days and fixed at daily intervals for examination of nuclear poly(ADP-ribosyl)ation with antiserum to PAR. After 3 days, the nuclei of all attached cells stained intensely for the PAR. The *in vivo* synthesis of PAR was observed to be markedly reduced after 4 days (**Fig.** 12).

The time course of PARP expression was similar to that of the synthesis of PAR, as shown in the **Fig.** 12. Low levels of PARP were detected after 1 day in culture. However, a substantial amount of PARP was detected in the nuclei of all cells after 2 days. PARP staining showed a punctate pattern throughout the nucleus. Staining was more intense in perinucleolar regions, but was excluded from the nucleoli. The intensity of PARP staining decreased between days 3 and 10, although weak staining was still apparent at 10 days. These observations suggest

that the initial catalytic activation of PARP is coincident with its synthesis in apoptotic osteosarcoma cells. Our results support the idea that nuclear disruption involving strand breaks may be present in the earliest stages of apoptosis (Neamati et al., 1995), before morphological changes and the appearance of the characteristic nucleosome ladder.

To confirm that this cleavage also occurs in intact cells, we subjected human osteosarcoma cells to immunofluorescence analysis with antibodies generated against a peptide corresponding to the DBD of PARP. As with the other markers, samples were analyzed each day throughout the total 10-day period; samples from immediate (day 1), early (day 3), mid- (day 6), and late (10) stages of apoptosis are shown in **Fig**. 12. Immunofluorescence analysis detected the PARP DBD in human osteosarcoma cells only after 6 to 7 days in culture, a time at which the abundance of both PARP and PAR is decreasing, PARP-cleavage activity is increasing, and internucleosomal DNA cleavage is present (Nicholson et al., 1995). The pattern of staining for the DBD also differed markedly from that of full-length PARP. Whereas PARP staining was present throughout the nucleus, the DBD showed a more localized punctate pattern in the region of the nucleolus and throughout the nucleus-disrupted cytoplasm.

DNA strand breaks and PAR status during late apoptosis in intact cells.

Using newly developed methodology (see published study below; Rosenthal et al., 1997), we assessed the levels of DNA strand breaks in the fixed intact cells by staining the human osteosarcoma cells with the biotinylated PARP DBD, followed by Texas red-conjugated streptavidin. Samples from immediate (day 1), early (day 3), mid-(day 6), and late (10) stages of apoptosis are shown in **Fig**. 12 (right). By day 10 the nuclei of many cells stained intensely. Significant internucleosomal DNA breaks were also detected from days 6-9 (Nicholson et al., 1995). Nuclear fluorescence was not detectable at day 1; however, a low level of staining, consistent with a small number of DNA strand breaks was observed at day 3, when PAR synthesis was most abundant and caspase-3 activity was only 15% of the maximum).

Taken together, the new immunofluorescent data further show that both protein expression and catalytic activation of PARP appear early in osteosarcoma cell growth, while the cleavage of PARP and the accumulation of a large number of DNA strand breaks confirm our earlier *in vitro* results by showing in intact cells that these events occur later in the process. They also confirm, in the context of the intact cell, that poly(ADP-ribosyl)ation is not associated with the late stages of apoptosis. Our results show with individual, intact cells that PARP cleavage and inactivation, the concomitant loss of poly(ADP-ribosyl)ation of target proteins and, hence, the maintenance of adequate cellular pools of NAD and ATP, appear to be characteristic of later stages of apoptosis during which cells become irreversibly committed to death. These techniques for the study of individual cells are useful methods for examining apoptosis in the graft system, putting us in a unique position to examine apoptosis induced by **SM** *in vivo*.

Simbulan-Rosenthal, C. M. G., **Rosenthal, D. S.**, Iyer, S., Boulares, A. H., and Smulson, M. E. Transient poly(ADP-ribosyl)ation of nuclear proteins and role of poly(ADP-ribose) polymerase in the early stages of apoptosis. *J. Biol. Chem.* **273**(22): 13703-13712 (1998).

A transient burst of poly(ADP-ribosyl)ation of nuclear proteins occurs early, prior to commitment to death, in human osteosarcoma cells undergoing apoptosis, followed by caspase-3-mediated cleavage of poly(ADP-ribose) polymerase (PARP). The generality of this early burst of poly(ADP-ribosyl)ation was investigated with human HL-60 cells, mouse 3T3-L1, and immortalized fibroblasts derived from wild-type mice. The effects of eliminating this early transient modification of nuclear proteins by depletion of PARP protein either by antisense RNA expression or by gene disruption on various morphological and biochemical markers of apoptosis were then examined. In the course of developing our antisense RNA system we discovered a novel feedback loop whereby the expression levels of PARP and/or its activity controlled the levels of the enzyme primarily responsible for its activity, i.e. caspase-3. When 3T3 L1 cells were transfected with inducible constructs expressing antisense to PARP, we found that the cells were unable to undergo Fas-mediated apoptosis. This was also true of Jurkat cells transfected with the same inducible vector expressing antisense RNA to PARP. In addition, cells derived from animals depleted of PARP where unable to undergo Fas-mediated apoptosis. Upon examination of pro-caspase-3, it was found that the precursor was not processed into its active form in the absence of PARP, indicating that some form of feedback mechanism was responsible. In addition, when PARP was retransfected back into PARP -/- cells, the phenotype reverted to a Fas-apoptosis inducible cell type confirming the fact that PARP was in fact responsible for the observed apoptosis.

The present study demonstrates the occurrence of a transient poly(ADP-ribosyl)ation of nuclear proteins at an early stage of apoptosis induced by serum deprivation, camptothecin, or antibodies to Fas in different cell lines. When this early poly(ADP-ribosyl)ation was prevented as a result of depletion of endogenous PARP, either by gene disruption or by antisense RNA expression, several morphological and biochemical markers of apoptosis were no longer observed in response to such inducers.

Incubation of cells with a combination of anti-Fas and cycloheximide resulted in a marked induction of caspase-3-like activity, as indicated by the generation of the 89- and 24-kDa cleavage fragments of PARP. Densitometric scanning showed that ~60% of [^{35}S]PARP substrate was converted to the 89-kDa cleavage product under these conditions. Cycloheximide alone did not induce apoptosis in these cells. The presence of Dex during the 72-h preincubation of mock-transfected 3T3-L1 cells had no effect on induction of caspase-3-like activity .

Immunoblot analysis revealed that the amount of PARP in mock-transfected 3T3-L1 cells was not affected by incubation with Dex. However, in the PARP-antisense cells, Dex induced a

time-dependent depletion of PARP, with only ~5% of the protein remaining after 72 h. Ponceau S staining for total protein on the same immunoblot confirmed essentially equal protein loading and transfer among lanes. Whereas the *in vitro* PARP activity of control cells was not affected by incubation with Dex, exposure of PARP-antisense cells to Dex for 72 h resulted in an ~80% decrease in PARP activity.

Effects of the absence of early transient poly(ADP-ribosyl)ation on morphological and biochemical markers of apoptosis in 3T3-L1 cells.

We next tried to determine whether prevention of the early burst of PAR synthesis by PARP antisense RNA expression could affect the development of other biochemical or morphological markers of apoptosis when these cells are exposed to apoptosis inducers. The combination of anti-Fas and cycloheximide induced a marked increase in caspase-3-like activity in mock-transfected 3T3-L1 cells that had been preincubated in the absence or presence of Dex; this effect was maximal 24 h after induction of apoptosis. Whereas PARP-antisense 3T3-L1 cells that were not exposed to Dex showed a similar increase in caspase-3-like activity in response to anti-Fas and cycloheximide, no such increase was apparent in PARP-antisense cells that had been depleted of PARP by preincubation with Dex before exposure to anti-Fas and cycloheximide (**Fig**. 13A).

Caspase-3, similar to other members of the caspase family, is expressed in cells as an inactive 32-kDa proenzyme (CPP32). During apoptosis, CPP32 is activated by cleavage at specific Asp residues, with the active enzyme (caspase-3) consisting of a heterodimer of a 17-kDa subunit (p17), containing the catalytic domain, and a 12-kDa subunit (p12) (Nicholson et al., 1995). To confirm that CPP32 is proteolytically processed to p17 during apoptosis in control 3T3-L1 cells, and to determine whether the transient early poly(ADP-ribosyl)ation is necessary for this activation, control and antisense cells were preincubated with Dex, exposed to anti-Fas and cycloheximide for indicated times, and cell extracts were subjected to immunoblot analysis with antibodies to the p17 subunit of caspase-3. The amount of CPP32 increased in both control and antisense cells after exposure to anti-Fas and cycloheximide. However, whereas CPP32 was proteolytically processed to p17 by 24 h, coinciding with the peak of *in vitro* caspase-3-like PARP-cleavage activity, in control cells, proteolytic processing of CPP32 was not apparent in the PARP-depleted antisense cells (**Fig**. 13C). Furthermore, using DNA fragmentation analysis as another assay for apoptosis, control 3T3-L1 cells exposed to anti-Fas and cycloheximide for 24 h exhibited marked internucleosomal DNA fragmentation (DNA ladders), but not the PARP-depleted antisense cells exposed to these inducers for the same time (**Fig**. 13B).

Consistently, whereas antisense cells preincubated in the absence of Dex showed changes in nuclear morphology typical of apoptosis when exposed to anti-Fas and cycloheximide, those depleted of PARP by preincubation with Dex did not.

<u>Immortalized fibroblasts derived from PARP knockout mice do not exhibit morphological and biochemical markers characteristic of apoptosis.</u>

Anti-Fas and cycloheximide induced a marked increase in caspase-3-like activity in PARP +/+ cells; this effect was maximal 24 h after induction of apoptosis, as indicated by the complete cleavage of PARP into 89-kDa and 24-kDa fragments. In contrast, no such increase in caspase-3-like activity was evident in PARP -/- cells after exposure to anti-Fas and cycloheximide for up to 24 h.

To verify that CPP32 is proteolytically activated to caspase-3 during induction of apoptosis in these cells, extracts of cells that had been exposed to anti-Fas and cycloheximide for various times were subjected to immunoblot analysis with antibodies to CPP32. Whereas CPP32 was proteolytically processed to p17 in PARP +/+ fibroblasts exposed to anti-Fas and cycloheximide, no such effect was evident in the PARP -/- cells.

PARP +/+ cells showed substantial nuclear fragmentation and chromatin condensation 24 h after induction of Fas-mediated apoptosis; ~97% of nuclei exhibited apoptotic morphology by this time. In contrast, no substantial changes in nuclear morphology were apparent in the PARP -/- fibroblasts even after exposure to anti-Fas and cycloheximide for 24 h or 48 h.

<u>Transfection of PARP -/- fibroblasts with wild-type PARP sensitizes these cells to Fas-mediated apoptosis.</u>

PARP -/- fibroblasts were stably transfected with pCD12, a plasmid expressing wild-type PARP (Alkhatib et al., 1987). Immunoblot analysis showed that three different cell clones (1, 2, and 3), and pooled clones (P) expressed PARP protein similar to the PARP +/+ cells, whereas PARP -/- cells and the clone transfected with the vector alone ("vec") did not (**Fig.** 13D). The ability of these clones to express PARP was also confirmed by *in vitro* PARP activity assays.

These cells were induced to undergo apoptosis by exposure to anti-Fas and cycloheximide for up to 48 h. *In vivo* caspase-3-like PARP-cleavage activity was monitored by immunoblot analysis with antisera to PARP that recognizes both the 116 kDa PARP and its 24 kDa cleavage fragment (F1-23, Biomol). PARP +/+ cells as well as PARP -/- clones stably transfected with PARP (clones 2 and 3) exhibited significant caspase-3-like activity after 48 h; ~95% of the PARP protein was cleaved *in vivo* to the 24 kDa cleavage fragment by 48 h (**Fig.** 13D). As expected, PARP was not expressed in the PARP -/- fibroblasts nor in -/- cells transfected with vector alone. Consistently, whereas exposure to anti-Fas and cycloheximide induced marked internucleosomal DNA fragmentation in PARP +/+ fibroblasts and PARP -/- cells stably transfected with PARP (clone 2), no apoptotic DNA ladders were evident in the PARP -/- cells when similarly treated (**Fig.** 13 E). Furthermore, exposure to anti-Fas plus cycloheximide for 48 h induced apoptotic nuclear morphology in PARP -/- cells transfected with PARP (clone 2), almost to the same extent as the PARP +/+ cells.

We have obtained some potentially relevant targets for poly(ADP-ribosyl)ation during the burst of PAR synthesis at the early stages of apoptosis. These results show that induction of spontaneous apoptosis in osteosarcoma cells is associated with an increase in the intracellular abundance of p53. Immunoprecipitation and immunoblot analysis further indicate that extensive poly(ADP-ribosyl)ation of p53 occurs concomitant with the burst of poly(ADP-ribosyl)ation, and that subsequent degradation of PAR attached to p53 occurs concomitant with the increase in caspase-3-like activity. Thus, this posttranslational modification may play a role in the regulation of p53 function or, alternatively, in its degradation during p53-dependent apoptosis. These results are consistent with recent studies showing substantial poly(ADP-ribosyl)ation of p53, with polymer chain lengths from 4 to 30 residues, in cells undergoing apoptosis in response to DNA damage (Kumari et al., 1997) (Nozaki et al., 1997). Electrophoretic mobility-shift analysis further showed that ADP-ribose polymers attached to p53 blocked its sequence-specific binding to a 26-bp oligonucleotide containing the palindromic p53 consensus binding sequence, suggesting that poly(ADP-ribosyl)ation of p53 may negatively regulate p53-mediated transcriptional activation of genes important in the cell cycle and apoptosis (Malanga and Althaus, 1997). Recently, primary fibroblasts from PARP -/- mice were further shown to have a two-fold lower basal level of p53 and are defective in the induction of p53 in response to DNA damage (Agarwal et al., 1997).

Relevance of Research Accomplishments: Part I to Original Hypothesis

By demonstrating that **SM** induces markers of terminal differentiation via a calmodulin-dependent pathway in keratinocytes, we accomplished tasks 1-4, and proved an important part of the original hypothesis: **SM** induces markers of terminal differentiation and cell death. Additionally, we demonstrated that a second mode of cell death: namely apoptosis, was induced by **SM** in both primary and immortalized human keratinocytes. The rest of the hypothesis is discussed under the heading of the other tasks below.

Recommended Changes and Future Work Relating to Research Accomplishments: Part I

Future work will further examine the mechanism for differentiation, although we have already established a role for calmodulin. In addition, we will further delineate the apoptotic pathways that lead to **SM** vesication in order to design prevention strategies, diagnostic markers, and treatments.

C.2.4 Task 5 and 6: pMAMneo CAM and NB-1 antisense constructs, as well as those containing the K1 keratinocyte-specific promoter, will be established for use in mouse skin graft studies (task 5), and in the construction of transgenic mice (task 6)

C.2.5 Task 7:

1) Stable lines of transfected keratinocytes that contain dexamethasone-inducible expression of antisense mRNA to CAM or NB-1 will be established. Transfected clones will be tested using polymerase chain reaction analysis (PCR), RNase protection (RPA) analysis, enzyme activity, and western blotting.

2) Keratinocytes with the K1 promoter constructs from C 2.4 will be transfected. Transfected clones will be tested using PCR analysis, RPA analysis, enzyme activity, and Western blotting. (ADDENDUM)

C.2.6 Task 8: The constructs expressing dexamethasone-inducible antisense mRNA to CAM and NB-1 (from C3.1) will be injected into mouse oocytes to obtain transgenic mice. Use of pMAMneo or the K1 keratinocyte-specific promoter will depend on the results of *the in vitro* experiments. Following oocyte implantation, screening for transgenic founder mice will commence.

Research Accomplishments: Part II

REDUCTION OF THE ENDOGENOUS LEVELS OF CALMODULIN BY ANTISENSE OLIGONUCLEOTIDES OR VECTORS ATTENUATES THE APOPTOTIC RESPONSE TO SM

Antisense oligonucleotide constructs to CaM block apoptosis.

We showed that antisense oligonucleotides to calmodulin were effective in lowering endogenous levels of calmodulin, and attenuated the apoptotic response. This strategy utilizes unmodified short oligonucleotides (20 residues) at a high concentration (40 µM). We synthesized antisense oligonucleotides directed against the human CaM 1, 2 and 3 genes, as well as against CaM-like protein (CLP). In addition to the antisense oligonucleotide, a "nonsense" oligonucleotide is synthesized that is identical in base composition to the antisense, but had a randomly generated sequence. This is an important control, since it rules out other effects of oligonucleotides on cells, including charge, etc. CaM I antisense oligonucleotide diminished the intracellular concentration of CaM in keratinocytes (**Fig. 14A**). Furthermore, treatment of keratinocytes with antisense oligonucleotides, but not with nonsense CaM nucleotides attenuated or eliminated the apoptotic response of keratinocytes in response to **SM**, as measured by either *in vitro* PARP cleavage (**Fig. 14B**) or by immunoblot analysis of caspase-3 processing (**Fig. 14C**).

Antisense vectors.

I originally proposed to establish stable lines of keratinocytes that express antisense RNA to calmodulin. We wished to use an improved strategy for the expression of CaM antisense in both primary and immortalized keratinocytes. A recent advance in molecular biological technology has been in the establishment of improved retroviral vectors that are capable of

delivering a cloned gene or cDNA into cells. These retroviral vectors, originally established from mouse murine leukemia virus (MMLV), have been engineered to infect any type of cell including human keratinocytes. For this purpose, we utilized a retroviral vector. In a published study (Stöppler et al., 1998) we first established the "proof of principal" by constructing and utilizing retroviral vectors that express E6, E7, or both in primary keratinocytes. I used these vectors to efficiently and stably deliver E6 and E7 genes of HPV into human keratinocytes in order to regulate p53 and study its role in **SM**-induced apoptosis. We therefore focused our efforts on the cloning and expression of antisense constructs that stably express antisense to different isoforms of calmodulin RNA. In the fifth quarter I reported on the cloning of calmodulin 2 and 3 cDNAs into retroviral expression vectors. In the sixth quarter I cloned both calmodulin-like protein (CLP) cDNA as well as the 3' end of the calmodulin 1 gene into the LXSN retroviral expression vector. I have also employed the use of RT-PCR for the analysis and cloning of calmodulin RNA from keratinocytes.

Calmodulin 2 and 3 were the two cDNAs that I first cloned into the retroviral vector LXSN. Calmodulin cDNA was obtained from Dr. Emmanuel Strehler (Children's Hospital Center of Cincinnati), who has cloned most calmodulin and CLP cDNAs. I took advantage of the unique site for Eco RI within the multicloning site of LXSN (**Fig.** 15A). Both calmodulin 3 and calmodulin 2 were cloned into this site. Digestion of the recombinant clones with Eco R1 revealed that the cDNA was inserted, while restriction digestion using wither Xho I, or Hpa I revealed the orientation of these clones with respect to the MMLV LTR promoter (not shown). Thus we have both sense constructs and antisense constructs. The constructs wereused to transfect a packaging cell line in order to produce infectious retroviral particles. These recombinant retroviruses can be used to infect cells, or even live animals in order to generate stable lines of keratinocytes that express antisense to calmodulin. In addition to these clones, we have also cloned the same calmodulin and CLP cDNA inserts into pMAMneo and K1 vectors.

For calmodulin 1, I also utilized the unique site for Eco RI within the multicloning site of LXSN. However, this cloning experiment was slightly more difficult, since there were no convenient compatible restriction sites for either calmodulin 1 and CLP. I thus utilized two different cloning strategies. The CLP cDNA and the calmodulin 1 gene fragment were digested with different restriction enzymes to generate approximately 1 kb fragments. This target size is suitable for antisense inhibition, as we have previously used a 1.1 kb fragment to completely inhibit the expression of mouse poly (ADP-ribose) polymerase. Both CLP and calmodulin 1 were blunt-ended with T4 polymerase, and ligated with Eco R1 linkers. This thus created compatible ends for the ligation ofboth inserts into the Eco R1 site of the LXSN vector in both the sense and antisense orientations . To determine the sense vs. antisense orientation of CLP-containing retrovirus, we digested the recombinant with Xba I, which revealed the presence of 4 antisense clones and one sense clone. For calmodulin 1, recombinant clones were also obtained. A second strategy that we employed is the direct cloning of cDNA using reverse-transcriptase-

mediated polymerase chain reaction (RT-PCR). In this technique, we have derived total mRNA from different keratinocyte cell lines. This RNA is then reverse transcribed to make a complementary DNA (cDNA) pool. Using the appropriate oligonucleotide primers, we then amplified regions of calmodulin 1, 2, 3, or CLP. **Fig.** 9 shows that we have been able to amplify calmodulin 1 cDNA from a total keratinocyte mRNA pool (unlike the other calmodulin cDNAs, calmodulin 1cDNA had not yet been cloned, and was only available as a gene fragment), and we cloned this region into a vector in order to express antisense RNA. We thus derived the cDNA for CaM I, utilizing RT-PCR of mRNA derived from NHEK, and specific primers. This 787 bp CaM I fragment was then ligated into pCR3.1 (Invitrogen). The pCR3.1-CaM I clone was then digested to remove the insert, which was then ligated in the sense and antisense orientation into the retroviral vector, LXSN (Clontech) (**Fig.** 15 B, C). Furthermore, this RT PCR technology clearly works well for the different isoforms of calmodulin RNAs, and can be used to screen cell lines either before or after transfection with antisense clones or retroviruses. The retroviral constructs were transfected into packaging cell lines in order to generate retroviral particles capable of efficient delivery of CAM antisense into human keratinocytes. High-titer viral supernatants from LXSN CaM I antisense constructs were used to transduce NHEK. Although viral titer is high, a 10-day selection in G418 (100 μg/ml medium) ensured that 100% of the cells are expressing CaM antisense RNA. The endogenous level of CaM protein was significantly inhibited by the CaM antisense RNA expression (**Fig.** 16A), as was processing of caspase-3 (**Fig.** 16B), and apoptotic morphology following exposure to **SM**. PARP cleavage was also inhibited (**Fig.** 16C), as was the processing of caspases-8 and -7 into their active forms (**Fig.** 17). This study suggests that inhibition of CaM protects keratinocytes from **SM**-induced apoptosis.

This work directly addresses Tasks 5 and 6, the construction of calmodulin antisense constructs for the generation of keratinocytes for grafting (Task 7), as well as generating transgenic animals (Task 8). The RT-PCR technique described for calmodulin specifically further addresses Task 7, in that it was used for the analysis of expression of calmodulin antisense and sense RNA in stable clones.

What is the mechanism by which CaM induces markers of apoptosis?

Bcl-2 is an anti-apoptotic protein located on the nuclear membrane, ER, and outer mitochondrial membrane. Several Bcl-2-related proteins have been described, including Bcl-xL, and Bcl-w, both of which are anti-apoptotic. In addition, some Bcl-2-related proteins are anti-apoptotic, including Bax, Bak, and BAD. In numerous recent studies, BAD has been implicated as a key player in programmed cell death (Datta et al., 1997; del Peso et al., 1997; Hsu et al., 1997; Scheid and Duronio, 1998; Yang et al., 1995; Zha et al., 1997; Zundel and Giaccia, 1998) and the Ca^{2+} /CaM-regulated protein, calcineurin, has been shown to interact with the Bcl-2 family members (Shibasaki et al., 1997), and to dephosphorylate BAD (Wang et al., 1997). This dephosphorylated form of BAD can interact with Bcl-2 or Bcl-xL and induce apoptosis (Zha et

al., 1997). We also obtained evidence that cam exerts its effects on apoptosis via activation of calcineurin which dephosphorylates BAD, destabilizes mitochondria, and induces apoptosis. This blot shows the dephosphorylation of BAD, which is blocked by the CaM inhibitor W-13, but not its inactive analogue, W-12 (**Fig.** 18, top), although the total levels of BAD protein were not significantly altered (**Fig.** 18, bottom).

Relevance of Research Accomplishments: Part II to Original Hypothesis

As outlined in the SOW tasks 5-8, we designed antisense oligonucleotides as well as retroviral vectors that express antisense to CaM. Furthermore, we were able to inhibit the apoptotic response to SM using these reagents.

Recommended Changes and Future Work Relating to Research Accomplishments: Part II

Future work will further examine the role for CaM in SM-mediated apoptosis. Since we have already established a role for CaM we are looking at downstream targets for therapeutic intervention, including Bad, which becomes dephosphorylated by calcineurin. Thus, inhibitors such as cyclosporin A (which inhibits calcineurin), which has been used clinically as an immunosuppressant, may reduce the response to **SM**.

C.2.7 Task 9

1) Stable keratinocyte cell lines will be grafted onto mice

2) Grafts in C.2.7 (1) will be exposed to **SM** to measure histological and immunocytochemical changes, as defined in c.2.1 and c.2.2 for comparison with effects on control grafts.

3) If **SM** effects can be attenuated, experiments will be undertaken in which animals will be either systemically of topically treated with antisense oligonucleotides to CAM or NB-1.

C.2.8 Task 10:

1) Breeding populations of transgenic mice will be established.

2) Mice will be tested for their ability to lower endogenous levels of CAM and NB1 in the epidermis as determined by methods similar to those used in c.2.7 (2).

Research Accomplishments: Part III

THE ROLE OF THE DEATH RECEPTOR PATHWAY FOR APOPTOSIS IN VIVO

SM induces apoptosis via FADD.

In the first year we focused primarily on caspase-3 in the apoptotic response. In order to further understand the apoptotic response, we have devoted much of our effort to assay for the activation of other key caspases, in particular the "upstream" caspases 8, 9, and 10, and the "executioner" caspases 3, 6, and 7 (**Fig.** 19), since a number of studies for the past several years have shown that the central signaling proteins for many of the pathways that coordinate apoptosis are members of this family of cysteine proteases (named for their preference for aspartate at their substrate cleavage site (Alnemri et al., 1996). Caspases cleave key proteins involved in the structure and integrity of the cell.

Accordingly, during the past two years, I focused on the roles of Ca^{2+}/calmodulin in the modulation of differentiation and apoptosis in epidermal cells, and potentially involved in vesication, as well as the role of the Fas/TNF receptor pathway. I have utilized much of the same technology that I have successfully employed in the first year to answer an essential question- How do Ca^{2+}/calmodulin and the Fas/TNF receptor family alter the apoptotic and differentiation responses in keratinocytes, and can these pathways be modulated to alter **SM** vesication in animal models (and ultimately, in humans)?

In the first year, we showed that **SM** induces both terminal differentiation and apoptosis in human keratinocytes. Further, we have demonstrated that these processes are Ca^{2+} and calmodulin dependent, and involve the activation of caspase-3. These responses may, in part, explain the death and detachment of basal cells of the epidermis that occurs following exposure to **SM**. Additionally, utilizing a combination of techniques including the stable expression of a dominant-negative inhibitor of **FADD**, we have begun to shown the potential role of a Fas/TNF family receptor in mediating the response of human keratinocytes to **SM** (Fig. **19**). Because of the unexpected results we obtained regarding apoptosis as well as differentiation, during the second and third years, I focused on the roles of both calmodulin and FADD in the (premature) induction of differentiation and apoptosis in epidermal cells leading to vesication (grafting experiments are still ongoing).

Accordingly, we further analyzed changes in the expression of apoptotic markers following exposure of primary keratinocytes to **SM**. Consistent with our previous results, we observed a strong activation of caspase-3 activity (detected by the PARP-cleavage assay, the fluorometric assay, and immunoblot analysis as described in Materials and Methods; Appendix). In addition to the activation of caspase-3, we tested whether other caspases within the cascade were similarly activated. We found that there was an early activation of caspase-8 and a later activation of caspases- 3, 6, and 7. Since this is similar to the pattern of caspase activation

following stimulation of the Fas receptor with either Fas ligand or with agonist antibody, we reasoned that **SM** may in fact induce apoptosis via the Fas pathway, or a related receptor within the Fas/TNF receptor family. First, we subjected primary keratinocytes to treatment with an anti-Fas agonist antibody to induce "pure" apoptosis, and compared the response to that of keratinocytes that were treated with **SM**. The response of the keratinocytes to each of these agents was remarkably similar with respect to the time course, dose response and the order of activation of different caspases, including the upstream caspase-8, which is activated by death receptors (**Fig.** 20).

Recent evidence has suggested that certain agents, in particular anticancer drugs, induce apoptosis by up-regulating the levels of Fas receptor, Fas ligand, or both, and experiments have shown that over-expression of either of these proteins can induce apoptosis. In addition, it has been shown that Fas transcription can be up-regulated by p53, which we have shown is rapidly induced in keratinocytes following treatment with **SM**. Thus, we examined the levels of Fas and Fas-ligand following treatment of primary keratinocytes with **SM** utilizing immunoblot analysis employing the antibodies and techniques described above. **Fig.** 21 shows that both Fas and Fas ligand are induced in primary keratinocytes following exposure to **SM**.

In order to determine if **SM** apoptosis was mediated by a death receptor pathway, we transfected keratinocytes with a construct expressing a dominant-negative mutant of FADD (FADD-DN). Upon stimulation of the death receptor, the truncated protein, lacking the N-terminal death effector domain (DED; **Fig.** 22A), occupies the Fas/TNFR binding site (death domain; DD) normally occupied by FADD, but does not transmit the downstream apoptotic signals, and thus acts as an inhibitor to Fas and other death receptor pathways. FADD-DN was stably expressed in several different clones of immortalized human keratinocytes, as determined using an antibody to either FADD or to AU1, which is an epitope tag that was placed on FADD (**Fig.** 22B).

A hallmark of apoptosis in a number of cell types is the appearance of nucleosome sized ladders due to the presence of a Ca^{2+}/Mg^{2+}-dependent endonuclease that is induced in apoptotic cells. Control or FADD-DN cells were then exposed to different concentrations of **SM**, followed by isolation of the DNA. In control keratinocytes, but not those stably transfected with FADD-DN, nucleosome-sized DNA ladders are observed (**Fig.** 23, top). In addition, the cleavage of nuclear lamin by caspase-6 is also inhibited in cells expressing FADD-DN, as determined by immunoblot analysis (**Fig.** 23, bottom).

We then examined the activation of caspase-3 by two different means. The first was by a quantitative fluorometric assay, which measures DEVDase activity, while the second assay is a Western analysis. In both cases, FADD-DN inhibited the apoptotic markers induced by **SM** (**Fig.** 24).

Grafting

In order to study the *in vivo* response of human keratinocytes to different gene products, as well as to topical agents, we have developed a graft system utilizing an immortalized human keratinocyte line, Nco. When these keratinocytes are grafted to the dorsal surface of athymic nude mice, a histologically normal epidermis is formed. In addition, immunocytochemical staining revealed a normal pattern of expression of markers compared to control skin sections derived from normal volunteers. K14 staining is restricted to the proliferating basal layer, while K1 expression is confined to the suprabasal layers of the epidermis. Since the pattern of K1 mRNA and protein expression is altered in cultured keratinocytes by **SM** exposure in a CaM-dependent manner (below), this graft system is being utilized for the *in vivo* studies of the role of CaM and **SM** in K1 expression.

In order to examine the role of FADD *in vivo*, the grafting system was utilized. A grafting chamber was used to graft engineered human keratinocytes to nude mice. The grafted human keratinocytes (parent line from which the FADD-DN clones were derived) form a morphologically normal epidermis. We next determined whether we could detect expression of FADD-DN in the grafted epidermis by using antibodies specific to the AU-1 epitope tag. An AU-1-specific antibody recognized grafted epidermis derived from FADD-DN, but not control keratinocytes (**Fig. 25**, top). Keratin K14 is also expressed normally in the epidermis derived from control or FADD-DN transfectants (**Fig. 25**, bottom). In addition, K1 is expressed normally, indicating that FADD-DN does not interfere with the expression of the differentiation-specific markers in grafted human skin (**Fig. 26**).

Utilizing Nco cells as recipients for transfection, we have thus demonstrated a normal pattern of expression of keratins K1, K14 within the grafted epidermis by immunofluorescence. These differentiation markers were detected employing an immunofluorescent technique, which affords greater sensitivity than Western analysis, and also provides additional information on which cell layers are expressing the marker under each experimental condition. In addition, the K1 antibody recognizes only the human, but not the mouse K1 protein.

The earliest stage of apoptosis is marked by the activation of PARP and the synthesis of poly(ADP-ribose). The requirement for the early synthesis of poly (ADP-ribose) for eventual morphological apoptosis has been shown in several of our recent publications (Rosenthal et al., 1997; Simbulan-Rosenthal et al., 1998). Using this technique on grafted skin sections, we demonstrated that poly(ADP-ribose) can be detected within the epidermis following exposure to **SM**. Following **SM** exposure, we determined if there are differences in the levels of poly(ADP-ribose) in control and FADD-DN grafts (**Fig. 27**, top), using indirect immunofluorescence of sections as described previously (Rosenthal et al., 1997). All exposure times are identical to allow comparisons of relative staining intensities at various times during apoptosis. These techniques for the study of individual cells are useful methods for examining apoptosis in the graft system, putting us in a unique position to examine apoptosis induced by **SM** *in vivo*. In

collaboration with Dana Anderson and Dr. Larry Micheltree (USAMRICD), we found that those grafts expressing FADD-DN are more resistant to vesication (**Fig.** 27, bottom; reproduced below).

Animal	Site	Exposure Time (min)	Pustular Epidermitis	Epidermal Necrosis	Microvesicle (Cleft)	Follicular Involvement
FADD-DN 1	**GRAFT**	6	0	0	0	0
FADD-DN 2	"	6	2	2	1	0
FADD-DN 3	"	8	0	0	0	0
FADD-DN 4	"	8	0	1	0	0
CONTROL1	"	6	0	0	0	0
CONTROL2	"	6	0	0	0	0
CONTROL3	"	8	0	0	2	0
CONTROL4	"	8	2	3	3	0
FADD-DN 1	**HOST**	6	2	4	2	3
FADD-DN 2	"	6	2	3	1	3
FADD-DN 3	"	8	1	2	0	2
FADD-DN 4	"	8	1	4	3	3
CONTROL1	"	6	2	4	2	4
CONTROL2	"	6	0	1	0	1
CONTROL3	"	8	4	1	2	3
CONTROL4	"	8	2	4	3	2

NEW TOOLS FOR DETECTING MARKERS OF APOPTOSIS *IN VIVO* FOR FURTHER STUDIES ON GRAFTED EPIDERMIS

Rosenthal, D. S., Ding, R., Simbulan-Rosenthal, C. M. G., Cherney, B., and Vanek, P. and Smulson, M. E. Detection of DNA breaks in apoptotic cells utilizing the DNA binding domain of poly(ADP-ribose) polymerase with fluorescence microscopy. *Nucleic Acids Research* **27**(7): 1437-1441 (1997).

The DNA binding domain of poly(ADP-ribose)polymerase (PARP) has proved to be a novel, highly sensitive probe for detecting DNA breaks in intact cells undergoing apoptosis. A recombinant peptide spanning the DNA-binding domain of PARP was expressed, purified, and used to detect DNA strand breaks in fixed cells. Fluorescence microscopy with this probe followed by detection with anti-PARP antisera initially revealed an increased binding following treatment of cells with DNA strand-breaking agents (such as MNNG), and subsequently, using biotinylated PARP DBD, during the later stages of apoptosis in several cell systems, when internucleosomal strand breaks become evident. This procedure was found to be at least as

sensitive and required fewer steps to detect DNA strand breaks than those utilizing a Klenow incorporation of biotinylated nucleotides.

Visualization at the level of individual cells allows for the assay of apoptosis. At the single cell level, the study of apoptosis requires morphological examination of cells and nuclei, using chromatin and DNA-specific fluorescent dyes, such as ethidium bromide, bis-benzamide, and DAPI. At the biochemical level, DNA breaks have been detected *in situ* utilizing the free 3'-OH ends of DNA as a substrate for either terminal transferase or the Klenow fragment of DNA pol I to incorporate biotin or digoxigenin, which can be subsequently visualized with either visible of fluorescent dyes.

Many of the currently available methods for examining DNA strand breaks *in situ* rely on the ability of exogenous enzymes such as DNA polymerase or terminal transferase to add labeled dNTPs to the 3'-OH ends of the strand breaks and subsequent detection of the incorporated nucleotides by immunofluorescence microscopy. We reasoned that the DBD of PARP might provide a more sensitive probe for DNA strand breaks that would eliminate the requirement for the often-labile enzymes and nucleotide substrates.

Clone pCD12, containing the full-length cDNA encoding human PARP in an Okayama-Berg vector, was used as a polymerase chain reaction (PCR) template for construction of a PARP DBD expression vector. The PARP cDNA fragment thus amplified encompassed the region that encodes the two zinc fingers of the enzyme as well as the KKKSKK nuclear localization signal. he product was then ligated into the bacterial protein expression vector pQE30 (Qiagen).

The DBD of PARP was subsequently expressed in *E coli*, and purified to more than 95% homogeneity by affinity chromatography using a Ni-NTA column. The PARP DBD fusion protein, but not full-length PARP, was recognized on immunoblot analysis by polyclonal antibodies, obtained subsequently, to this region of PARP (**Fig.** 28, bottom). To establish conditions for detecting DNA strand breaks in fixed mouse cells with the PARP DBD, we first adopted an immunofluorescence approach using anti-human PARP. The antibody used does not react with the murine PARP (Bhatia et al., 1990), even though the amino acid sequences of the proteins are >80% identical. We therefore incubated mouse 3T3 cells for 30 min in the absence or presence of 0.4 mM MNNG to induce a significant number of DNA breaks, after which the cells were fixed on slides, incubated at room temperature with excess purified PARP DBD (25 µg/ml) for 1 h, and washed with phosphate-buffered saline. DBD bound to DNA strand breaks was then detected by incubating the slides with the rabbit antibodies which recognize human PARP DBD followed by Texas red-conjugated goat antibodies to rabbit immunoglobulin IgG. Whereas no immunofluorescence was detected in 3T3 cells not incubated with MNNG, marked immunofluorescence was apparent in cells treated with the alkylating agent. These results indicated the feasibility of using PARP DBD to detect DNA strand breaks in fixed cells.

<u>Use of biotinylated PARP DBD.</u>

To avoid the use of antibodies to detect the PARP DBD bound to the DNA strand breaks, we conjugated the bacterially expressed DBD to biotin so as to allow detection by reaction with horseradish peroxidase-conjugated streptavidin and enhanced chemiluminescence (ECL, Amersham). We first tested the modified DBD detection system in two human B cell lines that are known to undergo apoptosis via endonuclease cleavage of DNA following serum depletion, unlike normal B cells which become quiescent upon serum withdrawal. Apoptosis was induced in either a B cell line immortalized with EBV *in vitro*, or in Burkitt Lymphoma-derived B cells by withdrawal of autocrine growth factor as described. The occurrence of apoptosis was confirmed by a morphology assay using fluorescence microscopy with a mixture of acridine orange and ethidium bromide (data not shown). The cells were then examined by phase-contrast microscopy and by fluorescence microscopy with biotinylated DBD and horseradish peroxidase-conjugated streptavidin. In virtually all instances, only those cells showing the morphological characteristics (cell shrinkage and nuclear condensation) of apoptosis were stained by the biotinylated PARP DBD. The number of stained cells increased with time after autocrine factor withdrawal (**Fig**. 28, top).

We first confirmed that the osteosarcoma cells were undergoing apoptosis, as measured by apopain activity. There was a marked increase in PARP cleavage activity by day 8. We then measured the ability of the PARP DBD to detect DNA breaks at these two time points. In both attached and floating cells, an increase in the binding of PARP DBD was observed in the late stage of apoptosis.

We then tested a well-established assay for DNA strand breaks in apoptotic cells which relies upon the ability of the Klenow fragment of DNA polymerase I to incorporate nucleotides *in situ*. We therefore measured the levels of DNA strand breaks in the fixed cells by incubating the human osteosarcoma cells with Klenow enzyme in the presence of biotinylated nucleotides. In general, the number of osteosarcoma cell nuclei positive for *in situ* nucleotide incorporation also increased with time, consistent with our other assays for apopain activity and DNA strand breaks. However, fewer apoptotic nuclei were detected by the Klenow assay than by the PARP-DBD assay. At day 3, none of the nuclei were stained. By day 6, several nuclei that appeared morphologically apoptotic stained positively for nucleotide incorporation. More nuclei stained positively for strand breaks by day 8, although the proportion of positive cells remained in the minority.

In a comparison with a commonly used system based on Klenow incorporation of biotinylated nucleotides for the detection of DNA strand breaks in fixed cells, our biotinylated DBD method proved at least as sensitive. The differential sensitivity of the two assays may relate to several factors including increased sensitivity of fluorescence. In addition, Klenow incorporation of biotinylated nucleotides only occurs at 5' dsDNA overhangs, but not with ssDNA, dsDNA with 3'-OH overhangs, or dsDNA with blunt ends. On the other hand, the

PARP DBD binds directly to all ssDNA and dsDNA breaks and requires no enzyme catalysis, indicating that this a useful and simple tool for detecting apoptotic DNA breaks *in situ*.

Smulson, M.E., Pang, D., Jung, M., Dimtchev, A., Chasovskikh, S., Spoonde, A., Simbulan-Rosenthal, C., **Rosenthal, D.**, Yakovlev, A., and Dritschilo, A. Irreversible binding of poly(ADP-ribose) polymerase cleavage product to DNA ends revealed by atomic force microscopy: possible role in apoptosis. *Cancer Research*, **58**: 3495-3498 (1998).

As described above, caspase-3 catalyzes the cleavage of PARP into a 24-kDa fragment containing the DNA binding domain (DBD) and an 89-kDa fragment containing the catalytic and automodification domains. These fragments persist in apoptotic cells for up to several days after exposure to ionizing radiation or drugs (10), suggesting that they are not substrates for further proteolytic processing and that they might play a role in the death program. In this study, the interaction of recombinant full-length PARP with plasmid DNA fragments was examined by atomic force microscopy (AFM), which reveals the topography of DNA and proteins at nanometer resolution. . In addition to binding to the DNA fragments, PARP was observed to link the fragments into chainlike structures. Automodification of PARP in the presence of nicotinamide adenine dinucleotide (NAD) resulted in its dissociation from the DNA fragments, which, nevertheless, remained physically aligned. A recombinant 28-kilodalton fragment of PARP containing the DBD but lacking the automodification domain bound to and linked DNA fragments in the absence or presence of NAD. Identical results were obtained on incubation of internucleosomal DNA fragments isolated from apoptotic cells with the products of *in vitro* cleavage of recombinant PARP by purified caspase-3. Our data demonstrate the usefulness of AFM for investigating the interactions of proteins with DNA and provide support for a role for PARP cleavage by caspase-3 in apoptosis. These data suggest that the 24-kilodalton product of PARP cleavage by caspase-3 may contribute to the irreversibility of apoptosis, possibly by blocking the access of DNA repair enzymes to DNA strand breaks.

CELL CYCLE AND DNA REPLICATION

Simbulan-Rosenthal, C. M. G., **Rosenthal, D. S.**, Boulares, A. H., Hickey, R., Malkas, L., Coll, J., and Smulson, M. E. Regulation of the expression or recruitment of components of the DNA synthesome by poly(ADP-ribose). *Biochemistry* **37**(26): 9363-9370 (1998).

Poly(ADP-ribose) polymerase (PARP) is a component of the multiprotein DNA replication complex (MRC, DNA synthesome) that catalyzes replication of viral DNA *in vitro*. PARP poly(ADP-ribosyl)ates 15 of the ~40 proteins of the MRC, including DNA polymerase α (DNA pol α), DNA topoisomerase I (topo I), and proliferating-cell nuclear antigen (PCNA). Although

about equal amounts of MRC-complexed and free forms of PCNA were detected by immunoblot analysis of HeLa cell extracts, only the complexed form was poly(ADP-ribosyl)ated, suggesting that poly(ADP-ribosyl)ation of PCNA may regulate its association with or its function within the MRC. NAD inhibited the activity of DNA pol δ in the MRC in a dose-dependent manner, whereas the PARP inhibitor, 3-AB, reversed this inhibitory effect. The roles of PARP in modulating the composition and enzyme activities of the DNA synthesome were further investigated by characterizing the complex purified from 3T3-L1 cells before and 24 h after induction of a round of DNA replication required for differentiation of these cells; at the latter time point, ~95% of the cells are in S phase and exhibit a transient peak of PARP expression. The MRC was also purified from similarly treated 3T3-L1 cells depleted of PARP by antisense RNA expression; these cells do not undergo DNA replication nor terminal differentiation. Both PARP protein and activity and essentially all of the DNA pol α and δ activities exclusively cosedimented with the MRC fractions from S phase control cells, and were not detected in the MRC fractions from PARP-antisense or uninduced control cells. Immunoblot analysis further revealed that, although PCNA and topo I were present in total extracts from both control and PARP-antisense cells, they were present in the MRC fraction only from induced control cells, indicating that PARP may play a role in their recruitment into the DNA synthesome. In contrast, DNA pol α, DNA primase, and RPA were absent from MRC fractions and total cell extracts of PARP-antisense cells, suggesting that PARP may be involved in the expression of these proteins. Depletion of PARP also prevented induction of the expression of the transcription factor E2F-1, which positively regulates transcription of the DNA pol α and PCNA genes, thus, PARP may be necessary for expression of these genes when quiescent cells are stimulated to proliferate. Note this study shows that PARP regulates expression of E2F1, and E2F1 in turn regulates p53, an important component of the SM-induced apoptotic pathway.

We next investigated the effect of PARP depletion on the abundance of E2F-1, a transcription factor that positively regulates the transcription of several gene products required for DNA replication and cell growth, including DNA pol α, PCNA, dihydrofolate reductase, thymidine kinase, c-MYC, c-MYB, cyclin D, and cyclin E (DeGregori et al., 1995) (Slansky et al., 1993) (Pearson et al., 1991) (Blake and Azizkhan, 1989) (Nevins, 1992). Immunoblot analysis of total cell extracts revealed that, whereas control cells exhibited a marked increase in the expression of E2F-1 as early as 1 h after induction of differentiation, consistent with the fact that the E2F-1 gene is an early-response gene (Johnson et al., 1994), PARP-depleted antisense cells contained negligible amounts of E2F-1 during the 24 h exposure to inducers of differentiation. The induction of both DNA pol α and PCNA in control cells occurred subsequent to that of E2F-1, consistent with their being encoded by late-response genes (Pearson et al., 1991). These results indicate that PARP may regulate the expression of DNA pol α and PCNA genes during early S-phase indirectly by affecting the expression of the transcriptional

factor, E2F-1, which in turn can regulate the transcription of both the DNA pol α and PCNA genes, as well as the E2F-1 gene itself.

Simbulan-Rosenthal, C. M. G., **Rosenthal, D. S.**, Hilz, H., Hickey, R., Malkas, L., Applegren, N., Wu, Y., Bers, G., and Smulson, M. E. The expression of poly(ADP-ribose) polymerase during differentiation-linked DNA replication reveals that this enzyme is a component of the multiprotein DNA replication complex. *Biochemistry.* **35**(36):11622-11633 (1996).

In this paper, we showed that the multireplication complex consists of approximately 40 different proteins including polymerases alpha delta, RPA, RPC, helicase, topoisomerases I and II, DNA ligase, PCNA, PARP, and that many of these proteins are modified by poly(ADP-ribosylation). During the cell cycle, this complex stays intact. However, during a complete withdrawal from the cell cycle, such as occurs during serum starvation, when the cells go into the G0 phase of the cell cycle, the MRC appears to be dissociated, and some of the components of the complex are not present either at the protein or the mRNA level. This appears to be due at least in part due to the absence of stimulation of E2F-1 responsive promoters, including polymerase alpha and E2F-1 itself. Upon restimulation with serum, control cells rapidly upregulated the E2F-1 transcripts and protein, by antisense cells lacking PARP were unable to stimulate E2F-1. These results may relate directly to the finding that these same antisense cells are unable to undergo apoptosis when stimulated with anti-Fas antibody

Relevance of Research Accomplishments: Parts I-III to Original Hypothesis

Keratinocytes respond to Ca^{2+}-signaling pathways in a fashion that makes them unique from other cells, which may explain the exquisite sensitivity of the skin to **SM** vesication. In collaboration with Dr. William Smith and Radharaman Ray at USAMRICD, I found that **SM** induced both the terminal differentiation response as well as the apoptotic response in keratinocytes. Furthermore, upon following up on previous studies by these two investigators in which they showed changes in Ca^{2+} fluxes in keratinocytes following exposure to **SM**, I found, using both chemical inhibitors and antisense oligonucleotides, that Ca^{2+} and calmodulin are important to both of these responses to **SM**, and that these two processes may in part play a role in the vesication response of skin to **SM**. In addition, we have found that the Fas/TNF receptor family also plays an important role in **SM**-induced apoptosis *in vivo*. A scheme of the role of **SM** in keratinocyte differentiation and apoptosis is presented in **Fig.** 29.

Recommended Changes and Future Work Relating to Research Accomplishments: Parts I-III

The roles of Ca^{2+}, calmodulin and Fas/TNF receptor family in the modulation of differentiation and apoptosis in epidermal cells leading to vesication will be further studied. This future work, which utilize much of the same technology that I have successfully employed in the last granting period, is designed to answer an essential question- How do Ca^{2+}, calmodulin and the Fas/TNF receptor family regulate the apoptotic and differentiation responses in keratinocytes, and can these pathways be modulated to alter **SM** vesication in animal models (and ultimately, in humans)?

KEY RESEARCH ACCOMPLISHMENTS

- We found that **SM** induces terminal differentiation and apoptosis.
- Inhibition of calmodulin inhibits both responses.
- Inhibition of the death receptor pathway inhibits apoptosis.
- Inhibiton of apoptosis reduces the vesication response in vivo.

REPORTABLE OUTCOMES

Manuscripts

1. Simbulan-Rosenthal, C. M., Haddad, B. R., **Rosenthal, D. S.**[*], Weaver, Z., Coleman, A., Luo, R., Young, H., Wang, Z.Q., Ried, T., and Smulson, M. E. Chromosomal aberrations in PARP-/- mice: genome stabilization in immortalized cells by reintroduction of PARP cDNA. *Proc. Natl. Acad. Sci. USA* **96**: 13191-13196 (1999). [*] **first three authors contributed equally**

2. **Rosenthal, D. S.**, Simbulan-Rosenthal, C. M, Liu, W.F., and Smulson, M. E. Poly(ADP-ribose) polymerase and Aging. In: *DNA Repair and Aging* (Gilchrest, B. and Bohr, W. (eds.)), in press (2000).

3. **Rosenthal, D. S.**, Simbulan-Rosenthal, C. M., Smith, W., Benton, B., Ray, R., and Smulson, M. E. Poly(ADP-ribose) polymerase is an active participant inprogrammed cell death and maintenance of genomic stability. In: *Cell Death: The Role of PARP* (Szabo, C. (ed.)), in press (2000).

4. Simbulan-Rosenthal, C. M., **Rosenthal, D. S.**, Luo, R., and Smulson, M. E. Poly(ADP-ribose) polymerase upregulates E2F-1 promoter activity and DNA pol α expression during entry into S-phase. Oncogene **18**(36) 5015-5023 (1999).

5. Simbulan-Rosenthal, C. M., **Rosenthal, D. S.**, Smulson, M. E. Poly(ADP-ribosyl)ation of p53 during apoptosis in human osteosarcoma cells. *Cancer Res.* **59**: 2190-2194 (1999).

6. Simbulan-Rosenthal, C. M. G., **Rosenthal, D. S.**, Iyer, S, Yoshihara, K., and Smulson, M. E. Requirement for PARP and poly(ADP-ribosyl)ation in apoptosis and DNA replication. *Mol. Cell. Biochem.* **193**: 137-148 (1999).

7. Simbulan-Rosenthal, C. M., **Rosenthal, D. S.**, and Smulson, M. E. Pleiotropic Roles of Poly(ADP-ribosyl)ation of DNA Binding Proteins. In: *Cell Death: The Role of PARP* (Szabo, C. (ed.)), in press (2000).

8. Stöppler, H., Stöppler, M. C., Johnson, E., Simbulan-Rosenthal, C. M. G., Iyer, S., Smulson, M. E., **Rosenthal, D. S.**[*], and Schlegel, R. The human papillomavirus 16 (HPV-16) E7 protein sensitizes primary human keratinocytes to apoptosis. *Oncogene* **17**: 1207-1214 (1998). ***corresponding author**

9. **Rosenthal, D. S.**, Rosenthal, C. M. G., Iyer, S., Smith, W., Ray, R., and Smulson, M. E. Sulfur mustard induces terminal differentiation and apoptosis in keratinocytes via a Ca^{2+}-calmodulin and apopain-dependent pathway. *J. Invest. Dermatol.* **111**(1): 64-71 (1998).

10. Iyer, S., Chaplin, D., **Rosenthal, D. S.**, Boulares, A. H., Li, L., and Smulson, M. Induction of apoptosis in proliferating human endothelial cells by the tumor-specific anti-angiogenesis agent combretastatin A-4. *Cancer Res.* **58**: 4510-4514 (1998).

11. Simbulan-Rosenthal, C. M. G., **Rosenthal, D. S.**, Iyer, S., Boulares, A. H., and Smulson, M. E. Transient poly(ADP-ribosyl)ation of nuclear proteins and role of poly(ADP-ribose) polymerase in the early stages of apoptosis. *J. Biol. Chem.* **273**(22): 13703-13712 (1998).

12. Simbulan-Rosenthal, C. M. G., **Rosenthal, D. S.**, Boulares, A. H., Hickey, R., Malkas, L., Coll, J., and Smulson, M. E. Regulation of the expression or recruitment of components of the DNA synthesome by poly(ADP-ribose). *Biochemistry* **37**(26): 9363-9370 (1998).

13. Cuvillier, O., **Rosenthal, D. S.**, Smulson, M. E., and Spiegel, S. Sphingosine 1-phosphate inhibits activation of caspases that cleave poly(ADP-ribose) polymerase and lamins during Fas- and ceramide-mediated apoptosis. *J. Biol. Chem.* **273**(5): 2910-2916 (1998).

14. Smulson, M.E., Pang, D., Jung, M., Dimtchev, A., Chasovskikh, S., Spoonde, A., Simbulan-Rosenthal, C., **Rosenthal, D.**, Yakovlev, A., and Dritschilo, A. Irreversible binding of poly(ADP-ribose) polymerase cleavage product to DNA ends revealed by atomic force microscopy: possible role in apoptosis. *Cancer Res.* **58**: 3495-3498 (1998).

15. Simbulan-Rosenthal, C. M., **Rosenthal, D. S.**, Ding, R., Bhatia, K., and Smulson, M. E. Prolongation of the p53 response to DNA strand breaks in cells depleted of PARP by antisense RNA expression. *Biochem. Biophys. Res. Commun.* **253**(3): 864-868 (1998).

16. **Rosenthal, D. S.**, Ding, R., Simbulan-Rosenthal, C. M. G., Cherney, B., and Vanek, P. and Smulson, M. E. Detection of DNA breaks in apoptotic cells utilizing the DNA binding domain of poly(ADP-ribose) polymerase with fluorescence microscopy. *Nucleic Acids Res.* **27**(7):1437-1441 (1997).

17. **Rosenthal, D. S.**, Ding, R., Simbulan-Rosenthal, C. M. G., Vaillancourt, J. P., and Nicholson, D. W. Intact cell evidence for the early synthesis, and subsequent late apopain-mediated suppression of poly(ADP-ribose) during apoptosis. *Exp. Cell Res.* **232**, 313-321 (1997).

18. **Rosenthal, D. S.**, and Smulson, M. E. PARP cleavage and apoptosis. *Bioradiations* **99:** 7-9 (1997)

19. Simbulan-Rosenthal, C. M. G., **Rosenthal, D. S.**, Hilz, H., Hickey, R., Malkas, L., Applegren, N., Wu, Y., Bers, G., and Smulson, M. E. The expression of poly(ADP-ribose) polymerase during differentiation-linked DNA replication reveals that this enzyme is a component of the multiprotein DNA replication complex. *Biochemistry.* **35**(36):11622-11633 (1996).

20. Simbulan-Rosenthal, C. M. G., **Rosenthal, D. S.**, Ding, R., Jackman, J., and Smulson, M. E. Depletion of nuclear poly (ADP-ribose) Polymerase by antisense RNA expression : Influence on genomic stability, chromatin organization, and DNA repair/replication. In: *Prog. Nucleic Acid Res. Mol. Biol.* **55**:135-156 (1996).

21. **Rosenthal, D. S.**, Smith, W. J., and Smulson, M. E. The roles of poly(ADP-ribose)polymerase in apoptosis and sulfur mustard vesication. In: *Proc. Med. Defense Bioscience Rev.* 1045-1054 (1996).

Abstracts

1. **Rosenthal, D.**, Simbulan-Rosenthal, C., Liu, W., Iyer, S., Stoppler, H., Schlegel, R., Smith, W., Ray, R., and Smulson, M. The roles of calmodulin, p53, and FADD in the induction of apoptosis in keratinocytes in response to the alkylating agent sulfur mustard. Proceedings of the American Association for Cancer Research **40**: 225, 90th Annual Meeting, Philadelphia, PA (1999)

2. **Rosenthal, D.**, Simbulan-Rosenthal, C., Boulares, H., Iyer, S., Smith, W., Ray, R., and Smulson, M. The role for apoptosis in the cytotoxic response to key military compounds. 38th Annual Meeting of the Society of Toxicology, New Orleans, LA (1999)

3. Simbulan-Rosenthal, C., **Rosenthal, D. S.**, Iyer, S., Boulares, H., and Smulson, M. Requirement for a transient poly(ADP-ribosyl)ation of p53 and other nuclear proteins at the early stages of apoptosis. Proceedings of the American Association for Cancer Research **40**: 222, 90th Annual Meeting, Philadelphia, PA (1999).

4. Simbulan-Rosenthal, C., **Rosenthal, D. S.**, Iyer, S., Boulares, H., and Smulson, M. Poly(ADP-ribose) polymerase (PARP) upregulates E2F-1 promoter activity during early S-phase. The FASEB Journal **13**(4): A351, Experimental Biology 99 Meeting, Washington DC (1999).

5. **Rosenthal, D. S.**, Simbulan-Rosenthal, C. M., Iyer, S., Smith, W., Ray, R., and Smulson, M. E. Calmodulin, poly(ADP-ribose) polymerase, and p53 are targets for modulating the effects of sulfur mustard. Medical Defense Bioscience Review (1998).

6. **Rosenthal, D. S.**, Iyer, S., Simbulan-Rosenthal, C. M. G., Smith, W., Ray, R., and Smulson, M. E. A Ca^{2+}-calmodulin and caspase-dependent pathway mediates sulfur-mustard induced keratinocyte terminal differentiation and apoptosis. Second Cold Spring Harbor Meeting on Programmed Cell Death, Cold Spring Harbor, N.Y. (1997).

7. Simbulan-Rosenthal, C., **Rosenthal, D.**, Iyer, S., Boulares, H., Yoshihara, K., and Smulson, M. Poly(ADP-ribosyl)ation may regulate the activity of a Ca^{2+}, Mg^{2+}-dependent endonuclease implicated in apoptotic internucleosomal DNA degradation. Second Cold Spring Harbor Meeting on Programmed Cell Death, Cold Spring Harbor, N.Y. (1997).

8. Simbulan-Rosenthal, C., **Rosenthal, D.**, Iyer, S., Yoshihara, K., and Smulson, M. PARP and poly(ADP-ribosyl)ation is required at an early stage in apoptosis in a variety of cell systems. Second Cold Spring Harbor Meeting on Programmed Cell Death, Cold Spring Harbor, N.Y. (1997).

9. **Rosenthal, D. S.**, Iyer, S., Simbulan-Rosenthal, C. M. G., Smith, W., Ray, R., and Smulson, M. E. Sulfur mustard induces terminal differentiation and apoptosis in keratinocytes via a Ca2+-calmodulin and apopain-dependent pathway. Annual meeting of the American Society for Biochemistry and Cell Biology: 17th International Congress of Biochemistry and Molecular Biology. San Francisco, CA. (1997).

10. Simbulan-Rosenthal, C., **Rosenthal, D.**, Hickey, R., Malkas, L., Coll, J., and Smulson, M. Poly(ADP-ribose) polymerase (PARP) is required for the expression or assembly of components of the multiprotein replication complex (MRC). 1997 annual meeting of the American Society for Biochemistry and Cell Biology: 17th International Congress of Biochemistry and Molecular Biology. San Francisco, CA. (1997).

11. Bhat, K. R., Benton, B. J., **Rosenthal, D. S.**, Smulson, M. E., and Ray, R. The role of poly(ADP-ribose) polymerase (PARP) in DNA repair in sulfur mustard exposed normal human epidermal keratinocytes (NHEK). 1997 annual meeting of the American Society for Biochemistry and Cell Biology: 17th International Congress of Biochemistry and Molecular Biology. San Francisco, CA (1997).

12. Simbulan-Rosenthal, C., **Rosenthal, D.**, Hickey, R., Malkas, L., and Smulson, M. Poly(ADP-Ribose) Polymerase (PARP) is a component of the multiprotein DNA replication complex. Proceedings of the eighty-seventh annual meeting of the American Association for Cancer Research, 510. (April 20-24, 1996).

13. **Rosenthal, D.**, Ding, R., Simbulan-Rosenthal, C., Cherney, B., Vaillancourt, J., Nicholson, D., Vanek, P., and Smulson, M. Intact cell evidence for the involvement of poly(ADP-ribose)polymerase in the early stages of apoptosis before undergoing an apopain-mediated proteolysis. Proceedings of the eighty-seventh annual meeting of the American Association for Cancer Research, 602. (April 20-24, 1996).

14. Smulson, M., **Rosenthal, D.**, Nicholson, D., and Ding, R. The role of PARP in HD-induced early stages of necrosis and/or apoptosis in primary skin cultures and molecularly engineered human skin grafts. In: Proceedings of the Medical Defense Bioscience Review 651-652 (1996).

15. Yakovlev, A. G., Knoblach, S. M., **Rosenthal, D.**, Smulson, M., and Faden, A. I. Upregulation of CPP32 cysteine protease associated with apoptosis in rat cortex following traumatic brain injury. 1996 annual meeting of the Society for Neuroscience (1996).

Presentations (Please also see above abstracts)

SM Induction of Keratinocyte Apoptosis, Medical Bioscience Review, Hunt Valley MD, 1999

Symposium on Regulation of Enzyme Activity and Synthesis in Normal and Neoplastic Tissues, Indiana University School of Medicine, Indianapolis, IN, October 4, 1999

CONCLUSIONS

Sulfur mustard (**SM**) causes blisters in the skin through a series of cellular changes that we are beginning to identify. We found a major role for Ca^{2+} and calmodulin in the induction of differentiation in human keratinocytes in response to **SM**. We also obtained the unexpected results that **SM** induces markers of apoptosis, and that this process also proceeds via a Ca^{2+}-calmodulin-dependent pathway. In addition, we found that **SM**-induced apoptosis was also mediated by a FADD-dependent pathway which induces caspase activation. The involvement of such varied molecules as Ca^{2+}, calmodulin, and FADD suggests a complex network involved in **SM**-induced differentiation and apoptosis. However, in our progress to date, we have found that blocking any one of these upstream signals can inhibit terminal differentiation or apoptosis, indicating that these molecular pathways are potential targets for therapeutic intervention. An understanding of the mechanisms for **SM** vesication will hopefully lead to strategies for prevention or treatment of **SM** toxicity. This study, which was performed in fulfillment of the Statement of Work, suggests that inhibition of calmodulin (upstream), or caspase-3 (downstream) may protect the epidermis from **SM**-induced apoptosis. Although the mechanism for their protection has not been described, calmodulin inhibitors have already been used successfully in the treatment of both thermal burns and frostbite (Beitner et al., 1989; Beitner et al., 1989), and may prove effective for **SM** as well, either alone, or in combination with caspase-3 inhibitors. We used antisense oligonucleotide and chemical inhibitors of calmodulin and have successfully attenuated the apoptotic response in cultured cells, and these inhibitors can be used in vivo as well.

Importantly, our initial inhibition experiments indicate that the Ca^{2+}-calmodulin and FADD pathways converge upstream of caspase-3 processing, **since inhibitors of either pathway inhibit SM-induced apoptosis**. Furthermore, since calmodulin inhibitors have been used clinically, and the FADD pathway can be manipulated at the level of a cell surface (Fas/TNF), receptor, these two molecules represent attractive targets for the modulation of the effects of **SM** in humans.

REFERENCES

Agarwal, M., Agarwal, A., Taylor, W., Wang, Z. Q., and Wagner, E. (1997). Defective induction but normal activation and function of p53 in mouse cells lacking PARP. *Oncogene* **15**, 1035-1041.

Alkhatib, H. M., Chen, D. F., Cherney, B., Bhatia, K., Notario, V., Giri, C., Stein, G., Slattery, E., Roeder, R. G., and Smulson, M. E. (1987). Cloning and expression of cDNA for human poly(ADP-ribose) polymerase. *Proc. Natl. Acad. Sci.* **84**, 1224-8.

Beitner, R., Chen-Zion, M., Sofer-Bassukevitz, Y., Morgenstern, H., and Ben-Porat, H. (1989). Treatment of frostbite with the calmodulin antagonists thioridazine and trifluoperazine. *Gen Pharmacol* **20**, 641-6.

Beitner, R., Chen-Zion, M., Sofer-Bassukevitz, Y., Oster, Y., Ben-Porat, H., and Morgenstern, H. (1989). Therapeutic and prophylactic treatment of skin burns with several calmodulin antagonists. *Gen Pharmacol* **20**, 165-73.

Blake, M., and Azizkhan, J. (1989). Transcription factor E2F is required for efficient expression of hamster dihydrofolate-reductase gene in vitro and in vivo. *Mol Cell Biol.* **9**, 4994-5002.

Chakravarthy, B. R., Isaacs, R. J., Morley, P., Durkin, J. P., and Whitfield, J. F. (1995). Stimulation of protein kinase C during calcium-induced keratinocyte differentiation: selective blockade of MARCKS phosphorylation by calmodulin. *J. Biol. Chem.* **270**, 1362-1368.

Datta, S. R., Dudek, H., Tao, X., Masters, S., Fu, H., Gotoh, Y., and Greenberg, M. E. (1997). Akt phosphorylation of BAD couples survival signals to the cell-intrinsic death machinery. *Cell* **91**, 231-41.

DeGregori, J., Kowalik, T., and Nevins, J. (1995). *Mol. Cell Biol.* **15**, 4215-4224.

del Peso, L., Gonzalez-Garcia, M., Page, C., Herrera, R., and Nunez, G. (1997). Interleukin-3-induced phosphorylation of BAD through the protein kinase Akt. *Science* **278**, 687-9.

Dlugosz, A. A., and Yuspa, S. H. (1993). Coordinate changes in gene expression which mark the spinous to granular cell transition in epidermis are regulated by protein kinase C. *J Cell Biol* **120**, 217-25.

Hennings, H., Michael, D., Cheng, C., Steinert, P., Holbrook, K., and Yuspa, S. H. (1980). Calcium regulation of growth and differentiation of mouse epidermal cells in culture. *Cell* **19**, 245-54.

Hockenberry, D., Zutter, M., Hickey, W., Nahm, M., and Korsmeyer, S. J. (1991). Bcl-2 protein is topographically restricted in tissues characterized by apoptotic cell death. *Proc. Natl. Acad. Sci. USA* **88**, 6961-6965.

Hsu, S. Y., Kaipia, A., Zhu, L., and Hsueh, A. J. (1997). Interference of BAD (Bcl-xL/Bcl-2-associated death promoter)-induced apoptosis in mammalian cells by 14-3-3 isoforms and P11. *Mol Endocrinol* **11**, 1858-67.

Huff, C. A., Yuspa, S. H., and Rosenthal, D. (1993). Identification of control elements 3' to the human keratin 1 gene that regulate cell type and differentiation-specific expression. *J Biol Chem* **268**, 377-84.

Johnson, D., Ohtani, K., and Nevins, J. (1994). *Genes & Dev.* **8**, 1514-1525.

Kumari, S., Mendoza-Alvarez, H., and Alvarez-Gonzalez, R. (1997). Poly(ADP-ribosyl)ation of p53 in apoptotic cells following DNA damage. In The 12th International Symposium on ADP-ribosylation reactions (Cancun, Mexico.

Li, L., Tucker, R. W., Hennings, H., and Yuspa, S. (1995). Chelation of intracellular calcium inhibits murine keratinocyte differentiation in vitro. *J. Cell. Physiol.* **163**, 105-114.

Malanga, M., and Althaus, F. (1997). Poly(ADP-ribose): a negative regulator of p53 functions. In The 12th International Symposium on ADP-ribosylation reactions (Cancun, Mexico.

Marthinuss, J., Lawrence, L., and Seiberg, M. (1995). Apoptosis in Pam212, an epidermal keratinocyte cell line: a possible role for bcl-2 in epidermal differentiation. .

McLean, W. H., Eady, R. A., Dopping-Hepenstal, P. J., McMillan, J. R., Leigh, I. M., Navsaria, H. A., Higgins, C., Harper, J. I., Paige, D. G., Morley, S. M., and et al. (1994). Mutations in the rod 1A domain of keratins 1 and 10 in bullous congenital ichthyosiform erythroderma (BCIE). *J Invest Dermatol* **102**, 24-30.

Mol, M. A. E., and Smith, W. (1996). Calcium homeostasis and calcium signalling in sulphur mustard-exposed normal human epidermal keratinocytes. In *Chemico-Biological Interactions* pp. 85-93 Elsevier,

Natoli, G., Ianni, A., Costanzo, A., De Petrillo, G., Ilari, I., Chirillo, P., Balsano, C., and M, L. (1995). Resistance to Fas-mediated apoptosis in human hepatoma cells. *Oncogene* **11**, 1157-1164.

Neamati, N., Fernandez, A., Wright, S., Kiefer, J., and McConkey, D. J. (1995). Degradation of lamin B1 precedes oligonucleosomal DNA fragmentation in apoptotic thymocytes and isolated thymocyte nuclei. *J. Immunology* **154**, 3788-3795.

Nevins, J. (1992). *Science* **258**, 424-429.

Nicholson, D. W., Ali, A., Thornberry, N. A., Vaillancourt, J. P., Ding, C. K., Gallant, M., Gareau, Y., Griffin, P. R., Labelle, M., Lazebnik, Y. A., Munday, N. A., Raju, S. M., Smulson, M. E., Yamin, T. T., Yu, V. L., and Miller, D. K. (1995). Identification and inhibition of the ICE/CED-3 protease necessary for mammalian apoptosis. *Nature* **376**, 37-43.

Nozaki, T., Masutani, M., Nishiyama, E., Shimokawa, T., Wkabayashi, K., and Sugimura, T. (1997). Interactions between poly(ADP-ribose) polymerase and p53. In The 12th International Symposium on ADP-ribosylation reactions (Cancun, Mexico.

Ogasawara, J., Suda, T., and Nagata, S. (1995). Selective apoptosis of CD4+CD8+thymocytes by the anti-Fas antibody. *J. Exp. Med.* **181**, 485-491.

Pearson, B., Nasheuer, H., and Wang, T. (1991). Human DNA polymerase a gene: sequences controlling expression in cycling and serum-stimulated cells. *Mol. Cell Biol.* **11**, 2081-2095.

Ray, R., Benton, B. J., Anderson, D. R., Byers, S. L., Shih, M. L., and Petrali, J. P. (1996). The intracellular free calcium chelator BAPTA prevents sulfur mustard toxicity in cultured normal human epidermal keratinocytes. In *Proc. Med. Defense Biosci. Rev.* pp. 1021-1027 US Army Medical Research Institute of Chemical Defense, Aberdeen Proving Ground.

Ray, R., Legere, R. H., Majerus, B. J., and and Petrali, J. P. (1995). Sulfur mustard-induced increase in intracellular free calcium level and arachidonic acid release from cell membrane. *Toxicology and Applied Pharmacology* **131**, 44-52.

Ray, R., Majerus, B. J., Munavalli, G. S., and Petrali, J. P. (1993). Sulfur mustard-Induced increase in intracellular calcium: A mechanism of mustard toxicity. In U.S. Army Medical Research Bioscience Review (Aberdeen, MD, pp. 267-276.

Robinson, N., La Celle, P., and Eckert, R. (1996). Involucrin is a covalently crosslinked constituent of highly purified epidermal corneocytes: evidence for a common pattern of involucrin crosslinking in vivo and in vitro. *J Invest Dermatol* **107**, 101-7.

Rosenthal, D. S., Chung, S., Steinert, P. M., Huff, C. A., Yuspa, S. H., and Roop, D. R. (1991). The human K1 gene is regulated independently by calcium and retinoids in transgenic mouse keratinocytes. *Cell Growth and Differentiation* **2**, 107-113.

Rosenthal, D. S., Ding, R., Simbulan-Rosenthal, C. M. G., Vaillancourt, J. P., Nicholson, D. W., and Smulson, M. E. (1997). Intact cell evidence fo the early snthesis, and subsequent late apopain-mediated suppression, of poly(ADP-ribose) during apoptosis. *Exp. Cell Res.* **232**, 313-321.

Rosenthal, D. S., Shima, T. B., Celli, G., De Luca, L. M., and Smulson, M. E. (1995). An engineered human skin model using poly(ADP-ribose) polymerase antisense expression shows a reduced response to DNA damage. *J. Invest. Dermatol.* **105**, 38-44.

Rosenthal, D. S., Simbulan-Rosenthal, C. M. G., Liu, W. F., and Smulson, M. E. (2000). SM induces keratin K1 at the level ot transcription. *Manuscript in preparation* .

Rosenthal, D. S., Steinert, P. M., Chung, S., Huff, C. A., Johnson, J., Yuspa, S. H., and Roop, D. R. (1991). A human epidermal differentiation-specific keratin gene is regulated by calcium but not negative modulators of differentiation in transgenic mouse keratinocytes. *Cell Growth Differ* **2**, 107-13.

Scheid, M. P., and Duronio, V. (1998). Dissociation of cytokine-induced phosphorylation of Bad and activation of PKB/akt: involvement of MEK upstream of Bad phosphorylation. *Proc Natl Acad Sci U S A* **95**, 7439-44.

Shibasaki, F., Kondo, E., Akagi, T., and McKeon, F. (1997). Suppression of signalling through transcription factor NF-AT by interactions between calcineurin and Bcl-2. *Nature* **386**, 728-31.

Simbulan-Rosenthal, C. M., Rosenthal, D. S., Iyer, S., Boulares, A. H., and Smulson, M. E. (1998). Transient poly(ADP-ribosyl)ation of nuclear proteins and role for poly(ADP-ribose) polymerase in the early stages of apoptosis. *J. Biol. Chem.* **273**, 13703-13712.

Slansky, J., Li, Y., Kaelin, W., and Farnham, P. (1993). *Mol. Cell Biol.* **13**, 1610-1618.

Stanley, J. R., and Yuspa, S. H. (1983). Specific epidermal protein markers are modulated during calcium-induced terminal differentiation. *J Cell Biol* **96**, 1809-14.

Steinert, P., and Marekov, L. (1997). Direct evidence that involucrin is a major early isopeptide cross-linked component of the keratinocyte cornified cell envelope. *J Biol Chem* **272**, 2021-30.

Stöppler, H., Stöppler, M. C., Johnson, E., Simbulan-Rosenthal, C. M., Smulson, M. E., Iyer, S., Rosenthal, D. S., and Schlegel, R. (1998). The E7 protein of human papillomavirus type 16 sensitizes primary human keratinocytes to apoptosis. *Oncogene* **17**, 1207-1214.

Totpal, K., Singh, S., Lapushin, R., and Aggarwal, B. (1996). Qualitative and quantitative differences in the cellular responses mediated through Fas antigen and TNFR. *J. Interferon Cytokine Res* **16**, 259-267.

Wang, H. G., Mckeon, F., and Reed, J. C. (1997). Dephosphorylation of pro-apoptotic protein Bad by calcineurin results in association with intracellular membranes. In Programmed Cell Death (Cold Spring Harbor, NY.

Wright, S., Kumar, M., Tam, A., Shen, N., Varma, M., and Larrick, J. (1992). Apoptosis and DNA fragmentation precede TNF-induced cytolysis in U937 cells. *J. Cell Biochem.* **48**, 344-355.

Wu, Y., Tewari, M., Cui, S., and Rubin, R. (1996). Activation of IGF-I receptor inhibits TNF-induced cell death. *J. Cell Physiol.* **168**, 499-509.

Yaffe, M., Murthy, S., and Eckert, R. (1993). Evidence that involucrin is a covalently linked constituent of highly purified cultured keratinocyte cornified envelopes. *J Invest Dermatol* **100**, :3-9.

Yang, E., Zha, J., Jockel, J., Boise, L. H., Thompson, C. B., and Korsmeyer, S. J. (1995). Bad, a heterodimeric partner for Bcl-XL and Bcl-2, displaces Bax and promotes cell death. *Cell* **80**, 285-91.

Yuspa, S. H., Kilkenny, A. E., Steinert, P. M., and Roop, D. R. (1989). Expression of murine epidermal differentiation markers is tightly regulated by restricted extracellular calcium concentrations in vitro. *J Cell Biol* **109**, 1207-17.

Zha, J., Harada, H., Osipov, K., Jockel, J., Waksman, G., and Korsmeyer, S. J. (1997). BH3 domain of BAD is required for heterodimerization with BCL-XL and pro-apoptotic activity. *J Biol Chem* **272**, 24101-4.

Zundel, W., and Giaccia, A. (1998). Inhibition of the anti-apoptotic PI(3)K/Akt/Bad pathway by stress. *Genes Dev* **12**, 1941-6.

APPENDICES
See attached

BIBLIOGRAPHY AND PERSONNEL

Bibliography- see above
Personnel:
Dean S. Rosenthal, PI (60% effort)
Wen Fang Liu, Research Technician (100% effort)

Fig. 1 Top
Rosenthal et al.

A Hours after
100 μM SM 0 2 4 8 24

kDa

67 —   ⎯ K1
59 —   ⎯ K10

B Hours after
100 μM SM 0 2 4 8 24

200 —   ⎤ Involucrin (cross-linked)
68 —   ⎦ Involucrin (monomer)

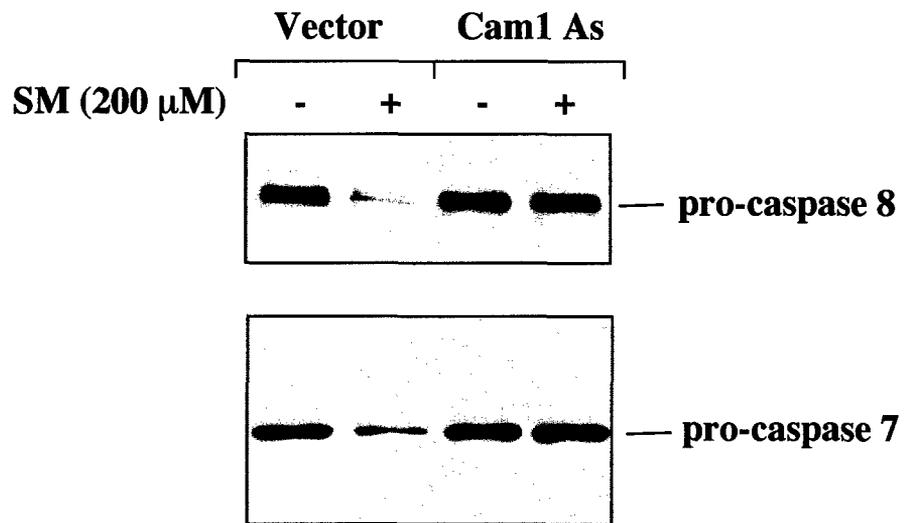**C**   100 μM SM   Control

Hours 0 2 4 8 24   0 2 4 8 24

220 —   ⎤ Fibronectin
94 —   ⎦

Fig. 2 Top
Rosenthal et al.

Fig. 3 Top
Rosenthal et al.

A **Hours after**
100 μM SM   0   2   4   8   24

— p53

B **Hours after**
100 μM SM   0   2   4   8   24
     kD

25 kDa —— —Bcl-2

Fig. 4 Top
Rosenthal et al.

Keratin K1 (644 aa) diagram showing VEID, Putative Caspase-6 cleavage site, Coil Regions, and epitope; Western blot showing NCO treatment with SM (μM): 0, 100, 200, 300, with K1 band and cleavage product.

Fig. 5 Top
Rosenthal et al.

A

Control
SM + BAPTA
100 μM SM
SM + W7 (10 μM)
SM + W7 (50 μM)

67 kDa — — K1

B

kDa
— 203
— 116
— 89

— 52

— 33
— 29

C Hours after
100 μM SM   0   2   4   8   24

17 kDa — — Calmodulin

Fig. 6 Top
Rosenthal et al.

A

B

Fig. 7 Top
Rosenthal et al.

A

SM (300μM)   -   +   +   +

BAPTA(20μM)   -   +

W-7(μM)   0   50

— PARP

— 89 kDa cleavage product

— 24 kDa cleavage product

B

SM (300 μM)   +   +

W-7(μM)   0   50

— CPP32

— p20

— p17 (active)

Fig. 8 Top
Rosenthal et al.

A

M +Cont CaM1 CaM2

Immortalized

B

Control　　　　　　SM

M +Cont CaM1 CaM2 CaM3 CLP CaM1 CaM2 CaM3 CLP

NHEK

Fig. 9 Top
Rosenthal et al.

A

B

Fig. 10 Top
Rosenthal et al.

A

Immuno-
precipitation: _____ **Anti-p53** _____   **C**   **B**

Time (days):   **1**   **2**   **3**   **4**   **7**   **9**   **4**   **4**

p53⟶

Immunoblot: ——————— **Anti-PAR** ———————

B

Immuno-
precipitation: _____ **Anti-p53** _____   **C**   **B**

Time (days):   **1**   **2**   **3**   **4**   **7**   **9**   **4**   **4**

p53⟶

Immunoblot: ——————— **Anti-p53** ———————

Fig. 11 Top
Rosenthal et al.

Fig. 12 Top
Rosenthal et al.

Fig. 13 Top
Rosenthal et al.

A

B

C

D

E

Fig. 14 Top
Rosenthal et al.

A

CaM3 CaM1 CaM1

kDa   AS   NS   AS

20 — ▬▬▬▬▬▬▬▬▬ — Calmodulin

7 —

B

Control   300 μM SM

CaM1   AS   NS   AS   NS

═══ PARP
═══ 89 kDa
Cleavage
product

C

Control   300 μM SM

CaM1   AS   NS   AS   NS

▬▬▬▬▬▬▬▬▬ — Pro-caspase-3

— p17

Fig. 15 Top
Rosenthal et al.

A

Hpa`(~1650)
123
Xba1
605
Xba1
229
Bam H1 (1660)

pLXSN
5.9 kb

MCS

EcoR1

B

Clones 1 2 3 4 5 6 7 9 10 11

← LXSN
vector
(6070 bp)

← AS insert
(787 bp)

CaM 1 AS Clones in LXSN Retroviral Vector
Eco R1 digest to confirm positive clones

C

Clones 3 6 7 9 10 11

Xba 1 Fragments:

← LXSN + 123 bp 3' end
of insert + 50 (4.5 Kb)

← LXSN + 229 bp 5' end
of insert+ 50 (1.78 Kb)

← middle part of
AS insert (0.6 Kb)
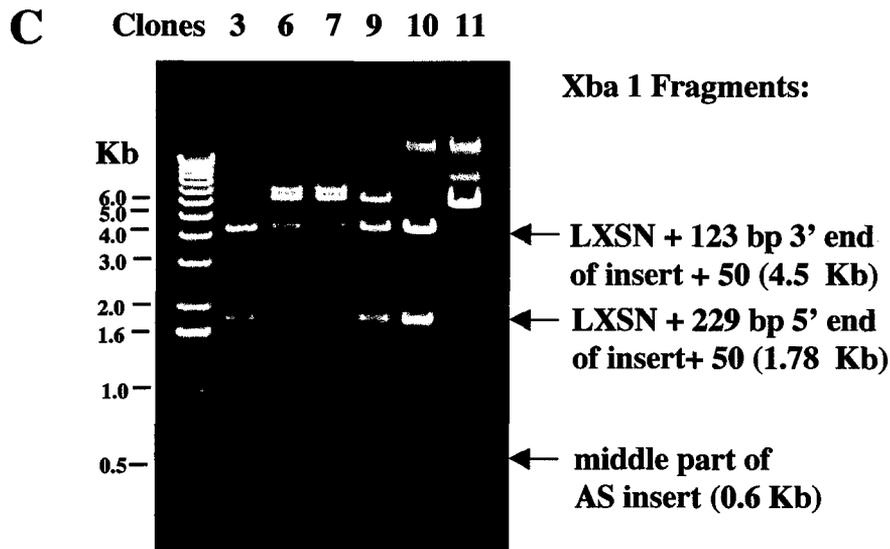
CaM 1 AS Clones in LXSN Retroviral Vector
Xba 1 digest to confirm orientation of insert

Fig. 16 Top
Rosenthal et al.

Calmodulin (17 kDa), pro-caspase 3, p17, PARP, 89 kDa cleavage product

Fig. 17 Top
Rosenthal et al.

Fig. 18 Top
Rosenthal et al.

| 0 | 24 | | 8 | | 24 | Hours after SM |
| - | - | W-12 | W-13 | W-12 | W-13 | Inhibitors |

← Phospho-Bad

← Bad

Fig. 19 Top
Rosenthal et al.

SM

Fas L

Ca²⁺-CAM

Calcineurin, (CAM Kinases II, IV)

BAD:Bcl2

Cytochrome c

Caspases-9, (8?)

Caspases-3,7

Caspase-6

PARP	Inactive	Lamin A	Inactive
Rb	Cleavage	Lamin B1	
PKC∂	Products		
K1?			

Apoptosis

Fas

FADD

Caspase-8

Caspases-3,7

Caspase-6

PARP	Inactive	Lamin A	Inactive
Rb	Cleavage	Lamin	Cleavage
PKC∂	e	B1	Products
DNA-PK	Products		
Keratin			
K1?	Morphological,	Nuclear	
	Biochemical	Breakdown	
	Apoptosis		

FIGURE 1: Two related pathways for SM-induced apoptosis

Fig. 20 Top
Rosenthal et al.

NCO

SM (µM) :	0	100	200	300

kDa

200 –

116 –

82 –

50 – — Caspase-8 (FLICE) proenzyme

33 –

29 –

20 –

Fig. 21 Top
Rosenthal et al.

NCO

SM (µM) :   0 100 200 300

kDa

50–

33–   — Fas

29–

33–   — Fas L

29–

Fas + CHX   **SM**
(µM Fas)   **(µM)**

0 100 200 500   0   100 200 300

200–
116–   –**PARP**
82–

50–   **89 kDa cleavage**
                                        product

In vivo **PARP cleavage**

Fig. 22 Top
Rosenthal et al.

A

Modulating the Fas-Activated "Death Domain" (FADD) by Utilizing a Dominant-negative Approach

UPSTREAM SIGNALS
(FAS, TNFR, DR3)

Death Effector Domain (DED)	Death Domain (DD)	

N   FADD (24 kDa)   C

Death Domain (DD)	

DOWNSTREAM SIGNALS   FADD-DN (16 kDa)
(CASPASES)

B

FADD-DN CLONES NCO FADD NCO

kDa	DN3	6	10	11	16	DN3
114 —						
82 —						
48 —						
33 —						← FADD
29 —						← FADD-DN
20 —						

Anti-FADD   Anti-AU1

Fig. 23 Top
Rosenthal et al.

SM (μM) : 0 50 100 200 300   0   50 100 200 300

bp

1000—
800—
600—
400—

Internucleosomal DNA fragmentation

SM (μM) :   0 100 200 300   0 100 200 300

kDa
200—

116—
82—
50—   — Lamin

33—   — cleavage
29—   product

Lamin B1 Cleavage

Fig. 24 Top
Rosenthal et al.

Caspase-3 Activation

Caspase-3 Processing

Fig. 25 Top
Rosenthal et al.

AU1-Tagged FADD-DN

Human K14 in Grafted Skin

Fig. 26 Top
Rosenthal et al.
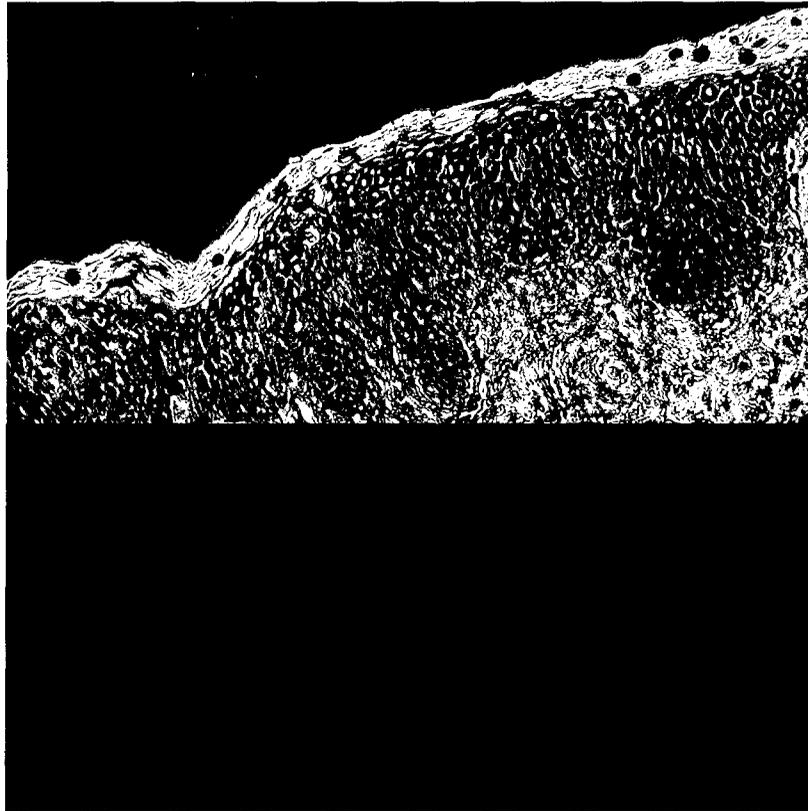
Human K1 in Human Skin

Human K1 in FADD-DN Graft

Fig. 27 Top
Rosenthal et al.
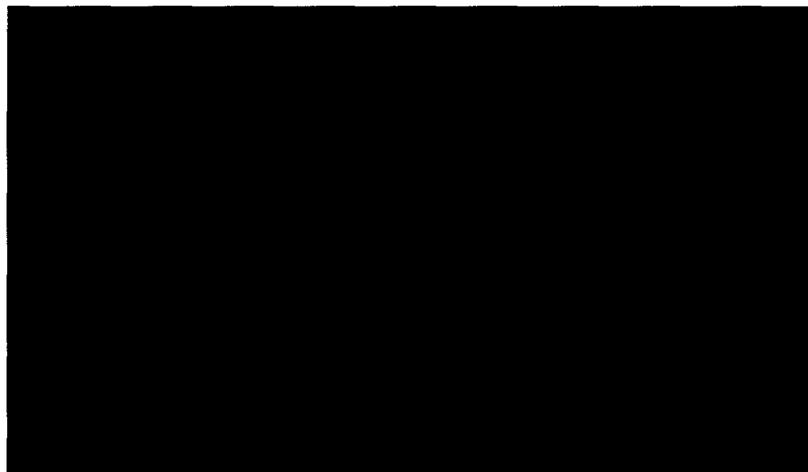
Human Keratinocytes Grafted onto Athymic Mice Form Normal Skin

PAR, an Early Marker of Apoptosis/Damage is Detected *in vivo* in SM-exposed Grafts

Grafted Cells

Human Skin

Untreated

Treated

Animal	Site	Exposure Time (min)	Pustular Epidermitis	Epidermal Necrosis	Microvesicle (Cleft)	Follicular Involvement
FADD-DN 1	GRAFT	6	0	0	0	0
FADD-DN 2	"	6	2	2	1	0
FADD-DN 3	"	8	0	0	0	0
FADD-DN 4	"	8	0	1	0	0
CONTROL1	"	6	0	0	0	0
CONTROL2	"	6	0	0	0	0
CONTROL3	"	8	0	0	2	0
CONTROL4	"	8	2	3	3	0
FADD-DN 1	HOST	6	2	4	2	3
FADD-DN 2	"	6	2	3	1	3
FADD-DN 3	"	8	1	2	0	2
FADD-DN 4	"	8	1	4	3	3
CONTROL1	"	6	2	4	2	4
CONTROL2	"	6	0	1	0	1
CONTROL3	"	8	4	1	2	3
CONTROL4	"	8	2	4	3	2

Fig. 28 Top
Rosenthal et al.

A   Phase contrast

B   PARP DBD fluorescence

Day one

C

D

Day three

E   Anti-PARP

F   Anti-DBD

Fig. 29 Top
Rosenthal et al.

Apoptosis

Differentiation

Prolongation of the p53 Response to DNA Strand Breaks in Cells Depleted of PARP by Antisense RNA Expression

Cynthia M. Simbulan-Rosenthal, Dean S. Rosenthal, Ruchuang Ding,
Kishor Bhatia, and Mark E. Smulson

Department of Biochemistry and Molecular Biology, Georgetown University School of Medicine, Washington, DC 20007

The observation that 3-aminobenzamide, which inhibits a variety of ADP-ribose transferases, prolongs the γ-irradiation-induced increase in intracellular p53 concentration suggested that one or more of such enzymes may determine the duration of the p53 response during G1 arrest. The role of poly(ADP-ribose) polymerase (PARP), an abundant nuclear enzyme activated by DNA strand breaks, in the p53 response to γ-irradiation was investigated in Burkitt's lymphoma AG876 cells stably transfected with an inducible PARP antisense construct. Immunoblot analysis revealed that the cellular content of PARP was reduced to virtually undetectable levels after incubation of transfected cells for 72 h with the inducer dexamethasone. In noninduced antisense cells, the p53 concentration reached a maximum 2 h after exposure to 6.3 Gy of γ-radiation and returned to control values by 4 h. In contrast, the p53 response in PARP-depleted antisense cells peaked at 4 h, with the levels of p53 remaining elevated for up to 12 h after γ-irradiation. The maximal increase in p53 concentration was similar in both induced and noninduced cells. These results thus indicate that PARP activity, in part, determines the duration, but not the magnitude, of the p53 response to DNA damage. © 1998 Academic Press

The tumor suppressor gene p53 encodes a nuclear phosphoprotein that presumably reduces the occurrence of mutations by either promoting cell cycle arrest in G1 or inducing apoptosis in cells that have accumulated substantial DNA damage (1–4); the arrest allows time for the cells to repair the DNA before proceeding in S-phase. Repair of DNA damage caused by γ-irradiation is usually complete within 1 h, at about the same time that the intracellular p53 concentration peaks before returning to control values. Treatment of cells with the nicotinamide analog 3-aminobenzamide (3-AB), an inhibitor of various ADP-ribose transferases including poly(ADP-ribose) polymerase (PARP) (5),

markedly prolongs the p53 response in γ-irradiated cells (6). Although many of the biological functions of PARP have been studied in cells treated with inhibitors such as 3-AB, these compounds lack specificity. In addition to their inhibitory effects on several cytoplasmic mono(ADP-ribosyl)ation reactions that require NAD and involve GTP-binding proteins (7, 8), these inhibitors markedly affect diverse metabolic reactions unrelated to (ADP-ribosyl)ation (9). Thus, whether the prolonged p53 response to γ-irradiation in 3-AB-treated cells is attributable to specific inhibition of PARP remains unclear.

One of the earliest nuclear events that follows DNA strand breakage during DNA replication, or during DNA repair in response to exposure of cells to such agents as γ-irradiation, carcinogens, free radicals, or alkylating agents, is the poly(ADP-ribosyl)ation of various proteins that are predominantly localized adjacent to the DNA strand breaks (10, 11). The doses of ultraviolet or γ-radiation or of alkylating agents that are used experimentally to induce G1 arrest and concomitant accumulation of p53 are similar to those that induce a rapid synthesis of long chains of poly(ADP-ribose) (PAR) covalently attached to various nuclear protein acceptors. PARP catalyzes the poly(ADP-ribosyl)ation of nuclear proteins only when bound to single- or double-stranded ends of DNA (12–14). Indeed, PARP cycles on and off the ends of DNA during DNA repair *in vitro* (15, 16). In addition to undergoing automodification, PARP catalyzes the poly(ADP-ribosyl)ation of such nuclear proteins as histones, topoisomerases I and II (17), SV40 large T antigen (18), DNA polymerase α, and proliferating cell nuclear antigen (PCNA) (19), all of which play a role in reactions involving DNA strand breaks. The poly(ADP-ribosyl)ation of nucleosomal proteins also alters the nucleosomal structure of DNA containing strand breaks and thereby, promotes the access of various replicative and repair enzymes to these sites (20, 21).

To clarify the role of PARP in the accumulation of p53 induced by DNA damage, in the absence of poten-

BIOCHEMICAL AND BIOPHYSICAL RESEARCH COMMUNICATIONS

tially nonspecific PARP inhibitors, we have now established and characterized a Burkitt's lymphoma cell line that both undergoes this response (3) and contains a stably integrated PARP antisense construct under the control of glucocorticoid-responsive promoter.

MATERIALS AND METHODS

Cell culture. The Burkitt's lymphoma cell line AG876 was maintained in RPMI 1640 medium (Mediatech) supplemented with 15% fetal bovine serum, 2 mM L-glutamine, penicillin (50 U/ml), and streptomycin (50 μg/ml). Cell cultures were maintained as exponentially growing cells in a humidified 5% CO2 incubator.

Transfection of Burkitt's lymphoma cell line AG876 with an inducible PARP antisense construct. A 3.9-kb human cDNA fragment encoding full-length PARP was subcloned previously in the antisense orientation into the expression vector pMAMneo (Clontech), under the control of the mouse mammary tumor virus promoter (Fig. 1). Burkitt's lymphoma AG876 cells, which have previously been shown to accumulate p53 in response to γ-radiation (3), were transfected with the pMAMneo containing PARP antisense construct or the empty vector by electroporation, with conditions optimized for this cell line. 10^7 cells were suspended in Hank's balanced salt solution containing 10 to 20 μg of DNA, and were exposed to pulses of 250 volts at 250 μF. Electroporated cells were allowed to grow without selection for 24 to 48 h, and were then maintained in RPMI 1640 supplemented with 15% charcoal-treated fetal bovine serum (Gibco), 2 mM L-glutamine, penicillin (50 U/ml), streptomycin (50 μg/ml), and G-418 (1.6 mg/ml).

Induction of PARP antisense RNA expression and irradiation of cells. Expression of PARP antisense RNA was induced by addition of 1 μM dexamethasone (Sigma) to the culture medium for up to 72 h. Exponentially growing cultures were exposed to 6.3 Gy of γ-radiation with a ^{137}Cs irradiator at a dose rate of 5.25 Gy/min.

PARP activity assays. At various indicated times after exposure to 1 μM dexamethasone, control and PARP-antisense cells were harvested and washed with ice-cold PBS. Samples were assayed for PARP activity by incorporation of [^{32}P]NAD into acid-insoluble acceptors at 25°C for 1 min, with 20 μg protein per determination and triplicate determinations per treatment as previously described (22).

Immunoblot analysis with antibodies to PARP or p53. SDS–polyacrylamide gel electrophoresis and protein transfer to nitrocellulose membranes were performed according to standard procedures. Membranes were stained with Ponceau S (0.1%) to confirm equal loading and transfer. After blocking of nonspecific sites, the blots were incubated with rabbit polyclonal antibodies to PARP (1:2000 dilution) (23) or to monoclonal antibodies to p53 (Ab-6, Calbiochem) and then detected with appropriate peroxidase-labeled secondary antibodies (1:3000 dilution) and enhanced chemiluminescence (ECL, Pierce).

RESULTS

Depletion of PARP protein by antisense RNA expression. The Burkitt's cell line AG876 was stably transfected with a vector containing human PARP cDNA in the antisense orientation under the control of a dexamethasone-responsive promoter (Fig. 1). Previous studies with HeLa cells (24, 25) and immortalized human keratinocytes (26) showed this construct to be effective in depleting cells of PARP protein and activity to concentrations of <5% of control values. Eighteen antisense and four control G-418 resistant colonies

PARP cDNA
(Antisense Orientation)
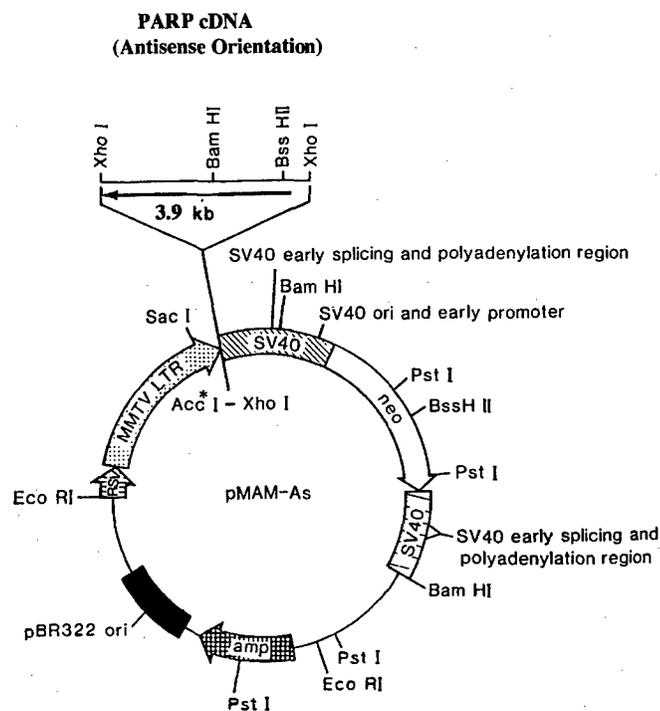
FIG. 1. Structure and restriction sites of the pMAM-As plasmids containing human PARP cDNA in the antisense orientation. The expression vector contains the dexamethasone-inducible MMTV promoter ligated to a reverse orientation of 3.9-kb human PARP cDNA comprising the entire PARP untranslated and translated regions as described previously. The PARP sequence is flanked downstream by the SV-40 early splicing and polyadenylylation regions and a transcription start site within the MMTV LTR is located 260 bp upstream of the cloning site. The entire expression plasmid is 12.2 kb.

were isolated and screened for PARP depletion after incubation with dexamethasone (1 μM) for 72 h; the half-life of PARP protein is estimated to be ~18 h in exponentially growing HeLa cells (27) and PARP antisense RNA expression for up to 72 h is required for maximal depletion of PARP (24–26). Burkitt's lymphoma antisense clone AG876-7 (AS-7) was selected for further analysis on the basis of depletion of PARP protein by immunoblot analysis with antibodies to PARP. Immunoblot analysis revealed that clone AS-7 showed almost complete depletion of PARP protein after incubation with dexamethasone for 72 h, whereas such treatment had no effect on the amount of PARP in control cells (transfected with the empty vector); incubation of AS-7 cells for 72 h in the absence of dexamethasone also had no effect on PARP concentration (Fig. 2). Densitometric analysis showed that the amount of PARP was reduced by ~98% in the induced antisense cells.

Inhibition of PARP activity by antisense RNA expression. To confirm whether the depletion of immunologically detectable PARP corresponds to a decrease in the levels of endogenous PARP activity, enzyme assays were performed on sonicated extracts of control and

Control Antisense

Dexamethasone: - + - +
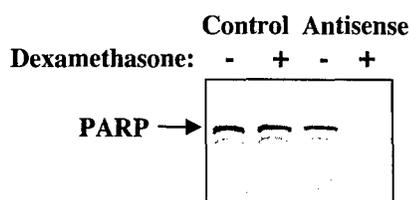
PARP →

FIG. 2. Effect of dexamethasone induction of PARP antisense RNA expression on PARP protein concentration in control and AS-7 Burkitt's lymphoma cells. Transfected control and antisense AS-7 cells were incubated in the absence (−) or presence (+) of dexamethasone (1 μM) for 72 h, after which cell lysates were prepared and subjected to immunoblot analysis with antibodies to PARP. The arrow at 116 kDa indicates the position of human PARP.

A

(−) Dex

p53 →

Time after
γ-irradiation (h): 0 0.5 2 4 6

(+) Dex

p53 →

Time after
γ-irradiation (h): 0 0.5 2 4 6

B

FIG. 3. Effect of depletion of PARP on p53 accumulation in response to γ-irradiation. (A) AS-7 cells were incubated for 72 h in the absence (top) or presence (bottom) of 1 μM dexamethasone, exposed to 6.3 Gy of γ-radiation, and, after incubation for the indicated times, subjected to immunoblot analysis with antibodies to p53. (B) The amount of p53 in noninduced (open squares) and PARP-depleted (closed circles) AS-7 cells was quantitated by densitometry. The densities of the p53 bands at the various incubation times were expressed relative to that of the corresponding p53 band of cells immediately after γ-irradiation (time 0).

antisense cells at various times after induction with dexamethasone. Consistent with the immunoblot analysis, endogenous PARP activity decreased by 55% in Burkitt AG876-AS-7 cells after 48 h after induction with 1 μM dexamethasone, with a maximal reduction in activity of nearly 100% by 72 h (Table 1). In contrast, uninduced antisense cells or control cells treated with dexamethasone for the same time periods exhibited no reduction in PARP activity.

Effect of PARP depletion on p53 accumulation in response to DNA strand breaks. Ionizing radiation induces rapid p53 accumulation in AG876 cells (3). AS-7 cells that had been incubated in the absence or presence of dexamethasone (1 μM) for 72 h were exposed to 6.3 Gy of γ-radiation and, after incubation for various times, subjected to immunoblot analysis with antibodies to p53. For cells preincubated in the absence of dexamethasone, p53 concentration showed a marked increase 30 min after γ-irradiation, peaked at 2 h, and returned to control values by 4 h (Fig. 3). The p53

TABLE 1

Effects of Antisense RNA Expression on Endogenous PARP Activity in Antisense Burkitt AG876 Cells[a]

Time after dexamethasone induction (h)	Endogenous PARP activity (% activity relative to uninduced cells)	
	Control	Antisense
0	~100	100
48	~100	45
72	~100	5

[a] Burkitt AG876 cells transfected with either vector alone (control) or PARP antisense constructs were induced with 1 μM dexamethasone for the indicated time periods and sonicated, and PARP activity assays were performed on cell extracts by measurement of [^{32}P]NAD incorporation into acid-insoluble acceptors at 25°C for 1 min, with triplicate determinations per time point. PARP activity of uninduced cells was taken as 100%, and PARP activity of treated cells was calculated relative to this value. Similar results were obtained in two independent experiments.

concentration in AS-7 cells depleted of PARP by preincubation with dexamethasone also increased after γ-irradiation. However, whereas the magnitude of the maximal increase was similar in induced and noninduced cells, the p53 concentration peaked later, at 4 h, and remained elevated for 6 to 12 h after γ-irradiation in the induced cells.

Since the exposure times were different in the two immunoblots in Fig. 3, densitometric analysis of the immunoblots was normalized by expressing the densities of the p53 bands at the various incubation times relative to that of the corresponding p53 band in cells immediately after γ-irradiation (time 0). The extent and kinetics of p53 accumulation was compared in noninduced antisense cells and in cells depleted of

PARP (Fig. 3B). In both cases, p53 concentration relative to levels prior to γ-irradiation was about 1.8-fold. The major difference in the p53 levels is apparent when the levels of p53 between the induced and non-induced cells are compared at late periods into the experiment. In noninduced antisense cells, p53 accumulation peaked ~2 h after treatment with 6.3 Gy of γ-radiation and decreased thereafter; whereas in PARP-depleted cells, p53 accumulation maximized ~4 h after irradiation and remained elevated for 6 h. The levels of p53 were still elevated at 12 h post irradiation in antisense cells (data not shown). Thus, depletion of PARP did not affect the magnitude of the p53 response, but rather prolonged the accumulation of this protein, presumably by a direct or indirect effect on its synthesis or degradation.

DISCUSSION

Both PARP activity and p53 accumulation are induced by DNA damage, and both proteins have been implicated in the normal cellular responses to such damage. Whereas PAR synthesis increases within seconds after induction of DNA strand breaks (28), the amount of wild-type p53, which is usually low because of the short half-life (20 min) of the protein and remains constant due to a balance between protein synthesis and degradation, increases several hours after DNA damage as a result of reduced degradation (29, 30). A functional association of PARP and p53 has recently been suggested by coimmunoprecipitation of each protein *in vitro* by antibodies to the other (31, 32). Furthermore, inhibition of PARP activity with a specific inhibitor 1,5-dihydroxy isoquinoline prior to γ-irradiation of cells suppresses the DNA binding activity of p53 and consequent expression of p53 target genes, such as those encoding p21 and MDM2 (32).

Our observation that PARP depletion by induction of PARP antisense RNA expression prolongs the p53 response to DNA damage is consistent with previous results showing that the PARP inhibitor 3-AB induces a delay of up to 5 h in the repair of DNA strand breaks and prolongs the p53 response by a similar extent in cells exposed to γ-irradiation (6). Our results thus confirm that the effect of 3-AB on the p53 response is indeed attributable to specific inhibition of PARP activity. We have also previously shown that of PARP depletion by antisense RNA expression reduces the survival of HeLa cells after exposure to methyl methane sulfonate or nitrogen mustard (25, 33). Both the overall repair of methyl methane sulfonate-induced DNA damage (25) and the preferential repair of the dihydrofolate reductase gene (33) are also delayed in these cells. The signaling mechanism(s) by which p53 accumulation occurs in response to DNA damage and how it is turned off following repair remain to be clarified. The prolonged accumulation of p53 in cells depleted of PARP by antisense RNA expression may be correlated with delayed DNA strand break rejoining in these cells and, consequently, delayed repair of DNA strand breaks.

Exposure of human cell lines expressing wild-type p53 to various DNA-damaging agents that also stimulate PAR synthesis (including ionizing radiation, bleomycin, and DNA topoisomerase-targeting drugs) results in a rapid increase in the intracellular concentration of p53 (34). Chinese hamster cells that are unable to synthesize PAR because of unavailability of NAD show a marked decrease in baseline p53 concentration and activity, and they fail to exhibit a p53 response and to undergo apoptosis in response to DNA-damaging agents (35). Moreover, compared with wild-type cells, primary fibroblasts from PARP−/− mice express lower constitutive levels of p53 protein and exhibit a defective p53 response to DNA damage (36), indicating that PARP-dependent signaling may influence the synthesis or degradation of p53 in response to DNA damage. In agreement with our results, exposure of primary splenocytes derived from PARP knockout mice to MNU show elevated p53 induction presumably associated with a lack of and/or delay in DNA repair (37). Consequently, these PARP knockout mice also exhibit extreme sensitivity to γ-irradiation and MNU (37). Thus, specific PARP inhibitors or antisense oligomers could be useful as chemo- or radio- potentiation agents for cancer therapy and a number of pharmaceutical companies have in the past and are currently targeting PARP for drug development (38). PARP antisense oligomers added extraneously to cells, have been shown to be capable of reducing endogenous PARP levels by up to 60%, prior to exposure to γ-irradiation (Vicente Notario, Georgetown University Medical Center, personal communication), but whether this has any effect on the sensitivity of the cells to γ-irradiation is still under study.

ACKNOWLEDGMENTS

REFERENCES

1. Kastan, M. B., Zhan, Q., El-Delry, W., S., Carrier, F., Jacks, T., Walsh, W. V., Plunkett, B., S., Vogelstein, B., and Fornace, A. J. J. (1992) *Cell* **71**, 587–597.

2. Lane, D. P. (1992) *Nature* **358**, 15–16.

3. O'Connor, P. M., Jackman, J., Jondle, D., Bhatia, K., Magrath, I., and Kohn, K. W. (1993) *Cancer Res.* **53**, 4776–4780.

4. Chowdary, D., R., Dermody, J. J., Jha, K. K., and Ozer, H. L. (1994) *Mol. Cell. Biol.* **14**(3), 1997–2003.

5. Banasik, M., and Ueda, K. (1994) *Mol. Cell. Biochem.* **138,** 185–197.

6. Lu, X., and Lane, D. P. (1993) *Cell* **75,** 1–20.

7. Moss, J., Stanley, S. J., and Watkins, P. (1980) *J. Biol. Chem.* **255,** 5838–5840.

8. Rankin, P. W., Jacobson, E. L., Benjamin, R. C., Moss, J., and Jacobson, M. K. (1989) *J. Biol. Chem.* **264,** 4312–4317.

9. Milam, K. M., and Cleaver, J. E. (1984) *Science* **223,** 589–591.

10. Jacobson, M. K., and Jacobson, E. L. (1989) *in* ADP-Ribose Transfer Reactions: Mechanisms and Biological Significance (Jacobson, M. K., and Jacobson, E. L., Eds.), 1st ed., Springer-Verlag, New York.

11. Poirier, G., and Moreau, P. (Eds.) (1992) *in* ADP-Ribosylation Reactions, Vol. I, 1st ed., Springer-Verlag, New York.

12. Malik, N., Miwa, M., Sugimura, T., Thraves, P., and Smulson, M. (1983) *Proc. Natl. Acad. Sci. USA* **80**(9), 2554–2558.

13. Thraves, P. J., Kasid, U., and Smulson, M. E. (1985) *Cancer Res.* **45**(1), 386–391.

14. Gradwohl, G., Menissier de-Murcia, J. M., Lolinete, M., Simonin, F., Koken, M., Hoeijimakers, J. H., and de Murcia, G. (1990) *Proc. Natl. Acad. Sci. USA* **87,** 2990–2994.

15. Satoh, M. S., and Lindahl, T. (1992) *Nature* **356**(6367), 356–358.

16. Satoh, M. S., Poirier, G. G., and Lindahl, T. (1993) *J. Biol. Chem.* **268**(8), 5480–5487.

17. Kasid, U. N., Halligan, B., Liu, L. F., Dritschilo, A., and Smulson, M. (1989) *J. Biol. Chem.* **264**(31), 18687–18692.

18. Baksi, K., Alkhatib, H., and Smulson, M. E. (1987) *Exp. Cell Res.* **172,** 110–123.

19. Simbulan-Rosenthal, C. M. G., Rosenthal, D. S., Hilz, H., Hickey, R., Malkas, L., Applegren, N., Wu, Y., Bers, G., and Smulson, M. (1996) *Biochemistry* **35**(36), 11622–11633.

20. Butt, T. R., and Smulson, M. E. (1980) *Biochemistry* **19,** 5235–5243.

21. Poirier, G. G., de Murcia, G., Jongstra-Bilen, J., Niedergang, C., and Mandel, P. (1982) *Proc. Natl. Acad. Sci. USA* **79,** 3423–3427.

22. Smulson, M. E., Kang, V. H., Ntambi, J. M., Rosenthal, D. S., Ding, R., and Simbulan, C. M. G. (1995) *J. Biol. Chem.* **270**(1), 119–127.

23. Ludwig, A., Behnke, B., Holtlund, J., and Hilz, H. (1988) *J. Biol. Chem.* **263,** 6993–6999.

24. Ding, R., Pommier, Y., Kang, V. H., and Smulson, M. (1992) *J. Biol. Chem.* **267**(18), 12804–12812.

25. Ding, R., and Smulson, M. (1994) *Cancer Res.* **54,** 4627–4634.

26. Rosenthal, D. S., Shima, T. B., Celli, G., De Luca, L. M., and Smulson, M. E. (1995) *J. Invest. Dermatol.* **105,** 38–44.

27. Althaus, F. R., Hilz, H., and Shall, S. (1985) *in* ADP-Ribosylation of Proteins, Springer-Verlag, Berlin.

28. Berger, N. A., and Petzold, S. J. (1985) *Biochemistry* **24,** 4352–4355.

29. Kastan, M. B., Onyekwere, O., Sidransky, D., Vogelstein, B., and Craig, R. W. (1991) *Cancer Res.* **51,** 6304–6311.

30. Fritsche, M., Haessler, C., and Brandner, G. (1993) *Oncogene* **8,** 307–318.

31. Wesierska-Gadek, J., Schmid, G., and Cerni, C. (1996) *Biochem. Biophys. Res. Commun.* **224,** 96–102.

32. Vaziri, H., West, M., Allsop, R., Davison, T., Wu, Y., Arrowsmith, C., Poirier, G., and Benchimol, S. (1997) *EMBO J.* **16,** 6018–6033.

33. Stevnsner, T., Ding, R., Smulson, M., and Bohr, V. A. (1994) *Nucleic Acids Res.* **22**(22), 4620–4624.

34. Nelson, W. G., and Kastan, M. B. (1994) *Mol. Cell. Biol.* **14**(3), 1815–1823.

35. Whitacre, C. M., Hashimoto, H., Tsai, M.-L., Chatterjee, S., Berger, S. J., and Berger, N. A. (1995) *Cancer Res.* **55,** 3697–3701.

36. Agarwal, M., Agarwal, A., Taylor, W., Wang, Z. Q., and Wagner, E. (1997) *Oncogene* **15,** 1035–1041.

37. de Murcia, J., Niedergang, C., Trucco, C., Ricoul, M., Dutrillaux, B., Mark, M., Oliver, J., Masson, M., Dierich, A., LeMeur, M., Waltzinger, C., Chambon, P., and deMurcia, G. (1997) *Proc. Natl. Acad. Sci. USA* **94,** 7303–7307.

38. Suto, M., Turner, W., Arundel-Suto, C., Werbel, L., and Sebolt-Leopold, J. (1991) *Anticancer Drug Des. (England)* **6,** 107–117.

Detection of DNA breaks in apoptotic cells utilizing the DNA binding domain of poly(ADP-ribose) polymerase with fluorescence microscopy

Dean S. Rosenthal[1], Ruchuang Ding[1], Cynthia M. G. Simbulan-Rosenthal[1], Barry Cherney[2], Philip Vanek[1,3] and Mark Smulson[1,*]

[1]Department of Biochemistry and Molecular Biology, Georgetown University School of Medicine, Washington, DC 20007, USA, [2]Food and Drug Administration, Bethesda, MD 20892, USA and [3]Trevigen Inc., Gaithersburg, MD 20898, USA

ABSTRACT

The DNA binding domain (DBD) of poly(ADP-ribose) polymerase (PARP) has proved to be a novel, highly sensitive probe for detecting DNA breaks in intact cells undergoing apoptosis. A recombinant peptide spanning the DNA binding domain of PARP was expressed, purified and used to detect DNA strand breaks in fixed cells. Fluorescence microscopy with this probe followed by detection with anti-PARP antisera initially revealed an increased binding following treatment of cells with DNA strand-breaking agents (such as N-methyl-N'-nitro-N-nitrosoguanidine) and, subsequently, using biotinylated PARP DBD, during the later stages of apoptosis in several cell systems, when internucleosomal strand breaks became evident. This procedure was found to be at least as sensitive and required fewer steps to detect DNA strand breaks than those utilizing Klenow incorporation of biotinylated nucleotides.

INTRODUCTION

Poly(ADP-ribose) polymerase (PARP) is an abundant nuclear protein that is associated with chromatin. This enzyme covalently attaches to and elongates homopolymers of poly(ADP-ribose) to a number of nuclear proteins, using NAD, an abundant nucleotide in eukaryotic nuclei, as substrate. PARP is a zinc finger-containing protein, allowing the enzyme to bind to either double- or single-strand DNA breaks without any apparent sequence preference. Cell culture systems have demonstrated that PARP is involved in numerous biological functions, all of which are associated with the breaking and rejoining of DNA strands (1–6). The enzyme has an absolute requirement for DNA for activity and is activated proportionately by the number of strand breaks in DNA. We recently demonstrated that one of the earliest stages of apoptosis is characterized by activation of PARP and poly(ADP-ribose) addition to nuclear proteins during the reversible stages of

apoptosis (7) and specific proteolysis of PARP has now been closely associated with a later stage of programed cell death (8–10). This process occurs in a variety of cell types during organogenesis and during maturation of the immune system. During apoptosis, clumps of heterochromatin form adjacent to the nuclear matrix, nuclear fragmentation occurs and, ultimately, membrane-enclosed apoptotic bodies appear. These changes are accompanied by an increase in intracellular free Ca^{2+} concentration. Increasing amounts of DNA strand breaks also occur during apoptosis. The first strand breaks that are associated with DNA cleavage at chromatin loops yield DNA fragment sizes >200 kb and can only be visualized by pulsed field electrophoresis. This is the stage that corresponds with activation of PARP (7). Later in apoptosis, a specific Ca^{2+}/Mg^{2+}-dependent nuclease is activated that cleaves DNA in the linker region between nucleosomes, yielding a characteristic nucleosome ladder when the chromosomal DNA is analyzed by agarose gel electrophoresis.

Visualization at the level of individual cells allows for the assay of apoptosis. At the single cell level, the study of apoptosis requires morphological examination of cells and nuclei, using chromatin- and DNA-specific fluorescent dyes, such as ethidium bromide, bis-benzamide and 4′,6-diamidino-2-phenylindole. At the biochemical level, DNA breaks have been detected *in situ* utilizing the free 3′-OH ends of DNA as a substrate for either terminal transferase or the Klenow fragment of DNA polymerase I to incorporate biotin or digoxigenin, which can be subsequently visualized with either visible or fluorescent dyes.

Proteolytic cleavage of PARP was first demonstrated in chemotherapy-induced apoptosis (11), where it was shown that PARP was processed into 85 and 24 kDa fragments. The 85 kDa fragment contains the catalytic and automodification domains, while the 24 kDa region consists of the DNA binding domain (DBD) of the enzyme. We recently explored the significance of PARP cleavage in the osteosarcoma cell model of apoptosis by examining the various participants in this specific aspect of programed cell death by immunofluorescence in whole cells (7). In doing so, we recognized the potential to utilize the unique aspect of the PARP DNA binding domain as a direct indicator of

---

* To whom correspondence should be addressed. Tel: +1 202 687 1718; Fax: +1 202 687 7186; Email: smulson@biocheml.basic-sci.georgetown.edu

DNA strand breaks that occur during apoptosis, as well as those that occur following DNA damage induced by alkylation. Accordingly, the experimental validity and general characterization of this new marker of apoptosis are described in detail below.

MATERIALS AND METHODS

Cells

Human osteosarcoma cells (American Type Culture Collection no. 11226) were cultured and apoptosis was induced as described previously (9). Burkitt lymphoma cell line BL-30 (12) and EBV-induced lymphoblastoid cell line YB-26 were maintained (13) and induced to undergo apoptosis (14,15).

Expression, purification, renaturation and biotinylation of the recombinant PARP DBD

The PARP DBD fusion protein was expressed in *Escherichia coli* (as described in detail in Results) and purified to >95% homogeneity in a single step by Ni resin column chromatography (Qiagen). Bacterial cell lysate was loaded onto a Ni–NTA column pre-equilibrated in buffer A (10 mM Tris–HCl, pH 8.0, 1% NP-40, 10 mM 2-mercaptoethanol, 6 M guanidine–HCl). After the column was washed extensively in buffer A, buffer B (containing 8 M urea instead of guanidine–HCl) and buffer C (buffer B adjusted to pH 6.3), recombinant protein was eluted with buffer D (buffer B adjusted to pH 5.7). Fractions were then collected and analyzed by SDS–PAGE. SDS–PAGE revealed the size of the fusion protein to be ~30 kDa, consistent with the predicted molecular mass of the PARP DBD attached to six histidine residues. PARP DBD protein was subsequently renatured by dialysis against seven changes of dialysis buffer (50 mM NaCl, 0.5 mM $ZnCl_2$ and 10 mM $MgCl_2$ in 50 mM phosphate buffer, pH 7.2) containing decreasing concentrations of urea (6, 4, 2 and 1 M), followed by decreasing concentrations of NaCl (1 M and 100 mM). Biotin labeling of PARP DBD was performed by incubating 5 μl biotin (long arm) *N*-hydroxysuccinimide ester in dimethylsulfoxide (5 mg/ml) with 250 μl PARP DBD (1 μg/μl) for 2 h at room temperature. The reaction was terminated with 5 mg glycine and the biotinylated PARP DBD protein was then dialyzed against 50 mM HEPES, pH 7.2, 20 mM $ZnCl_2$, 100 mM NaCl and 70 μl 2-mercaptoethanol.

Immunofluorescence and immunoblot analysis

Antibodies to PARP DBD were derived by immunization of rabbits with a peptide corresponding to amino acids 25–41 of human PARP. Fixation of cells, immunofluorescence and immunoblot analysis were performed as previously described (7,16).

Detection of DNA fragmentation

DNA breaks were detected *in situ* using a Klenow fragment-based assay system (TACS1; Trevigen). Cells were fixed and labeled with biotinylated nucleotides, using streptavidin-conjugated horseradish peroxidase and diaminobenzidine for detection. Cells were counterstained with methyl green. Brown nuclei were positive for Klenow labeling. DNA nucleosome ladders were observed by isolation of total genomic DNA and agarose gel electrophoresis as described previously (9).

PARP cleavage assay

Cytosolic extracts were prepared from cultured human osteosarcoma cells by homogenizing phosphate-buffered saline (PBS) washed cell pellets in 10 mM HEPES–KOH, pH 7.4, 2 mM EDTA, 0.1% (w,v) CHAPS, 5 mM dithiothreitol, 1 mM phenylmethylsulfonyl fluoride, 10 μg/ml pepstatin A, 20 μg/ml leupeptin, 10 μg/ml aprotinin (at 1×10^8 cells/ml) and collecting the post-100 000 g supernatant. Assays contained 10 μg protein from the cytosol fractions of osteosarcoma cells derived from days 2 and 8 with purified [^{35}S]PARP (~5×10^4 c.p.m.), 50 mM PIPES–KOH, 2 mM EDTA, 0.1% (w/v) CHAPS and 5 mM dithiothreitol in a volume of 25 μl. Incubations were performed at 37 C for 1 h and terminated by the addition of 25 μl 2× SDS–PAGE sample buffer containing 4% SDS, 4% β-mercaptoethanol, 10% glycerol, 0.125 M Tris–HCl, pH 6.8 and 0.02% bromophenol blue. Samples were analyzed by SDS–PAGE and fluorography.

RESULTS

Development of a new cytochemical assay for apoptotic DNA strand breaks based on a recombinant PARP cleavage product

Many of the currently available methods for examining DNA strand breaks *in situ* rely on the ability of exogenous enzymes such as DNA polymerase or terminal transferase to add labeled dNTPs to the 3'-OH ends of the strand breaks and subsequent detection of the incorporated nucleotides by immunofluorescence microscopy. We reasoned that the DBD of PARP might provide a more sensitive probe for DNA strand breaks that would eliminate the requirement for the often labile enzymes and nucleotide substrates.

Clone pCD12, containing the full-length cDNA encoding human PARP in an Okayama–Berg vector (17), was used as a polymerase chain reaction (PCR) template for construction of a PARP DBD expression vector. PCR was performed with: (i) a 28 bp primer that contained a *Bam*HI restriction site upstream (nt 164–180) of PARP cDNA; (ii) a 22 bp primer that contained a *Hind*III restriction site downstream (nt 837–854) of PARP cDNA. The PARP cDNA fragment thus amplified encompassed the region that encodes the two zinc fingers of the enzyme as well as the KKKSKK nuclear localization signal. Amplification was performed for 21 cycles and the product was then ligated into the bacterial protein expression vector pQE30 (Qiagen).

The DBD of PARP was subsequently expressed in *E.coli* and purified to >95% homogeneity by affinity chromatography using a Ni–NTA column (Fig. 1). The PARP DBD fusion protein was recognized on immunoblot analysis by polyclonal antibodies, obtained subsequently, to this region of PARP (7). The double bands of the PARP DBD shown in the Coomassie stained gel in Figure 1 may be due to premature termination of transcription or translation, although both of these proteins reacted specifically to antibodies to PARP DBD (not shown). To establish conditions for detecting DNA strand breaks in fixed mouse cells with the PARP DBD, we first adopted an immunofluorescence approach using anti-human PARP. The antibody used does not react with the murine PARP (18), even though the amino acid sequences of the proteins are >80% identical (17,19). We therefore incubated mouse 3T3 cells for 30 min in the absence or presence of 0.4 mM *N*-methyl-*N'*-nitro-*N*-nitrosoguanidine (MNNG) to induce a significant number of DNA breaks, after which the cells were
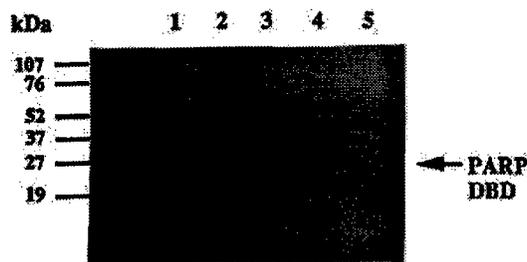
Figure 1. Expression and purification of the DBD of PARP. The PARP DBD was expressed in bacteria and purified as described in Materials and Methods. Samples obtained from five different clones were resolved by PAGE and stained for total proteins with Coomasie blue. Molecular size standards are indicated on the left in kilodaltons.

fixed on slides, incubated at room temperature with excess purified PARP DBD (25 μg/ml) for 1 h and washed with PBS. DBD bound to DNA strand breaks was then detected by incubating the slides with the rabbit antibodies which recognize human PARP DBD, followed by Texas red-conjugated goat antibodies to rabbit immunoglobulin IgG. Whereas no immuno-fluorescence was detected in 3T3 cells not incubated with MNNG, marked immunofluorescence was apparent in cells treated with the alkylating agent (data not shown). These results indicated the feasibility of using PARP DBD to detect DNA strand breaks in fixed cells.

Use of biotinylated PARP DBD

To avoid the use of antibodies to detect the PARP DBD bound to DNA strand breaks, we conjugated the bacterially expressed DBD to biotin so as to allow detection by reaction with horseradish peroxidase-conjugated streptavidin and enhanced chemiluminescence (ECL; Amersham). We first tested the

modified DBD detection system in two human B cell lines that are known to undergo apoptosis via endonuclease cleavage of DNA following serum depletion, unlike normal B cells which become quiescent upon serum withdrawal (15). Apoptosis was induced in either a B cell line immortalized with EBV *in vitro* (Fig. 2) or in Burkitt lymphoma-derived B cells (Fig. 3) by withdrawal of autocrine growth factor as described (15). The occurrence of apoptosis was confirmed by a morphological assay (20) using fluorescence microscopy with a mixture of acridine orange and ethidium bromide (data not shown). The cells were then examined by phase contrast microscopy and by fluorescence microscopy with biotinylated DBD and horseradish peroxidase-conjugated streptavidin (Figs 2 and 3). In virtually all instances, only those cells showing the morphological characteristics (cell shrinkage and nuclear condensation) of apoptosis were stained by the biotinylated PARP DBD. The number of stained cells increased with time after autocrine factor withdrawal.

We recently characterized the stages of apoptosis with respect to PARP activation, PARP proteolysis and DNA fragmentation in a human osteosarcoma cell line that undergoes a slow (8–10 days), spontaneous and reproducible death program in culture (7). Activation of PARP occurred early, within 2 days of cell plating for apoptosis, while PARP proteolysis was detected immunocytochemi-cally between 4 and 6 days. DNA fragmentation was not evident until 6–10 days in culture, as determined by nucleosome ladder formation. In the current study we wished to compare the sensitivity of this new methodology for detecting strand breaks, using the osteosarcoma system, to a widely used technique. We first confirmed that the osteosarcoma cells were undergoing apoptosis, as measured by apopain activity (9). Figure 4 shows a marked increase in PARP cleavage activity by day 8. We then measured the ability of the PARP DBD to detect DNA breaks at these two time points (Fig. 5). In both attached and floating cells, an increase in the binding of PARP DBD was observed in the late stage of apoptosis.
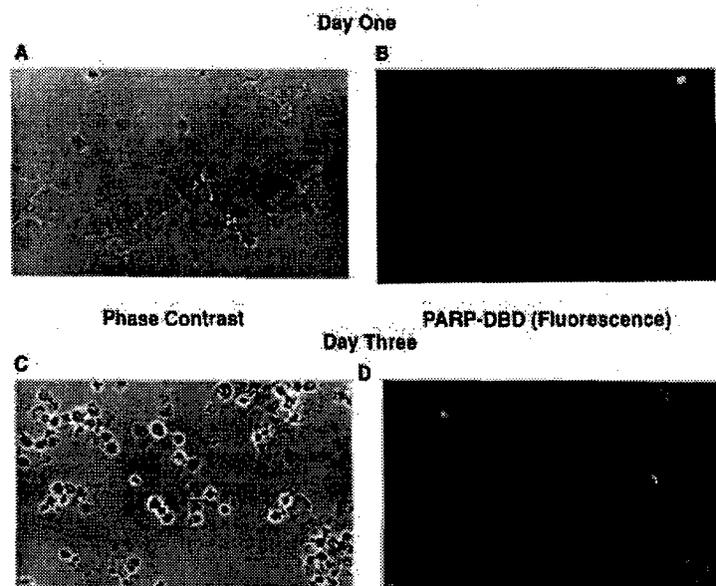
Figure 2. Binding of the PARP DBD to DNA strand breaks in apoptotic, EBV-immortalized human B cells. B lymphocytes were immortalized by EBV infection of peripheral B cells as described (25). Apoptosis was induced by culturing the cells at low density in the absence of serum (15). Cells were fixed after 1 (A and B) or 3 (C and D) days and incubated with biotinylated PARP DBD followed by streptavidin–Texas red. (A and C) Phase contrast microscopy; (B and D) fluorescence microscopy.
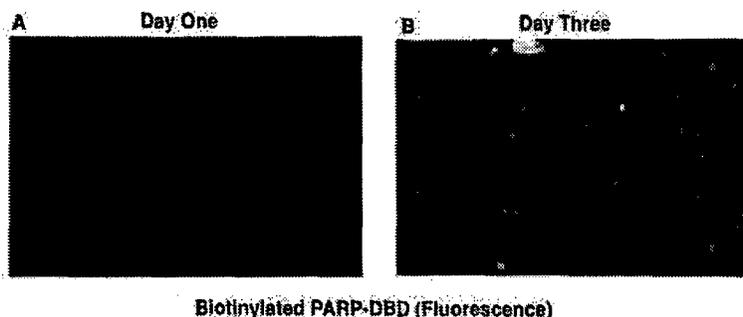
Biotinylated PARP-DBD (Fluorescence)

Figure 3. Binding of the PARP DBD to DNA strand breaks in apoptotic clonal Burkitt lymphoma cells. BL-30 cells were cultured in the absence of autocrine factor to induce apoptosis, fixed after 1 (A) or 3 (B) days and incubated with DBD as above.
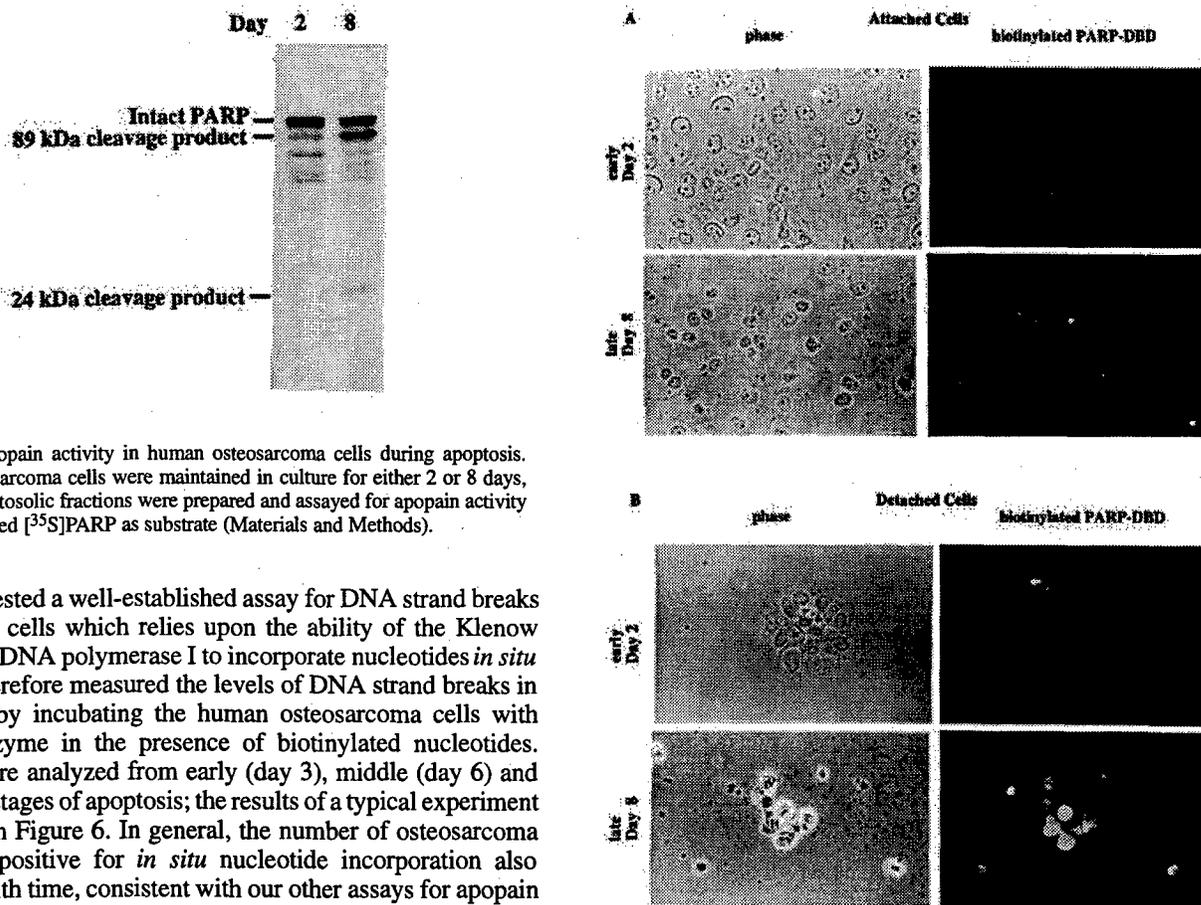
Figure 4. Apopain activity in human osteosarcoma cells during apoptosis. Human osteosarcoma cells were maintained in culture for either 2 or 8 days, after which cytosolic fractions were prepared and assayed for apopain activity (9) with purified [^{35}S]PARP as substrate (Materials and Methods).

Figure 5. Time course of staining of human osteosarcoma cells for the presence of DNA strand breaks using biotinylated recombinant PARP DBD in attached (upper panel) and detached cells (lower panel).

We then tested a well-established assay for DNA strand breaks in apoptotic cells which relies upon the ability of the Klenow fragment of DNA polymerase I to incorporate nucleotides *in situ* (21). We therefore measured the levels of DNA strand breaks in fixed cells by incubating the human osteosarcoma cells with Klenow enzyme in the presence of biotinylated nucleotides. Samples were analyzed from early (day 3), middle (day 6) and late (day 8) stages of apoptosis; the results of a typical experiment are shown in Figure 6. In general, the number of osteosarcoma cell nuclei positive for *in situ* nucleotide incorporation also increased with time, consistent with our other assays for apopain activity and DNA strand breaks. However, fewer apoptotic nuclei were detected by the Klenow assay than by the PARP DBD assay (Figs 5 and 6). At day 3, none of the nuclei were stained. By day 6, several nuclei that appeared morphologically apoptotic stained positively for nucleotide incorporation. More nuclei stained positively for strand breaks by day 8, although the proportion of positive cells remained in the minority (Fig. 6). At this time point <30% of attached cells were Klenow-positive, compared with >80% that were DBD-positive.

DISCUSSION

Satoh and Lindahl (4,5) recently demonstrated that unmodified PARP binds to a damaged DNA plasmid *in vitro* and inhibits repair in the absence of NAD. It is hypothesized that PARP cycles

between an unmodified form, which blocks DNA strand ends, and a modified form, which is released from DNA, thereby allowing access of repair enzymes. Automodification of intact PARP by long chains of branched ADP-ribose polymers has in fact been shown to result in a loss of affinity of the enzyme for DNA (22). We recently tested this model by cycling PARP *in vitro* with bacterially expressed deletion mutants of PARP (6). Our data using this *in vitro* assay of DNA showed that those mutants that
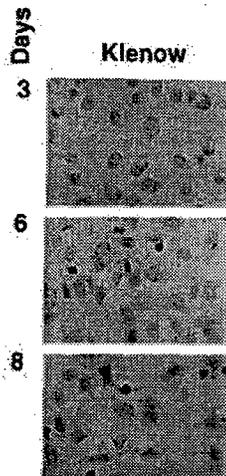
Figure 6. Time course of the labeling of DNA strand breaks with the Klenow fragment during apoptosis of human osteosarcoma cells. Cells were cultured for 3, 6 or 8 days and fixed and labeled by a Klenow-based assay, using horseradish peroxidase and diaminobenzidine for detection. Cells were counter-stained with methyl green. Brown nuclei are positive for Klenow labeling.

and double-stranded DNA breaks and requires no enzyme catalysis, indicating that this a useful and simple tool for detecting apoptotic DNA breaks *in situ*.

ACKNOWLEDGEMENTS

possess an intact DBD and are therefore able to bind to single-strand breaks inhibit DNA repair when added to a PARP-depleted HeLa cell extract. However, deletions in the automodification domain or the NAD binding domain prevented alleviation of the inhibition exerted by these mutants by NAD. We thus reasoned that the DBD could be used as a tool to detect DNA damage in intact cells.

The cleavage of PARP into a separate DBD that cannot be automodified also suggests the possibility that the 24 kDa cleavage product binds irreversibly to the numerous strand breaks characteristic of the final stages of apoptosis. This may account for the fact that expression of the DBD in living cells has been shown to interfere with the DNA repair function of endogenous PARP (23,24).

We examined the above hypotheses directly by synthesizing a recombinant peptide spanning this proteolytic fragment of PARP. We tested this new assay by measuring binding of the recombinant DBD in 3T3 cells treated with MNNG, which is known to induce strand breaks, as well as in other well-defined apoptotic systems. Immunofluorescence analysis demonstrated an increased binding of excess biotinylated PARP DBD during the later stages of apoptosis in osteosarcoma cells. This analysis was easier to perform and was at least as sensitive as an assay utilizing Klenow incorporation of biotinylated nucleotides.

In a comparison with a commonly used system based on Klenow incorporation of biotinylated nucleotides for the detection of DNA strand breaks in fixed cells, our biotinylated DBD method proved at least as sensitive (compare Figs 5 and 6). The differential sensitivity of the two assays may relate to several factors, including increased sensitivity of fluorescence. In addition, Klenow incorporation of biotinylated nucleotides only occurs at double-stranded DNA 5′ overhangs, but not with single-stranded DNA, double-stranded DNA with 3′-OH overhangs or double-stranded DNA with blunt ends. On the other hand, the PARP DBD binds directly to all single-stranded DNA

REFERENCES

1 Berger,N.A., Petzold,S.J. and Berger,S.J. (1979) *Biochim. Biophys. Acta*, **564**, 90–104.
2 Stevnsner,T., Ding,R., Smulson,M. and Bohr,V.A. (1994) *Nucleic Acid Res.*, **22**, 4620–4624.
3 Jacobson,M.K. and Jacobson,E.L. (eds) (1989) *ADP-Ribose Transfer Reactions: Mechanisms and Biological Significance.* Springer-Verlag, New York, NY.
4 Satoh,M.S. and Lindahl,T. (1992) *Nature*, **356**, 356–358.
5 Satoh,M.S., Poirier,G.G. and Lindahl,T. (1993) *J. Biol. Chem.*, **268**, 5480–5487.
6 Smulson,M., Istock,N., Ding,R. and Cherney,B. (1994) *Biochemistry*, **33**, 6186–6191.
7 Rosenthal,D.S., Ding,R., Simbulan-Rosenthal,C.M.G., Vaillancourt,J.P., Nicholson,D.W. and Smulson,M.E. (1997) *Exp. Cell Res.*, in press.
8 Tewari,M., Quan,L.T., O'Rourke,K., Desnoyers,S., Zeng,Z., Beidler,D.R., Poirier,G.G., Salvesen,G.S. and Dixit,V.M. (1995) *Cell*, **81**, 801–809.
9 Nicholson,D.W., Ali,A., Thornberry,N.A., Vaillancourt,J.P., Ding,C.K., Gallant,M., Gareau,Y., Griffin,P.R., Labelle,M., Lazebnik,Y.A., Munday,N.A., Raju,S.M., Smulson,M.E., Yamin,T.T., Yu,V.L. and Miller,D.K. (1995) *Nature*, **376**, 37–43.
10 Neamati,N., Fernandez,A., Wright,S., Kiefer,J. and McConkey,D.J. (1995) *J. Immunol.*, **154**, 3788–3795.
11 Kaufmann,S.H., Desnoyers,S., Ottaviano,Y., Davidson,N.E. and Poirier,G.G. (1993) *Cancer Res.*, **53**, 3976–3985.
12 Lenoic,G.M., Vuillaume,M. and Bonnardel,C. (1985) *The Use of Lymphomatous and Lymphoblast Lines in the Study of Burkitt's Lymphoma*, IARC Publication no. 2. IARC, Lyon, France, pp. 309–318.
13 Pike,S.E., Markey,S.P., Ijames,C., Jones,K.D. and Tosato,G. (1991) *Proc. Natl. Acad. Sci. USA*, **88**, 11081–11085.
14 Falk,M.H., Hultner,L., Milner,A., Gregory,C.D. and Bornkamm,G.W. (1993) *Int. J. Cancer*, **55**, 485–491.
15 Cherney,B.W., Bhatia,K. and Tosato,G. (1994) *Proc. Natl. Acad. Sci. USA*, **91**, 12967–12971.
16 Rosenthal,D.S., Shima,T.B., Celli,G., De Luca,L.M. and Smulson,M.E. (1995) *J. Invest. Dermatol.*, **105**, 38–44.
17 Cherney,B.W., McBride,O.W., Chen,D.F., Alkhatib,H., Bhatia,K., Hensley, P. and Smulson,M.E. (1987) *Proc. Natl. Acad. Sci. USA*, **84**, 8370–8374.
18 Bhatia,K., Kang,V.H., Stein,G.S., Bustin,M., Cherney,B.W., Notario,V., Haque,S.J., Huppi,K. and Smulson,M.E. (1990) *J. Cell Physiol.*, **144**, 345–353.
19 Huppi,K., Bhatia,K., Siwarski,D., Klinman,D., Cherney,B., Dritschilo,A. and Smulson,M.E. (1989) *Nucleic Acid Res.*, **17**, 3387–3401.
20 Duke,R.C. and Cohen,J.J. (1992) In Coligan,J.E., Kruisbeek,A.M., Margulies,D.H. Shevach,E.M. and Strober,W. (eds), *Current Protocols in Immunology.* Green/Wiley, New York, NY, pp. 3.17.1–3.17.3.
21 Fehsel,K., Kolb-Bachofen,V. and Kolb,H. (1991) *Am. J. Pathol.*, **139**, 251–254.
22 Zahradka,P. and Ebisuzaki,K. (1982) *Eur. J. Biochem.*, **127**, 579–585.
23 Kupper,J.H., de Murcia,G. and Burkle,A. (1990) *J. Biol. Chem.*, **265**, 18721–18724.
24 Molinete,M., Vermeulen,W., Burkle,A., de Murcia,J.M., Kupper,J.H., Hoeijmakers,J.H.J. and de Murcia,G. (1993) *EMBO J.*, **12**, 2109–2117.
25 Tosato,G. (1992) In Coligan,J.E., Kruisbeek,A.M., Margulies,D.H., Shevach,E.M. and Strober,W. (eds), *Current Protocols in Immunology.* Green/Wiley, New York, NY, pp. 7.22.1–7.22.3.

Intact Cell Evidence for the Early Synthesis, and Subsequent Late Apopain-Mediated Suppression, of Poly(ADP-ribose) during Apoptosis

Dean S. Rosenthal,* Ruchuang Ding,* Cynthia M. G. Simbulan-Rosenthal,* John P. Vaillancourt,† Donald W. Nicholson,† and Mark Smulson*,1

*Department of Biochemistry and Molecular Biology, Georgetown University School of Medicine, Washington, DC 20007; and †Department of Biochemistry and Molecular Biology, Merck Frosst Centre for Therapeutic Research, Pointe Claire-Dorval, Quebec, H9R 4P8, Canada

Poly(ADP-ribose) polymerase (PARP), which is catalytically activated by DNA strand breaks, has been implicated in apoptosis, or programmed cell death. A protease (CPP32) responsible for the cleavage of PARP and necessary for apoptosis was recently purified and characterized. The coordinated sequence of events related to PARP activation and cleavage in apoptosis has now been examined in individual cells. Apoptosis was studied in a human osteosarcoma cell line that undergoes a slow (8 to 10 days), spontaneous, and reproducible death program in culture. Changes in the abundance of intact PARP, poly(ADP-ribose) (PAR), and a proteolytic cleavage product of PARP that contains the DNA-binding domain were examined during apoptosis in the context of individual, whole cells by immunofluorescence with specific antibodies. The synthesis of PAR from NAD increased early, within 2 days of cell plating for apoptosis, prior to the appearance of internucleosomal DNA cleavage and before the cells become irreversibly committed to apoptosis, since replating yields viable, nonapoptotic cells. Strong expression of full-length PARP was also detected, by immunofluorescence as well as by Western analysis, during this same time period. However, after ~4 days in culture, the abundance of both full-length PARP and PAR decreased markedly. After 6 days, a proteolytic cleavage product containing the DNA-binding domain of PARP was detected immunocytochemically and confirmed by Western analysis, both in the nuclei and in the cytoplasm of cells. A recombinant peptide spanning the DNA-binding domain of PARP was expressed, purified, and biotinylated, and was then used as a probe for DNA strand breaks. Fluorescence microscopy with this probe revealed extensive DNA fragmentation during the later stages of apoptosis. This is the first report, using individual, *intact cells*, demonstrating that poly(ADP-ribosyl)ation of nuclear proteins occurs prior to the commitment to apoptosis, that inactivation and cleavage of PARP begin shortly thereafter, and that very little PAR per se is present during the later stages of apoptosis, despite the presence of a very large number of DNA strand breaks. These results suggest a negative regulatory role for PARP during apoptosis, which in turn may reflect the requirement for adequate NAD and ATP during the later stages of programmed cell death. © 1997 Academic Press

INTRODUCTION

Poly(ADP-ribose) polymerase (PARP)[2] catalyzes the poly(ADP-ribosyl)ation of nuclear histone and nonhistone proteins, using NAD, an abundant nucleotide in eukaryotic nuclei, as substrate. PARP contains two zinc fingers, which are sequence-nonspecific but facilitate the binding of the enzyme to either double- or single-strand breaks. Exposure of cells to agents that induce severe DNA strand breakage results in a rapid depletion of nuclear NAD and cellular ATP [1, 2]. Specialized tissue culture systems have demonstrated that PARP plays pleiotropic biological roles, all of which are associated with the breaking and rejoining of DNA strands [3–5]. For example, we have established and characterized several mammalian cell lines, including HeLa cells [6], keratinocytes [7], and 3T3-L1 preadipocytes [8], that are stably transfected with PARP antisense cDNA under the control of an inducible promoter. Induction of PARP antisense RNA in these cells results in depletion of endogenous PARP protein and activity and has revealed that the lack of PARP and hence poly-(ADP-ribosyl)ation suppresses an early event of DNA repair in HeLa cells [6]. Survival after exposure to DNA damaging agents is reduced, chromatin structure is altered, and gene amplification is increased in PARP-depleted cells [9].

2 Abbreviations used: DBD, DNA-binding domain; PAR, poly(ADP-ribose); PARP, poly(ADP-ribose)polymerase.

Wang *et al.* [10] recently showed that PARP knockout mice appear to exhibit normal development, fertility, and health, although one-third of the animals developed a hyperproliferative skin disorder. Fibroblasts derived from these mice apparently retain the normal capacity for DNA excision repair and nucleotide excision repair; however, their proliferation is impaired in culture. More recently, de Murcia and colleagues [10a] have noted stronger phenotypic abnormalities in PARP knockout animals, including reduced fertility and abnormal apoptosis. These data suggest that the roles of PARP and poly(ADP-ribosyl)ation may be more complex than anticipated and might best be studied in the context of specialized cells grown in culture.

Recently, PARP has been implicated in the induction of p53 and apoptosis [11], and the specific proteolysis of PARP has now been closely associated with programmed cell death [12–14]. This process is important for a variety of cells during embryogenesis and also for immunological competence. During apoptosis, clumps of heterochromatin form adjacent to the nuclear matrix, nuclear fragmentation occurs, and, ultimately, membrane-enclosed apoptotic bodies appear. These changes are accompanied by an increase in intracellular free Ca^{2+} concentration and internucleosomal DNA degradation. Because poly(ADP-ribosyl)ation is stimulated by DNA fragmentation, the potential role for PARP in cell death via NAD and ATP depletion has been proposed [15].

Kaufmann *et al.* [16] have shown that PARP undergoes proteolytic cleavage during chemotherapy-induced apoptosis. By immunoblot analysis with epitope-specific antibodies, it was demonstrated that programmed cell death was accompanied by early cleavage of PARP into 85- and 24-kDa fragments that contain the active site and the DNA-binding domain of the enzyme, respectively. This latter domain is required for full PARP activity.

We have recently participated in a study involving the purification and characterization of an enzyme, termed "apopain," that is responsible for the cleavage of PARP during apoptosis [13]. This enzyme is composed of two subunits of 17 and 12 kDa that are derived from a common proenzyme identified as CPP32, which is related to interleukin-1β-converting enzyme and to CED-3, the product of a gene required for programmed cell death in *Caenorhabditis elegans* [17]. The identity of this protease as CPP32 was also demonstrated by Tewari *et al.* [12]. We developed a highly specific assay with [35S]PARP and also used a specific fluorescent substrate to study this cleavage activity in cultured human osteosarcoma cells that undergo confluence-associated apoptosis over a 10-day period. With these *in vitro* assays, it was shown that apopain achieved maximum activity 6 to 7 days after initiation of apoptosis, which coincided with the onset of production of 200-bp inter-nucleosomal DNA ladders. A tetrapeptide aldehyde (Ac-DEVD-CHO) that specifically inhibits apopain was also synthesized, and we showed that this inhibitor also blocked apoptotic events studied *in vitro,* suggesting that the protease plays a key role in the initiation of apoptosis. Clearly, PARP and apopain may prove to be pivotal targets for pharmacological development especially under those conditions where inappropriate apoptosis occurs, such as in Alzheimer's, Parkinson's, and Huntington diseases and in immune deficiency disorders.

Most of the early research on apoptosis, including our own studies, has relied on *in vitro* assays or immunoblot analysis. We have now further explored the significance of PARP activation and cleavage in the osteosarcoma cell model of apoptosis by examining the various participants in this specific aspect of programmed cell death by immunofluorescence in individual cells.

MATERIALS AND METHODS

Cell lines and cell culture. Human osteosarcoma cells (American Type Culture Collection No. 11226) were cultured and apoptosis was induced as described previously [13]. Briefly, 1.5×10^5 cells were plated in 10-cm dishes in DMEM with 10% fetal calf serum. Cells were allowed to grow for 10 days without medium changes to induce apoptosis.

PARP cleavage assay. The full-length cDNA clone for PARP [18] (pcD-12) was excised and ligated into the *Xho*I site of pBluescript II SK(+) (Stratagene) and then used to drive the synthesis of PARP labeled with [35S]methionine (Dupont-NEN) by coupled T7 transcription/translation in a reticulocyte lysate system (Promega). [35S]PARP was separated from the other constituents by gel filtration chromatography on a Superdex-75 FPLC column (Pharmacia; 1×30 cm) in 10 m*M* Hepes–KOH (pH 7.4), 2 m*M* EDTA, 0.1% (w/v) Chaps, and 5 m*M* dithiothreitol.

Cytosolic extracts were prepared from cultured human osteosarcoma cells by homogenizing PBS-washed cell pellets in 10 m*M* Hepes/KOH (pH 7.4), 2 m*M* EDTA, 0.1% Chaps, 5 m*M* dithiothreitol, 1 m*M* phenylmethylsulfonyl fluoride, 10 μg/ml pepstatin A, 20 μg/ml leupeptin, 10 μg/ml aprotinin (at 1×10^8 cells/ml). The post-100,000*g* supernatant was recovered after centrifugation.

PARP cleavage activity was measured in mixtures containing 4.5 μg protein from the cytosol fractions of osteosarcoma cells derived every 24 h during the 10-day apoptotic program. Assay mixtures also contained purified [35S]PARP ($\approx 5 \times 10^4$ cpm), 50 m*M* Pipes–KOH, 2 m*M* EDTA, 0.1% (w/v) Chaps, and 5 m*M* dithiothreitol in a total volume of 25 μl. Incubations were performed at 37°C for 1 h and terminated by the addition of 25 μl of 2× SDS–PAGE sample buffer containing 4% SDS, 4% β-mercaptoethanol, 10% glycerol, 0.125 *M* Tris–HCl (pH 6.8), and 0.02% bromophenol blue. Samples were resolved by 10% SDS–polyacrylamide gels and PARP cleavage products were visualized by fluorography. The 24-kDa cleavage product of [35S]PARP was quantified by laser densitometry of the resulting films and data are expressed as percentage of the maximum cleavage activity.

Indirect immunofluorescence microscopy and immunoblot analysis. The details for fixation and staining with rabbit antiserum to human PARP [6] and guinea pig antiserum to PAR [7] have been described previously in detail. Antibodies to PARP DBD were derived by immunization of rabbits with a peptide corresponding to amino acids 25 to 41 of human PARP and were a kind gift from Dr. Intisar Husain (Glaxo Inc. Research Institute). The specificity of the antisera for

the PARP DBD vs full-length PARP was tested by immunoblot and immunofluorescence analysis. Both recombinant PARP DBD and DBD generated by apopain cleavage of PARP *in vitro* were stained strongly by this antibody using Western analysis. However, this anti-peptide antibody possessed negligible reactivity to full-length PARP in experiments repeated in two independent laboratories, using different cell and tissue extracts.

Osteosarcoma cells were grown on coverslips, fixed as previously described for antibody staining [7], and then incubated with biotin-DBD (20 μg/ml) in PBS containing 12% BSA for 4 h at room temperature. Cells were washed with PBS and then incubated with streptavidin conjugated to Texas Red (Life Technologies) diluted 1:800 in PBS with 12% BSA for $\frac{1}{2}$ h at room temperature. Cells were then washed with PBS, mounted, and visualized using a Zeiss immunofluorescence microscope. To allow comparisons of relative staining intensities at different time points during apoptosis, all film exposure times were identical.

Synthesis and purification of the DNA strand break probe. Clone pcD12, containing the full-length cDNA encoding human PARP in an Okayama-Berg vector, has been described [18]. This clone was used as a polymerase chain reaction (PCR) template to amplify the DNA fragment encoding the PARP DBD (PARP aa 1–234, encompassing the zinc fingers as well as the nuclear localization signal KKKSKK), which was then cloned into bacterial protein expression vector pQE30 (Qiagen).

The PARP DBD fusion protein was expressed in *Escherichia coli* and purified to >95% homogeneity in a single step by Ni-resin column chromatography (Qiagen). SDS–polyacrylamide gel electrophoresis revealed the size of the fusion protein to be ~30 kDa, consistent with the predicted molecular mass of the PARP DBD attached to six histidine residues. The bacterially expressed DBD was renatured and biotinylated by reaction with biotin *N*-hydroxysuccinimide ester at room temperature for 2 h, as recommended by the manufacturer (Vector Labs). The ability of the PARP DBD to bind to cellular DNA strand breaks was verified by the use of HeLa cells treated with MNNG. The ability of the probe to detect DNA breaks arising during apoptosis was also confirmed using several serum-starved Burkitt lymphoma-derived cell lines. Briefly, cells were fixed on coverslips, incubated with excess biotinylated PARP DBD (~25 μg/ml), and washed with PBS; strand break-DBD complexes were then detected utilizing streptavidin-conjugated Texas red. Fluorescence was localized to the nuclei of cells only under apoptotic conditions, when increases in the TUNEL labeling index, nucleosome ladders, and apopain activity were observed. A characterization of this DNA strand break assay will be described in greater detail elsewhere (18a).

RESULTS

Spontaneous Program of Apopain Activation and Cell Death in Human Osteosarcoma Cells.

In the previous study on PARP-cleavage activity [13], we used a human osteosarcoma cell line that undergoes a "slow," spontaneous apoptotic death. On reaching confluency, these cells undergo the morphological and biochemical changes characteristic of apoptosis, including cell shrinkage, membrane blebbing, chromatin condensation and fragmentation, and internucleosomal DNA cleavage. We incubated osteosarcoma cells in culture for various times, after which DNA was extracted and resolved on agarose gels as previously described [13]. The cells achieve confluency after ~6 days under our culture conditions. Internucleosomal DNA cleavage became evident around Day 7 and increased until Day

TABLE 1

Apopain Activity in Human Osteosarcoma
Cells during Apoptosis

Time (days)	Apopain activity (% of maximum)
3	15
4	26
5	34
6	70
7	96
8	96
9	96
10	100

Note. Human osteosarcoma cells were maintained in culture for the indicated times, after which cytosolic fractions were prepared and assayed for apopain activity with purified [^{35}S]PARP as substrate (Materials and Methods).

10, at which time virtually all of the cells have completed the death program [13].

By *in vitro* transcription of the originally isolated pcD12 clone encoding human PARP [18], and translation, we produced [^{35}S]met-labeled PARP as a substrate with which to assay apopain activity. Cytosolic fractions of cells incubated for various times in culture were assayed for PARP cleavage activity to confirm that the proenzyme CPP32 was converted from its latent form during the current experiments (Table 1). Subsequently, cells from the same cultures were fixed onto slides for immunofluorescence studies. Consistent with our previous data [13], PARP cleavage activity increased with time in culture, reaching 70% of maximum after 6 days, when the cells achieve confluence, and 96% shortly thereafter (Table 1).

PAR Is Synthesized Early, but Not Late during Apoptosis of Human Osteosarcoma Cells

Human osteosarcoma cells grown on coverslips were incubated for up to 10 days and fixed at daily intervals for examination of nuclear poly(ADP-ribosyl)ation with a guinea pig antiserum to PAR. Polymer was not detected after 24 h of culture, indicating the absence of DNA strand breaks, PARP, or both (Fig. 1). After 2 days of culture, substantial amounts of PAR, not observed earlier in this spontaneous apoptosis system, were detected within the nuclei of all attached cells. After 3 days, the nuclei of all attached cells stained intensely for the PAR. These cells are all viable at this stage, since ~100% of the cells can be replated at this time point without undergoing apoptosis. Recently, Neamati *et al.* [14] demonstrated large DNA fragments (1 Mb) and lamin B1 degradation early in apoptosis, prior to any evidence of internucleosomal cleavage. The *in vivo* synthesis of PAR was observed to be markedly reduced
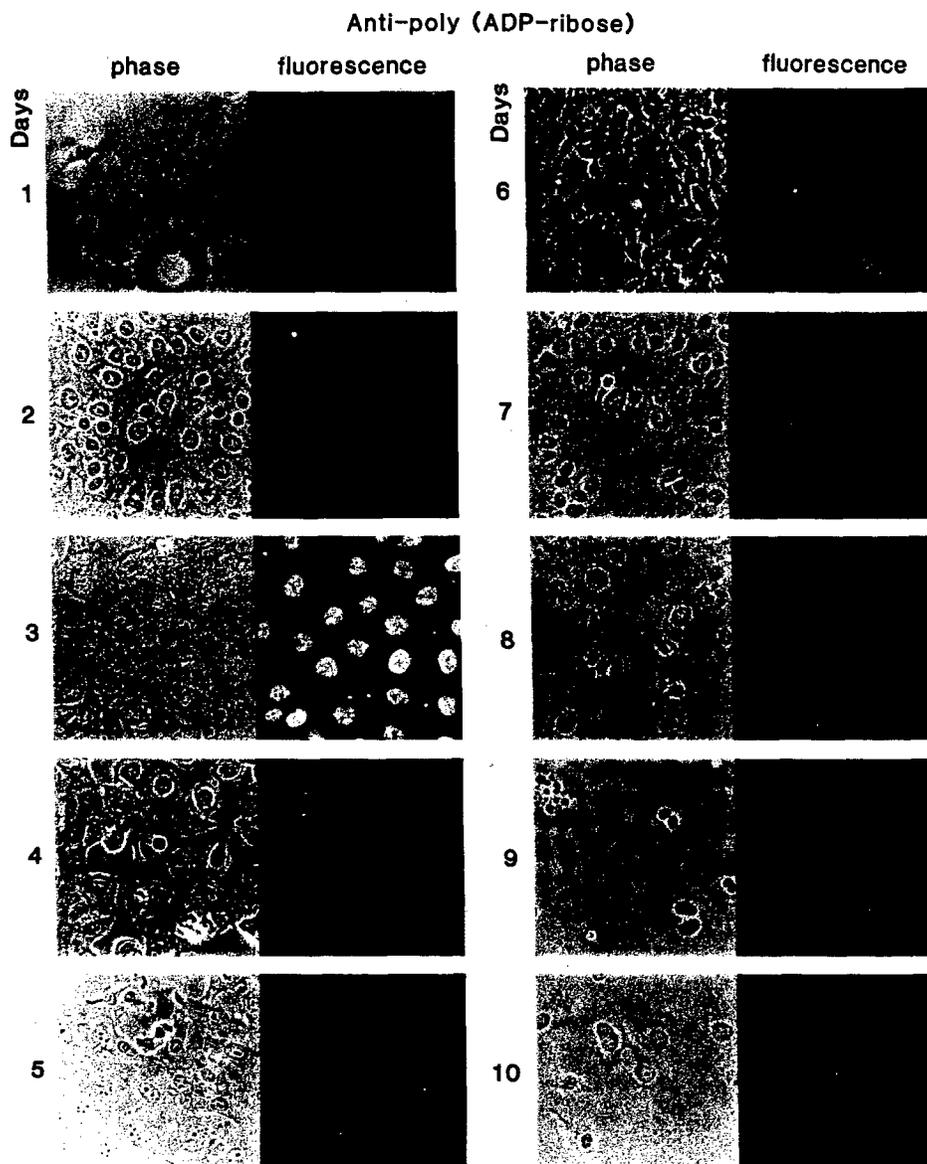
Anti-poly (ADP-ribose)

FIG. 1. Time course of poly(ADP-ribosyl)ation during apoptosis of human osteosarcoma cells. Cells were cultured for 1 to 10 days, fixed, and subjected to phase-contrast microscopy and immunofluorescence analysis with antibodies to PAR.

after 4 days (Fig. 1). Subsequently, only a faint diffuse staining pattern was detected, even though we observed the occurrence of substantial DNA fragmentation during this period [13]. If intact PARP were present in cells during these later time points, PAR would be very elevated and NAD and ATP levels would be expected to be almost totally depleted, based upon earlier studies [19]. However, high apopain activity accounts for the loss of catalytically active PARP (Table 1; see also below).

To determine whether the time course of this early nuclear poly(ADP-ribosyl)ation reflected that of PARP expression, we subjected the cells to immunofluorescence analysis with antibodies specific for full-length

PARP. In all subsequent experiments, samples were analyzed each day throughout the total 10-day period; representative samples from immediate (Day 1), early (Day 3), middle (Day 6), and late (Day 10) stages of apoptosis are shown in all cases. The time course of PARP expression was similar to that of the synthesis of PAR, as shown in Fig. 2A. Low levels of PARP were detected after 1 day in culture, perhaps reflecting a time lag after cell plating. However, a substantial amount of PARP was detected in the nuclei of all cells after 2 days. PARP staining showed a punctate pattern throughout the nucleus. Staining was more intense in perinucleolar regions, but was excluded from the nucleoli. The intensity of PARP staining decreased be-
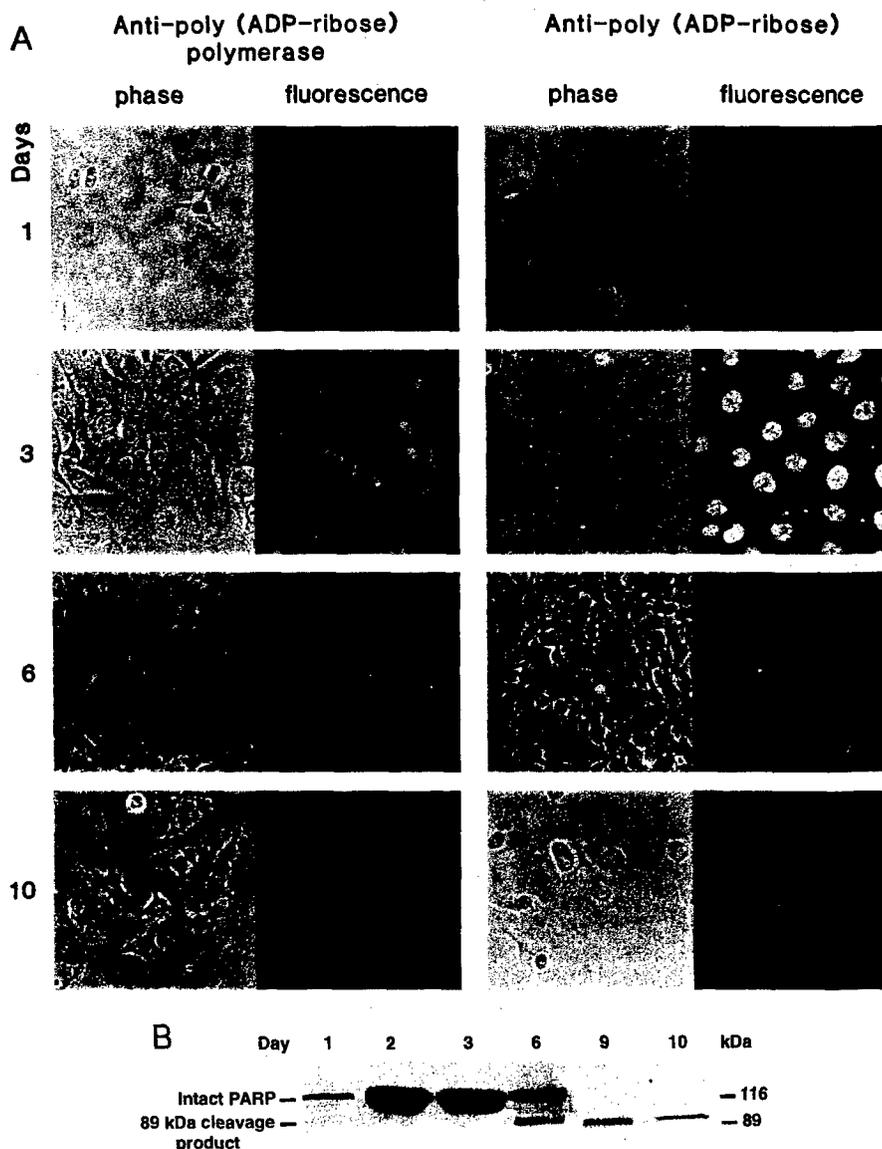
FIG. 2. (A) Time course of PARP vs PAR levels during apoptosis of human osteosarcoma cells. Cells were cultured for the indicated times, fixed, and stained with antibodies to PARP (left) or to PAR (right). (B) Time course of PARP expression and cleavage during apoptosis of human osteosarcoma cells. Cells were cultured for the indicated times. Total cell extracts containing equal amounts of protein (20 μg) were subjected to immunoblot analysis with rabbit antiserum recognizing both the full-length (116 kDa) and the 89-kDa cleavage product of PARP. Cells from Days 1–6 were predominantly attached, while most cells after this time were already detached.

tween Days 3 and 10, although weak staining was still apparent at 10 days. Using the same immunological staining procedure with the same PAR antisera, we recently showed extensive fluorescence of cells exposed to MNNG; it was also demonstrated that PARP-depleted cells (following PARP antisense expression) did not react with either anti-PARP or anti-PAR after MNNG treatment [7]. These observations suggest that the initial catalytic activation of PARP (Days 2–3; Fig. 2A) may be coincident with its expression in apoptotic osteosarcoma cells. To help rule out other possibilities (e.g., PARP is present, but not recognized by the anti-

sera used at this stage), total cellular protein was extracted at different time points and subjected to immunoblot analysis, using a different anti-PARP antibody that recognizes both the full-length PARP (116 kDa) and the 89-kDa cleavage product. Extracts were derived from both attached cells (which were in the majority from Day 1 to Day 6) and detached cells (predominant from Day 7 to Day 10). Figure 2B shows that only a small quantity of PARP is present at Day 1, which increases significantly (~10-fold) up to Days 3–4 and decreases thereafter. Immunoblot analysis with this particular antibody also reveals that PARP proteolysis
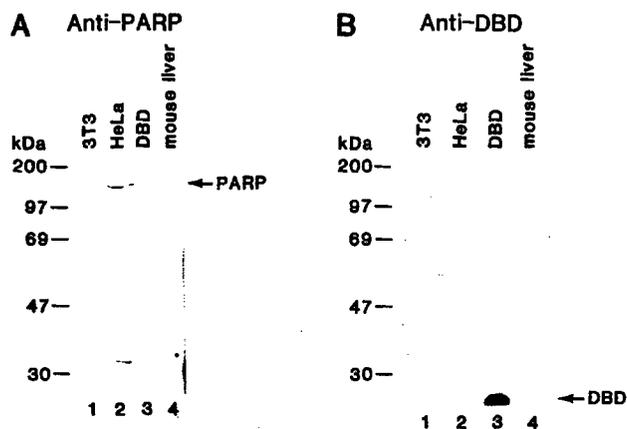
FIG. 3. Specificity of anti-PARP and anti-PARP N-terminal antibodies. Total cell extracts containing equal amounts of protein (20 μg) from mouse 3T3 cells, HeLa, and mouse liver, as well as 10 ng of purified recombinant PARP DBD, were subjected to immunoblot analysis with rabbit antisera either to human full-length PARP (A) or to a peptide (amino acid residues 25–41) within the PARP 24-kDa cleavage product (B). Immunoreactivity was visualized using horseradish peroxidase-conjugated anti-rabbit antibodies and ECL.

in vivo also yields the characteristic 89-kDa cleavage product which increases with time (Fig. 2B, lanes 4–6). The early detection of both PARP and PAR supports the idea that nuclear disruption involving strand breaks may be present in the earliest stages of apoptosis [14], before morphological changes and the appearance of the characteristic nucleosome ladder.

Generation of a 24-kDa PARP Cleavage Product during Apoptosis of Human Osteosarcoma Cells

The transient nature of the appearance of both PARP and PAR during apoptosis of human osteosarcoma cells suggests that these molecules are degraded or altered in these cells. The half-life of PAR within the nucleus is short, on the order of 1 min, which is primarily attributable to the action of the degradative enzyme poly(-ADP-ribose) glycohydrolase [2, 20]. PARP is also degraded (Table 1) during programmed cell death [12, 13, 16]. Using *in vitro* assays, we showed that PARP is cleaved by apopain into an NH_2-terminal 24-kDa fragment encompassing the DBD and a COOH-terminal 89-kDa fragment containing the automodification and catalytic domains. To confirm that this cleavage also occurs in intact cells, we subjected human osteosarcoma cells to immunofluorescence analysis with antibodies generated against a peptide corresponding to the DBD of PARP. The specificities of the anti-DBD and anti-PARP antisera were compared by immunoblot analysis of extracts of mouse 3T3 cells, mouse liver, and HeLa cells, as well as with purified recombinant DBD (Fig. 3). The antipeptide antibodies had high titer to the DBD of PARP but not full-length PARP (Fig.

3B; see also Materials and Methods), whereas the anti-PARP antibodies primarily recognized the full-length human PARP protein in HeLa cells (Fig. 3A). The failure of the antipeptide antibody to recognize full-length PARP in immunoblots was consistently observed and may be related to differences in conformation of the DBD and full-length PARP (see Discussion). The failure of either the anti-DBD or the anti-human PARP to recognize mouse PARP (Fig. 3, lanes 1 and 4), even though mouse and human PARP are 85% homologous, further illustrates the (unexpected) specificities of these antibodies. As with the other markers, samples were analyzed each day throughout the total 10-day period; samples from immediate (Day 1), early (Day 3), middle (Day 6), and late (Day 10) stages of apoptosis are shown in Fig. 4. Immunofluorescence analysis detected the PARP DBD in human osteosarcoma cells only after 6 to 7 days in culture (Fig. 4), a time at which the abundance of both PARP and PAR is decreasing (Fig. 2A), PARP-cleavage activity is increasing (Table 1), and internucleosomal DNA cleavage is present [13]. The pattern of staining for the DBD also differed markedly from that of full-length PARP. Whereas PARP staining was present throughout the nucleus, the DBD showed a more localized punctate pattern in the region of the nucleolus and throughout the nucleus-disrupted cytoplasm.

DNA Strand Breaks and PAR Status during Late Apoptosis in Intact Cells

Using newly developed methodology (Materials and Methods), we assessed the levels of DNA strand breaks in the fixed intact cells by staining the human osteosarcoma cells with the biotinylated PARP DBD, followed by Texas red-conjugated streptavidin (18a). Samples from immediate (Day 1), early (Day 3), middle (Day 6), and late (Day 10) stages of apoptosis are shown in Fig. 4 (although samples were analyzed each day throughout the total 10-day period). By Day 10 the nuclei of many cells stained intensely. Significant internucleosomal DNA breaks were also detected from Day 6 to Day 9 (Fig. 4; and [13]). Nuclear fluorescence was not detectable at Day 1; however, a low level of staining, consistent with a small number of DNA strand breaks, was observed at Day 3, when PAR synthesis was most abundant (Fig. 2A) and apopain activity was only 15% of the maximum (Table 1).

Taken together, the new immunofluorescence data further show that both detectable protein amount and catalytic activation of PARP appear early in osteosarcoma cell growth (Figs. 1, 2A, and 2B), while the cleavage of PARP and the accumulation of a large number of DNA strand breaks (Figs. 2B, 3, and 4) confirm our earlier *in vitro* results by showing in intact cells that these events occur later in the process. They also con-
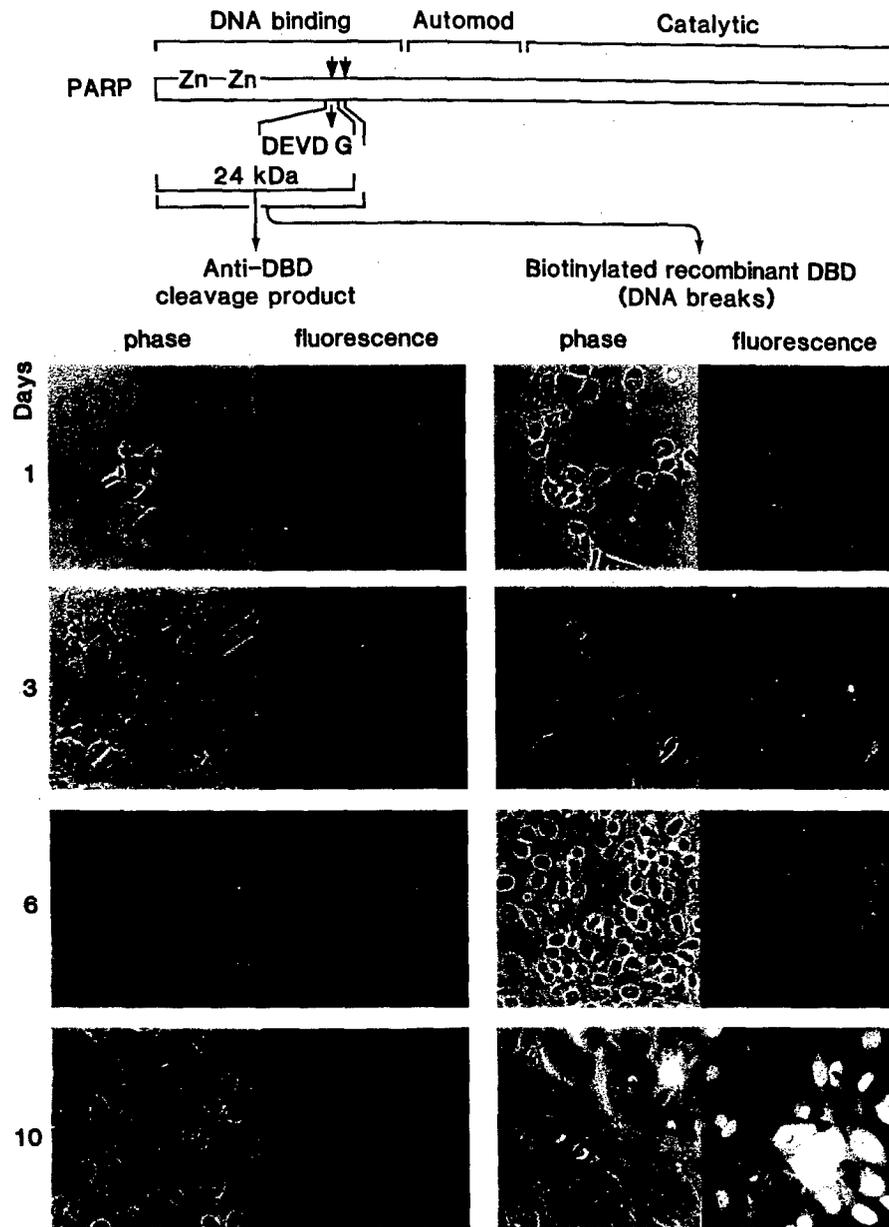
FIG. 4. Time course of staining of human osteosarcoma cells during apoptosis for the 24-kDa cleavage product of PARP (left) or the presence of DNA strand breaks using biotinylated recombinant PARP DBD (right).

firm, in the context of the intact cell, that poly(ADP-ribosyl)ation is not associated with the late stages of apoptosis.

DISCUSSION

The current study shows for the first time, in intact cells, that PAR is synthesized in all cells prior to the commitment to apoptosis. We have also shown that very little PAR is synthesized, hence sparing NAD and ATP, in the later stages of apoptosis, in spite of the massive DNA fragmentation that occurs. Recent studies have indicated that cleavage of PARP by the protease apopain occurs during programmed cell death [12, 13]. Thus, we showed that a peptide inhibitor of this protease prevents both the cleavage and the inactivation of PARP and apoptotic events *in vitro* [13]. Our present data support and extend these earlier observations by suggesting that PARP cleavage may be a necessary event in the later stages of apoptosis in intact cells. Poly(ADP-ribosyl)ation is important in a variety of nuclear processes, including DNA repair, DNA repli-

cation, recombination, and cellular differentiation, all of which require cleavage and rejoining of DNA strands.

Past studies of the role of PARP in nuclear processes have relied largely on the employment of chemical inhibitors of PARP, whose usefulness may be somewhat limited because of a lack of specificity and their consequent unrelated effects on other biological processes [23–25]. Adopting a more specific approach, we have established and characterized several mammalian cell lines, including HeLa cells [6], keratinocytes [7], and 3T3-L1 preadipocytes [8], that are stably transfected with PARP antisense cDNA under the control of an inducible promoter. Induction of PARP antisense RNA in these cells results in depletion of endogenous PARP protein and activity and has revealed that the lack of PARP and hence poly(ADP-ribosyl)ation inhibits the initial rate of DNA repair in HeLa cells [6]. Survival after exposure to DNA-damaging agents is reduced, chromatin structure is altered, and gene amplification is increased in PARP-depleted cells [9]. Wang et al. [10] recently showed that knock-out mice lacking PARP protein and activity are viable and fertile; on the other hand, PARP-deficient fibroblasts derived from these mice exhibited proliferation deficiencies in culture, while PARP-minus thymocytes showed a delayed recovery following exposure to gamma irradiation. Apparently, isolated cells and specialized systems may show more subtle effects due to the lack of PARP which are not evident in intact animals.

Because the catalytic activation of PARP is absolutely dependent on DNA strand breaks, our observation of a substantial amount of PARP expression and nuclear poly(ADP-ribosyl)ation 2 to 3 days into the apoptosis program of human osteosarcoma cells (Fig. 2A) confirms the presence of large (1 Mb) chromatin fragments at this early stage as described by Neamati et al. [14] and suggests a potential role for PAR synthesis and/or NAD depletion early in apoptosis. Previous studies with cells that undergo more rapid apoptosis have revealed a marked decrease in NAD concentration in the early stages of death followed by a recovery prior to the appearance of internucleosomal DNA cleavage [26]. The increase in PARP and PAR in human osteosarcoma cells occurs prior to a commitment to cell death; the cultures are less than 50% confluent at this stage and have a plating efficiency near 100%. Furthermore, no obvious morphological characteristics of apoptosis, such as nuclear condensation and cell shrinkage, are apparent at this early stage. Minimal DNA strand breaks were detected (Fig. 4). Thus, it is possible that the extent of catalytic activation of PARP at this critical time reflects the decision to live or die. Indeed, exposure of cells to chemical inhibitors of PARP at this time, but not later, can stave off the death program [26]. This early reversible time period of PARP

expression may be similar to that described in other studies [14] when the initial events of nuclear breakdown are occurring and poly(ADP-ribosyl)ation may play an accessory role in these early nuclear changes. This topic, accordingly, is under current investigation.

PARP cleavage begins early and maximizes at a later stage of apoptosis, as revealed by the accumulation of the 24-kDa fragment of the enzyme after 6 days in culture as well as by the increase in in vitro PARP cleavage activity during this same time period. The in vitro activity of apopain was shown earlier to be inhibited by the peptide active site aldehyde Ac-DEVD-CHO with a K_i of inhibition of <1 nM, making this among the most potent peptide aldehydes known for inhibiting a protease. This inhibitor totally repressed apoptosis in an in vitro isolated nuclear apoptosis system incubated with extracts containing PARP cleavage activity from Day 7 of a typical experiment and subsequently was also shown to be able to inhibit protease activity and apoptosis when added to intact osteosarcoma cells undergoing apoptosis [13].

We showed that the antibodies used to detect the 24-kDa N-terminal fragment of PARP had negligible, if any, affinity for the full-length PARP protein. The specificity of this antisera for the N-terminal region of PARP was confirmed by four lines of evidence. First, this antibody recognizes both recombinant PARP DBD (Fig. 3B) and the homologous 24-kDa fragment generated by apopain cleavage of PARP in vitro by immunoblot analysis (not shown). Second, perhaps related to partial renaturation of full-length PARP into a structure that is not recognized by this anti-peptide antisera, the antibody also did not recognize full-length PARP by immunoblot analysis in repeated experiments using extracts from different cells and tissues (Fig. 3B). Other investigators have also observed that certain antisera can recognize peptide fragments of proteins, including PARP, but not even the full-length protein itself can be recognized by Western analysis [27, 28]. Third, the antibody failed to recognize full-length PARP in the nuclei of control cells, or early apoptotic cells, as determined by indirect immunofluorescence (compare Fig. 2A, Day 3 vs Fig. 4, Day 3). Fourth, during the middle and later stages of apoptosis, the pattern of staining using the N-terminal-specific antibody (Fig. 4, left column) differed markedly from that obtained when using anti-PARP (Fig. 2A, left column), indicating that these antibodies do not cross-react.

The accumulation of the PARP cleavage product in intact cells was accompanied by the reduction of both intact PARP and PAR in the nuclei of cells between Days 4 and 10. The appearance of the 24-kDa cleavage product of PARP was also detected by immunoblot analysis of protein extracts of cells at the later stages of apoptosis (data not shown). In contrast with the lack of extensive synthesis of polymer, the appearance of

the PARP cleavage product coincided with the appearance of DNA strand breaks, as revealed by internucleosomal DNA cleavage [13] and fluorescence microscopy with a new marker of DNA breaks (Fig. 4). Our data indicate that the cleavage product localized to regions of heterochromatin, which presumably contain the majority of the DNA strand breaks as determined by terminal transferase labeling techniques [29].

Together, our results show with individual, intact cells that PARP cleavage and inactivation, the concomitant loss of poly(ADP-ribosyl)ation of target proteins and, hence, the maintenance of adequate cellular pools of NAD and ATP appear to be characteristic of later stages of apoptosis during which cells become irreversibly committed to death.

REFERENCES

1. Alvarez, G. R., Eichenberger, R., and Althaus, F. R. (1986) *Biochem. Biophys. Res. Commun.* **138**, 1051–1057.

2. Wielckens, K., Schmidt, A., George, E., Bredehorst, R., and Hilz, H. (1982) *J. Biol. Chem.* **257**, 12872–12877.

3. Satoh, M. S., and Lindahl, T. (1992) *Nature* **356**, 356–358.

4. Satoh, M. S., Poirier, G. G., and Lindahl, T. (1993) *J. Biol. Chem.* **268**, 5480–5487.

5. Smulson, M., Istock, N., Ding, R., and Cherney, B. (1994) *Biochemistry* **33**, 6186–6191.

6. Ding, R., Pommier, Y., Kang, V. H., and Smulson, M. (1992) *J. Biol. Chem.* **267**, 12804–12812.

7. Rosenthal, D. S., Shima, T. B., Celli, G., De Luca, L. M., and Smulson, M. E. (1995) *J. Invest. Dermatol.* **105**, 38–44.

8. Smulson, M. E., Kang, V. H., Ntambi, J. M., Rosenthal, D. S., Ding, R., and Simbulan, C. M. G. (1995) *J. Biol. Chem.* **270**, 119–127.

9. Ding, R., and Smulson, M. (1994) *Cancer Res.* **54**, 4627–4634.

10. Wang, Z. Q., Auer, B., Stingl, L., Berghammer, H., Haidacher, D., Schweiger, M., and Wagner, E. F. (1995) *Genes Dev.* **9**, 509–520; (a) de Murcia, J., Trucco, C., Nidergang, C., Masson, M., and de Murcia, G. (1996) "Workshop on Processing of DNA damage: "Molecular Mechanisms and Biological Effects, Noordwijkerhout, The Netherlands, April 20–25, 1996," p. 186.

11. Whitacre, C. M., Hashimoto, H., Tsai, M.-L., Chatterjee, S., Berger, S. J., and Berger, N. A. (1995) *Cancer Res.* **55**, 3697–3701.

12. Tewari, M., Quan, L. T., O'Rourke, K., Desnoyers, S., Zeng, Z., Beidler, D. R., Poirier, G. G., Salvesen, G. S., and Dixit, V. M. (1995) *Cell* **81**, 801–809.

13. Nicholson, D. W., Ali, A., Thornberry, N. A., Vaillancourt, J. P., Ding, C. K., Gallant, M., Gareau, Y., Griffin, P. R., Labelle, M., Lazebnik, Y. A., Munday, N. A., Raju, S. M., Smulson, M. E., Yamin, T. T., Yu, V. L., and Miller, D. K. (1995) *Nature* **376**, 37–43.

14. Neamati, N., Fernandez, A., Wright, S., Kiefer, J., and McConkey, D. J. (1995) *J. Immunol.* **154**, 3788–3795.

15. Berger, N. A., Sims, J. L., Catino, D. M., and Berger, S. J. (1983) *in* ADP-Ribosylation, DNA Repair and Cancer (M. Miwa, O. Hayaishi, S. Shall, M. Smulson, and T. Sugimura, Eds.), Proceedings of the 13th International Symposium of the Princess Takamatsu Cancer Research Fund, pp. 219–226, Japan Scientific Societies Press, Tokyo.

16. Kaufmann, S. H., Desnoyers, S., Ottaviano, Y., Davidson, N. E., and Poirier, G. G. (1993) *Cancer Res.* **53**, 3976–3985.

17. Yuan, J., Shaham, S., Ledoux, S., Ellis, H. M., and Horvitz, H. R. (1993) *Cell* **75**, 641–652.

18. Alkhatib, H. M., Chen, D. F., Cherney, B., Bhatia, K., Notario, V., Giri, C., Stein, G., Slattery, E., Roeder, R. G., and Smulson, M. E. (1987) *Proc. Natl. Acad. Sci. USA* **84**, 1224–1228.

18a. Rosenthal, D. S., Ding, R., Simbulan-Rosenthal, C. M. G., Cherney, B., Vanck, P., and Smulson, M. (1997) *Nucl. Acids Res.*, in press.

19. Durkacz, B. W., Omidiji, O., Gray, D. A., and Shall, S. (1980) *Nature* **283**, 593–596.

20. Wielckens, K., George, E., Pless, T., and Hilz, H. (1983) *J. Biol. Chem.* **258**, 4098–4104.

21. Le Cam, E., Fack, F., Menissier-de Murcia, J., Cognet, J. A., Barbin, A., Sarantoglou, V., Revet, B., Delain, E., and de Murcia, G. (1994) *J. Mol. Biol.* **235**, 1062–1071.

22. Jacobson, E. L., Meadows, R., and Measel, J. (1985) *Carcinogenesis* **6**, 711–714.

23. Cleaver, J. E., Borek, C., Milam, K., and Morgan, W. F. (1985) *Pharmacol. Ther.* **31**, 269–293.

24. Hunting, D., Gowans, B., and Henderson, J. F. (1985) *Biochem Pharmacol.* **34**, 3999–4003.

25. Milam, K. M., and Cleaver, J. E. (1984) *Science* **223**, 589–591.

26. Nosseri, C., Coppola, S., and Ghibelli, L. (1994) *Exp. Cell Res.* **212**, 367–373.

27. Liang, T. C., Luo, W., Hsieh, J.-T., and Lin, S.-H. (1996) *Arch. Biochem. Biophys.* **329**, 208–214.

28. Muller, S., Briand, J.-P., Barakkkat, S., Lagueux, J., Poirier, G. G., De Murcia, G., and Isenberg, D. A. (1994) *Clin. Immunol. Immunopathol.* **73**, 187–196.

29. Kressel, M., and Groscurth, P. (1994) *Cell Tissue Res.* **278**, 549–556.

The E7 protein of human papillomavirus type 16 sensitizes primary human keratinocytes to apoptosis

Hubert Stöppler[1], Melissa Conrad Stöppler[2], Elizabeth Johnson[3], Cynthia M Simbulan-Rosenthal[4], Mark E Smulson[4], Sudha Iyer[4], Dean S Rosenthal[4] and Richard Schlegel[3]

[1]Institute of Pharmacology and Toxicology, Philipps University of Marburg, Karl-von-Frisch Str. 1, 35033 Marburg, Germany; [2]Department of Pathology, Philipps University of Marburg, Klinikum Lahnberge, Baldingerstr. 35043 Marburg, Germany; [3]Molecular Pathology Program, Department of Pathology and [4]Department of Biochemistry and Molecular Biology, Georgetown University, 3900 Reservoir Road, Washington, DC 20007, USA

The 'high risk' human papillomaviruses are associated with the development of anogenital carcinomas and their E6 and E7 genes possess immortalizing and transforming functions in several in vitro culture systems. Recently the E6 gene has also been shown to enhance the apoptosis of human mammary epithelial cells. To determine the apoptotic activity of these oncogenes in the natural host cell, we infected genital keratinocytes with retroviruses expressing either HPV-16 E6, E7, or both the E6 and E7 (E6/7) genes. Apoptosis was quantitated under normal growth conditions or when induced by tumor necrosis factor α/cycloheximide or sulfur mustard. In contrast to previous findings with mammary epithelial cells, the E6 gene did not significantly augment either spontaneous or induced apoptosis. E6 also did not suppress apoptosis in normal keratinocytes (despite dramatically reducing their p53 levels), suggesting that p53-independent events mediated this effect. In contrast, E7 increased both spontaneous and induced apoptosis as well as the cellular levels of p53 and p21 protein. Interestingly, co-expression of E6 abrogated E7-facilitated apoptosis by tumor necrosis factor α nearly completely, but had only a minor protective effect on sulfur mustard induced apoptosis in these cells, demonstrating at least in part the p53-dependence and -independence of these two apoptotic pathways. Finally, our results indicate that the apoptosis of normal and E7-expressing keratinocytes is differentially affected by E6 expression and that E7, when unaccompanied by E6, sensitizes keratinocytes to apoptosis.

Keywords: HPV E6 and E7 oncogenes; apoptosis; p53; primary keratinocytes; extended life span

Introduction

Human papillomaviruses (HPV) infect and replicate in stratified squamous epithelia at specific anatomic sites and induce a concomitant hyperplasia of the infected tissues (de Villiers, 1989). A subgroup of the HPV's infecting the genital mucosa are the 'high-risk' human papillomaviruses (e.g. HPV-16 and -18) which are strongly associated with the malignant conversions of anogenital tract lesions (zur Hausen, 1991). The E6 and E7 genes of the 'high-risk' HPV's are responsible for the transforming/immortalizing activity of the viral genome (Mansur and Androphy, 1993; Stöppler et al., 1994). For example, the co-expression of the E6 or E7 gene with an activated oncogene (e.g. ras) leads to immortalization of primary rodent cells (Chesters and McCance, 1989; Crook et al., 1991a; Liu et al., 1994; Peacock et al., 1990; Phelps et al., 1988; Storey and Banks, 1993; Storey et al., 1988). The expression of either the E6 or E7 genes is also sufficient to transform immortalized rodent cells (Bedell et al., 1989; Kanda et al., 1988; Sedman et al., 1991; Tanaka et al., 1989; Vousden et al., 1988). Finally, the combined expression of E6 and E7 efficiently immortalizes primary human keratinocytes (Barbosa and Schlegel, 1989; Hawley-Nelson et al., 1989; Hudson et al., 1990; Münger et al., 1989; Sedman et al., 1991), although it does not induce directly the tumorigenic phenotype. Additional cellular genetic changes appear requisite for malignant progression.

The oncogenic properties of E6 and E7 viral proteins correlate with their ability to interfere respectively with the functions of two cellular tumor suppressor proteins, p53 (Huibregtse et al., 1991, 1993; Scheffner et al., 1990, 1992) and Rb (or Rb-related proteins) (Davies et al., 1993; Dyson et al., 1989, 1992). Thus, the oncogenic activity of 'high risk' E7 proteins is at least partly due to its interference with Rb/E2F interactions and the consequent loss of cell cycle control functions of the Rb protein (Goodrich and Lee, 1993). Similarly, the transforming activity of E6 appears partly due to its ability to target p53 protein for ubiquitination and consequent degradation (Crook et al., 1991b; Goodrich and Lee, 1993; Hubbert et al., 1992; Huibregtse et al., 1991, 1993; Li and Coffino, 1996; Scheffner et al., 1990, 1992; Werness et al., 1990). However, since E6 proteins which are unable to target p53 for degradation have a weak immortalizing activity (Band et al., 1993), it is possible that there is an additional cellular target(s) for the E6 protein. Recently two additional E6-associated proteins, E6-BP (Chen et al., 1995) and paxillin (Tong and Howley, 1997), have been discovered which may play a role in cellular transformation. Furthermore, the expression of high risk E6 proteins in primary keratinocytes increases telomerase activity prior to cell immortalization. Normally, telomerase activity is lost in keratinocytes prior to cell senescence (Klingelhutz et al., 1996; Stöppler et al., 1997).

The p53 degradation functions of the E6 proteins are necessary for the efficient immortalization of mammary epithelial cells (MEC) (Band et al., 1990, 1991; Dalal et al., 1996; Wazer et al., 1995) and human kidney cells (Nakagawa et al., 1995). However, despite the loss of p53 protein in E6-immortalized mammary epithelial cells, there is an increased sensitivity to the induction of apoptosis (Xu et al., 1995). In direct contrast, the expression of E6 in transformed cells increases the resistance to the induction of apoptosis (Xu et al., 1995; Thomas et al., 1996; Hickman et al., 1997). The influence of an E6 or E7 expression on apoptosis has been further analysed in the lens morphogenesis of transgenic mice expressing E6, E7 or E6 and E7 (Pan and Griep, 1994, 1995). E6 expression inhibits apoptotic events necessary for the normal development of the eye, whereas E7 transgenic mice demonstrate spatially inappropriate cell proliferation and apoptosis during lens development.

To determine the effects of a HPV-16 E6 or E7 expression on the apoptosis of the natural host cell, the genital keratinocyte, we used retroviruses expressing the E6, E7, or E6 plus E7 (E6/7) genes. Foreskin keratinocytes transduced with any of these recombinant retroviruses exhibit an 'extended life span', compared to keratinocytes infected with control retrovirus (Klingelhutz et al., 1994, 1996; Stöppler et al., 1997). 'Extended life span' cells have not yet undergone an immortalization (M2) crisis, which allows the analysis of effects of viral gene expression independently from the immortalization event. When HPV oncogene transduced cells were evaluated for apoptosis induced by either TNF α or sulfur mustard, E6-transduced cells showed a slight increase in comparison to control cells whereas E7-transduced cells showed a 5–10-fold increase in apoptotic signaling. Cells transduced with E6/7 showed either a slight increase in apoptotic response in comparison to control cells or an intermediate apoptotic response between that of control cells and E7 transduced cells, depending upon the agent used for inducing apoptosis. E7 was also able to enhance spontaneous apoptosis in keratinocytes, although the effect was less pronounced than that observed during induced apoptosis.

Results

Induction of an 'extended life span' in primary human keratinocytes

Primary human foreskin keratinocytes, which possess a limited life span in vitro and can be passaged only 10–12 times (equivalent to 50–60 population doublings) prior to senescence, were infected with recombinant retroviruses encoding E6, E7, or E6/7 genes as well as the neomycin resistance gene. The cells were then selected in G418 and analysed for their sensitivity to apoptosis. The cells could be cultured for at least twenty passages, indicating that they had an 'extended life span' and had bypassed M1 crisis (the point at which control-transduced cells ceased cell division (Klingelhutz et al., 1994; Stöppler et al., 1997). These cells, however, had not bypassed M2 crisis (cell immortalization) (Shay et al., 1991; Wright et al., 1989) and could not routinely be established

into cell lines. All evaluations of apoptosis were performed on these non-immortalized, post M1 crisis cells.

E7-transduced keratinocytes exhibit the highest levels of spontaneous apoptosis

The percentage of apoptotic cells in post M1 crisis cultures of primary keratinocytes was evaluated by both morphological and biochemical methods. Figure 1 demonstrates an in situ DNA-labeling of fragmented DNA of confluent, primary epithelial cells infected with the control (LXSN), E6, E7, or E6/7 retroviruses. This staining technique visualizes cells with nicked chromosomal DNA, a hallmark of apoptotic cells. E7-expressing cells showed the highest level of nuclear staining, indicating a greater degree of DNA breakage. Control transduced cells showed the lowest levels of staining.

The in situ DNA labeling results were confirmed by staining these same keratinocyte strains with bisbenzimide (Hoechst 33258) to detect chromatin condensation and fragmentation in the nuclei of apoptotic cells. Figure 2 summarizes the results of three independent experiments in which the percentage of apoptotic cells was quantitated. Approximately 1.5–2.0% of the E7-expressing cells were spontaneously apoptotic, in contrast to 0.5% of control cells. An intermediate apoptosis rate (1%) was observed in E6 or E6/7 cells. The overlap in experimental values between E6 and E6/7 expressing cells precluded making definitive conclusions regarding the differences in the activities of these constructs.
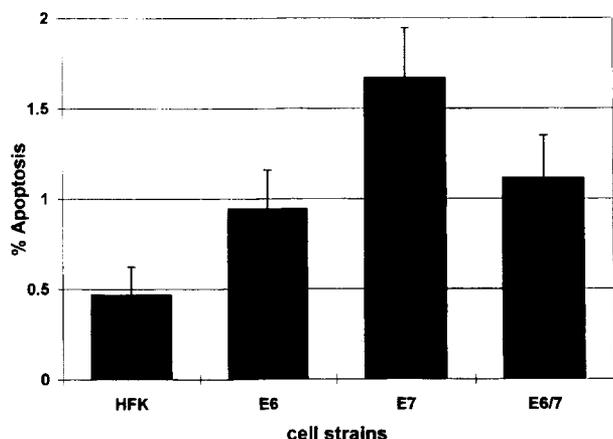

LXSN   E6

E7   E6/7
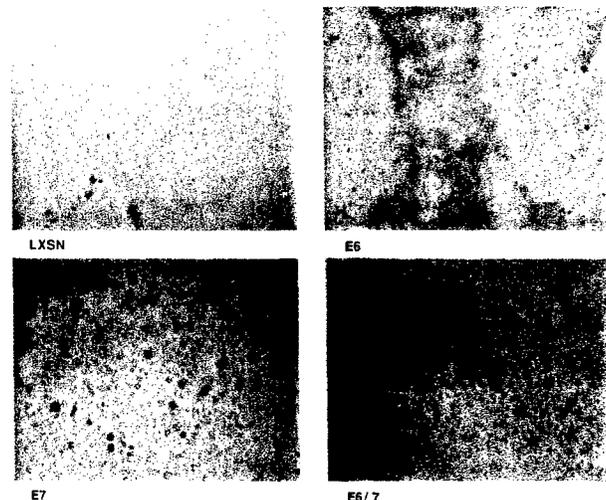
Figure 1 In situ labeling of fragmented DNA is highest in the nuclei of E7-transduced keratinocytes. Keratinocytes were transduced with retroviruses expressing either the empty vector, LXSN, or the HPV-16 E6, E7, or E6/7 genes. Spontaneous keratinocyte apoptosis during growth in culture medium was monitored by in situ DNA labeling of fragmented DNA (see Materials and methods) in which staining of the nucleus is an indicator of DNA breakage. The highest number of in situ DNA-labeled nuclei was observed in E7-expressing cells whereas the nuclei of vector- and E6-transduced were nearly completely negative. Cells transduced with E6/7 showed an intermediate number of positive nuclei. The small spots in E6/7-expressing cells are artifacts of the staining procedure. Microscopic magnification 100×

TNF α/cycloheximide treatment augments the apoptotic-inducing activity of E7

In an effort to amplify the apoptotic signal in the transduced keratinocytes and to better differentiate between control and transduced cells, we utilized a well-characterized inducer of apoptosis, TNF α. Primary keratinocytes were treated with 10 ng/ml TNF α and 30 μg/ml cycloheximide and then assayed for apoptotic cells by staining with bisbenzimide as described in the legend of Figure 3a. Qualitatively, E7-transduced cells showed the highest percentage of apoptotic nuclei. When the staining was quantitated (Figure 3b), approximately 1.0% of the TNF α-treated control cells were apoptotic, representing a twofold increase compared to the spontaneous rate (0.5%). Primary keratinocytes were relatively resistant to this induction procedure. In contrast, TNF α induced 12% of the E7-expressing keratinocytes to undergo apoptosis, indicating that E7 had preferentially sensitized these cells. There was now a 12-fold difference in apoptosis between control and E7-transduced cells. E6- and E6/7-transduced cells showed only minimal induction of apoptosis by TNF α (2–3-fold).

A cell death ELISA confirms the sensitization of E7-transduced cells to apoptosis

To validate the morphologic increase of apoptosis in E7-transduced keratinocytes, we performed an ELISA technique (see Materials and methods) to quantitate the amount of histone/DNA fragment complexes which are present in the cytoplasm of apoptotic cells (Figure 4). This independent assay confirmed that E7-transduced keratinocytes were more sensitive (in this case, eightfold) to TNF α-induced apoptosis than control cells. As previously shown in Figure 3, the co-expression of E6 reduced E7-induced apoptotic sensitivity in E6/7-transduced cells close to the levels of E6 cells. The values for apoptosis in non-induced

control cells were near the limit of experimental detection and, although no reliable conclusion can be made with respect to quantitative differences, cells expressing the E7 and E6/7 genes showed a slight increase in apoptosis in comparison to E6 or control cells in this assay.

Keratinocytes sensitized to apoptosis by E7 contain increased amounts of p53 and p21 protein

To determine whether there was any correlation between the apoptotic sensitivity of the transduced keratinocytes and their expression of p53 protein, a regulator of cellular apoptosis, we screened the above cell strains by Western blotting analysis using a p53-specific monoclonal antibody (Figure 5). The expression of E6 or E6/7 induced a dramatic decrease in p53 levels, a finding which is consistent with the known

a

HFK   E6

E7   E6/7

b
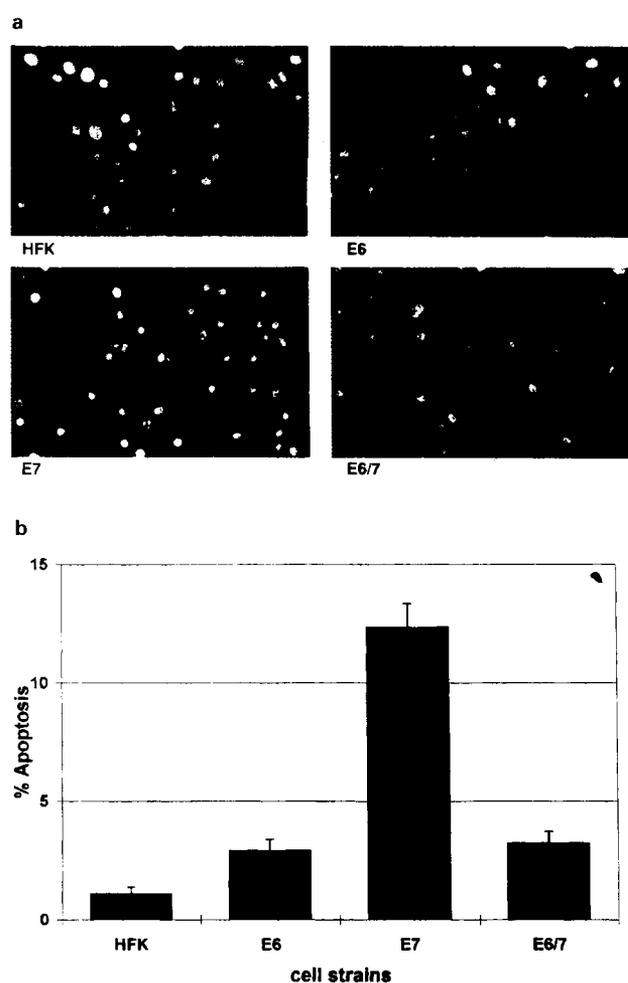
Figure 3 TNF α/cycloheximide treatment augments E7-facilitated apoptosis. (a) Keratinocytes transduced with vector (HFK), E6, E7, and E6/7 were treated for 6 h with TNF α/cycloheximide (see Materials and methods) and then fixed with methanol and stained with bisbenzimide (Hoechst 33258). Characteristic apoptotic changes of chromatin condensation and nuclear fragmentation were observed in a portion of the cell nuclei. E7-expressing cells demonstrated the most prominent degree of nuclear fragmentation. Microscopic magnification 400 ×. (b) For quantitation, 300 cells were counted and evaluated for nuclear morphological evidence of apoptosis. The percentage of apoptotic nuclei for each of the keratinocyte strains is indicated and the bar indicates the standard error of the mean for three independent experiments

Figure 2 E7-transduced keratinocytes display increased nuclear fragmentation. The spontaneous rate of apoptosis in subconfluent, transduced keratinocytes was analysed in three separate experiments utilizing bisbenzimide (Hoechst 33258) staining (see Materials and methods) to detect the nuclear fragmentation characteristic of apoptosis. In each experiment 300 cells were counted and evaluated for nuclear changes (e.g. Figure 3). Bars indicate the standard error of the mean

ability of E6 to target p53 for ubiquitination and degradation. In marked contrast, E7-transduced cells with an 'extended life span' showed increased amounts of p53 protein, which is in agreement with the previous finding of elevated steady state p53 levels in cells immortalized by E7 (Demers et al., 1994).

To determine whether the increase in p53 had functional consequences, we evaluated the expression
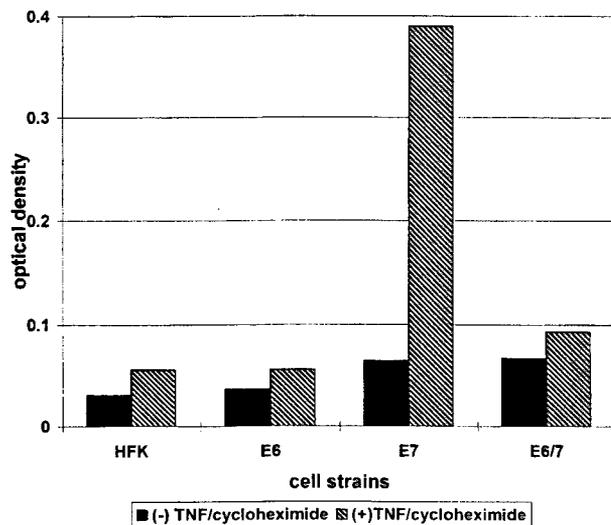
Figure 4 A cell death ELISA confirms that TNF α/cyclohex-imide treatment enhances the apoptosis of E7-transduced keratinocytes. Cytoplasmic extracts of untreated and TNF α/cycloheximide-treated keratinocytes were prepared as described in Materials and methods. An ELISA technique was used to quantitate the amount of histone/DNA fragment complexes present in the cytoplasm, an independent indicator of apoptotic change. Similar to the morphological findings in Figure 3, the ELISA demonstrated that TNF α-treated, E7-transduced keratinocytes displayed the highest level of apoptosis
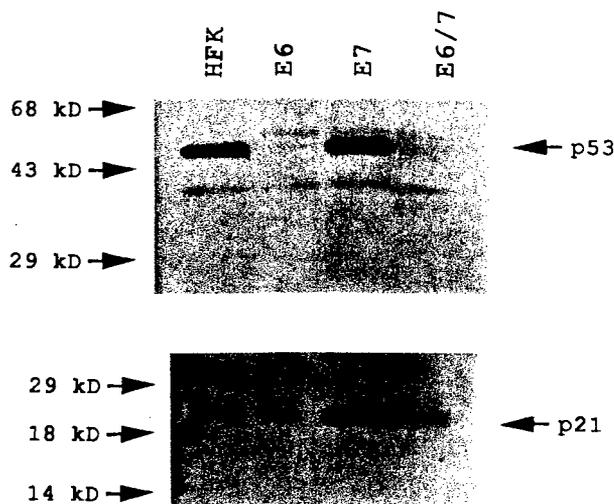
Figure 5 E7-transduced keratinocytes have elevated levels of p53 and p21 protein. The expression of p53 and p21 in control primary keratinocytes and HPV-16 E6, E7 and E6/7 transduced primary keratinocytes was analysed by Western blot using 50 μg of whole protein cell extract (see Materials and methods). The steady state level of p53 was elevated in E7-expressing cells in comparison to vector-transduced keratinocytes. Little or no p53 protein was detected in the E6 or E6/7 transduced cells. The increased steady state level of p53 in E7-expressing cells correlated ...

of a cell regulatory protein, p21, which is normally up-regulated at the transcriptional level by p53 (El-Deiry et al., 1993, 1994). p21 protein was increased in E7-transduced cells (high p53) and decreased in E6- or E6/7-expressing cells (low p53), although the decrease of p21 in E6-expressing cells was not as profound as the loss of cellular p53 (Figure 5). Regardless, it is apparent that the increase in cellular p53 in E7-transduced cells was biologically functional.

Sulfur mustard further increases keratinocyte apoptosis, permitting the detection of poly(ADP-ribose)polymerase (PARP) breakdown

Treatment of keratinocytes by TNF α cycloheximide induced an apoptosis rate of approximately 12%. However, these levels were insufficient to detect the apoptotic-specific breakdown of poly(ADP-ribose) polymerase (PARP) through the ICE like protease, caspase (also known as 'apopain'). Caspase-3 appears to be a converging point for distinct apoptotic pathways (Nicholson et al., 1995) and, in an number of analysed systems, caspase-3 cleaves key proteins involved in the structure and integrity of the cell, including PARP. We treated transduced keratinocytes with sulfur mustard in order to induce a higher rate of apoptosis in these cells (Dabrowska et al., 1996; Rosenthal et al., 1998) and thereby allow us to determine whether the caspase pathway was activated during E7-augmented apoptosis. Preliminary studies showed that the treatment of the cells with 50 μM sulfur mustard was sufficient to induce apoptosis (by bisbenzimide staining) in 40% of the E7-transduced cells (data not shown). Protein extracts of sulfur mustard treated cells were evaluated for their ability to cleave the 116 kD PARP protein to an 89 kD product (Figure 6a). Control cells and E6-transduced keratinocytes demonstrated the weakest response; in each case approximately 3% of PARP (measured with a Phos-phorimager; see Materials and methods) was cleaved following treatment with 50 μM sulfur mustard (Figure 6b). E7-transduced cells, however, cleaved approximately 24% of PARP and E6/7-expressing cells showed a somewhat lower conversion (20%). Treatment of the cells with 100 μM sulfur mustard increased the apoptotic breakdown of PARP in primary keratinocytes and E6-expressing cells to approximately 12%, while E7- and E6/7-expressing cells demonstrated no further increase in PARP breakdown.

Discussion

In the current study, we analysed the effects of expressing the E6 and E7 oncogenes (alone or together) on the rate of spontaneous and induced apoptosis in the natural host cell for HPV-16, the genital keratinocyte. In contrast to previous studies with mammary epithelial cells (Xu et al., 1995), the E6 gene had only a minor effect on cellular apoptosis. Rather, the E7 gene was found to strongly sensitize keratinocytes to apoptosis, despite the observation that this gene can independently, but infrequently, immortalize keratinocytes (Halbert et al., 1991). There are parallels for E7 biological activity at the molecular

level; the interaction of E7 with Rb appears not only responsible for the transforming and immortalizing activity of E7, but it might also be responsible for cell sensitization to apoptosis. E7 is known to uncouple E2F function from Rb regulation, and a deregulated E2F activity has been shown to induce apoptosis (Qin et al., 1994; Shan and Lee, 1994; Wu and Levine, 1994) in 32D.3 cells, apparently by a p53-independent mechanism (Hiebert et al., 1995).

The observed sensitization to apoptosis in the E7-transduced cells is in agreement with the effect of E7 expression on the lens development in transgenic mice (Pan and Griep, 1994, 1995). E7 expression in the murine lens, in which apoptosis is necessary for an orderly development of the eye during embryogenesis,

leads to spatially inappropriate cell proliferation and apoptosis. The cell proliferation and apoptotic effects of E7 on murine lens development correlate with its known extension of life span (Klingelhutz et al., 1994; Stöppler et al., 1997) as well as its apoptosis sensitizing activity (current study).

The E6 and E6/7-dependent induction of the 'extended life span' in primary keratinocytes was also accompanied by a slight increase in spontaneous apoptosis in comparison to the non HPV gene expressing control cells. Interestingly, even the expression of E6 alone in these cells, which led to a drastic reduction in cellular p53 levels, was unable to protect the keratinocytes from a higher rate (about twofold) of spontaneous apoptosis in comparison to the control cells. A similar effect was observed in E6-transduced cells following the induction of apoptosis by TNF α. The increased rate of apoptosis in E6 expressing cells together with the drastic decrease of p53 levels in these cells suggests that keratinocytes are able to undergo, at least in part, a p53 independent apoptosis. The inability of E6 to inhibit, or at least reduce, the apoptotic rate of primary control keratinocytes is in contrast with the observed ability of E6 to inhibit p53 dependent and independent apoptosis events in the transgenic mouse lens (Pan and Griep, 1994, 1995).

When expressed alone, E7 induced p53 expression in post M1 crisis ('extended life span') cells in comparison to control cells. The increase in p53 levels subsequent to E7 expression has been described previously in epithelial cells (Demers et al., 1994), and in our study the elevated levels of p53 were accompanied by an increase in p21 protein, a downstream target of p53. It is probable that the overexpression of p53 plays a role in E7-induced apoptosis as it does in other systems (Gottlieb and Oren, 1996) and that the reduction of apoptosis in E6/7-transduced cells (either spontaneous or TNF α-induced) is a consequence of degradation of cellular p53 protein by E6 as observed in other cell types (Thomas et al., 1996; Yu et al., 1997). Nevertheless the observation that E6/7-transduced primary human keratinocytes demonstrated slightly higher levels of spontaneous and TNF α-induced apoptosis than control cells, suggested that the E6 expression in E6/7 transduced cells could not fully counteract the E7 induced apoptotic effects. This was most obvious when using a stronger inducer of apoptosis, sulfur mustard. Sulfur mustard-induced E6/7 cells clearly demonstrated a significantly higher apoptotic rate than E6 expressing cells, which was intermediate between the apoptotic rates of E6 and E7 cells. The simplest explanation for these opposite phenotypes induced by TNF α and sulfur mustard is the hypothesis that the apoptotic pathways used are at least in part p53-dependent and -independent mechanisms, respectively.

It is possible that the apoptotic-tempering effects of E6 on E7 may explain the synergistic interactions between these two genes for mediating cell immortalization. By reducing E7-induced apoptosis, E6 would facilitate the progression of a greater number of cells from the M1 'extended life span' phase of cell growth to the M2 phase of cell immortalization crisis. The frequency of cell immortalization would thereby be increased.

In contrast to our current studies with pre-immortalized keratinocytes it appears that immorta-
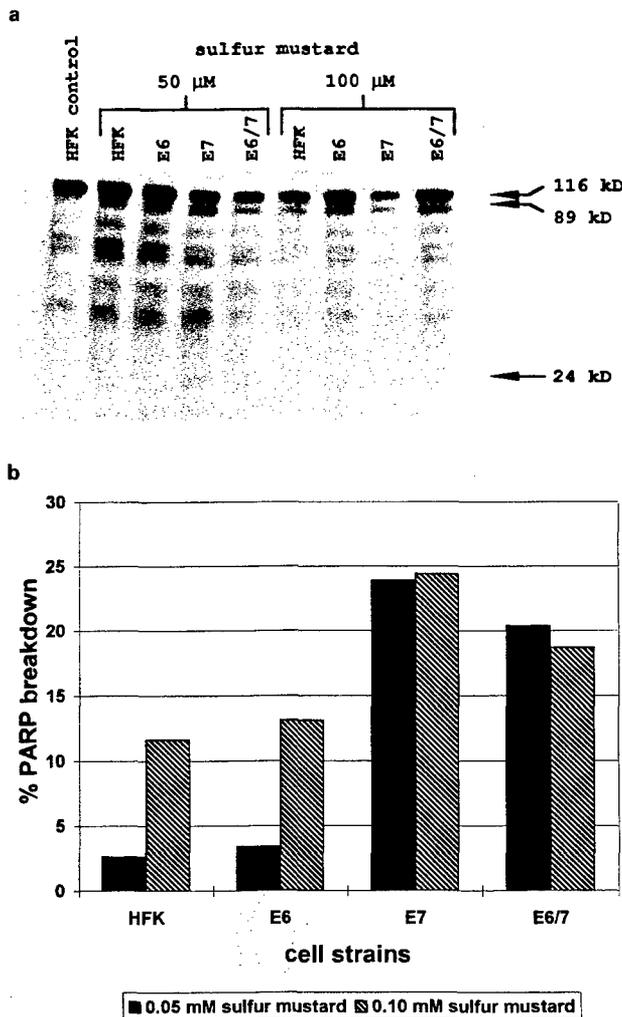
Figure 6 Sulfur mustard-induced apoptosis is enhanced by both E7 and E6/7 and is accompanied by PARP cleavage. (a) The keratinocyte strains described in the previous figures were treated with 50 or 100 μM sulfur mustard for 24 h. Cytoplasmic extracts were then prepared and assayed for apopain activity using [^{35}S]PARP as a substrate (see Materials and methods). Full-length PARP (119 kD) can be visualized in all lanes. The 89 kD PARP cleavage product is readily detected in cells expressing E7 following treatment with 50 μM sulfur mustard. (b) Quantitative autoradiography of the above experiment was performed with a phosphorimage analyser and evaluated for the conversion of the 119 to the 89 kD form of PARP. Both the E7- and E6/7-transduced keratinocytes displayed increased apopain cleavage activity indicative of an enhanced apoptotic response.

lized keratinocytes (expressing the E6/E7 genes) are resistant to some effects of TNF α (Villa *et al.*, 1992). For example, while primary keratinocytes are sensitive to TNF-mediated growth inhibition, HPV-16- or HPV-18-immortalized keratinocytes are resistant, with HPV-18 cells being the most resistant. Evidently there are additional genetic or epigenetic alterations which occur during immortalization which render keratinocytes less sensitive to the effects of TNF. However, as shown in the current study, pre-immortal cells expressing E6/E7 still retain their sensitivity to TNF-induced apoptosis.

Materials and methods

Cell culture

Primary human keratinocytes were derived from neonatal foreskins as described and grown in KSF medium (Life Technologies Inc., Rockville, Maryland, USA) supplemented with gentamycin. The primary cells were infected with derivatives of the amphotropic LXSN retrovirus expressing the various HPV-16 open reading frames (E6, E7, or E6 plus E7). The retroviruses were generated as described (Miller and Rosman, 1989) using existing recombinant vectors (Sherman and Schlegel, 1996). Retrovirus-infected cells were selected in G418 (100 μg/ml medium) for 10 days. G418- resistant colonies were pooled from each transduction and passed every 3–4 days (ratio of 1:5).

TNF α/cycloheximide treatment

The various cells strains were trypsinized 24 h before the induction of apoptosis and passaged at equal cell densities. Twenty-four hours after passaging, cells were treated for 6 h with medium containing 10 ng/ml TNF α (human recombinant expressed in yeast, Sigma) and 30 μg/ml cycloheximide (Sigma) in tissue culture medium.

Sulfur mustard treatment

Sulfur mustard (bis-(2-chloroethyl)sulfide; >98% purity) was obtained from the US Army Edgewood Research, Development and Engineering Center. Cells were grown in 75 cm^2 tissue culture flasks to 60–80% confluency, then exposed to sulfur mustard in KSF medium to final concentration of 50 or 100 μM. Media was not changed for the duration of the experiments (24 h).

Bisbenzimide (Hoechst 33258) staining

Following TNF α treatment, the cells were fixed for 5–10 min over methanol fumes at room temperature and then submerged for an additional 5–10 min in methanol at room temperature. Fixed cells were then allowed to air dry and stained for 10 min with bisbenzimide (Hoechst 33258 dye (Sigma) 0.5 μg/ml in PBS). The cells were washed three times with PBS followed by mounting (Fluoromount-G, Southern Biotechnology Associates, Inc.) the cells with a cover slip. The morphology of nuclei was evaluated under a Zeiss Axioskope microscope at a magnification of 400 $\times$.

Detection of DNA fragmentation / in situ DNA-labeling

DNA breaks were detected *in situ* using a Klenow fragment-based assay. Cells were fixed and labeled with biotinylated dUTP (200 pM) for 30 min at room temperature in reaction buffer containing 200 μM dA,G,CTP, 50 U/ml Klenow, 50 mM Tris-Cl (pH 7.5), 5 mM MgCl$_2$ 10 mM β-mercap-

detected using streptavidin-conjugated horseradish peroxidase and VIP substrate (Vector).

PARP cleavage assay

The full-length cDNA clone for PARP (pcD-12 (Alkhatib *et al.*, 1987)) was excised and ligated into the *Xho*I site of pBluescript-II SK$^+$ (Stratagene) then used to drive the synthesis of PARP labeled with ^{35}S-methionine (Dupont-NEN) by coupled T7 transcription/translation in a reticulocyte lysate system (Promega). [^{35}S]PARP was separated from the other constituents by gel filtration chromatography on a Superdex-75 FPLC column (Pharmacia; 1 $\times$ 30 cm) in 10 mM HEPES-KOH (pH 7.4), 2 mM EDTA; 0.1% (w/v) CHAPS and 5 mM dithiothreitol.

Cytosolic extracts were prepared from the cells by scraping PBS-washed monolayers in 10 mM HEPES/KOH (pH 7.4), 2 mM EDTA, 0.1% CHAPS, 5 mM dithiothreitol, 1 mM phenylmethylsulphonylfluoride, 10 μg/ml pepstatin A, 20 μg/ml leupeptin, 10 μg/ml aprotinin (at 1 $\times$ 10^8 cell/ml). The post-100 000 g supernatant was recovered after centrifugation.

PARP cleavage activity was measured in mixtures containing 5 μg protein from the cytosol fractions of keratinocytes. Assay mixtures also contained purified [^{35}S]PARP ($\sim$5 $\times$ 10^4 c.p.m.), 50 mM PIPES-KOH, 2 mM EDTA, 0.1% (w/v) CHAPS, and 5 mM dithiothreitol in a total volume of 25 μl. Incubations were performed at 37°C for 1 h, and terminated by addition of 25 μl of 2 $\times$ SDS–PAGE sample buffer containing 4% SDS, 4% β-mercaptoethanol, 10% glycerol, 0.125 M Tris-Cl (pH 6.8) and 0.02% bromophenol blue. Samples were resolved by 10% SDS-polyacrylamide gels.

PARP cleavage products were visualized by fluorography and the 89 kDa cleavage product of [^{35}S]PARP was quantified relative to full-length PARP using a Storm 840 PhosphorImage analyzer (Molecular Dynamics). Quantification included a correction for background, as well as for the difference in methionine residues present in the 89 kDa fragment (18 methionine residues) *vs* full-length PARP (25 methionine residues).

Cell death ELISA

A cell death ELISA kit from Boehringer Mannheim (Indianapolis, IN, USA) was used for the ELISA assay. The cells were prepared as follows for the ELISA. The cells of the various cell strains were trypsinized and then suspended in DMEM medium containing 10% fetal calf serum. 7.5 $\times$ 10^6 cells of each cell strain were aliquoted into plastic tubes and pelleted by centrifugation (4°C, 900 g for 10 min). After removing the supernatant, 500 μl of lysis buffer was added. The pellets were carefully resuspended and kept for 30 min on ice for complete cell lysis. The ELISA conditions were in accordance with the manufacturer's instructions.

Western blot

Whole cell extracts were either obtained by repeated freezing and thawing (three times) of harvested cell pellets or by extracting the cells in protein sample buffer containing 2% SDS. The extracts were centrifuged at 10 000 g for 10 min at 4°C, the supernatant was separated from undissolved debris, and the protein concentrations of the supernatants were determined using a DC Protein Assay kit (Bio-Rad). Fifty μg of protein extract were separated on 10% SDS-polyacrylamide gels and blotted onto PVDF membranes (Millipore). p53 was detected using a monoclonal anti p53 antibody (anti p53 Ab2, Oncogene Science) and p21 with a monoclonal anti p21 antibody (clone 6B6, PharMingen) in conjunction with a

References

Alkhatib HM, Chen DF, Cherney B, Bhatia K, Notario V, Giri C, Stein G, Slattery E, Roeder RG and Smulson ME. (1987). *Proc. Natl. Acad. Sci.*, **84**, 1224–1228.

Band V, Dalal S, Delmolino L and Androphy EJ. (1993). *EMBO J.*, **12**, 1847–1852.

Band V, DeCaprio JA, Delmolino L, Kulesa V and Sager R. (1991). *J. Virol.*, **65**, 6671–6676.

Band V, Zajchowski D, Kulesa V and Sager R. (1990). *Proc. Natl. Acad. Sci. USA*, **87**, 463–467.

Barbosa MS and Schlegel R. (1989). *Oncogene*, **4**, 1529–1532.

Bedell MA, Jones KH, Grossman SR and Laimins LA. (1989). *J. Virol.*, **63**, 1247–1255.

Chen JJ, Reid CE, Band V and Androphy EJ. (1995). *Science*, **269**, 529–531.

Chesters PM and McCance DJ. (1989). *J. Gen. Virol.*, **70**, 353–365.

Crook T, Fisher C and Vousden KH. (1991a) *J. Virol.*, **65**, 505–510.

Crook T, Tidy JA and Vousden KH. (1991b) *Cell*, **67**, 547–556.

Dabrowska MI, Becks LL, Lelli Jr JL, Levee MG and Hinshaw DB. (1996). *Toxicol. Appl. Pharmacol.*, **141**, 568–583.

Dalal S, Gao Q, Androphy EJ and Band V. (1996). *J. Virol.*, **70**, 683–688.

Davies R, Hicks R, Crook T, Morris J and Vousden K. (1993). *J. Virol.*, **67**, 2521–2528.

de Villiers E-M. (1989). *J. Virol.*, **63**, 4898–4903.

Demers WG, Halbert CL and Galloway DA. (1994). *Virology*, **198**, 169–174.

Dyson N, Guida P, Münger K and Harlow E. (1992). *J. Virol.*, **66**, 6893–6902.

Dyson N, Howley PM, Münger K and Harlow E. (1989). *Science*, **243**, 934–937.

El-Deiry WS, Harper JW, O'Connor PM, Velculescu VE, Canman CE, Jackman J, Pietnepol JA, Burrell M, Hill DE, Wang Y, Wiman KG, Mercer WE, Kastan MB, Kohn KW, Elledge SJ, Kinzler KW and Vogelstein B. (1994). *Cancer Res.*, **54**, 1169–1174.

El-Deiry WS, Tokino T, Velculescu VE, Levy DB, Parsons R, Trent JM, Lin D, Mercer WE, Kinzler KW and Vogelstein B. (1993). *Cell*, **75**, 817–825.

Goodrich DW and Lee WH. (1993). *Biochim. Biophys. Acta*, **1155**, 43–61.

Gottlieb TM and Oren M. (1996). *Biochim. Biophys. Acta*, **1287**, 77–102.

Halbert CL, Demers GW and Galloway DA. (1991). *J. Virol.*, **65**, 473–478.

Hawley-Nelson P, Vousden KH, Hubbert NL, Lowy DR and Schiller JT. (1989). *EMBO J.*, **8**, 3905–3910.

Hickman EA, Bates S and Vousden KH. (1997). *J. Virol.*, **71**, 3710–3718.

Hiebert SW, Packham G, Storm DK, Haffner R, Oren M, Zambetti G and Cleveland JL. (1995). *Mol. Cell. Biol.*, **15**, 6864–6874.

Hubbert NL, Sedman SA and Schiller JT. (1992). *J. Virol.*, **66**, 6237–6241.

Hudson JB, Bedell MA, McCance DJ and Laimins LA. (1990). *J. Virol.*, **64**, 519–526.

Huibregtse JM, Scheffner M and Howley PM. (1991). *EMBO J.*, **10**, 4129–4135.

Huibregtse JM, Scheffner M and Howley PM. (1993). *Mol. Cell. Biol.*, **13**, 4918–4927.

Kanda T, Watanabe S and Yoshiike K. (1988). *Virology*, **165**, 321–325.

Klingelhutz AJ, Barber SA, Smith PP, Dyer K and McDougall JK. (1994). *Mol. Cell. Biol.*, **14**, 961–969.

Klingelhutz AJ, Foster SA and McDougall JK. (1996). *Nature*, **380**, 79–81.

Li X and Coffino P. (1996). *J. Virol.*, **70**, 4509–4516.

Liu Z, Ghai J, Ostrow RS, McGlennen RC and Faras AJ. (1994). *Virology*, **201**, 388–396.

Mansur CP and Androphy EJ. (1993). *Biochim. Biophys. Acta*, **1155**, 323–345.

Miller AD and Rosman GJ. (1989). *BioTechniques*, **7**, 980–990.

Münger K, Phelps WC, Bubb V, Howley PH and Schlegel R. (1989). *J. Virol.*, **63**, 4417–4421.

Nakagawa S, Watanabe S, Yoshikawa H, Taketani Y, Yoshiike K and Kanda T. (1995). *Virology*, **212**, 535–542.

Nicholson DW, Ali A, Thornberry NA, Vaillancourt JP, Ding CK, Gallant M, Gareau Y, Griffin PR, Labelle M, Lazebnik YA, Munday NA, Raju SM, Smulson ME, Yamin TT, Yu VL and Miller DK. (1995). *Nature*, **376**, 37–43.

Pan H and Griep AE. (1994). *Genes and Dev.*, **8**, 1285–1299.

Pan H and Griep AE. (1995). *Genes and Dev.*, **9**, 2157–2169.

Peacock JW, Matlashewski GJ and Benchimol S. (1990). *Oncogene*, **5**, 1769–1779.

Phelps WC, Yee CL, Munger K and Howley PM. (1988). *Cell*, **53**, 539–47.

Qin X-Q, Livingston DM, Kaelin Jr WG and Adams PD. (1994). *Proc. Natl. Acad. Sci. USA*, **91**, 10918–10922.

Rosenthal DS, Simbulan-Rosentnal CMG, Iyer S, Spoonde A, Smith W, Ray R and Smulson M. (1998). *J. Invest. Dermatol.*, **111**, 64–71.

Scheffner M, Takahashi T, Huibregtse JM, Minna JD and Howley PM. (1992). *J. Virol.*, **66**, 5100–5105.

Scheffner M, Werness BA, Huibregtse JM, Levine AJ and Howley PM. (1990). *Cell*, **63**, 1129–1136.

Sedman SA, Barbosa MS, Vass WC, Hubbert NL, Haas JA, Lowy DR and Schiller JT. (1991). *J. Virol.*, **65**, 4860–4866.

Shan B and Lee WE. (1994). *Mol. Cell. Biol.*, **14**, 8166–8173.

Shay JW, Wright WE and Werbin H. (1991). *Biochim. Biophys. Acta*, **1072**, 1–7.

Sherman L and Schlegel R. (1996). *J. Virol.*, **70**, 3269–3279.

Stöppler H, Conrad Stöppler M and Schlegel R. (1994). *Intervirology*, **37**, 168–179.

Stöppler H, Hartmann D-P, Sherman L and Schlegel R. (1997). *J. Biol. Chem.*, **272**, 13332–13337.

Storey A and Banks L. (1993). *Oncogene*, **8**, 919–924.

Storey A, Pim D, Murray A, Osborn K, Banks L and Crawford L. (1988). *EMBO J.*, **7**, 1815–1820.

Tanaka A, Noda T, Yajima H, Hatanaka M and Ito Y. (1989). *J. Virol.*, **63**, 1465–1469.

Thomas M, Matlashewski G, Pim D and Banks L. (1996). *Oncogene*, **13**, 265–273.

Tong X and Howley PM. (1997). *Proc. Natl. Acad. Sci. USA*, **94**, 4412–4417.

Villa LL and Schlegel R. (1991). *Virology*, **181**, 374–377.

Villa LL, Vieira KB, Pei XF and Schlegel R. (1992). *Mol. Carcinog.*, **6**, 5–9.

Vousden KH, Doniger J, DiPaolo JA and Lowy DR. (1988). *Oncogene Res.*, **3**, 167–175.

Wazer DE, Liu X-L, Chu Q, Gao Q and Band V. (1995). *Proc. Natl. Acad. Sci. USA*, **92**, 3687–3691.

Werness BA, Levine AJ and Howley PM. (1990). *Science*, **248**, 76–79.

Wright WE, Pereira-Smith OM and Shay JW. (1989). *Mol. Cell. Biol.*, **9**, 3088–3092.

Wu X and Levine AJ. (1994). *Proc. Natl. Acad. Sci. USA*, **91**, 3602–3606.

Xu C, Meikrantz W, Schlegel R and Sager R. (1995). *Proc. Natl. Acad. Sci. USA*, **92**, 7829–7833.

Yu Y, Li CY and Little Jb. (1997). *Oncogene*, **14**, 1661–1667.

zur Hausen H. (1991). *Virology*, **184**, 9–13.

Sulfur Mustard Induces Markers of Terminal Differentiation and Apoptosis in Keratinocytes Via a Ca²⁺-Calmodulin and Caspase-Dependent Pathway

Dean S. Rosenthal, Cynthia M.G. Simbulan-Rosenthal, Sudha Iyer, Alexander Spoonde,* William Smith,† Radharaman Ray,† and Mark E. Smulson

Department of Biochemistry and Molecular Biology, Georgetown University School of Medicine, Washington D.C., U.S.A.; *Pacific NW National Laboratories, Richland, Washington, U.S.A.; †US Army Medical Research Institute of Chemical Defense, Aberdeen Proving Ground, Maryland, U.S.A.

Sulfur mustard (SM) induces vesication via poorly understood pathways. The blisters that are formed result primarily from the detachment of the epidermis from the dermis at the level of the basement membrane. In addition, there is toxicity to the basal cells, although no careful study has been performed to determine the precise mode of cell death biochemically. We describe here two potential mechanisms by which SM causes basal cell death and detachment: namely, induction of terminal differentiation and apoptosis. In the presence of 100 µM SM, terminal differentiation was rapidly induced in primary human keratinocytes that included the expression of the differentiation-specific markers K1 and K10 and the cross-linking of the cornified envelope precursor protein involucrin. The expression of the attachment protein, fibronectin, was also reduced in a time- and dose-dependent fashion. Features common to both differentiation and apoptosis were also induced in 100 µM SM, including the rapid induction of p53 and the reduction of Bcl-2. At higher concentrations of SM (i.e., 300 µM), formation of the characteristic nucleosome-sized DNA ladders, TUNEL-positive staining of cells, activation of the cysteine protease caspase-3/apopain, and cleavage of the death substrate poly(ADP-ribose) polymerase, were observed both *in vivo* and *in vitro*. Both the differentiation and the apoptotic processes appeared to be calmodulin dependent, because the calmodulin inhibitor W-7 blocked the expression of the differentiation-specific markers, as well as the apoptotic response, in a concentration-dependent fashion. In addition, the intracellular Ca²⁺ chelator, BAPTA-AM, blocked the differentiation response and attenuated the apoptotic response. These results suggest a strategy for designing inhibitors of SM vesication via the Ca²⁺-calmodulin or caspase-3/PARP pathway. *Key words: BAPTA/caspase-3/poly(ADP-ribose) polymerase/W-7. J Invest Dermatol 111:64–71, 1998*

Sulfur mustard [bis-(2-chloroethyl) sulfide; SM] causes blisters in the skin via poorly understood mechanisms. Because SM is a strong alkylating agent, its ability to induce DNA damage via apurinic sites and endonucleolytic activation has been advanced as one possible pathway leading to vesication (Papirmeister *et al*, 1985). Similar to other agents that induce DNA strand breakage, SM activates the nuclear protein poly(ADP-ribose) polymerase (PARP), which drastically depletes levels of cellular nicotinamide adenine dinucleotide and adenosinetriphosphate (Wielckens *et al*, 1982; Alvarez *et al*, 1986), a mechanism proposed to induce cell death (Berger *et al*, 1983). We have recently examined this mechanism using a human skin graft derived from human keratinocytes stably transfected with a PARP anti-sense inducible vector (Rosenthal *et al*, 1995). Recent studies have further implicated PARP as an important player in apoptosis. Proteolytic cleavage of PARP was first demonstrated in

chemotherapy-induced apoptosis (Kaufmann *et al*, 1993) and the specific proteolysis of PARP is now closely associated with apoptosis in different systems (Neamati *et al*, 1995; Nicholson *et al*, 1995; Tewari *et al*, 1995). We recently showed that the reversible stage of apoptosis is characterized by the transient activation of PARP, and poly(ADP-ribosyl)ation of nuclear proteins followed by the breakdown of poly (ADP-ribose) and PARP (Rosenthal *et al*, 1997b).

Ca²⁺ also plays an important role in apoptosis, as well as in the maintenance and homeostasis of the skin, and SM has been shown to elevate intracellular levels of Ca²⁺ in keratinocytes (Ray *et al*, 1995; Mol and Smith, 1996). Several laboratories, including our own, have shown that terminal differentiation can be induced in both murine and human keratinocytes by the elevation of extracellular Ca²⁺ (Hennings *et al*, 1980; Stanley and Yuspa, 1983; Rosenthal *et al*, 1991b). This in turn results in an increase in intracellular free Ca²⁺ (Ca$_i$). Ca$_i$ appears to be an important signal for terminal differentiation, because agents that chelate and buffer Ca$_i$ can block markers of terminal differentiation (Li *et al*, 1995). Ca²⁺ has also been shown to play a role in apoptosis in a number of systems. Studies by Kaiser and Edelman (1977) showed the first evidence that Ca$_i$ may trigger apoptosis in glucocorticoid-stimulated thymocytes. Since then, several other studies have confirmed this role for Ca²⁺. The observed Ca$_i$ increase during apoptosis appears to occur by two different mechanisms. The first mechanism involves the activation of protein tyrosine kinases, leading to the activation of phospholipase C, the formation of IP3, and Ca²⁺

mobilization (Takata *et al*, 1995; Silvennoinen *et al*, 1996). The second pathway involves oxidative stress, which can occur in response to cytotoxic agents, such as SM, that generate reactive oxygen species. Oxygen radicals can damage Ca^{2+} transport systems localized in the endoplasmic reticulum (ER), mitochondria, and plasma membrane, leading to a disruption in Ca^{2+} homeostasis and a sustained increase in Ca_i (Orrenius *et al*, 1989).

Ca^{2+}-buffering experiments have supported the role of Ca^{2+} in the etiology of SM-induced cytotoxicity (Ray *et al*, 1996). Experiments utilizing specific inhibitors of calmodulin have also demonstrated the importance of Ca^{2+}-calmodulin complexes in programmed cell death. Cyclosporine A-sensitivity of apoptosis in certain systems also suggests a role for Ca^{2+}-calmodulin complexes in programmed cell death. Cyclosporine binds to a family of cytosolic receptors (cyclophilins); the complex then binds to and suppresses the serine/threonine phosphatase calcineurin, which in turn is regulated by Ca^{2+}-calmodulin complexes in programmed cell death (Shi *et al*, 1989). Ca^{2+} also plays a role in the induction of the endonuclease responsible for the internucleosomal DNA cleavage, yielding the characteristic apoptotic DNA ladders (Shiokawa *et al*, 1994).

Numerous recent studies have suggested that the ultimate targets for many of these signaling pathways that lead to apoptosis are a family of cysteine proteases, known as "caspases," named for their preference for aspartate at their substrate cleavage site (Alnemri *et al*, 1996). In collaboration with others, our laboratory has been particularly active in studying the characterization of caspase-3 (also known as "apopain"), which appears to be a converging point for different apoptotic pathways (Nicholson *et al*, 1995). In several apoptotic systems, caspase-3 cleaves key proteins involved in the structure and integrity of the cell, including PARP (Nicholson *et al*, 1995; Tewari *et al*, 1995; Casciola-Rosen *et al*, 1996; Song *et al*, 1996).

In this study, we show that SM induces both terminal differentiation and apoptosis in human keratinocytes. Further, we demonstrate that these processes are Ca^{2+} and/or calmodulin dependent, and involve the activation of caspase-3 as well as the activation and specific cleavage of PARP. These responses may, in part, explain the death and detachment of basal cells of the epidermis that occurs following exposure to SM.

MATERIALS AND METHODS

Cells Normal human epidermal keratinocytes (NHEK) were obtained as primary cultures from Clonetics (San Diego, CA) and maintained in serum-free keratinocyte growth medium. NHEK were grown in 75 cm^2 tissue culture flasks to 60–80% confluency, then exposed to SM diluted in keratinocyte growth medium to final concentrations of 100 μM or 300 μM. Media was not changed for the duration of the experiments. Cell viability was measured by the ability of cells to exclude trypan blue. For all studies, similar results were obtained from three independent experiments utilizing human primary adult keratinocytes and from three independent experiments utilizing human primary neonatal keratinocytes.

Chemicals SM (>98% purity) was obtained from the US Army Edgewood Research, Development and Engineering Center. Glycine, N,N'-[1,2-ethane-diylbis(oxy-2,1-phenylene)]bis[N-[2-[(acetyloxy)methoxy]-2-oxo-ethyl]]-bis[(acetyloxy)methyl]ester (BAPTA-AM) was purchased from Molecular Probes (Eugene, OR), as was Pluronic F-127, used to facilitate loading of BAPTA-AM into cells. N-(6-Aminohexyl)-5-chloro-1-napthalene-sulfonamide (W-7) was obtained from Sigma (St. Louis, MO). The tetrapeptide aldehyde inhibitor of caspase-3 (AcDEVD-CHO) was obtained from Biomol (Plymouth Meeting, PA).

Antibodies

Immunoblotting The following antibodies were obtained from Sigma: (i) mouse monoclonal antibody (clone 8.60) that recognizes both K1 and K10 keratins; (ii) monoclonal antibody (clone SY5) against the 68 kDa cornified envelope precursor, involucrin; (iii) a mixture of three monoclonal antibodies (clones 2D1, 1F11, and 6D4), recognizing a 17 kDa band corresponding to calmodulin; and (iv) affinity purified rabbit anti-serum against the attachment protein, fibronectin, recognizing both a 220 kDa and a 94 kDa form of the protein. Rabbit affinity-purified anti-peptide anti-sera specific for human K1 (AF87) was from Babco (Richmond, CA). Mouse monoclonal antibody (clone DO-1) recognizing human p53 is from Calbiochem (Cambridge, MA). Monoclonal

anti-human Bcl-2 antibody (clone 4D7) is from Biomol. Rabbit anti-peptide anti-sera specific for the N-terminal propeptide sequence of pro-caspase-3/apopain (CPP32) was obtained from Transduction Labs (Lexington, KY). Rabbit anti-sera against the p17 subunit of CPP32 was obtained from Donald Nicholson (Merck Frosst Center for Therapeutic Research, Pointe Claire-Dorval, Quebec, Canada). Rabbit anti-sera recognizing both full-length PARP, as well as the 89 kDa apoptotic cleavage product of PARP, was a kind gift from Eric Ackerman (Pacific NW National Laboratories, Richland, WA). Guinea pig anti-sera specific for poly(ADP-ribose) has been described (Rosenthal *et al*, 1995).

Fluorescence-activated cell sorter analysis FITC-conjugated anti-human cytokeratin ("CK") antibody (MNF116), recognizing keratins 10, 17, and 18, was from DAKO (Carpinteria, CA).

Immunoblot analysis For immunoblot analysis, sodium dodecyl sulfate-polyacrylamide gel electrophoresis-separated proteins were transferred to nitro-cellulose filters. Proteins were measured (DCA protein assay; BioRad), and normalized prior to gel-loading, and all filters were stained with Ponceau-S, in order to reduce the possibility of loading artifacts. The details for using rabbit anti-serum to human PARP (Ding *et al*, 1992) and guinea pig anti-serum to poly(ADP-ribose) (Rosenthal *et al*, 1995) for immunoblot analysis have been described previously in detail. Immune complexes were visualized by electro-chemiluminescence (Amersham Life Sciences, Arlington Heights, IL).

Fluorescence-activated cell sorter analysis At the designated time points, monolayer culture medium was decanted, trypsin-ethylenediamine tetraacetic acid was added for 5 min, and the cells were removed from the flasks by scraping. The cell suspension was mixed with trypsin neutralizing solution, washed in keratinocyte growth medium, and fixed with 1% formaldehyde for 15 min followed by 70% ethanol. Fixed cells were stored at –200°C until stained for cytometry. Flow cytometric analyses were conducted on a Becton-Dickinson (Franklin Lakes, NJ) FACStar Plus cytometer using a 100 mW air-cooled argon laser at 488 nm.

PARP cleavage assay The full-length cDNA clone for PARP (pcD-12) (Alkhatib *et al*, 1987) was excised and ligated into the XhoI site of pBluescript-II SK+ (Stratagene, La Jolla, CA), and then used to drive the synthesis of PARP labeled with [^{35}S]methionine (Dupont-NEN, Wilmington, DE) by coupled T7 transcription/translation in a reticulocyte lysate system (Promega, Madison, WI). [^{35}S]PARP was separated from the other constituents by gel filtration chromatography on a Superdex-75 FPLC column (Pharmacia, Piscataway, NJ; 1 × 30 cm) in 10 mM HEPES-KOH (pH 7.4), 2 mM ethylenediamine tetraacetic acid, 0.1% (wt/vol) CHAPS, and 5 mM dithio-threitol.

Cytosolic extracts were prepared from NHEK by scraping phosphate-buffered saline-washed monolayers in 10 mM HEPES/KOH (pH 7.4), 2 mM ethylenediamine tetraacetic acid, 0.1% CHAPS, 5 mM dithiothreitol, 1 mM phenylmethylsulfonylfluoride, 10 μg pepstatin A per ml, 20 μg leupeptin per ml, and 10 μg aprotinin per ml (at 1×10^8 cells per ml). The post-100,000 $\times$ g supernatant was recovered after centrifugation.

PARP cleavage activity was measured in mixtures containing 5 μg protein from the cytosol fractions of keratinocytes. Assay mixtures also contained purified [^{35}S]PARP ($\approx 5 \times 10^4$ cpm), 50 mM PIPES-KOH, 2 mM ethylenedia-mine tetraacetic acid, 0.1% (wt/vol) CHAPS, and 5 mM dithiothreitol in a total volume of 25 μl. Incubations were performed at 37°C for 1 h, and terminated by the addition of 25 μl of 2×sodium dodecyl sulfate-polyacrylamide gel electrophoresis sample buffer containing 4% sodium dodecyl sulfate, 4% β-mercaptoethanol, 10% glycerol, 0.125 M Tris-HCl (pH 6.8), and 0.02% bromophenol blue. Samples were resolved by 10% sodium dodecyl sulfate-polyacrylamide gels.

PARP cleavage products were visualized either by fluorography, or else the 89 kDa cleavage product of [^{35}S]PARP was quantitated relative to the full-length PARP using a Storm 840 PhosphorImage analyzer (Molecular Dynamics, Sunningvale, CA). Quantitation included a correction for background, as well as for the difference in methionine residues present in the 89 kDa fragment (18 met residues) *versus* full-length PARP (25 met residues).

DNA isolation Cells were lysed for 2 h in 10 mM Tris-Cl pH 7.5, 10 mM ethylenediamine tetraacetic acid, 0.5% sodium dodecyl sulfate, containing 144 μg proteinase K per ml, and 500 μg RNase A per ml (Boehringer Mannheim, Indianapolis, IN). Lysates were extracted twice with phenol:chloroform (1:1), and precipitated by the addition of ethanol to 70%. Precipitates were resuspended in distilled water. Glycerol was added to 10% and DNA was resolved on 1% agarose gels and visualized by ethidium bromide staining.

[^{35}S]Methionine labeling To measure total protein synthesis, cells were pulse-labeled with [^{35}S]methionine (10 μCi per ml; Dupont-NEN) for 1 h.

A Hours after

B Hours after

C
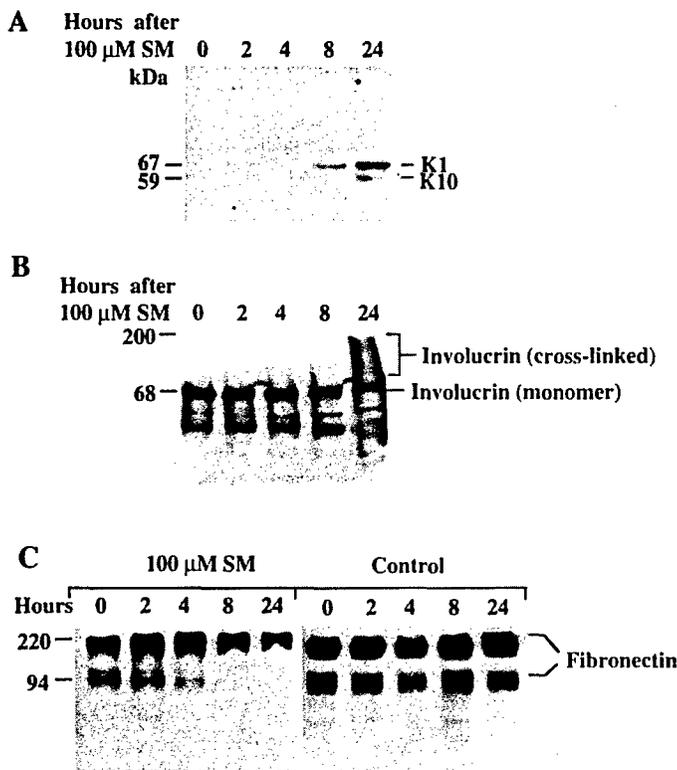
Figure 1. Modulation of differentiation markers and attachment proteins by SM. NHEK were treated with 100 μM SM for the indicated times, harvested, and total cell extracts were immunoblotted using antibodies specific for K1 + K10 (*A*), involucrin (*B*), or fibronectin (*C*). For all studies, similar results were obtained from three independent experiments utilizing human primary adult keratinocytes and three independent experiments utilizing human primary neonatal keratinocytes.

Cells were then washed twice with phosphate-buffered saline, and harvested. Cells were lysed in 10% trichloroacetic acid, and the precipitated protein was collected on glass filters. Filters were washed successively with 10% trichloroacetic acid, 70% ethanol, and absolute ethanol, and dried. Protein-incorporated [^{35}S]methionine on filters was measured by scintillation spectroscopy.

RESULTS

SM induces markers of terminal differentiation in both primary and immortalized keratinocytes To determine if SM altered keratin expression, NHEK were exposed to 100 μM SM, fixed after 24 h, and then subjected to fluorescence-activated cell sorter analysis, using the broad-range-reactive cytokeratin (CK) antibody as a tag. Following SM exposure, the number of CK+ cells increased significantly (data not shown). Because the CK antibody recognizes the suprabasal keratin K10, we were curious to determine if SM altered the expression of any differentiation-specific proteins. Immunoblot analysis with specific anti-sera revealed that both K1 and K10 were induced in the presence of 100 μM SM (**Fig 1A**). The viability of NHEK throughout the time course was greater than 90% as measured by dye exclusion. We also examined the expression of involucrin, a precursor protein that becomes cross-linked in the fully differentiated cornified envelope (Yaffe *et al*, 1993; Robinson *et al*, 1996; Steinert and Marekov, 1997). In extracts derived from untreated cells, involucrin migrated as a 68 kDa monomer form. Following 24 h exposure to SM, the staining pattern shifted to higher molecular weight forms (**Fig 1B**), suggesting that the protein is cross-linked in response to SM.

We next examined the levels of fibronectin expressed in NHEK following SM treatment, for two reasons. First, fibronectin is expressed in basal cells, but is suppressed in suprabasal cells *in vivo*, and in response to differentiating agents *in vitro* (Adams and Watt, 1990; Nicholson and Watt, 1991). In turn, contact with fibronectin also inhibits keratinocyte differentiation (Staiano-Coico and Higgins, 1992; Drozdoff and Pledger, 1993; Watt *et al*, 1993). Second, fibronectin is

a major component of the basal lamina, and forms an attachment site for the alpha 5 beta 1 integrin of the basal cells (Adams and Watt, 1990). Thus, suppression of this protein by SM could in part explain the detachment of basal cells from the basal lamina during vesication *in vivo*. Fibronectin is produced in keratinocytes (as well as fibroblasts), in two isoforms. Both the 220 kDa and the 94 kDa forms of fibronectin were reduced with time after SM exposure. In contrast, untreated NHEK showed no decrease in the levels of fibronectin (**Fig 1C**).

Because previous studies have shown that SM can induce an increase in Ca$_i$ (Ray *et al*, 1995), and because we have observed that a rise in Ca$_i$ is associated with the normal terminal differentiation response of keratinocytes (Yuspa *et al*, 1989; Rosenthal *et al*, 1991), the expression of these markers suggested a role for Ca^{2+} in the SM response that was observed. Furthermore, we have shown that the K1 gene contains specific Ca^{2+}-inducible enhancer sequences located 3' to the gene (Huff *et al*, 1993) and expression of K1 (and other differentiation-specific genes) can be blocked by the Ca$_i$ chelator BAPTA (Li *et al*, 1995). BAPTA also enhances the survival of keratinocytes in the presence of SM (Ray *et al*, 1996). We therefore preincubated keratinocytes with 20 μM BAPTA-AM (+ Pluronic F-127; see *Materials and Methods*) for 30 min prior to SM treatment. When NHEK were subsequently treated for 24 h with 100 μM SM, keratin K1 was suppressed (**Fig 2A**). Although BAPTA treatment suppressed total protein synthesis by 50% after 24 h (not shown), this effect was not enough to account for the complete suppression of K1. Ca^{2+} may induce differentiation via its role in the activation of protein kinase C (Dlugosz and Yuspa, 1993). In addition, Ca^{2+}-calmodulin complexes are also generated that modulate this protein kinase C response (Chakravarthy *et al*, 1995). We therefore determined whether the calmodulin inhibitor W-7 could alter the differentiation response to SM. **Figure 2(A)** shows that a 30 min pretreatment with W-7 prior to exposure to 100 μM SM inhibited the expression of K1. Protein calibration prior to gel-loading, followed by Ponceau-S-staining of the immunoblot (**Fig 2B**), eliminated the possibility of loading artifact, indicating that SM induces the expression of this differentiation-specific marker via a Ca^{2+}-calmodulin-dependent pathway. Interestingly, calmodulin itself was downregulated by SM (**Fig 2C**).

SM suppresses Bcl-2 and induces p53 To examine possible mechanisms by which SM altered the differentiation response, we initially examined the expression of p53, which has been postulated to play important roles in both the differentiation and the apoptotic responses. Immunoblot analysis showed a significant increase in the protein levels of p53 after exposure to 100 μM SM, and that this increase in p53 levels occurs within 2 h (**Fig 3A**).

We also examined the levels of the *bcl-2* gene product, which inhibits both keratinocyte differentiation and apoptosis. Bcl-2 levels are high in basal keratinocytes and are reduced in the differentiating layers of the epidermis (Hockenberry *et al*, 1991). Furthermore, expression of *bcl-2* anti-sense RNA can lower endogenous levels of Bcl-2 and induce markers of terminal differentiation in mouse keratinocytes (Marthinuss *et al*, 1995). Following SM treatment, there is a time-dependent decrease in Bcl-2 protein levels in NHEK as determined by immunoblot analysis (**Fig 3B**).

SM induces apoptosis via caspase-3 The striking decrease in Bcl-2 levels and the increase in p53 levels suggested that in addition to modulating differentiation, SM may induce apoptosis as well. Thus, we assayed for markers of apoptosis following SM treatment. A hallmark of apoptosis in several cell types is the appearance of nucleosome-sized ladders due to the presence of a Ca^{2+}/Mg^{2+}-dependent endonuclease that is induced in apoptotic cells. DNA isolated from NHEK treated with 0 or 100 μM SM was intact; however, at 300 μM SM, NHEK showed nucleosome-sized ladders analyzed by agarose gel electrophoresis, although some nonspecific fragmentation was also apparent (**Fig 4**). Accordingly, trypan blue exclusion at 24 h was 98% in control cells, 90% following 100 μM SM treatment, and 60% after 300 μM SM (not shown). W-7 suppressed DNA fragmentation, whereas BAPTA partially inhibited DNA cleavage (see below).
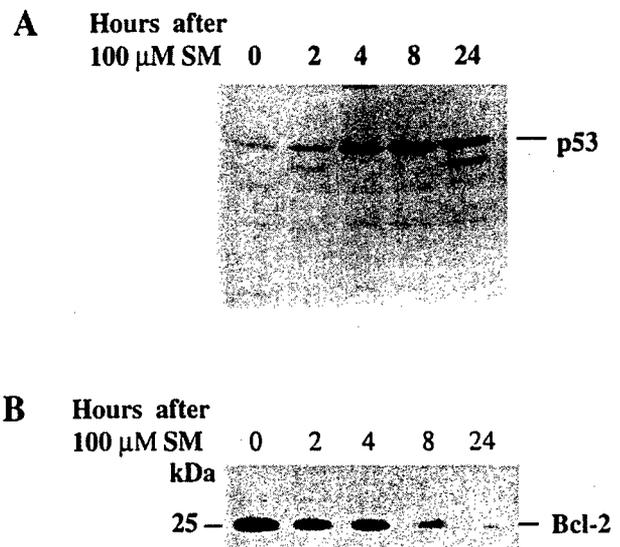
We have recently determined that the activation of PARP plays a role in the etiology of apoptosis in osteosarcoma cells induced to
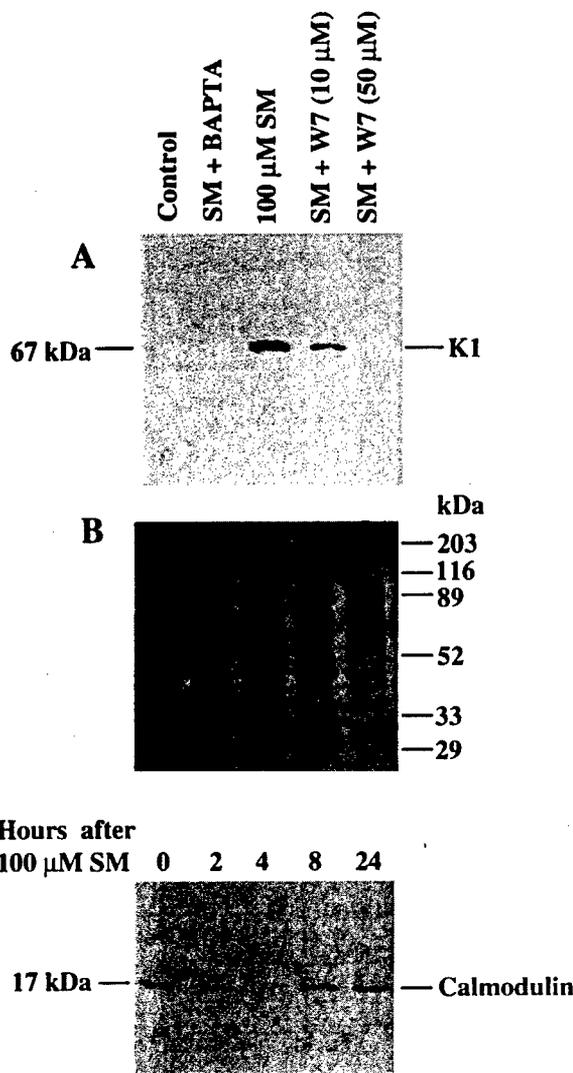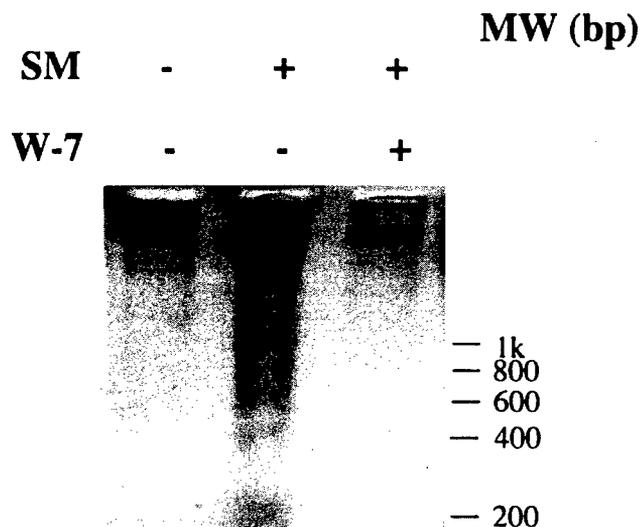
Figure 2. Ca^{2+} and calmodulin are required for the induction of markers of terminal differentiation by SM. NHEK were treated with SM as above, either with or without pretreatment with 20 µM BAPTA-AM or W-7 (A). Cell extracts were immunoblotted using antibodies specific for K1 (A), or calmodulin (C). (B) Ponceau-S stain of total cell protein on nitrocellulose prior to immunostaining shown in (A).

Figure 3. SM induces an increase in p53 levels, and a decrease in Bcl-2. NHEK were treated with 100 µM SM for the indicated times. Total cell extracts were derived, resolved by polyacrylamide gel electrophoresis, and subjected to immunoblot analysis using anti-sera specific for p53 (A) or Bcl-2 (B).

Figure 4. SM treatment induces DNA fragmentation in keratinocytes. NHEK were treated with 100 µM or 300 µM SM, with or without W-7 or BAPTA. Total genomic DNA was isolated, resolved by agarose gel electrophoresis, and stained with ethidium bromide.

undergo programmed cell death, in which poly(ADP-ribosyl)ation corresponds with the early reversible stages of apoptosis (Rosenthal et al, 1997b). We therefore determined whether we could detect increased levels of poly(ADP-ribosyl)ation following exposure of NHEK to SM. Because PARP itself is the main acceptor protein for poly(ADP-ribosyl)ation, via intermolecular "automodification" (Mendoza-Alvarez and Alvarez-Gonzalez, 1993), the presence of a 116 kDa antipoly(ADP-ribose)-crossreactive band is a sensitive indicator of poly(ADP-ribosyl)ation within the nucleus. Anti-sera specific for poly(ADP-ribose) did in fact detect a strong band at 116 kDa in extracts of primary keratinocytes treated with all concentrations of SM tested, whereas no such band was present in extracts of control keratinocytes, indicating that SM induces DNA strand breaks and PARP is activated. **Figure 5**(A) shows that, at 100 µM SM, activation of PARP occurs and automodification is apparent by 2 h. The molecular weight of automodified PARP was similar to that of unmodified PARP (116 kDa), indicating that the average polymer length is relatively short at this time point. After this time, the level of poly(ADP-ribose) decreases precipitously, similar to our previous observations using osteosarcoma cells induced to undergo apoptosis (Rosenthal et al, 1997b).

We previously determined that this characteristic rise and rapid

decline in poly(ADP-ribose) levels could be attributed not only to poly(ADP-ribose) glycohydrolase activity (Wielckens et al, 1983), but also to the proteolytic cleavage of PARP into the characteristic 89 kDa and 24 kDa fragments, the latter of which contains the Zn^{2+} finger region and DNA-binding domain. We therefore performed western analysis to monitor the cleavage of PARP using an antibody that recognizes both the full-length 116 kDa protein as well as the 89 kDa fragment of PARP. **Figure 5**(B) shows a significant conversion of full-length PARP to the 89 kDa fragment following 300 µM SM treatment.

We have previously described an ICE-like protease similar to the Ced-3 protein of C. elegans and closely associated with apoptosis (Nicholson et al, 1995), now known as "caspase-3" (Alnemri et al, 1996). Accordingly, a sensitive technique to verify that SM induces apoptosis is to determine the activation of caspase-3 from its precursor (pro-caspase-3; CPP32) via the use of in vitro translated PARP. We therefore used a combination transcription/translation system to radiolabel full-length PARP (see Materials and Methods) that was subsequently incubated with extracts derived from keratinocytes treated
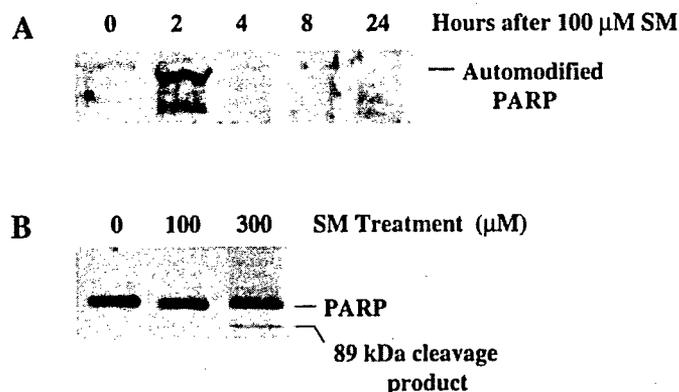
Figure 5. SM treatment induces in vivo PARP activation and cleavage in keratinocytes. NHEK were treated with 100 μM (A, B) or 300 μM (B) SM. Total cell extracts were derived, resolved by polyacrylamide gel electrophoresis, and subjected to immunoblot analysis using anti-sera specific for poly(ADP-ribose) (A), or for both the full-length and the 89 kDa cleavage product of PARP (B).
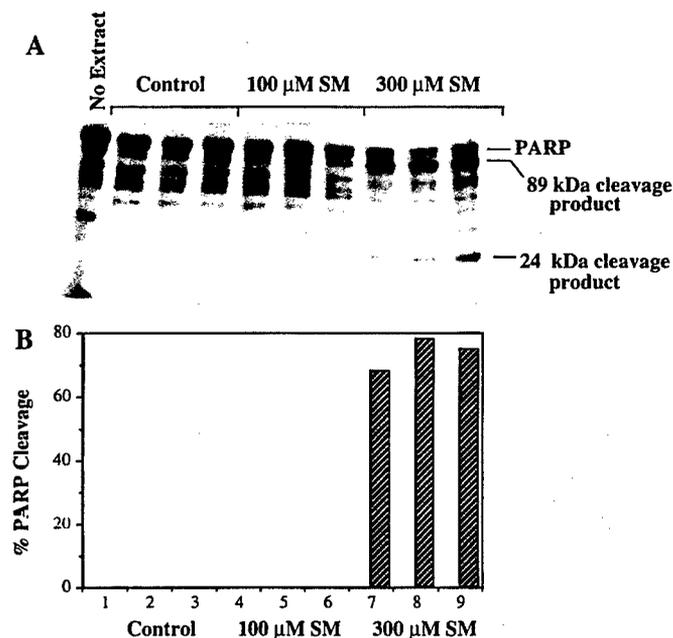
Figure 6. Extracts of keratinocytes treated with SM show in vitro PARP-cleavage activity. Triplicate cultures of NHEK were treated with 100 μM or 300 μM SM. Cytoplasmic extracts were then derived after 24 h and assayed for caspase-3 activity, using [^{35}S]PARP as a substrate (Materials and Methods). (B) Quantitation of PARP-cleavage activity by phosphorimage analysis.

with SM. **Figure 6(A)** shows that PARP cleavage activity is clearly seen in NHEK in 300 μM SM (but not 100 μM SM) after 24 h, as evidenced by the strong appearance of the 24 kDa and 89 kDa cleavage products. **Figure 6(B)** shows, by quantitative phosphorimage analysis, the relative PARP cleavage activities that result from the treatment of NHEK with SM for 24 h. The high level of PARP-cleavage activity observed in 300 μM SM is indicative that this vesicant is also a strong inducer of apoptosis in primary keratinocytes, and that apoptosis is occurring via a caspase-3-like pathway.

We next further verified that SM induces apoptosis by determining whether the observed caspase-3 activity in vitro could be associated with the processing of pro-caspase-3/CPP32 into its active protease form. During apoptosis, procaspase-3/CPP32 is processed into 17 kDa and 12 kDa peptides, with the removal of a pro-peptide sequence from the N-terminus. The 17 kDa and 12 kDa fragments then form the active proteolytic heterodimer. Using an antibody that recognizes both the active (p17) and the inactive (CPP32) forms of caspase-3, a
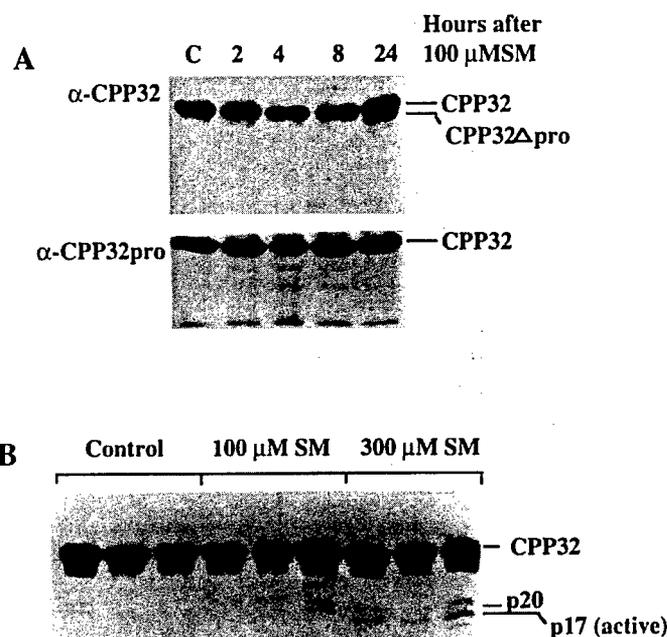
Figure 7. SM induces processing of procaspase-3/CPP32 to its active form. Triplicate cultures of NHEK were treated with 100 μM or 300 μM SM for the indicated times (A), or for 24 h (B). Total cell extracts were derived, resolved by polyacrylamide gel electrophoresis, and subjected to immunoblot analysis using anti-sera specific for the p17 subunit (A, top; B), or the N-terminal pro-peptide sequence (A, bottom) of caspase-3.

slightly smaller form of CPP32 was observed 24 h after the cells were exposed to 100 μM SM, equivalent in size to CPP32 minus the pro-peptide sequence, suggesting that processing of the N-terminus of the precursor protein was occurring (**Fig 7A**, top). To confirm this, the same extracts were analyzed utilizing an antibody that is specific for the pro-sequence that is removed when caspase-3 is processed into its active form. The disappearance of the slightly smaller MW band previously observed at 24 h in 100 μM SM (**Fig 7A**, bottom), indicates that this band is missing the propeptide sequence, and is thus the result of CPP32 N-terminal processing. Following treatment with 300 μM SM, NHEK showed complete processing of a portion of CPP32 into the active p17 form (**Fig 7B**). A small amount of the partially processed p20, which represents p17 and the N-terminal pro-sequence, is also observed. Thus, in both 100 μM and 300 μM SM, markers of apoptosis are induced, although complete activation of caspase-3, PARP cleavage, and DNA fragmentation are only observed at the higher concentration of SM.

A Ca^{2+} calmodulin-dependent pathway for SM-induced apoptosis To determine if SM-induced apoptosis was proceeding via Ca^{2+}-calmodulin dependent pathways, BAPTA and W-7 were utilized as pretreatment agents. BAPTA had a small effect on in vitro PARP-cleavage activity, whereas greater suppression was observed following W-7 pretreatment (**Fig 8A**). W-7 also suppressed the level of DNA fragmentation (**Fig 4**).

We next determined whether this W-7-sensitive repression was related to the processing of CPP32 into its active form. In control NHEK, one of the two subunits of the active form of apopain, p17, can clearly be detected 24 h following treatment with 300 μM SM; however, p17 is completely suppressed by 50 μM W-7 (**Fig 8B**). Thus, SM induces apoptosis via a calmodulin-dependent pathway that involves the activation of caspase-3.

DISCUSSION

SM vesication clearly involves both cytotoxicity and detachment of the epidermal basal layer in vivo. Using a cell culture model in this

A

— PARP

89 kDa cleavage product

— 24 kDa cleavage product

B

— CPP32

p20

p17 (active)
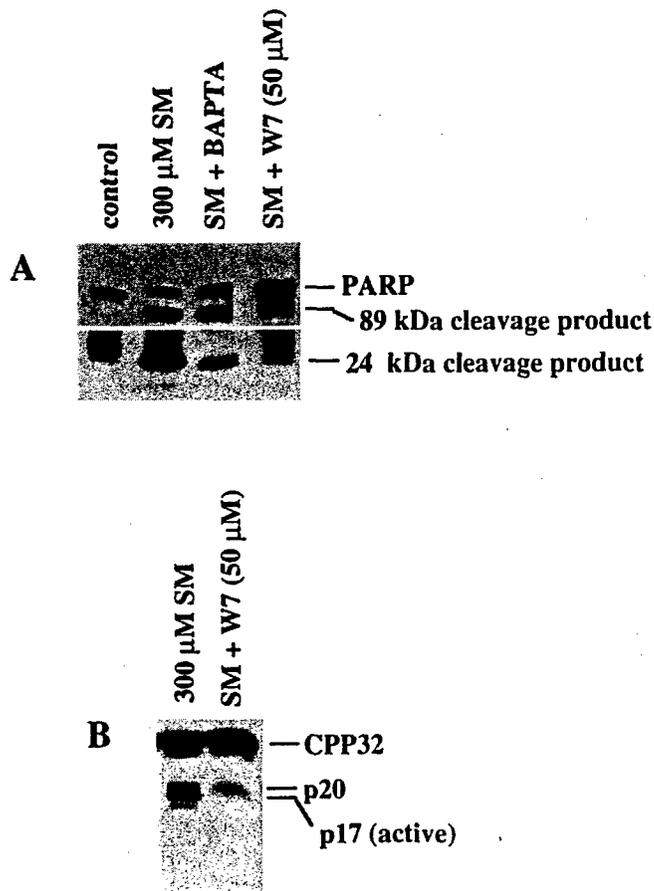
Figure 8. Caspase-3 activity and processing induced by SM is suppressed by inhibitors of Ca_i and calmodulin. Cells were treated with 300 μM SM for 24 h with or without a 30 min pretreatment with BAPTA-AM or W-7. Cytoplasmic extracts were then derived and assayed for caspase-3 activity, using [^{35}S]PARP as a substrate. (B) Extracts of cells treated with 300 μM SM, plus a 30 min W-7 pretreatment, were resolved by polyacrylamide gel electrophoresis, and subjected to immunoblot analysis using anti-sera specific for p17.

study, we have described two potential mechanisms for SM-induced keratinocyte basal cell death and detachment: induction of terminal differentiation and apoptosis. SM induced the differentiation-specific markers K1 and K10, cross-linking of the cornified envelope precursor protein involucrin, and suppressed fibronectin. SM also induced markers of apoptosis in NHEK, including the transient elevation of poly(ADP-ribose), the processing of CPP32 into caspase-3, and the specific cleavage of PARP both *in vivo* and in cell-free PARP-cleavage assays. Differentiation markers were suppressed by the intracellular Ca^{2+}-chelator BAPTA-AM, and the calmodulin inhibitor W-7, whereas markers of apoptosis were suppressed by W-7. Thus, both the differentiation and the apoptotic responses appear to be Ca^{2+}-calmodulin dependent.

Because SM induces an increase in Ca_i (Ray et al, 1995; Mol and Smith, 1996), it seems likely that this elevation in Ca_i accounts for the induction of the markers of terminal differentiation observed in this study, because terminal differentiation of keratinocytes is closely associated with an elevation in Ca^{2+} (Hennings et al, 1980; Stanley and Yuspa, 1983; Kruszewski et al, 1991a, b; Rosenthal et al, 1991; Li et al, 1995). The suppression of these markers by BAPTA also lends support to the idea that the rise in Ca_i is an important event in SM-induced expression of differentiation markers (**Fig** 2). How SM induces a rise in Ca_i is unknown, but may stem from its ability to alkylate several molecules within the cell, including glutathione (Gross et al, 1993) or other molecules involved in cellular homeostasis, ultimately resulting in disruptions of plasma, ER, and mitochondrial membranes. Disruption of these membranes could easily lead to perturbations in Ca_i within the cell.

The role of SM in the induction of apoptosis may also involve Ca_i and/or Ca^{2+}-calmodulin complexes, because these molecules have been shown to be involved in apoptosis in other systems (Kaiser and Edelman, 1977; Shi et al, 1989). The suppression of apoptotic markers by the Ca_i buffer BAPTA and the calmodulin inhibitor W-7 in this study supports this idea. It is also likely that DNA strand breaks and the activation of PARP play a role in the SM-induced expression of apoptotic markers in keratinocytes. SM is a strong alkylating agent with a high affinity for DNA, and has been shown to induce DNA strand breaks and consequently activate PARP. PARP inhibitors can extend the lifespan of lymphocytes treated with SM (Meier and Johnson, 1992; Meier, 1996), and inhibitors of PARP have previously been reported to significantly affect the extent of apoptosis in response to other agents (Rice et al, 1992; Ghibelli et al, 1994; Monti et al, 1994; Kuo et al, 1996). PARP may thus be an important signaling molecule for cell death either via the lowering of NAD and/or ATP levels (Wielckens et al, 1982; Berger et al, 1983; Alvarez et al, 1986), or by poly(ADP-ribosyl)ation of other key cellular proteins involved in apoptosis, such as p53 (Whitacre et al, 1995) and the Ca^{2+}/Mg^{2+} dependent nuclease involved in the apoptotic cleavage of DNA (Rice et al, 1992).

The early and short-lived poly(ADP-ribosyl)ation, followed by caspase-3 activation and PARP cleavage detected in this study (**Figs** 5–7), is consistent with our previous findings during spontaneous apoptosis in the osteosarcoma system (Rosenthal et al, 1997a,b). The synthesis of poly(ADP-ribose) from nicotinamide adenine dinucleotide increased early after initiation of apoptosis. The abundance of both poly(ADP-ribose) and PARP then decreased markedly, corresponding to the appearance of the proteolytic cleavage product containing the DNA-binding domain of PARP; no poly(ADP-ribose) was observed during this time, in spite of the fact that there was massive DNA internucleosomal degradation. This coincided with earlier data indicating that caspase-3 activity maximized in osteosarcoma cells at this time. These data suggested that there appears to be not only a requirement for destruction of PARP during apoptosis, but also a stage in early apoptosis that appeared to require the presence of PARP protein and presumably poly(ADP-ribosyl)ation of certain proteins. Recently, we utilized antisense RNA expression to deplete endogenous PARP in order to examine the requirement of this protein early in apoptosis, and found that the apoptotic response was modulated (Simbulan-Rosenthal et al, 1998). Likewise, in recent PARP-knockout animals, apoptosis was found to be altered (de Murcia et al, 1997).

The involvement of such varied molecules as Ca^{2+}, calmodulin, p53, Bcl-2, and caspase-3 suggests a complex network involved in SM-induced apoptosis; however, it seems that the activation of caspase-3 (or the closely related caspase-7) may be a final converging point for apoptosis, because (i) procaspase-3/CPP32 knockout mice show altered programmed cell death in the nervous system (Kuida et al, 1996), (ii) caspase-3 (and −7) is a target for granzyme B-mediated apoptosis, as well as apoptosis mediated by other caspases (Darmon et al, 1995, 1996; Chinnaiyan et al, 1996; Gu et al, 1996; Quan et al, 1996), and (iii) a tetrapeptide aldehyde (Ac-DEVD-CHO) that inhibits caspase-3 activity blocks apoptotic events in isolated nuclei (Nicholson et al, 1995). In this study, the convergence of these signals at the level of caspase-3 activation is supported by the facts that: (i) p53 and Bcl-2, which act upstream of caspase-3, are strongly and rapidly modulated by SM; (ii) inhibitors of Ca^{2+} and calmodulin, which have been found in previous studies to prolong the lifespan of keratinocytes exposed to SM (Ray et al, 1996), and to block apoptosis in this study, prevent the processing and activation of caspase-3; and (iii) in preliminary experiments, NHEK pretreated with AcDEVD-CHO showed both inhibition of *in vitro* PARP-cleavage activity and a reduced apoptotic index in response to SM, as determined by TUNEL labeling (not shown).

An understanding of the mechanisms for SM vesication will hopefully lead to strategies for prevention or treatment of SM toxicity. This study suggests that inhibition of calmodulin (upstream) or caspase-3 (downstream) may protect the epidermis from SM-induced apoptosis. Although the mechanism for their protection has not been described, calmodulin inhibitors have already been successfully employed in the

treatment of both thermal burns and frostbite (Beitner *et al*, 1989a, b), and may prove effective for SM as well, either alone or in combination with caspase-3 inhibitors.

REFERENCES

Adams JC, Watt FM: Changes in keratinocyte adhesion during terminal differentiation: reduction in fibronectin binding precedes alpha 5 beta 1 integrin loss from the cell surface. *Cell* 63:425–435, 1990

Alkhatib HM, Chen DF, Cherney B, *et al*: Cloning and expression of cDNA for human poly (ADP-ribose) polymerase. *Proc Natl Acad Sci* 84:1224–1228, 1987

Alnemri E, Livingston D, Nicholson D, Salvesen G, Thornberry N, Wong W, Yuan J: Human ICE/CED-3 protease nomenclature [letter]. *Cell* 87:171, 1996

Alvarez GR, Eichenberger R, Althaus FR: Poly (ADP-ribose) biosynthesis and suicidal NAD+ depletion following carcinogen exposure of mammalian cells. *Biochem Biophys Res Commun* 138:1051–1057, 1986

Beitner R, Chen-Zion M, Sofer-Bassukevitz Y, Morgenstern H, Ben-Porat H: Treatment of frostbite with the calmodulin antagonists thioridazine and trifluoperazine. *Gen Pharmacol* 20:641–646, 1989a

Beitner R, Chen-Zion M, Sofer-Bassukevitz Y, Oster Y, Ben-Porat H, Morgenstern H: Therapeutic and prophylactic treatment of skin burns with several calmodulin antagonists. *Gen Pharmacol* 20:165–173, 1989b

Berger NA, Sims JL, Catino DM, Berger SJ: Poly (ADP-ribose) polymerase mediates the suicide response to massive DNA damage: Studies in normal and DNA-repair defective cells. In: Miwa M *et al*. (eds). *ADP-ribosylation, DNA Repair and Cancer*, Japan Scientific Societies Press, Tokyo, 1983, pp. 219–226

Casciola-Rosen L, Nicholson D, Chong T, Rowan K, Thornberry N, Miller D, Rosen A: Apopain/CPP 32 cleaves proteins that are essential for cellular repair: a fundamental principle of apoptotic death. *J Exp Med* 183:1957–1964, 1996

Chakravarthy BR, Isaacs RJ, Morley P, Durkin JP, Whitfield JF: Stimulation of protein kinase C during calcium-induced keratinocyte differentiation: selective blockade of MARCKS phosphorylation by calmodulin. *J Biol Chem* 270:1362–1368, 1995

Chinnaiyan A, Hanna W, Orth K, Duan H, Poirier G, Froelich C, Dixit V: Cytotoxic T-cell-derived granzyme B activates the apoptotic protease ICE-LAP3. *Curr Biol* 6:897–899, 1996

Darmon A, Nicholson D, Bleackley R: Activation of the apoptotic protease CPP 32 by cytotoxic T-cell-derived granzyme B. *Nature* 377:446–448, 1995

Darmon A, Ley T, Nicholson D, Bleackley R: Cleavage of CPP 32 by granzyme B represents a critical role for granzyme B in the induction of target cell DNA fragmentation. *J Biol Chem* 271:21709–21712, 1996

Ding R, Pommier Y, Kang VH, Smulson M: Depletion of poly (ADP-ribose) polymerase by antisense RNA expression results in a delay in DNA strand break rejoining. *J Biol Chem* 267:12804–12812, 1992

Dlugosz AA, Yuspa SH: Coordinate changes in gene expression which mark the spinous to granular cell transition in epidermis are regulated by protein kinase C. *J Cell Biol* 120:217–225, 1993

Drozdoff V, Pledger W: Commitment to differentiation and expression of early differentiation markers in murine keratinocytes in vitro are regulated independently of extracellular calcium concentrations. *J Cell Biol* 123:909–919, 1993

Ghibelli L, Coppola S, Nosseri C, Bergamini A, Beninati S: A protein produced by a monocytic human cell line can induce apoptosis on tumor cells. *Febs Lett* 344:35–40, 1994

Gross C, Innace J, Hovatter R, Meier H, Smith W: Biochemical manipulation of intracellular glutathione levels influences cytotoxicity to isolated human lymphocytes by sulfur mustard. *Cell Biol Toxicol* 9:259–267, 1993

Gu Y, Sarnecki C, Fleming M, Lippke J, Bleackley R, Su M: Processing and activation of CMH-1 by granzyme B. *J Biol Chem* 271:10816–10820, 1996

Hennings H, Michael D, Cheng C, Steinert P, Holbrook K, Yuspa SH: Calcium regulation of growth and differentiation of mouse epidermal cells in culture. *Cell* 19:245–254, 1980

Hockenberry D, Zutter M, Hickey W, Nahm M, Korsmeyer SJ: Bcl-2 protein is topographically restricted in tissues characterized by apoptotic cell death. *Proc Natl Acad Sci USA* 88:6961–6965, 1991

Huff CA, Yuspa SH, Rosenthal D: Identification of control elements 3′ to the human keratin 1 gene that regulate cell type and differentiation-specific expression. *J Biol Chem* 268:377–384, 1993

Kaiser N, Edelman IS: Calcium dependence of glucocorticoid-induced lymphocytolysis. *Proc Natl Acad Sci USA* 74:638–642, 1977

Kaufmann SH, Desnoyers S, Ottaviano Y, Davidson NE, Poirier GG: Specific proteolytic cleavage of poly (ADP-ribose) polymerase: an early marker of chemotherapy-induced apoptosis. *Cancer Res* 53:3976–3985, 1993

Kruszewski FH, Hennings H, Tucker RW, Yuspa SH: Differences in the regulation of intracellular calcium in normal and neoplastic keratinocytes are not caused by ras gene mutations. *Cancer Res* 51:4206–4212, 1991a

Kruszewski FH, Hennings H, Yuspa SH, Tucker RW: Regulation of intracellular free calcium in normal murine keratinocytes. *Am J Physiol* 261:C767–C773, 1991b

Kuida K, Zheng T, Na S, *et al*: Decreased apoptosis in the brain and premature lethality in CPP 32-deficient mice. *Nature* 384:368–372, 1996

Kuo M, Chau Y, Wang J, Shiah S: Inhibitors of poly (ADP-ribose) polymerase block nitric oxide-induced apoptosis but not differentiation in human leukemia HL-60 cells. *Biochem Biophys Res Commun* 219:502–508, 1996

Li L, Tucker RW, Hennings H, Yuspa S: Chelation of intracellular calcium inhibits murine keratinocyte differentiation in vitro. *J Cell Physiol* 163:105–114, 1995

Marthinuss J, Lawrence L, Seiberg M: Apoptosis in Pam212, an epidermal keratinocyte cell line: a possible role for bcl-2 in epidermal differentiation. 1995.

Meier H: The time-dependent effect of 2,2′-dichlorodiethyl sulfide (sulfur mustard, HD, 1, 1′-thiobis [2-chloroethane]) on the lymphocyte viability and the kinetics of protection by poly (ADP-ribose) polymerase inhibitors. *Cell Biol Toxicol* 12:147–153, 1996

Meier H, Johnson J: The determination and prevention of cytotoxic effects induced in human lymphocytes by the alkylating agent 2,2″-dichlorodiethyl sulfide (sulfur mustard, HD). *Toxicol Appl Pharmacol* 113:234–239, 1992

Mendoza-Alvarez H, Alvarez-Gonzalez R: Poly (ADP-ribose) polymerase is a catalytic dimer and the automodification reaction is intermolecular. *J Biol Chem* 268:22575–22580, 1993

Mol MAE, Smith W: Calcium homeostasis and calcium signalling in sulphur mustard-exposed normal human epidermal keratinocytes. In *Chemico–Biological Interactions*, Elsevier), pp 85–93. 1996.

Monti D, Cossarizza A, Salvioli S, *et al*: Cell death protection by 3-aminobenzamide and other poly (ADP-ribose) polymerase inhibitors: different effects on human natural killer and lymphokine activated killer cell activities. *Biochem Biophys Res Commun* 199:525–530, 1994

de Murcia JM, Niedergang C, Trucco C, *et al*: Requirement of poly (ADP-ribose) polymerase in recovery from DNA damage in mice and in cells. *Proc Natl Acad Sci USA* 94:7303–7307, 1997

Neamati N, Fernandez A, Wright S, Kiefer J, McConkey DJ: Degradation of lamin B1 precedes oligonucleosomal DNA fragmentation in apoptotic thymocytes and isolated thymocyte nuclei. *J Immunol* 154:3788–3795, 1995

Nicholson DW, Ali A, Thornberry NA, *et al*: Identification and inhibition of the ICE/CED-3 protease necessary for mammalian apoptosis. *Nature* 376:37–43, 1995

Nicholson L, Watt F: Decreased expression of fibronectin and the alpha 5 beta 1 integrin during terminal differentiation of human keratinocytes. *J Cell Sci* 98:225–232, 1991

Orrenius S, McConkey DJ, Bellomo G, Nicotera P: Role of Ca2+ in toxic cell killing. *Tends Pharmacol Sci* 10:281–285, 1989

Papirmeister B, Gross CL, Meier HL, Petrali JP, Johnson JB: Molecular basis for mustard-induced vesication. *Fund Appl Toxicol* 5:S134–S149, 1985

Quan L, Tewari M, O'Rourke K, *et al*: Proteolytic activation cell death protease Yama/CPP 32 by granzyme B. *Proc Natl Acad Sci USA* 93:1972–1976, 1996

Ray R, Legere RH, Majerus BJ, Petrali JP: Sulfur mustard-induced increase in intracellular free calcium level and arachidonic acid release from cell membrane. *Toxicol Appl Pharmacol* 131:44–52, 1995

Ray R, Benton BJ, Anderson DR, Byers SL, Shih ML, Petrali JP: The intracellular free calcium chelator BAPTA prevents sulfur mustard toxicity in cultured normal human epidermal keratinocytes. In: *Proceedings of the Medical Defense Bioscience Review*, US Army Medical Research Institute of Chemical Defense, Aberdeen Proving Ground, Maryland, 1996, pp. 1021–1027

Rice WG, Hillyer CD, Harten B, *et al*: Induction of endonuclease-mediated apoptosis in tumor cells by C-nitroso-substituted ligands of poly (ADP-ribose) polymerase. *Proc Natl Acad Sci USA* 89:7703–7707, 1992

Robinson N, La Celle P, Eckert R: Involucrin is a covalently crosslinked constituent of highly purified epidermal corneocytes: evidence for a common pattern of involucrin crosslinking in vivo and in vitro. *J Invest Dermatol* 107:101–107, 1996

Rosenthal DS, Steinert PM, Chung S, Huff CA, Johnson J, Yuspa SH, Roop DR: A human epidermal differentiation-specific keratin gene is regulated by calcium but not negative modulators of differentiation in transgenic mouse keratinocytes. *Cell Growth Differ* 2:107–113, 1991

Rosenthal DS, Shima TB, Celli G, De Luca LM, Smulson ME: An engineered human skin model using poly (ADP-ribose) polymerase antisense expression shows a reduced response to DNA damage. *J Invest Dermatol* 105:38–44, 1995

Rosenthal DS, Ding R, Simbulan-Rosenthal CMG, Cherney B, Vanek P, Smulson ME: Detection of DNA breaks in apoptotic cells utilizing the DNA binding domain of poly (ADP-ribose) polymerase with fluorescence microscopy. *Nucl Acids Res* 25:1437–1441, 1997a

Rosenthal DS, Ding R, Simbulan-Rosenthal CMG, Vaillancourt JP, Nicholson DW, Smulson ME: Intact cell evidence fo the early snthesis, and subsequent late apopain-mediated suppression, of poly (ADP-ribose) during apoptosis. *Exp Cell Res* 232:313–321, 1997b

Shi Y, Sahai BM, Green DR: Cyclosporin A inhibits activation-induced cell death in T-cell hybidomas and thymocytes. *Nature* 339:625–626, 1989

Shiokawa D, Ohyama H, Yamada T, Takahashi K, Tanuma S: Identification of an endonuclease responsible for apoptosis in rat thymocytes. *European J Biochem* 226:23–30, 1994

Silvennoinen O, Nishigaki H, Kitanaka A, *et al*: CD38 signal transduction in human B cell precursors. Rapid induction of tyrosine phosphorylation, activation of syk tyrosine kinase, and phosphorylation of phospholipase C-gamma and phosphatidylinositol 3-kinase. *J Immunol* 156:100–107, 1996

Simbulan-Rosenthal CMG, Rosenthal DS, Iyer S, Boulares AH, Smulson ME: Transient poly(ADP-ribosyl)ation of nuclear proteins and role of poly(ADP-ribose) polymerase in the early stages of apoptosis. *J Biol Chem* 273:13703–13712, 1998

Song Q, Lees-Miller S, Kumar S, *et al*: DNA-dependent protein kinase catalytic subunit a target for an ICE-like protease in apoptosis. *EMBO J* 15:3238–3246, 1996

Staiano-Coico L, Higgins P: Cell shape changes during transition of basal keratinocytes to mature enucleate-cornified envelopes: modulation of terminal differentiation by fibronectin. *Exp Cell Res* 201:126–136, 1992

Stanley JR, Yuspa SH: Specific epidermal protein markers are modulated during calcium-induced terminal differentiation. *J Cell Biol* 96:1809–1814, 1983

Steinert P, Marekov L: Direct evidence that involucrin is a major early isopeptide cross-linked component of the keratinocyte cornified cell envelope. *J Biol Chem* 272:2021–2030, 1997

Takata M, Homma Y, Kurosaki T: Requirement of phospholipase C-gamma 2 activation in surface immunoglobulin M-induced B cell apoptosis. *J Exp Med* 182:907–914, 1995

Tewari M, Quan LT, O'Rourke K, *et al*: Yama/CPP 32β, a mammalian homolog of CED-3, is a crmA-inhibitable protease that cleaves the death substrate poly (ADP-ribose) polymerase. *Cell* 81:801–809, 1995

Watt F, Kubler M, Hotchin N, Nicholson L, Adams J: Regulation of keratinocyte terminal differentiation by integrin-extracellular matrix interactions. *J Cell Sc* 106:175–182, 1993

Whitacre CM, Hashimoto H, Tsai M-L, Chatterjee S, Berger SJ, Berger NA: Involvement of NAD-poly (ADP-ribose) metabolism in p53 regulation and its consequences. *Cancer Res* 55:3697–3701, 1995

Wielckens K, Schmidt A, George E, Bredehorst R, Hilz H: DNA fragmentation and NAD depletion. Their relation to the turnover of endogenous mono (ADP-ribosyl) and poly (ADP-ribosyl) proteins. *J Biol Chem* 257:12872–12877, 1982

Wielckens K, George E, Pless T, Hilz H: Stimulation of poly (ADP-ribosyl) ation during Ehrlich ascites tumor cell "starvation" and suppression of concomitant DNA fragmentation by benzamide. *J Biol Chem* 258:4098–4104, 1983

Yaffe M, Murthy S, Eckert R: Evidence that involucrin is a covalently linked constituent of highly purified cultured keratinocyte cornified envelopes. *J Invest Dermatol* 100:3–9, 1993

Yuspa SH, Kilkenny AE, Steinert PM, Roop DR: Expression of murine epidermal differentiation markers is tightly regulated by restricted extracellular calcium concentrations in vitro. *J Cell Biol* 109:1207–1217, 1989

Regulation of the Expression or Recruitment of Components of the DNA Synthesome by Poly(ADP-Ribose) Polymerase

Cynthia M. Simbulan-Rosenthal, Dean S. Rosenthal,
A. Hamid Boulares, Robert J. Hickey, Linda H. Malkas,
Jennifer M. Coll, and Mark E. Smulson

Department of Biochemistry and Molecular Biology, Georgetown
University School of Medicine, Washington, DC 20007, and
Department of Pharmacology and Experimental Therapeutics,
Greenebaum Cancer Center, University of Maryland
School of Medicine, Baltimore, Maryland 21201

Biochemistry®

Regulation of the Expression or Recruitment of Components of the DNA Synthesome by Poly(ADP-Ribose) Polymerase[†]

Cynthia M. Simbulan-Rosenthal,[‡] Dean S. Rosenthal,[‡] A. Hamid Boulares,[‡] Robert J. Hickey,[§] Linda H. Malkas,[§] Jennifer M. Coll,[§] and Mark E. Smulson*[,‡]

Department of Biochemistry and Molecular Biology, Georgetown University School of Medicine, Washington, DC 20007, and Department of Pharmacology and Experimental Therapeutics, Greenebaum Cancer Center, University of Maryland School of Medicine, Baltimore, Maryland 21201

Received December 18, 1997; Revised Manuscript Received April 10, 1998

ABSTRACT: Poly(ADP-ribose) polymerase (PARP) is a component of the multiprotein DNA replication complex (MRC, DNA synthesome) that catalyzes replication of viral DNA in vitro. PARP poly(ADP-ribosyl)ates 15 of the ~40 proteins of the MRC, including DNA polymerase α (DNA pol α), DNA topoisomerase I (topo I), and proliferating-cell nuclear antigen (PCNA). Although about equal amounts of MRC-complexed and free forms of PCNA were detected by immunoblot analysis of HeLa cell extracts, only the complexed form was poly(ADP-ribosyl)ated, suggesting that poly(ADP-ribosyl)ation of PCNA may regulate its function within the MRC. NAD inhibited the activity of DNA pol δ in the MRC in a dose-dependent manner, whereas the PARP inhibitor, 3-AB, reversed this inhibitory effect. The roles of PARP in modulating the composition and enzyme activities of the DNA synthesome were further investigated by characterizing the complex purified from 3T3-L1 cells before and 24 h after induction of a round of DNA replication required for differentiation of these cells; at the latter time point, ~95% of the cells are in S phase and exhibit a transient peak of PARP expression. The MRC was also purified from similarly treated 3T3-L1 cells depleted of PARP by antisense RNA expression; these cells do not undergo DNA replication nor terminal differentiation. Both PARP protein and activity and essentially all of the DNA pol α and δ activities exclusively cosedimented with the MRC fractions from S phase control cells, and were not detected in the MRC fractions from PARP-antisense or uninduced control cells. Immunoblot analysis further revealed that, although PCNA and topo I were present in total extracts from both control and PARP-antisense cells, they were present in the MRC fraction only from induced control cells, indicating that PARP may play a role in their assembly into an active DNA synthesome. In contrast, expression of DNA pol α, DNA primase, and RPA was down-regulated in PARP-antisense cells, suggesting that PARP may be involved in the expression of these proteins. Depletion of PARP also prevented induction of the expression of the transcription factor E2F-1, which positively regulates transcription of the DNA pol α and PCNA genes; thus, PARP may be necessary for expression of these genes when quiescent cells are stimulated to proliferate.

Poly(ADP-ribose) polymerase (PARP) catalyzes the covalent attachment of poly(ADP-ribose) chains to a variety of nuclear proteins, with NAD as substrate. Consistent with earlier studies with chemical inhibitors of PARP, depletion of PARP from cells by expression of antisense RNA has shown that the enzyme plays important accessory roles in various nuclear processes that involve rejoining of DNA strand breaks. These antisense studies have indicated that depletion of PARP results in a decrease in the initial rate of

DNA repair in HeLa cells (Ding et al., 1992) and keratinocytes (Rosenthal et al., 1995), a reduction in the survival of cells exposed to mutagenic agents, an alteration in chromatin structure, and an increase in gene amplification (Ding and Smulson, 1994). In a related approach, fibroblasts derived from PARP knockout mice exhibit proliferation deficiencies in culture, and thymocytes from these animals show a delayed recovery after exposure to γ-irradiation (Wang et al., 1995). More recently, other PARP knockout mice showed reduced survival after exposure to sublethal doses of ionizing radiation, and splenocytes derived from these animals undergo abnormal apoptosis (de Murcia et al., 1997).

We have previously shown that 3T3-L1 cells expressing PARP antisense RNA do not show a transient peak of PARP expression and activity normally apparent 24 h after exposure to insulin, dexamethasone, and methylisobutylxanthine (inducers of differentiation in this system). Consequently, the PARP-depleted cells fail to differentiate into adipocytes (Simbulan-Rosenthal et al., 1996; Smulson et al., 1995). PARP is apparently required for a necessary round of DNA

* Author to whom correspondence should be addressed at Department of Biochemistry and Molecular Biology, Georgetown University School of Medicine, Basic Science Building, Room 351, 3900 Reservoir Road NW, Washington, DC 20007. Tel.: (202) 687-1718 or 1089. Fax: (202) 687-7186. E-mail: smulson@bc.georgetown.edu.
[‡] Georgetown University School of Medicine.
[§] University of Maryland School of Medicine.

replication that occurs within the first 24 h of differentiation in these cells. Confocal microscopy revealed that, during this early stage of differentiation, when essentially all control cells have entered the S phase of the cell cycle, PARP is localized within distinct intranuclear granular foci that are associated with replication centers (Simbulan-Rosenthal et al., 1996). Furthermore, PARP specifically coimmunoprecipitated with DNA pol α during this time in control cells, but not in PARP-antisense cells.

PARP also exclusively copurifies through a series of centrifugation and chromatography steps with core proteins of a multiprotein DNA replication complex (known as MRC, or DNA synthesome) from HeLa cells and mouse FM3A cells; this complex catalyzes replication of viral DNA in vitro and contains DNA pol α and δ, DNA primase, DNA helicase, DNA ligase, and topoisomerase I and II, as well as accessory proteins such as proliferating-cell nuclear antigen (PCNA), RFC, and RPA. Furthermore, immunoblot analysis of MRC from both these cell types with antibodies to poly(ADP-ribose) (PAR) revealed that 15 of the ~40 component proteins, including DNA pol α, topoisomerase I, and PCNA, were poly(ADP-ribosyl)ated.

To clarify the role(s) of PARP within the DNA synthesome during the round of DNA replication in the early stages of differentiation in 3T3-L1 cells, we have now purified and characterized replicative complexes from control cells that had entered S phase after induction of differentiation and from cells depleted of PARP by expression of PARP antisense RNA. In the present study, we demonstrate that the DNA polymerase activities of the DNA synthesome from the S-phase control cells were markedly increased relative to uninduced control cells, whereas, the complex from PARP-deficient antisense cells was devoid of any DNA polymerase activities. To further investigate whether the lack of DNA pol α and δ activities in the PARP-antisense cells can be attributed to present but inactive enzymes, their absence from the complex, or a down-regulation of their expression in the cells, immunoblot analysis was performed with antibodies to replicative enzymes or accessory proteins. Interestingly, we show for the first time that PARP may play a role in the recruitment of PCNA and topo I into the DNA synthesome. These two proteins have been shown to be loosely associated with the core proteins of the DNA synthesome and form a so-called initiation complex (Applegren et al., 1995). On the other hand, PARP also appears to play a role in the regulation of the expression of a number of the proteins comprising the tightly associated core proteins of the MRC, such as DNA pol α, DNA primase, and RPA.

MATERIALS AND METHODS

Cells, Vectors, and Transfection. Monolayer cultures of control and PARP antisense 3T3-L1 preadipocytes were grown in Dulbecco's modified Eagle's medium (DMEM) supplemented with 10% fetal bovine serum (FBS), penicillin (100 units/mL), and streptomycin (100 μg/mL), and subcultured every 4 days. The PARP-antisense cell lines were obtained as previously described (Smulson et al., 1995) by transfection of 3T3-L1 preadipocytes with pMAM-As, a 1.1-kb Xho I fragment of murine PARP cDNA subcloned in the antisense orientation into the expression vector pMAM-neo (Clontech) under the control of the mouse mammary tumor

virus long terminal repeat, followed by selection of transfectants in medium containing G-418 (400 μg/mL). Expression of PARP antisense RNA was confirmed by RNA, DNA, and immunoblot analysis of control and stably transfected antisense cell lines after incubation with dexamethasone for various times.

Induction of Differentiation. Control and PARP-antisense 3T3-L1 preadipocyte cells were grown to confluence in DMEM supplemented with 10% FBS and then maintained for an additional 2 days, after which differentiation was induced by addition of 0.5 mM methylisobutyl xanthine, 1 μM dexamethasone, and 1.7 μM insulin. This medium was replaced with DMEM containing 10% FBS and 1.7 μM insulin after 48 h, and cells were placed back in regular medium after another 48 h. Terminal differentiation was monitored by washing the cells in phosphate-buffered saline (PBS), followed by fixation for 10 min in PBS containing 3.7% formaldehyde, staining with 0.3% Oil-Red-O dye for triglyceride droplets for 1 h, and observation under a phase-contrast microscope.

Enzyme Assays. At various indicated times after exposure to inducers of differentiation, control and PARP-antisense cells were harvested, they were washed with ice-cold PBS, and duplicate samples were subjected to enzyme assays to measure PARP, DNA pol α, and DNA pol δ activities. Purified MRC fractions from induced and uninduced control and PARP-antisense cells, as well as from HeLa cells, were also assayed for these enzyme activities. For PARP activity assays, incorporation of [^{32}P]NAD into acid-insoluble acceptors was measured at 25 °C for 1 min, with 20 μg protein per determination and triplicate determinations per treatment (Smulson et al., 1995). In vitro DNA pol α activity was assayed by measuring the incorporation of [^{3}H]TTP into DNA for 1 h at 37 °C by scintillation spectroscopy, with activated calf thymus DNA as template as previously described (Simbulan et al., 1993). DNA pol δ activity assays were performed by measuring the incorporation of [^{3}H]TTP into DNA for 1 h at 37 °C, with polydA-dT as template according to published procedures (Syvaoja et al., 1990).

Purification of the MRC from 3T3-L1 and HeLa Cells. Fractionation of cells and purification of the MRC were performed by a series of centrifugation steps and chromatography on two different columns as previously described (Applegren et al., 1995; Malkas et al., 1990; Wu et al., 1994). The replication-competent MRC partitions exclusively with the P4, Q-Sepharose peak, and sucrose gradient peak fractions, which also exhibit peak activities for DNA pol α, DNA pol δ, and PARP.

Immunoprecipitation Protocols. Immunoprecipitation was performed according to procedures described previously (Simbulan et al., 1993). Briefly, equal amounts (10 μg) of purified MRC (SG fraction) were added with 200 μL of EBC buffer (50 mM Tris-HCl pH 8, 120 mM NaCl, 0.5% NP-40, and 0.1 TIU of aprotinin), pre-cleared overnight with 10 μL/sample of protein A-Sepharose at 4 °C. After centrifugation, the supernatants were rocked for an hour with 0.5 mL of NET-N buffer (20 mM Tris-HCl pH 8.0, 100 mM NaCl, 1 mM EDTA, and 0.5% NP-40) containing anti-PCNA (1 μg of antibody per sample), followed by another incubation for 20 min with 20 μL of protein A-Sepharose in Tris-buffered saline with 10% BSA (1:1). After extensive washing of the beads with NET-N buffer, the immunocomplex bound to the

beads was then separated by SDS–polyacrylamide gel electrophoresis, transferred to nitrocellulose, and immuno-detected with monoclonal antibody against poly(ADP-ribose), provided by Drs. M. Miwa and T. Sugimura, Japan (1:250) (Kawamitsu et al., 1983).

Immunoblot Analysis with Antibodies to PARP, DNA pol α, DNA Primase, Topoisomerase I, RPA, and PCNA. SDS–polyacrylamide gel electrophoresis and protein transfer to nitrocellulose membranes were performed according to standard procedures. Membranes were stained with Ponceau S (0.1%) to confirm equal loading and transfer. After blocking of nonspecific sites, the blots were incubated with rabbit polyclonal antibodies to PARP (1:2000 dilution) (Ludwig et al., 1988) and then detected with appropriate peroxidase-labeled secondary antibodies (1:3000 dilution) and enhanced chemiluminescence (ECL, Amersham). Im-munoblots were sequentially stripped by incubation for 30 min at 50 °C with a solution containing 100 mM 2-mercap-toethanol, 2% SDS, and 62.5 mM Tris-HCl (pH 6.7), reblocked, and reprobed with antibodies to different DNA replication proteins. The monoclonal anti-DNA pol α (purified ascites) was used at 1:250 dilution and recognizes the 180 kDa polypeptide (Spriggs et al., 1992). The monoclonal antibody to RPA (1:500 dilution; recognizes the RPA p70) was kindly provided by Dr. B. Stillman; and the anti-DNA primase antibody (1:500 dilution; detects the DNA primase p58) by Dr. W. Copeland. The antibodies to topo I (1:1000 dilution; reacts with the topo I p100), PCNA (1:1000 dilution; detects the PCNA p36), and E2F-1 (1:1000; reacts with the E2F p60) were obtained from TopoGEN, Calbiochem, and Santa Cruz Biotech., respectively.

RESULTS

The Complexed Form of PCNA is Poly(ADP-ribosyl)ated. We have previously shown by immunoprecipitation experi-ments that PCNA is one of the poly(ADP-ribosyl)ated proteins of the HeLa MRC, together with DNA pol α and topo I. To further characterize the poly(ADP-ribosyl)ation state of PCNA in these cells, we subjected various fractions obtained during the purification of the MRC to immunopre-cipitation with anti-PCNA and then to immunoblot analysis with antibodies to PCNA and to PAR. Purification of the MRC was performed by fractionation of cells in a series of centrifugation steps, followed by discontinuous gradient centrifugation on a sucrose cushion (P4 and S4 fractions), chromatography on a Q-sepharose column (QS and FT fractions), and the peak fractions subjected to sucrose gradient centrifugation (SG) as previously described (Apple-gren et al., 1995; Malkas et al., 1990; Wu et al., 1994). The replication-competent MRC partitions exclusively with the P4, QS peak, and SG peak fractions, which also exhibit peak activities for DNA pol α, DNA pol δ, and PARP. Two forms of PCNA were detected: a complexed form that associated with the replication-competent fractions of the MRC, and a free form present in the replication-inactive fractions (Figure 1). Although approximately equal amounts of these two forms of PCNA were detected in the cell, only the complexed form was poly(ADP-ribosyl)ated (Figure 1), indicating that poly(ADP-ribosyl)ation of PCNA in the MRC may play a role in regulating its functions within the MRC.

Because PCNA is required for synthesis of leading strand DNA synthesis by DNA pol δ (Tsurimoto and Stillman,
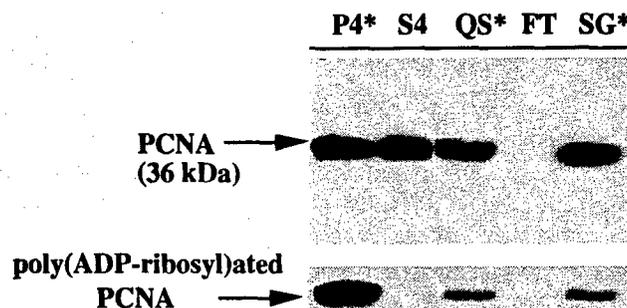

FIGURE 1: Immunoblot analysis with antibodies to PCNA (upper panel) or to PAR (lower panel) of immunoprecipitated fractions obtained during purification of the MRC from HeLa cells. Equal amounts of protein fractions (10 μg) were immunoprecipitated with antibody to PCNA and then subjected to immunoblot analysis with anti-PCNA (1:1000 dilution). Asterisks indicate the replication-competent MRC fractions, including the P4, Q-Sepharose (QS) peak, and sucrose gradient (SG) peak fractions (Applegren et al., 1995; Malkas et al., 1990). The positions of molecular size standards (in kilodaltons) are indicated on the right; the arrow indicates the position of PCNA. The immunoblot in the upper panel was stripped of antibodies and reprobed with monoclonal antibodies to PAR (1:250 dilution).

1991), we next investigated the effects of further poly(ADP-ribosyl)ation (in the presence of NAD) and the PARP inhibitor 3-aminobenzamide (3-AB) on in vitro DNA pol δ activity within the DNA synthesome. NAD inhibited the activity of DNA pol δ in the HeLa MRC (SG fraction) in a dose-dependent manner (Figure 2A), whereas 3-AB reversed the inhibitory effect of 100 μM NAD (Figure 2B). Es-sentially identical results were obtained when the effects of NAD and 3-AB on DNA pol α activity in the purified HeLa MRC (SG fraction) were assayed (data not shown). This is the first time that PARP or poly(ADP-ribosyl)ation has been shown to affect the activity of DNA pol δ in vitro, suggesting that PARP may play a regulatory role in the MRC by modulating the activity of component MRC replicative enzymes by catalyzing their poly(ADP-ribosyl)ation. As with other acceptor proteins of PARP (Yoshihara et al., 1985; Darby et al., 1985; Ferro and Olivera, 1984; Kasid et al., 1989; Eki and Hurwitz, 1991), further poly(ADP-ribosyl)-ation of these enzymes or their cofactors in the presence of increasing NAD may confer a large negative charge which promotes the dissociation of these enzymes from the DNA template-primer, thereby inhibiting their activity.
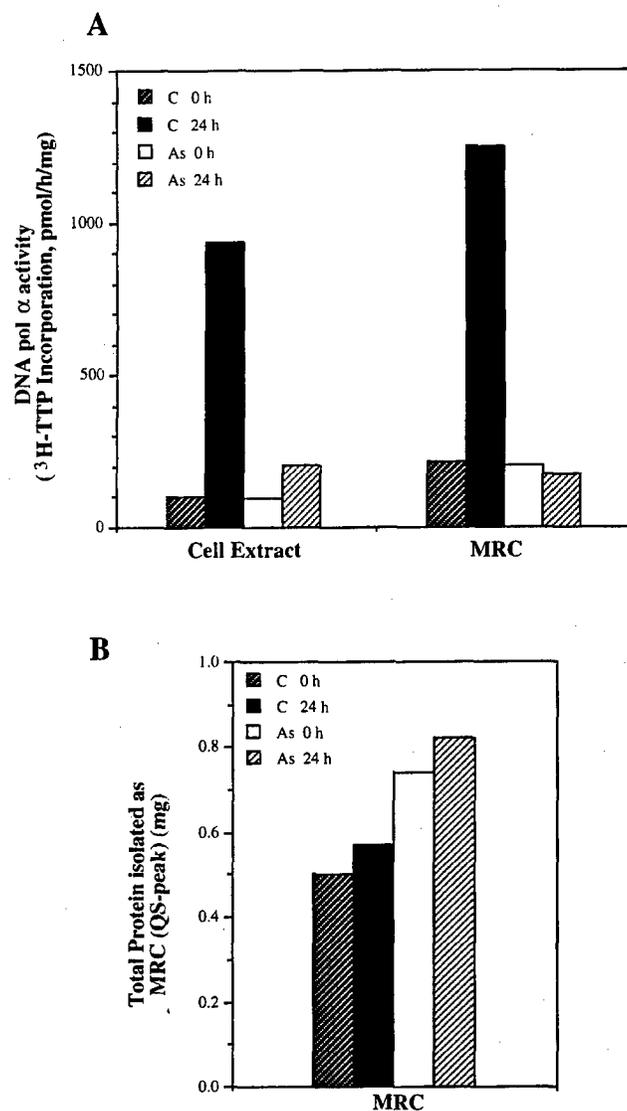
Effects of Depletion of PARP by Antisense RNA Expression on the Activities of DNA pol α and δ in the MRC of 3T3-L1 Cells. To further elucidate the role(s) of PARP in the MRC, we next investigated the effects of PARP depletion by expression of antisense RNA on the activities of DNA pol α and δ in the MRC (QS peak fractions) purified from 3T3-L1 cells. We have previously shown by flow cytometry that 80% of both 3T3-L1 control and PARP-antisense cells had a predominant G_0-G_1 DNA content prior to induction of differentiation. However, whereas 95% of the control cells had synchronously entered S phase 24 h after induction, 60% of the PARP antisense cells remained blocked at G_0-G_1 and had not entered S phase at this time (Simbulan-Rosenthal et al., 1996). Thus, under these conditions, quiescent control cells are induced to proliferate and go through one round of the cell cycle, but not the PARP-depleted antisense cells. Accordingly, the MRC was purified from 3T3-L1 control and PARP-antisense cells harvested before (0 h) and 24 h

A

B

3AB Concentration (μM)
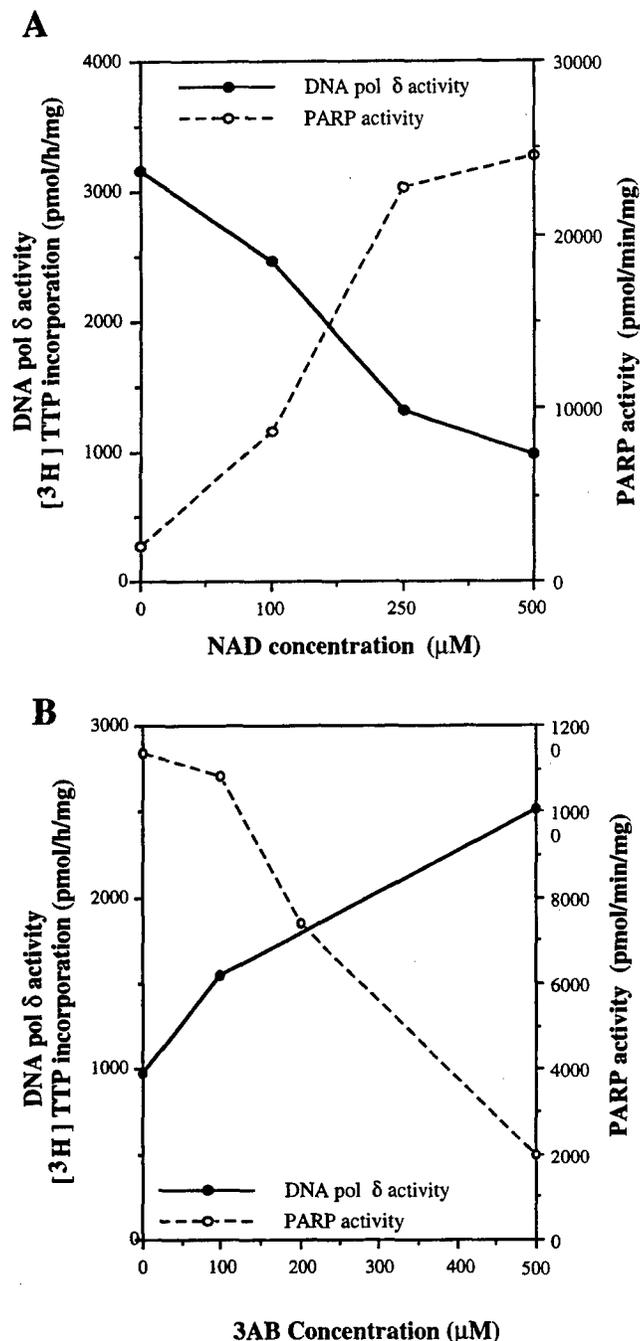
FIGURE 2: Concentration-dependent effects of NAD (A) and 3-AB (B) on DNA pol δ and PARP activities of the purified HeLa cell MRC. PARP and DNA pol δ activities of purified HeLa cell MRC (SG peak fraction) were assayed in the presence of various concentrations of NAD (A), or in the presence of 100 μM NAD and various concentrations of 3-AB (B), as described in Materials and Methods. Data are expressed as pmoles of [³H]dTTP incorporated into DNA per hour per milligram (DNA pol δ) or nanomoles of [³²P]NAD per minute per milligram of protein (PARP), and are means of triplicate determinations. Essentially identical results were obtained in three independent experiments.

after induction of differentiation as described in Materials and Methods. The Q-Sepharose peak fractions of MRC purified from the induced control cells which were used in the subsequent experiments were found to be competent to support viral DNA replication in vitro (data not shown).

DNA pol α activity in total cell extracts from uninduced control cells or from the PARP-antisense cells either before or 24 h after induction was only ~15% of that in total

A

B

FIGURE 3: Effects of PARP depletion by antisense RNA expression on DNA pol α activity of extracts and MRC fractions of 3T3-L1 cells prepared before or 24 h after induction of differentiation. (A) Total cell extracts and MRC (QS peak) fractions were prepared from 3T3-L1 control (C) and PARP-antisense (As) cells before and 24 h after exposure to inducers of differentiation. DNA pol α activity (pmoles of [³H]dTTP incorporated into DNA per hour per milligram) was assayed as described in Materials and Methods. Data are means of triplicate determinations, and essentially identical results were obtained in two additional experiments. (B) Amounts of protein isolated as MRC (QS peak) from 3T3-L1 (C) and PARP anstisense (As) cells prior to (0 h) and 24 h after induction.

extracts of the S phase control cells (Figure 3). Essentially all of the DNA pol α activity of the replicating control cells was recovered in the MRC fraction; the MRC fractions from PARP-antisense and uninduced control cells contained only ~15% of the DNA pol α activity associated with the MRC fraction of induced control cells (Figure 3A). Comparable amounts of protein were isolated as MRC (QS peak fraction) from the control and antisense cells, before (0 h) and 24 h after induction of differentiation (Figure 3B).

PARP activity assays were performed to confirm that the replicative complex purified from PARP-antisense cells lacked PARP activity. As expected, virtually all PARP activity cosedimented with the replication-competent MRC fractions (P4, QS peak), whereas the replication-inactive fractions (S4, QS flowthrough) contained essentially no

A

B
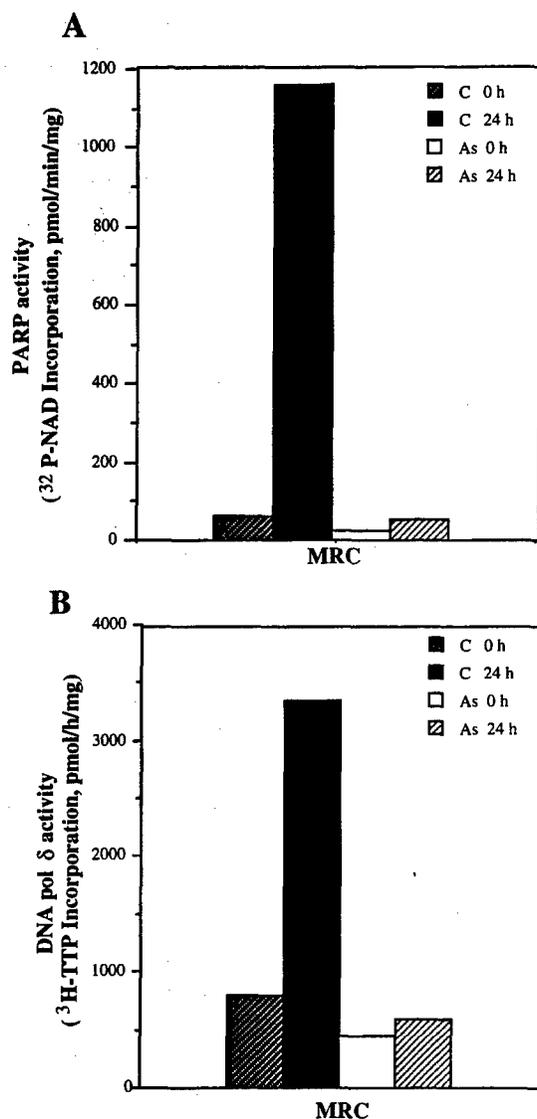
FIGURE 4: Effects of PARP depletion on PARP (A) and DNA pol δ (B) activities in the MRC fractions of 3T3-L1 cells. The MRC (QS peak) fraction was purified from 3T3-L1 control and PARP-antisense cells before and 24 h after induction of differentiation, and subjected to PARP and DNA pol δ activity assays as described in Materials and Methods. Data are means of triplicate determinations, and essentially identical results were obtained in two additional experiments.

PARP activity (data not shown), consistent with PARP being a "core" component of the MRC in these cells. However, as with DNA pol α activity, whereas substantial PARP activity was detected in MRC from control cells in S phase, the MRC fraction from PARP-antisense and uninduced control cells exhibited only ~5% of this activity (Figure 4A). The effect of PARP depletion on DNA pol δ activity of the MRC fraction was virtually identical to that on DNA pol α activity. Only the MRC fraction from replicating control cells contained substantial DNA pol δ activity (Figure 4B). These results are consistent with our earlier results showing that in vivo DNA replication, as assessed by incorporation of bromodeoxyuridine or [^{3}H]thymidine into newly synthesized DNA, occurred only in 3T3-L1 control cells 24 h after induction of differentiation, but not in the PARP-depleted antisense cells. Accordingly, depletion of PARP by antisense RNA expression resulted in a replicative complex devoid of any significant DNA pol α or δ activity.
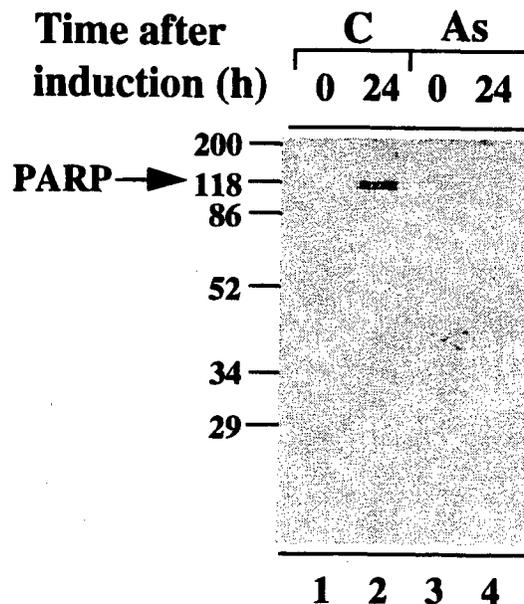
FIGURE 5: Immunoblot analysis with antibody to PARP of MRC fractions purified from 3T3-L1 control and PARP-depleted antisense cells. The MRC (QS peak) fraction was purified from 3T3-L1 control and PARP-antisense cells before and 24 h after induction of differentiation and equal amounts (20 μg) were subjected to immunoblot analysis with antibodies to murine PARP (1:2000 dilution). The positions of molecular size standards (in kilodaltons) are indicated on the left, as is the position of PARP (arrow).

Effects of PARP Depletion on the Protein Composition of the DNA Synthesome of 3T3-L1 Cells. SDS−polyacrylamide gel electrophoresis and silver staining of MRC fractions prepared from control and PARP-antisense cells, before or 24 h after induction of differentiation, revealed that the most prominent difference was the presence of a 116-kDa protein, corresponding to the size of intact PARP, in the fraction from control cells in S phase but not in those from PARP antisense cells or uninduced control cells. Although MRC purified from both control and antisense cells have approximately 35 to 40 protein bands, some proteins are evident only in the control MRC, while other proteins appear to be present in higher amounts in the antisense MRC (data not shown). What these proteins are, whether these bands represent different proteins, or whether some of these bands represent different modified forms of the same proteins, however, remain to be clarified. Consistent with the PARP activity data, immunoblot analysis with polyclonal antibodies to PARP showed that PARP protein was present exclusively in the MRC fraction from control 3T3-L1 cells in S phase, and not in the MRC fractions from PARP-antisense cells or nonreplicating control cells (Figure 5). The polyclonal antibody to PARP used here has previously been shown to react with a 116 kDa protein, corresponding to full-length PARP, and a smaller truncated PARP around 100 kDa which is observed only in murine cell extracts (Ludwig et al., 1988).

We next investigated the effects of PARP depletion on the protein composition of the MRC by immunoblot analysis with antibodies to specific MRC protein components. Immunoblot analysis of total cell extracts revealed that the amounts of PCNA and topo I were markedly increased in control cells exposed to inducers of differentiation (Figure 6). Ponceau S staining for total protein on the same immunoblot confirmed essentially equal protein loading and
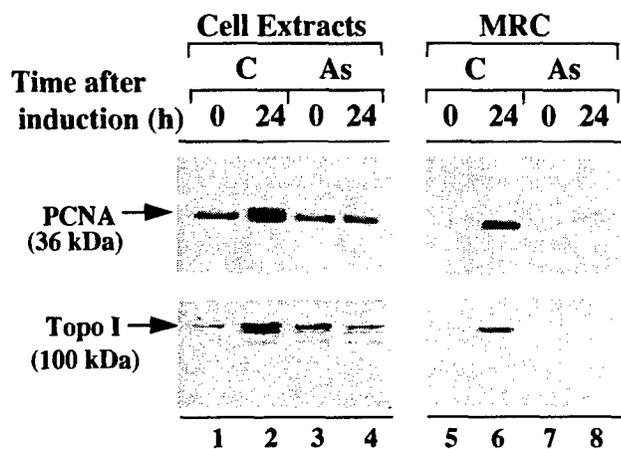
FIGURE 6: Immunoblot analysis of PCNA and topoisomerase I in total cell extracts and MRC fractions prepared from 3T3-L1 control and PARP-depleted antisense cells. Equal amounts (20 μg) of total cell extracts (left panels) and MRC (QS peak) fractions (right panels) from 3T3-L1 control and PARP-antisense cells prepared before and 24 h after induction of differentiation were subjected to immunoblot analysis with antibodies to PCNA (1:1000 dilution) (upper panels) or to DNA topoisomerase I (1:1000 dilution) (lower panels). Arrows indicate the positions of PCNA and topoisomerase I.

FIGURE 7: Immunoblot analysis of PARP, DNA polα, DNA primase, and RPA in total cell extracts derived from 3T3-L1 control and PARP-depleted antisense cells. Total cell extracts from 3T3-L1 control and PARP-antisense cells were prepared before and 24 h after induction of differentiation and equal amounts (20 μg protein) were subjected to immunoblot analysis with antibodies to PARP, DNA pol α, DNA primase, or RPA. Arrows indicate the positions of the various proteins, and their molecular sizes (in kilodaltons) are indicated on the right.

transfer among lanes (data not shown). It is unclear why topo I was detected in the uninduced PARP-antisense cells, but not in the uninduced control cells; nevertheless, both PCNA and topo I were present in antisense cells (Figure 6). However, the two proteins appeared to be present in antisense cells and uninduced control cells only in the free, uncomplexed form, because they were detected in the MRC fraction only from replicating control cells. These results suggest that these replication proteins are not recruited into the complex in PARP-depleted antisense cells and that PARP may play a role in their assembly into the DNA synthesome.

Immunoblot analysis of total cell extracts with antibodies to other component replicative proteins of the MRC such as DNA pol α, DNA primase, and RPA revealed a significant induction of each of these proteins on exposure of control cells to inducers of differentiation, but not in the PARP antisense cells (Figure 7). These results indicate that PARP and/or poly(ADP-ribosyl)ation may play a role in the regulation of expression of these MRC components when quiescent cells are induced to proliferate. Since there was no effect of PARP depletion on the expression of topo I in these cells (Figure 6), the lack of any DNA pol α, DNA primase, and RPA gene expression could not be attributed to a general inability of the PARP-depleted cells to undergo protein or RNA synthesis.

Effects of PARP Depletion by Antisense RNA Expression on the Expression of E2F-1, a Transcription Factor Implicated in the Transcriptional Regulation of the DNA pol α Gene. We next investigated the effect of PARP depletion on the abundance of E2F-1, a transcription factor that positively regulates the transcription of several gene products required for DNA replication and cell growth, including DNA pol α, PCNA, dihydrofolate reductase, thymidine kinase, c-MYC, c-MYB, cyclin D, and cyclin E (Blake and Azizkhan, 1989; DeGregori et al., 1995; Nevins, 1992; Pearson et al., 1991; Slansky et al., 1993). Immunoblot analysis of total cell extracts revealed that, whereas control cells exhibited a marked increase in the expression of E2F-1
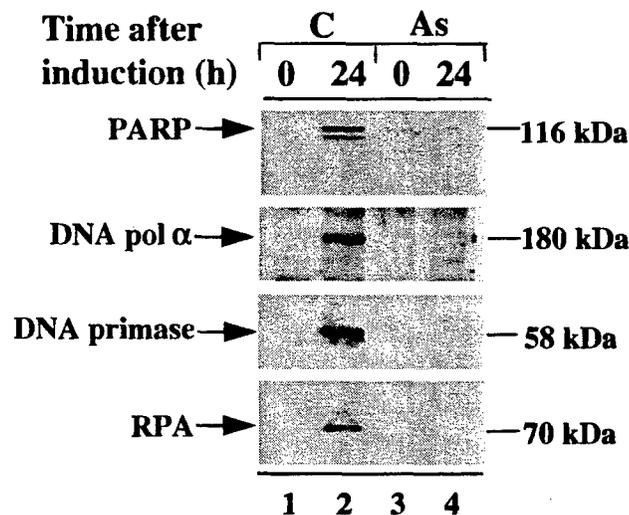
as early as 1 h after induction of differentiation, consistent with the fact that the E2F-1 gene is an early-response gene (Johnson et al., 1994), PARP-depleted antisense cells contained negligible amounts of E2F-1 during the 24 h exposure to inducers of differentiation (Figure 8). The induction of both DNA pol α and PCNA in control cells occurred after that of E2F-1, consistent with their being encoded by late-response genes (Pearson et al., 1991). These results indicate that PARP may regulate the expression of DNA pol α and PCNA genes during early S-phase indirectly by affecting the expression of the transcriptional factor, E2F-1, which in turn can regulate the transcription of both the DNA pol α and PCNA genes, as well as the E2F-1 gene itself.

DISCUSSION

We had previously shown that PARP depletion by expression of antisense RNA inhibits the differentiation of 3T3-L1 preadipocytes, including the differentiation-linked round of DNA replication (Smulson et al., 1995). The requirement for DNA replication prior to differentiation is thought to reflect a need to reconfigure chromatin in order to set and change committed patterns of gene expression (Villarreal, 1991). Differentiation of both 3T3-L1 cells (Smulson et al., 1995) and Friend erythroleukemia cells (Spriggs et al., 1992) is prevented by blocking the associated DNA replication at the early stages of this process. Thus, the failure of PARP-depleted 3T3-L1 cells to undergo terminal differentiation into adipocytes is likely attributable to their inability to undergo replication in the early stages of differentiation, indicating that PARP plays a role in this replication.

The roles of PARP have also been examined by gene disruption in PARP knockout mice. While certain strains of PARP knockout mice are viable and fertile, primary fibroblasts derived from these animals exhibit proliferation deficiencies in culture (de Murcia et al., 1997; Wang et al., 1995). Although both DNA replication and differentiation
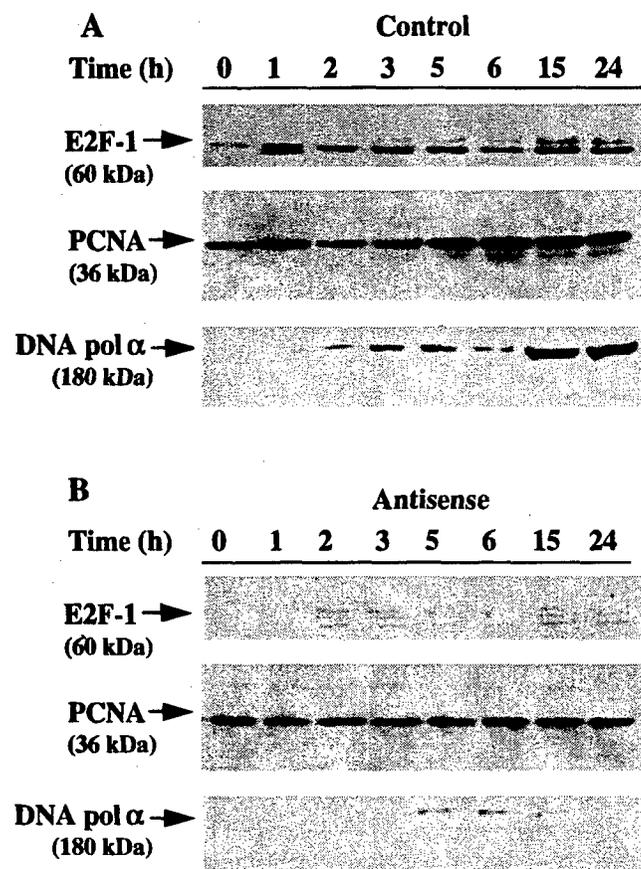
FIGURE 8: Time courses of the expression of DNA pol α, PCNA, and E2F-1 in 3T3-L1 control and PARP-antisense cells after exposure to inducers of differentiation. 3T3-L1 control and PARP-antisense cells were exposed to inducers of differentiation and harvested at the indicated times. Total cell extracts were then prepared and subjected to immunoblot analysis with antibodies to DNA pol α, PCNA, or E2F-1.

must be occurring in these animals, in the absence of PARP, apparently, in clonal cultured cell systems, PARP plays auxiliary roles in these processes, and isolated cell systems show more profound effects due to the lack of PARP that are not apparent in the animals.

We have also shown previously that PARP is tightly associated with the core proteins of the MRC purified from HeLa and FM3A cells (Simbulan-Rosenthal et al., 1996). These purified MRCs support viral DNA replication in vitro and migrates as discrete, high molecular weight complexes on native polyacrylamide gel electrophoresis (Tom et al., 1996). PARP has been thought to play a regulatory role within these complexes because it is capable of modulating the catalytic activity of some of the replicative enzymes or factors either by directly associating with them [DNA pol α (Simbulan et al., 1993)] or by catalyzing their poly(ADP-ribosyl)ation [DNA pol α (Yoshihara et al., 1985), and DNA topoisomerase I and II (Darby et al., 1985; Ferro and Olivera, 1984; Kasid et al., 1989), and RPA (Eki and Hurwitz, 1991)]. In most instances, poly(ADP-ribosyl)ation results in a reduction in enzyme activity of the modified protein, presumably because of a marked decrease in DNA-binding affinity caused by electrostatic repulsion between DNA and PAR.

About 15 of the ∼40 polypeptides of the MRC including DNA pol α, topo I, and PCNA, were shown to be poly-(ADP-ribosyl)ated by immunoblot analysis to PAR (Sim-

bulan-Rosenthal et al., 1996). We have now shown that, although there are approximately equal amounts of MRC-complexed and free forms of PCNA in HeLa cells, only the complexed form is poly(ADP-ribosyl)ated (Figure 1), suggesting that such modification may regulate its activity within the complex. The modified, complexed form of PCNA may correspond to the -35% of total cellular PCNA previously shown to be associated with replication foci during the peak of S phase (Morris and Mathews, 1989).

DNA pol α-primase synthesizes RNA primers and Okazaki fragments required for initiation of the lagging strand, while DNA pol δ mediates leading and lagging strand DNA synthesis during the elongation phase of DNA replication (Waga and Stillman, 1994). PCNA is required for DNA pol δ-mediated synthesis of the leading strand (Tsurimoto and Stillman, 1991). Consistent with previous studies with other purified enzymes, poly(ADP-ribosyl)ation inhibited the activities of DNA pol α and DNA pol δ within the MRC purified from HeLa cells in a manner that was dependent on NAD concentration and sensitive to 3-AB. Thus, poly-(ADP-ribosyl)ation may regulate the catalytic activities of these enzymes within the replication complex.

We also purified the MRC from 3T3-L1 cells harvested before and 24 h after exposure to inducers of DNA replication and differentiation; at the latter time point, ∼95% of control cells are in S phase and exhibit a transient peak of PARP expression. Only the MRC fraction from S phase control cells, not those from uninduced control cells or from PARP-antisense cells, contained PARP protein and activity as well as DNA pol α and δ activities (Figures 3 and 4). The observation that the MRC from PARP-depleted antisense cells do not have any DNA pol α and δ activities indicated three possibilities: (i) PARP may be essential for the functions of these replicative enzymes within the complex (they are present but inactive in the PARP-depleted antisense MRC); (ii) PARP may play a role in its assembly into the complex (they are present in total cell extracts, but not in the replicative complex); or (iii) PARP may be implicated in regulation of the expression of the genes for these proteins during entry into S phase (they are not present in cell extracts of the PARP-depleted antisense cells). Thus, the effect of PARP-depletion by antisense RNA expression on the protein composition of the complex was next investigated by immunoblot analyses using antibodies to MRC proteins which were available to us, i.e., PARP, DNA pol α, DNA primase, PCNA, topo I, and RPA.

PCNA and topo I were present in the MRC fraction only from S phase control cells, although they were both detected in total cell extracts from control and PARP-antisense cells exposed or not to inducers of differentiation (Figure 6). These results indicate that PARP may play a role in the assembly of PCNA and topo I into the DNA synthesome during entry into S phase. The mechanism by which this occurs, however, remains unclear. PARP has previously been shown by immunoprecipitation experiments to physically associate with DNA pol α in vitro (Simbulan et al., 1993) and in vivo (Smulson et al., 1995), as well as with topo I (Ferro et al., 1983). This physical association with other proteins may represent a mechanism by which PARP can recruit certain proteins into the replication complex. Whether poly(ADP-ribosyl)ation regulates recruitment of proteins to the MRC remains to be elucidated since it is still unclear whether

modification of component proteins occurs prior to, during, or after association with the MRC.

DNA pol α /DNA primase form a complex of four subunits, the largest of which is the catalytic subunit (~180 kDa) (Wong et al., 1986), and the two smallest subunits comprise the DNA primase (~58- and ~48 kDa) (Bambara and Jessee, 1991). When quiescent cells are stimulated to proliferate, mRNA levels of all four subunits increase simultaneously prior to DNA synthesis; thus, transcription of the genes for DNA pol α and DNA primase are likely regulated by a common mechanism (Miyazawa et al., 1993). Expression of DNA pol α, DNA primase, and RPA were significantly reduced in PARP-depleted antisense cells (Figure 7), suggesting that PARP may be implicated in the expression of the corresponding genes during entry of cells into S phase.

Under the conditions prior to induction of differentiation in this system, cells were stimulated to proliferate from essentially serum-deprived, spatially restricted quiescent cultures. In response to growth stimulation, expression of genes involved in DNA replication has been shown to increase dramatically at late G_1 (Baserga, 1991; Miyazawa et al., 1993), including PCNA, DNA pol α, and DNA primase genes. In mammalian cells, the transcription factor E2F-1 binds to a specific recognition site (5′-TTTCGCGC) and thereby activates the promoters of several genes that encode proteins required for DNA replication and cell growth, including DNA pol α, dihydrofolate reductase, thymidine kinase, c-MYC, c-MYB, PCNA, cyclin D, and cyclin E (Blake and Azizkhan, 1989; DeGregori et al., 1995; Nevins, 1992; Pearson et al., 1991; Slansky et al., 1993). Transcription of the E2F-1 gene, in turn, is also regulated during the cell cycle (Neuman et al., 1994). Interestingly, depletion of PARP by antisense RNA expression also prevented the increase in the abundance of E2F-1 associated with the early stage of differentiation in 3T3-L1 cells (Figure 8). Recently, PARP has also been shown to enhance activator-dependent transcription, presumably by interacting with RNA polymerase II-associated factors (Meisterernst et al., 1997), and a basal transcription factor, TFIIF, was reported to be a highly specific substrate for poly(ADP-ribosyl)ation (Rawling and Alvarez-Gonzalez, 1997). Thus, experiments are now underway to determine whether PARP plays a more direct role in the transcription of DNA pol α, PCNA, and E2F-1 genes by binding to the promoter sequences of the E2F-1 and/or DNA pol α genes during early S phase. Alternatively, since PARP depletion by antisense RNA expression has also been shown to result in significant changes in chromatin structure (Ding et al., 1992), it is also possible that the effects of PARP depletion may be due to indirect alterations in chromatin structure.

REFERENCES

Applegren, N., Hickey, R., Kleinschmidt, A., Zhou, Q., Coll, J., Bachur, N., Swaby, R., Wu, Y., Quan, J., Lee, M., & Malkas, L. (1995) *J. Cell. Biochem. 59*, 91−107.

Bambara, R., & Jessee, C. (1991) *Biochim. Biophys. Acta 1088*, 11−17.

Baserga, R. (1991) *J. Cell Sci. 98*, 433−436.

Blake, M., & Azizkhan, J. (1989) *Mol. Cell. Biol. 9*, 4994−5002.

Darby, M. K., Schmitt, B., Jongstra, B. J., & Vosberg, H. P. (1985) *Embo J. 4*, 2129−2134.

DeGregori, J., Kowalik, T., & Nevins, J. (1995) *Mol. Cell. Biol. 15*, 4215−4224.

de Murcia, J., Niedergang, C., Trucco, C., Ricoul, M., Dutrillaux, B., Mark, M., Oliver, J., Masson, M., Dierich, A., LeMeur, M., Waltzinger, C., Chambon, P., & deMurcia, G. (1997) *Proc. Natl. Acad. Sci. U.S.A. 94*, 7303−7307.

Ding, R., & Smulson, M. (1994) *Cancer Res. 54*, 4627−4634.

Ding, R., Pommier, Y., Kang, V. H., & Smulson, M. (1992) *J. Biol. Chem. 267*, 12804−12812.

Eki, T., & Hurwitz, J. (1991) *J. Biol. Chem. 266*, 3087−3100.

Ferro, A. M., Higgins, N. P., & Olivera, B. M. (1983) *J. Biol. Chem. 258*, 6000−6003.

Ferro, A. M., & Olivera, B. M. (1984) *J. Biol. Chem. 259*, 547−554.

Johnson, D., Ohtani, K., & Nevins, J. (1994) *Genes Dev. 8*, 1514−1525.

Kasid, U. N., Halligan, B., Liu, L. F., Dritschilo, A., & Smulson, M. (1989) *J. Biol. Chem. 264*, 18687−18692.

Kawamitsu, H., Hoshino, H., Miwa, M., & Sugimura, T. (1983) *Proc. Int. Symp. Princess Takamatsu Cancer Res. Fund 13*, 41−47.

Ludwig, A., Behnke, B., Holtlund, J., & Hilz, H. (1988) *J. Biol. Chem. 263*, 6993−6999.

Malkas, L. H., Hickey, R. J., Li, C., Pedersen, N., & Baril, E. F. (1990) *Biochemistry 29*, 6362−6374.

Meisterernst, M., Stelzer, G., & Roeder, R. (1997) *Proc. Natl. Acad. Sci. U.S.A. 94*, 2261−2265.

Miyazawa, H., Izumi, M., Tada, S., Takada, R., Masutani, M., Ui, M., & Hanaoka, F. (1993) *J. Biol. Chem. 268*, 8111−8122.

Morris, G., & Mathews, M. (1989) *J. Biol. Chem. 23*, 13856−13864.

Neuman, E., Flemington, E., Sellers, W., & Kaelin, W. (1994) *Mol. Cell. Biol. 14*, 6607−6615.

Nevins, J. (1992) *Science 258*, 424−429.

Pearson, B., Nasheuer, H., & Wang, T. (1991) *Mol. Cell. Biol. 11*, 2081−2095.

Rawling, J., & Alvarez-Gonzalez, R. (1997) *Biochem. J. 324*, 249−253.

Rosenthal, D. S., Shima, T. B., Celli, G., De Luca, L. M., & Smulson, M. E. (1995) *J. Invest. Dermatol. 105*, 38−44.

Simbulan, C., Suzuki, M., Izuta, S., Sakurai, T., Savoysky, E., Kojima, K., Miyahara, K., Shizuta, Y., & Yoshida, S. (1993) *J. Biol. Chem. 268*, 93−99.

Simbulan-Rosenthal, C. M. G., Rosenthal, D. S., Hilz, H., Hickey, R., Malkas, L., Applegren, N., Wu, Y., Bers, G., & Smulson, M. (1996) *Biochemistry 35*, 11622−11633.

Slansky, J., Li, Y., Kaelin, W., & Farnham, P. (1993) *Mol. Cell. Biol. 13*, 1610−1618.

Smulson, M. E., Kang, V. H., Ntambi, J. M., Rosenthal, D. S., Ding, R., & Simbulan, C. M. G. (1995) *J. Biol. Chem. 270*, 119−127.

Spriggs, L., Hill, S., & Jeter, J. (1992) *Biochem. Cell Biol. 70*, 555.

Syvaoja, J., Suomensari, S., Nishida, C., Goldsmith, J., Chui, G., Jain, S., & Linn, S. (1990) *Proc. Natl. Acad. Sci. U.S.A. 87*, 6664−6668.

Tom, T., Malkas, L., & Hickey, R. (1996) *J. Cell. Biochem. 63*, 259.

Villarreal, L. P. (1991) *Microbiol. Rev. 55*, 512−542.

Waga, S., & Stillman, B. (1994) *Nature 369*, 207−212.

Wang, Z. Q., Auer, B., Stingl, L., Berghammer, H., Haidacher, D., Schweiger, M., & Wagner, E. F. (1995) *Genes Dev. 9*, 509−520.

Wong, S., Paborsky, L., Fisher, P., Wang, T. S.-F., & Korn, D. (1986) *J. Biol. Chem. 261*, 7958−7968.

Wu, Y., Hickey, R., Lawlor, K., Wills, P., Yu, F., Ozer, H., Starr, R., Quan, J. Y., Lee, M., & Malkas, L. (1994) *J. Cell. Biochem. 54*, 32−46.

Yoshihara, K., Itaya, A., Tanaka, Y., Ohashi, Y., Ito, K., Teraoka, H., Tsukada, K., Matsukage, A., & Kamiya, T. (1985) *Biochem. Biophys. Res. Commun. 128*, 61−67.

Transient Poly(ADP-ribosyl)ation of Nuclear Proteins and Role of Poly(ADP-ribose) Polymerase in the Early Stages of Apoptosis*

Cynthia M. Simbulan-Rosenthal, Dean S. Rosenthal, Sudha Iyer, A. Hamid Boulares, and Mark E. Smulson‡

From the Department of Biochemistry and Molecular Biology, Georgetown University School of Medicine, Washington, D. C. 20007

A transient burst of poly(ADP-ribosyl)ation of nuclear proteins occurs early, prior to commitment to death, in human osteosarcoma cells undergoing apoptosis, followed by caspase-3-mediated cleavage of poly(ADP-ribose) polymerase (PARP). The generality of this early burst of poly(ADP-ribosyl)ation has now been investigated with human HL-60 cells, mouse 3T3-L1, and immortalized fibroblasts derived from wild-type mice. The effects of eliminating this early transient modification of nuclear proteins by depletion of PARP protein either by antisense RNA expression or by gene disruption on various morphological and biochemical markers of apoptosis were then examined. Marked caspase-3-like PARP cleavage activity, proteolytic processing of CPP32 to its active form, internucleosomal DNA fragmentation, and nuclear morphological changes associated with apoptosis were induced in control 3T3-L1 cells treated for 24 h with anti-Fas and cycloheximide but not in PARP-depleted 3T3-L1 antisense cells exposed to these inducers. Similar results were obtained with control and PARP-depleted human Jurkat T cells. Whereas immortalized PARP +/+ fibroblasts showed the early burst of poly(ADP-ribosyl)ation and a rapid apoptotic response when exposed to anti-Fas and cycloheximide, PARP −/− fibroblasts exhibited neither the early poly(ADP-ribosyl)ation nor any of the biochemical or morphological changes characteristic of apoptosis when similarly treated. Stable transfection of PARP −/− fibroblasts with wild-type PARP rendered the cells sensitive to Fas-mediated apoptosis. These results suggest that PARP and poly(ADP-ribosyl)ation may trigger key steps in the apoptotic program. Subsequent degradation of PARP by caspase-3-like proteases may prevent depletion of NAD and ATP or release certain nuclear proteins from poly(ADP-ribosyl)ation-induced inhibition, both of which might be required for late stages of apoptosis.

Apoptosis, or programmed cell death, plays important roles in development, homeostasis, and immunological competence.

It is characterized by marked morphological changes such as membrane blebbing, chromatin condensation, nuclear breakdown, and the appearance of membrane-associated apoptotic bodies, as well as by internucleosomal DNA fragmentation. The enzyme poly(ADP-ribose) polymerase (PARP)[1] catalyzes the poly(ADP-ribosyl)ation of various nuclear proteins with NAD as substrate, and, because it is activated by binding to DNA ends or strand breaks, PARP has been suggested to contribute to cell death by depleting the cell of NAD and ATP (1). PARP undergoes proteolytic cleavage into 89- and 24-kDa fragments that contain the active site and the DNA-binding domain of the enzyme, respectively, during drug-induced apoptosis in a variety of cells (2). More recently, PARP has been implicated in the induction of both p53 expression and apoptosis (3), with the specific proteolysis of the enzyme thought to be a key apoptotic event (4–6).

Caspase-3, a member of the caspase family of 10 or more aspartate-specific cysteine proteases that play a central role in the execution of the apoptotic program (7), is primarily responsible for the cleavage of PARP during cell death (4, 5). Other caspases, such as caspase-7, also cleave PARP *in vivo*, but at lower efficiencies. Composed of two subunits of 17 and 12 kDa that are derived from a common proenzyme (CPP32), caspase-3 is related to interleukin-1β-converting enzyme and CED-3, which is required for apoptosis in *Caenorhabditis elegans* (8). In human osteosarcoma cells that undergo confluence-associated apoptosis over a 10-day period, caspase-3-like activity, measured with a specific [^{35}S]PARP-cleavage assay *in vitro*, peaks at 6–7 days after initiation of apoptosis, concomitant with the onset of internucleosomal DNA fragmentation (4).

We recently examined the time course of PARP activation and cleavage during apoptosis in intact osteosarcoma cells by immunofluorescence microscopy with antibodies to PARP, to the 24-kDa cleavage product of PARP, and to poly(ADP-ribose) (PAR) (9). We observed a transient burst of synthesis of PAR from NAD that increased early and was maximal 3 days after initiation of apoptosis, prior to the appearance of internucleosomal DNA cleavage (at day 7) and before the cells became irreversibly committed to apoptosis. During this early period, expression of full-length PARP was detected by both immunofluorescence and immunoblot analysis. The amounts of both PAR and PARP decreased thereafter, and at 6 days, the 24-kDa cleavage product of PARP was detected both immunocytochemically and by immunoblot analysis. PAR was not observed during days 8 to 10, despite the presence of abundant DNA strand breaks, potential activators of PARP, during this time.

[1] The abbreviations used are: PARP, poly(ADP-ribose) polymerase; PAR, poly(ADP-ribose); MNU, *N*-methyl-*N*-nitrosourea; CHAPS, 3-[(3-cholamidopropyl)dimethylammonio]-1-propanesulfonic acid; Pipes, 1,4-piperazinediethanesulfonic acid; PBS, phosphate-buffered saline; TNF-α, tumor necrosis factor-α.

These observations suggested that short-lived PARP-catalyzed poly(ADP-ribosyl)ation may be important at an early stage of apoptosis and is followed by the cleavage of PARP by mid-apoptosis. We have now investigated whether this transient poly(ADP-ribosyl)ation occurs in other cell lines and with other inducers of apoptosis. We examined both cell lines stably transfected with inducible PARP antisense constructs (9–11) and immortalized fibroblasts derived from PARP knockout mice (12) to determine the effect of preventing the early burst in PARP activity on specific markers of apoptosis.

Several PARP knockout mice have been established by disrupting the PARP gene in embryonic stem cells; these animals neither express PARP nor exhibit any poly(ADP-ribosyl)ation (12, 13). Despite variations in the physiological phenotypes of these animals, developmental apoptosis seems to take place in the absence of PARP. Furthermore, primary cells (fibroblasts, splenocytes, thymocytes) from these animals undergo apoptosis induced by *N*-methyl-*N*-nitrosourea (MNU) and other agents (13, 14). The more recent PARP knockout mice exhibit extreme sensitivity to γ-irradiation and MNU, and primary cells derived from these mice showed an abnormal apoptotic response to MNU (13). In contrast, >80% of primary embryonic fibroblasts derived from the earlier PARP knockout mice lost viability when exposed to anti-Fas (1000 ng/ml) for 8 h; thus, the absence of PARP does not seem to interfere with programmed cell death in these primary cells (14).

Our previous studies with clonal cells depleted of PARP by expression of PARP antisense RNA have supported accessory roles for PARP and/or poly(ADP-ribosyl)ation in adipocyte differentiation (11), DNA replication associated with this differentiation (15, 63), genomic stability (10), and DNA repair (33, 16). In DNA repair, for example, although the absence of PARP did not totally prevent the repair of single-strand breaks, it resulted in a significant delay in this process (16). Primary cell cultures presumably consist of a mosaic of different stages of development, many of which perhaps possess compensatory routes to overcome gene disruption. It is possible that biochemical roles, not easily observable in the context of the whole animal or in primary cultures of cells, can be identified in clonal cells because of more profound effects observed in these cells.

The present study demonstrates the occurrence of a transient poly(ADP-ribosyl)ation of nuclear proteins at an early stage of apoptosis induced by serum deprivation, camptothecin, or antibodies to Fas in different cell lines. When this early poly(ADP-ribosyl)ation was prevented as a result of depletion of endogenous PARP, either by gene disruption or by antisense RNA expression, several morphological and biochemical markers of apoptosis were no longer observed in response to such inducers.

EXPERIMENTAL PROCEDURES

Cell Culture, Vectors, and Transfection—A 1.1-kilobase fragment of murine PARP cDNA encoding the DNA-binding domain and the NH_2-terminal automodification domain (for the mouse 3T3-L1 cell transfections) or a 3.7-kilobase *Xho*I full-length human PARP cDNA (for human Jurkat T cell transfection) was subcloned in an antisense orientation in the expression vector pMAM-neo (CLONTECH) under the control of the dexamethasone-inducible mouse mammary tumor virus promoter. The resulting pMAM-As (antisense) or pMAM-neo (control) plasmids were transfected into cells by calcium phosphate precipitation (3T3-L1 cells) or by electroporation (Jurkat cells). Transfectants were selected in appropriate medium with G-418 (400 μg/ml) (Life Technologies, Inc.). Stably transfected 3T3-L1 cells and fibroblasts derived from both wild-type and PARP knockout mice (12) were cultured in Dulbecco's modified Eagle's medium supplemented with 10% fetal bovine serum, penicillin (100 units/ml), and streptomycin (100 μg/ml). The PARP +/+ and −/− fibroblasts, immortalized by a standard 3T3 protocol, were kindly provided by Z. Q. Wang (International Agency for Research on Cancer,

Lyon, France). Jurkat T cells and HL-60 cells were maintained in RPMI 1640 supplemented with 10% and 20% fetal bovine serum, respectively. PARP −/− fibroblasts were either cotransfected with a plasmid expressing wild-type PARP (pcD-12; Ref. 17) along with the plasmid pTracer-CMV (Invitrogen), a zeocin-based vector system, or with pTracer-CMV alone using lipofectamine (Life Technologies, Inc.). This vector system was utilized as the PARP −/− fibroblasts expressed an endogenous neo gene, which was used to establish the original PARP knockout mice. Stable transfectants were colony-selected in growth medium containing 500 μg/ml Zeocin.

PARP-cleavage Assay—*In vitro* PARP-cleavage assays were performed as described previously (4, 9). In brief, full-length human PARP cDNA was excised from pcD-12 (17), ligated into the *Xho*I site of pBluescript-II SK+ (Stratagene), and used to synthesize [^{35}S]methionine-labeled PARP by coupled T7 RNA polymerase-mediated transcription and translation in a reticulocyte lysate system (Promega). Cytosolic extracts of various cells were prepared by rapid freezing and thawing of cells in a solution containing 10 mM Hepes-KOH (pH 7.4), 2 mM EDTA, 0.1% CHAPS detergent, 5 mM dithiothreitol, 1 mM phenylmethylsulfonyl fluoride, pepstatin A (10 μg/ml), leupeptin (10 μg/ml), and aprotinin (10 μg/ml), followed by centrifugation of the cell lysate at 100,000 × g for 30 min and recovery of the supernatant. *In vitro* PARP-cleavage activity was measured in 25-μl reaction mixtures containing 5 μg of cytosolic protein, [^{35}S]PARP (~5 × 104 cpm), 50 mM Pipes-KOH (pH 6.5), 2 mM EDTA, 0.1% CHAPS, and 5 mM dithiothreitol. After incubation for 1 h at 37 °C, reactions were terminated by the addition of SDS sample buffer (4% SDS, 4% 2-mercaptoethanol, 10% glycerol, 125 mM Tris-HCl (pH 6.8), and 0.02% bromphenol blue). Proteins were resolved by SDS-polyacrylamide gel electrophoresis, and PARP-cleavage products were visualized by fluorography.

Indirect Immunofluorescence Microscopy and Immunoblot Analysis—The procedures for fixation and staining with monoclonal antibodies to PAR (10HA) (18) have been described previously (9). Cells were transferred to a slide in a Cytospin (IEC Centra), fixed with 10% (w/v) ice-cold trichloroacetic acid for 10 min, and dehydrated in 70%, 90%, and absolute ethanol for 3 min each at −20 °C. The slides were then incubated overnight in a humid chamber at room temperature with antibodies to PAR (1:250 dilution) in phosphate-buffered saline (PBS) containing 12% bovine serum albumin. After washing with PBS, cells were incubated for 1 h with biotinylated anti-mouse IgG (1:400 dilution in PBS-bovine serum albumin), washed, and incubated for 30 min with streptavidin-conjugated Texas red (1:800 dilution in PBS-bovine serum albumin). Cells were finally mounted with PBS containing 80% glycerol and observed with a Zeiss fluorescence microscope. All exposure times were identical to allow comparisons of relative staining intensities at various times during apoptosis.

For immunoblot analysis, SDS-polyacrylamide gel electrophoresis and transfer of proteins (30 μg per lane) to nitrocellulose membranes were performed according to standard procedures. Membranes were stained with Ponceau S (0.1%) to confirm equal loading and transfer. After blocking of nonspecific sites, membranes were incubated with antibodies to PARP (1:2000 dilution) (19) or to caspase-3 (1:10,000 dilution; kindly provided by Dr. D. Nicholson, Merck Labs). The membranes were subsequently probed with appropriate peroxidase-labeled antibodies to mouse or rabbit IgG (1:3000 dilution), and immune complexes were detected by enhanced chemiluminescence (Pierce). For detection of PAR bound to the separated proteins in the same blots, the membranes were stripped of antibodies by incubation at 50 °C for 30 min in a solution containing 100 mM 2-mercaptoethanol, 2% SDS, and 62.5 mM Tris-HCl (pH 6.7); after blocking of nonspecific sites, they were reprobed with monoclonal antibodies to PAR (1:250 dilution).

PARP Activity Assays—At indicated time intervals, cells were harvested by scraping, washed with ice-cold PBS, and assayed for PARP activity as described previously (20). Briefly, cells were sonicated for 20 s (three times) to lyse cells and introduce DNA strand breaks required for PARP activity, followed by measurement of [^{32}P]NAD incorporation into acid-insoluble acceptors at 25 °C for 1 min.

Detection of Apoptotic Internucleosomal DNA Fragmentation—Cells were washed in PBS and lysed in 7 M guanidine hydrochloride, and total genomic DNA was extracted and purified using a Wizard Miniprep DNA Purification Resin (Promega). After RNase A treatment (1 μg/50 μl) of the DNA samples for 30 min, apoptotic internucleosomal DNA fragmentation was detected by gel electrophoresis on a 1% agarose gel and ethidium bromide staining (0.5 μg/ml) as described previously (64).

Hoechst Staining for Apoptotic Morphology—Cells were centrifuged at 1000 rpm for 5 min, fixed for 10 min in PBS containing 4% formalin, washed with PBS, and stained with Hoechst 33258 (24 mg/ml) in PBS containing 80% glycerol. An aliquot (25 μl) of the cell suspension was

Time (h): 0 1 2 4 6 8 24
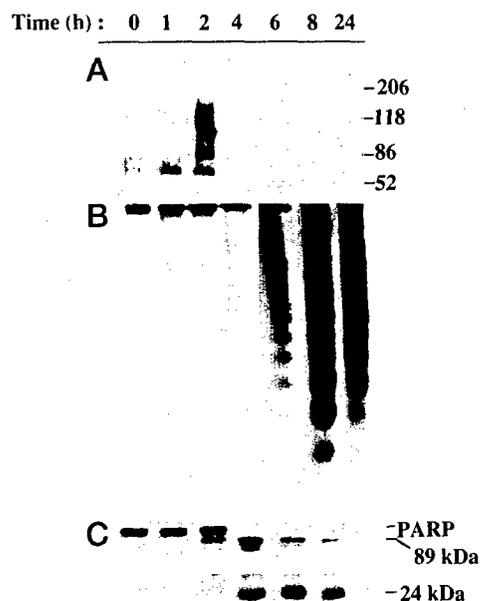
FIG. 1. **Time course of poly(ADP-ribosyl)ation of nuclear proteins (A), DNA fragmentation (B), and PARP-cleavage activity (C) during camptothecin-induced apoptosis in human HL-60 cells.** A, apoptosis was induced in human HL-60 cells by incubation with camptothecin (10 μM); at the indicated times, cell extracts were prepared and subjected to immunoblot analysis with antibodies to PAR. B, apoptosis was monitored by extraction of total genomic DNA and detection of characteristic internucleosomal DNA ladders by agarose gel electrophoresis and ethidium bromide staining. C, caspase-3-like PARP-cleavage activity in cytosolic extracts was assayed with [^{35}S]PARP as substrate.

then dropped onto a slide, and nuclear morphology was observed with an Olympus BH2 fluorescence microscope.

RESULTS

A Transient Burst of Poly(ADP-ribosyl)ation of Nuclear Proteins Occurs during Early Stages of Apoptosis in HL-60 Cells—To investigate whether the brief activation of PARP during the early stages of apoptosis, detected initially by immunofluorescence in osteosarcoma cells (9), is a general phenomenon, we examined several different cell types. The transient PARP activation occurs prior to the induction of caspase-3-like activity, as measured by the *in vitro* cleavage of [^{35}S]methionine-labeled PARP into 89- and 24-kDa fragments by cell extracts derived at various stages of apoptosis. This burst of PAR synthesis also occurs before the onset of internucleosomal DNA fragmentation, a biochemical hallmark of apoptosis, which has been shown to begin on day 7 and peak at day 10, when almost 100% of the cells have undergone apoptosis (4, 9). Although caspase-3 is the major protease responsible for the *in vivo* cleavage of PARP, other caspases have also been shown to partially cleave PARP at much lower efficiencies; thus, we refer to this activity as caspase-3-like.

The time course of apoptosis induced by the topoisomerase inhibitor camptothecin in HL-60 cells is shorter than spontaneous apoptosis occurring in osteosarcoma cells, as evidenced by the detection of internucleosomal DNA fragmentation by 6 h after induction (Fig. 1*B*). Caspase-3-like PARP-cleavage activity was apparent at 4 h and maximal at 6–8 h after induction (Fig. 1*C*). Immunoblot analysis with antibodies to PAR revealed an early transient peak of poly(ADP-ribosyl)ation of nuclear proteins 2 h after induction of apoptosis (Fig. 1*A*), prior to the onset of caspase-3-like activity and DNA fragmentation, similar to that observed in osteosarcoma cells. Caspase-3-like cleavage of PARP apparently results in PARP inactivation as there are no poly(ADP-ribosyl)ated acceptors at the peak of

TNF-α: - + - - -
Camptothecin: - - + - -
Anti-Fas: - - - + +
Cycloheximide: - - - - +
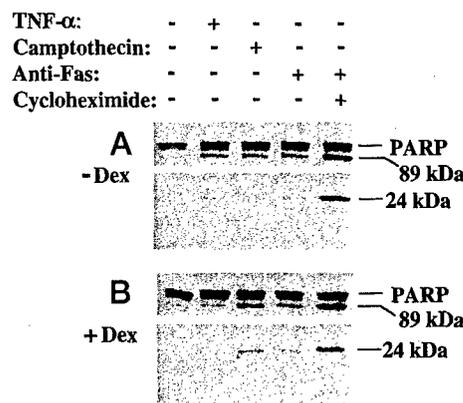
FIG. 2. **Induction of *in vitro* caspase-3-like PARP-cleavage activity in 3T3-L1 cells by a combination of anti-Fas and cycloheximide.** Mock-transfected cells were preincubated in the absence (A) or presence (B) of 1 μM dexamethasone (Dex) for 72 h and subsequently incubated for 24 h in the absence or presence of TNF-α (1000 units/ml), camptothecin (10 μM), anti-Fas (500 ng/ml), or a combination of anti-Fas (50 ng/ml) and cycloheximide (10 μg/ml). Cytosolic extracts were then prepared and assayed for caspase-3-like activity with [^{35}S]PARP as substrate.

caspase-3 like activity (6–8 h), even in the presence of massive DNA fragments (Fig. 1*B*) at this time.

Transient Poly(ADP-ribosyl)ation of Nuclear Proteins Occurs Early during Fas-mediated Apoptosis in Murine 3T3-L1 Cells but Not in PARP-depleted 3T3-L1 Antisense Cells—We next examined murine 3T3-L1 cells that can be depleted of endogenous PARP by antisense RNA expression. We have previously used these cells, which are stably transfected with a dexamethasone-inducible PARP antisense construct, to investigate the role of PARP in differentiation (11, 15, 63). PARP was shown to be required for a round of DNA replication that precedes the onset of differentiation in these cells.

Because apoptosis has previously been induced in 3T3-L1 cells only by deregulated expression of c-Myc under conditions of serum deprivation (21), it was first necessary to establish conditions under which apoptosis could be triggered by exogenous inducers. 3T3-L1 cells transfected with the control vector (mock-transfected) were preincubated in the presence or absence of 1 mM dexamethasone for 72 h and then treated with various inducers of apoptosis. Tumor necrosis factor-α (TNF-α), camptothecin, or antibodies to Fas (anti-Fas) (even at a dose of 500 ng/ml, which is 10 times the concentration required to induce apoptosis in other cell lines) induced only a slight increase in caspase-3-like activity in mock-transfected cells (Fig. 2). However, incubation of cells with a combination of anti-Fas and cycloheximide resulted in a marked induction of caspase-3-like activity, as indicated by the generation of the 89- and 24-kDa cleavage fragments of PARP. Densitometric scanning showed that ~60% of [^{35}S]PARP substrate was converted to the 89-kDa cleavage product under these conditions. Cycloheximide alone did not induce apoptosis in these cells (data not shown). Cycloheximide has been previously shown to potentiate TNF-α-induced apoptosis (22–24) as well as overcome resistance to Fas-mediated apoptosis in various cells (24–26); this latter effect of cycloheximide does not seem to be mediated by inhibition of translation because resistant cells can be sensitized to anti-Fas by subinhibitory concentrations of the drug. The presence of dexamethasone during the 72-h preincubation of mock-transfected 3T3-L1 cells had no effect on induction of caspase-3-like activity (Fig. 2*B*).
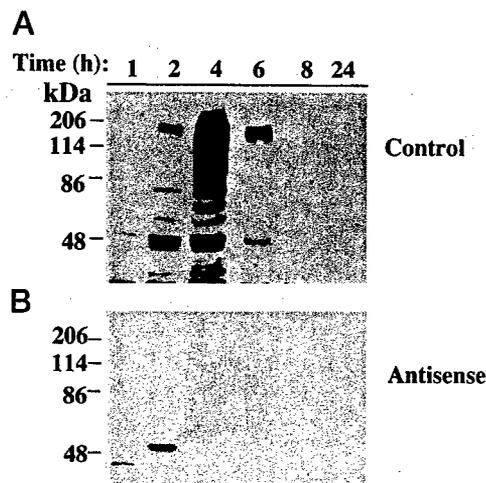
It was important to determine the kinetics of PARP depletion induced by antisense RNA expression in 3T3-L1 cells under the present conditions, given that our previous studies with this cell line had focused on the role of PARP in differentiation.
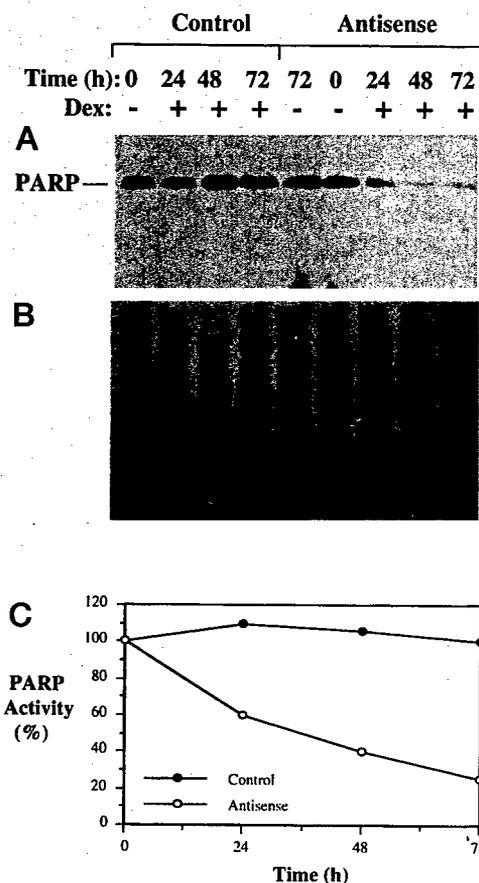
FIG. 3. **PARP depletion by antisense RNA expression in 3T3-L1 cells.** Mock-transfected (control) and PARP-antisense 3T3-L1 cells were incubated in the absence or presence of 1 μM dexamethasone (Dex) for the indicated times, after which equal amounts of total cellular protein (30 μg) were resolved by SDS-polyacrylamide gel electrophoresis and subjected to immunoblot analysis with rabbit antibodies to full-length PARP (A). The immunoblot was also stained with Ponceau S to confirm equal protein loading and transfer among the lanes (B). At indicated time intervals after exposure to dexamethasone, control and PARP antisense cells were harvested by scraping, washed with ice-cold PBS, and assayed for PARP activity as described under "Experimental Procedures" (C).

FIG. 4. **Time course of poly(ADP-ribosyl)ation of nuclear proteins in 3T3-L1 control and PARP-depleted antisense cells exposed to anti-Fas and cycloheximide.** 3T3-L1 control (A) and PARP-antisense (B) cells were preincubated in the presence of 1 μM dexamethasone for 72 h and then exposed to anti-Fas (50 ng/ml) and cycloheximide (10 μg/ml) for the indicated times. Equal amounts of total cellular protein (30 μg) were then subjected to immunoblot analysis with monoclonal antibodies to PAR. The positions of molecular size standards (in kilodaltons) are indicated.

Immunoblot analysis revealed that the amount of PARP in mock-transfected 3T3-L1 cells was not affected by incubation with dexamethasone (Fig. 3A). However, in the PARP-antisense cells, dexamethasone induced a time-dependent depletion of PARP, with only ~5% of the protein remaining after 72 h. Ponceau S staining for total protein on the same immunoblot confirmed essentially equal protein loading and transfer among lanes (Fig. 3B). Whereas the *in vitro* PARP activity of control cells was not affected by incubation with dexamethasone, exposure of PARP-antisense cells to dexamethasone for 72 h resulted in an ~80% decrease in PARP activity (Fig. 3C).

3T3-L1 control cells that had been preincubated with dexamethasone for 72 h were exposed to anti-Fas and cycloheximide for various times and then subjected to immunoblot analysis with antibodies to PAR. As in HL-60 and osteosarcoma cells, the extent of poly(ADP-ribosyl)ation of nuclear proteins peaked early, 4 h after the induction of apoptosis in control 3T3-L1 cells, a stage at which all the cells were still viable and could be replated, and subsequently decreased (Fig. 4A). The array of poly(ADP-ribosyl)ated nuclear proteins was consistent with automodification of PARP as well as the poly(ADP-ribosyl)ation of histones and other nuclear acceptor proteins (27). As anticipated, poly(ADP-ribosyl)ation of nuclear proteins was not detected in PARP-depleted 3T3-L1 antisense cells exposed to

anti-Fas and cycloheximide (Fig. 4B).

Effects of the Absence of Early Transient Poly(ADP-ribosyl)ation on Morphological and Biochemical Markers of Apoptosis in 3T3-L1 Cells—We next tried to determine whether prevention of the early burst of PAR synthesis by PARP antisense RNA expression could affect the development of other biochemical or morphological markers of apoptosis when these cells are exposed to apoptosis inducers. The combination of anti-Fas and cycloheximide induced a marked increase in caspase-3-like activity in mock-transfected 3T3-L1 cells that had been preincubated in the absence or presence of dexamethasone (Fig. 5A); this effect was maximal 24 h after induction of apoptosis. Whereas PARP-antisense 3T3-L1 cells that were not exposed to dexamethasone showed a similar increase in caspase-3-like activity in response to anti-Fas and cycloheximide, no such increase was apparent in PARP-antisense cells that had been depleted of PARP by preincubation with dexamethasone before exposure to anti-Fas and cycloheximide (Fig. 5B).

Caspase-3, similar to other members of the caspase family, is expressed in cells as an inactive 32-kDa proenzyme (CPP32). During apoptosis, CPP32 is activated by cleavage at specific Asp residues, with the active enzyme (caspase-3) consisting of a heterodimer of a 17-kDa subunit (p17), containing the catalytic domain, and a 12-kDa subunit (p12) (4). To confirm that CPP32 is proteolytically processed to p17 during apoptosis in control 3T3-L1 cells and to determine whether the transient early poly(ADP-ribosyl)ation is necessary for this activation, control and antisense cells were preincubated with dexamethasone and exposed to anti-Fas and cycloheximide for the indicated times; cell extracts were then subjected to immunoblot analysis with antibodies to the p17 subunit of caspase-3 (Fig. 5C). The amount of CPP32 increased in both control and antisense cells after exposure to anti-Fas and cycloheximide. However, whereas CPP32 was proteolytically processed to p17 by 24 h, coinciding with the peak of *in vitro* caspase-3-like PARP-cleavage activity, in control cells, proteolytic processing of CPP32 was not apparent in the PARP-depleted antisense cells. Furthermore, using DNA fragmentation analysis as another assay for apoptosis, control 3T3-L1 cells exposed to anti-Fas and cycloheximide for 24 h exhibited marked internucleosomal DNA fragmentation (DNA ladders), but not the PARP-depleted
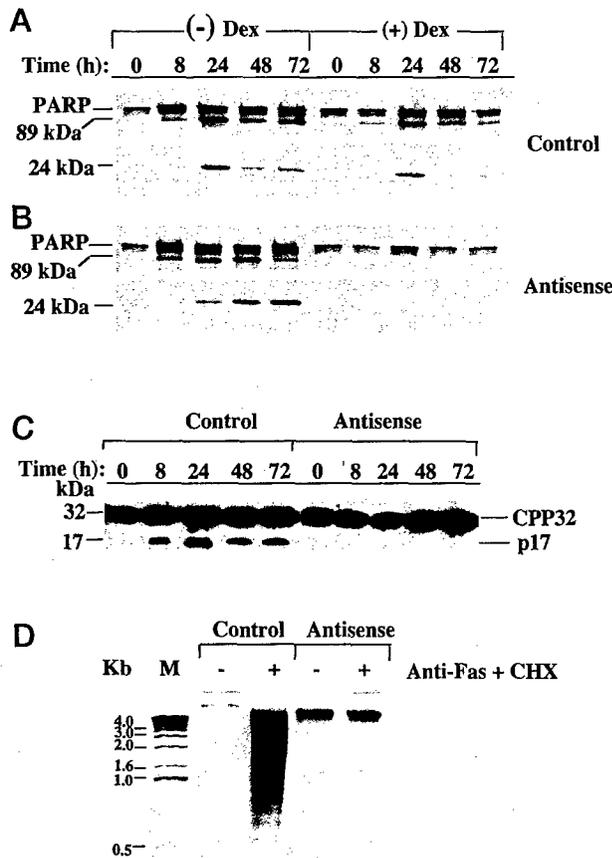
FIG. 5. **Effects of PARP depletion by antisense RNA expression on the increase in caspase-3-like activity (*A* and *B*), proteolytic processing of CPP32 (*C*), and internucleosomal DNA fragmentation (*D*) during Fas-mediated apoptosis in 3T3-L1 cells.** Mock-transfected (*A*) and PARP-antisense (*B*) 3T3-L1 cells were preincubated in the absence or presence of 1 μM dexamethasone (Dex) for 72 h and then incubated with anti-Fas (50 ng/ml) and cycloheximide (CHX) (10 μg/ml) for the indicated times. Cytosolic extracts were prepared and assayed for *in vitro* PARP-cleavage activity with [^{35}S]PARP as substrate. (*C*) 3T3-L1 control and antisense cells were preincubated with dexamethasone for 72 h and then exposed to anti-Fas and cycloheximide for the indicated times as in (*A*) and (*B*). Cell extracts were subjected to immunoblot analysis with a monoclonal antibody to the p17 subunit of caspase-3. The positions of CPP32 and p17 are indicated. (*D*) Total genomic DNA was extracted, and internucleosomal DNA ladders characteristic of apoptosis were detected by agarose gel electrophoresis and ethidium bromide staining. The positions of DNA size standards (in kilobases) are indicated (M).

antisense cells exposed to these inducers for the same time (Fig. 5*D*).

Consistently, whereas antisense cells preincubated in the absence of dexamethasone showed changes in nuclear morphology typical of apoptosis when exposed to anti-Fas and cycloheximide, those depleted of PARP by preincubation with dexamethasone did not (Fig. 6*A*). Whereas ~75% of the antisense cells, which were not preincubated with dexamethasone, exhibited chromatin condensation (*arrowheads*) and nuclear fragmentation (*arrows*) after 48 h of exposure to anti-Fas and cycloheximide, only ~1% of PARP-depleted antisense cells did (Fig. 6*A*). Exposure of the PARP-depleted antisense cells to these agents for >72 h failed to induce any morphological or biochemical markers of apoptosis (data not shown). In contrast, more than 90% of the control cells contained apoptotic nuclei by 48 h and thereafter (Fig. 6*B*).
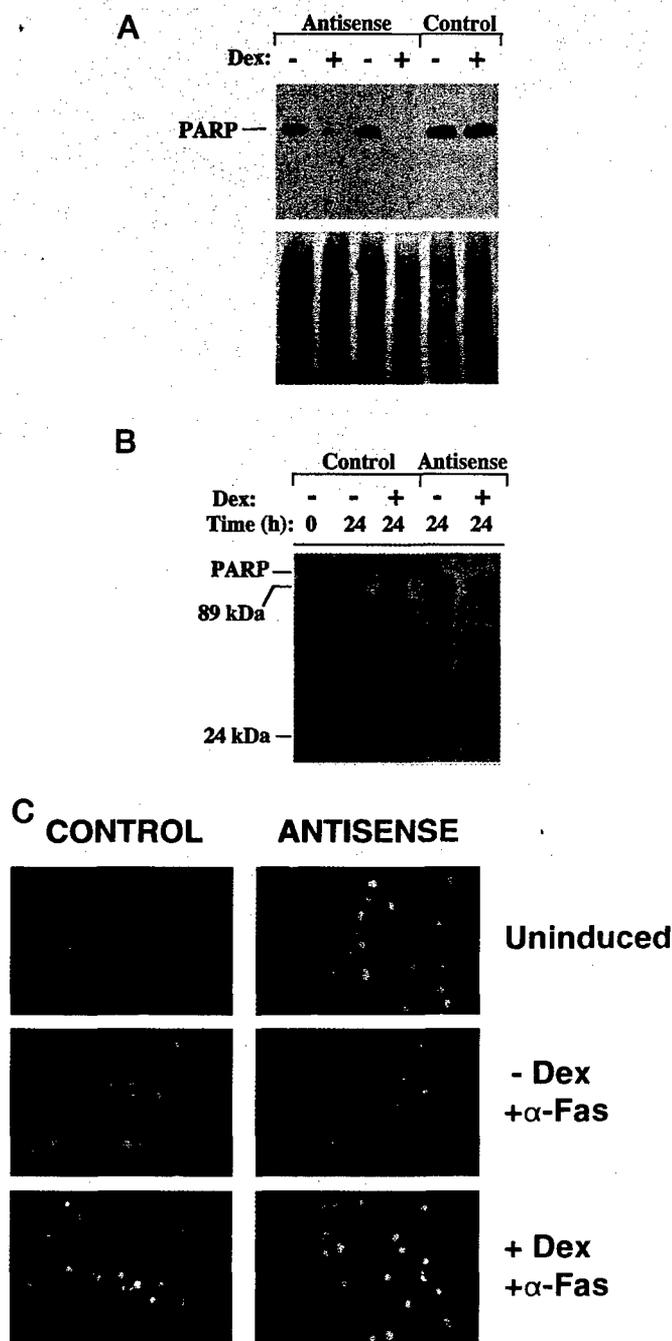
Effects of PARP Depletion by Antisense RNA Expression on Induction of Apoptosis in Human Jurkat Cells—To confirm our results with 3T3-L1 control and antisense cells, we examined human Jurkat T cells stably transfected with either a PARP
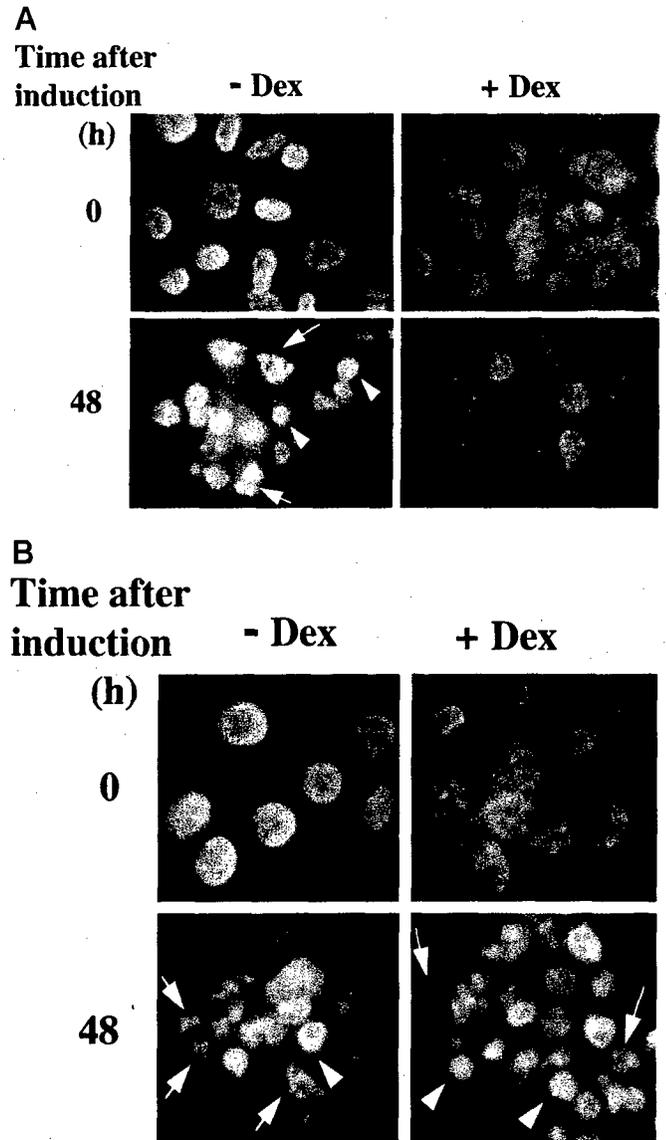
FIG. 6. **Time course of apoptosis in 3T3-L1 cells as monitored by Hoechst staining for nuclear morphology.** PARP-antisense (*A*) and mock-transfected (*B*) cells were preincubated for 72 h in the absence (*left panels*) or presence (*right panels*) of 1 μM dexamethasone and then exposed to anti-Fas (50 ng/ml) and cycloheximide (10 μg/ml) for the indicated times. Cells were fixed, stained with Hoechst stain, and observed with a fluorescence microscope for morphological changes associated with apoptosis (pyknotic nuclei, chromatin condensation, nuclear fragmentation). Original magnification, 40×. *Arrows* indicate nuclear fragmentation; *arrowheads* indicate chromatin condensation.

antisense RNA construct or the empty vector. Immunoblot analysis showed that preincubation of two different Jurkat antisense cell clones for 72 h with dexamethasone resulted in depletion of endogenous PARP by ~99% (Fig. 7*A*).

Because Jurkat cells express high levels of the Fas antigen (24, 29), anti-Fas alone was used to induce apoptosis in these cells. Similar to the other cell lines used in this study, Jurkat cells also exhibited an early transient peak of PAR synthesis 3 h after induction with anti-Fas (data not shown). Mock-transfected Jurkat cells preincubated in the absence or presence of dexamethasone, as well as antisense cells preincubated in the absence of dexamethasone, showed a marked increase in caspase-3-like activity; ~80% of the [^{35}S]PARP substrate was cleaved into 89- and 24-kDa fragments by cytosolic extracts derived from cells exposed to anti-Fas for 24 h (Fig. 7*B*). In contrast, caspase-3-like activity remained negligible in PARP-

A

B

C

FIG. 7. **Effects of PARP depletion by antisense RNA expression on markers of Fas-mediated apoptosis in human Jurkat cells.** *A*, Jurkat control and two antisense cell clones were incubated in the absence or presence of 1 µM dexamethasone (Dex) for 72 h, after which cell extracts (30 µg) were subjected to immunoblot analysis with antibodies to PARP (*upper panel*). The immunoblot was also stained with Ponceau S for confirmation of equal protein loading (*lower panel*). *B*, mock-transfected (control) and PARP-antisense Jurkat cells were preincubated in the absence or presence of 1 µM dexamethasone for 72 h and then treated with anti-Fas (50 ng/ml) for the indicated times. Cytosolic extracts were prepared and equal amounts assayed for PARP-cleavage activity *in vitro* with [35S]PARP as substrate. *C*, control or PARP antisense Jurkat cells were preincubated in the absence or presence of 1 µM dexamethasone for 72 h and then incubated in the absence or presence of anti-Fas (50 ng/ml) for 24 h. Cells were then fixed, stained with Hoechst stain, and observed with a fluorescence microscope for nuclear apoptotic morphology. Original magnification, 40×.

depleted antisense cells treated with anti-Fas for the same time (Fig. 7*B*).

Anti-Fas also induced changes in nuclear morphological consistent with apoptosis in control Jurkat cells (Fig. 7*C*). More

A

B
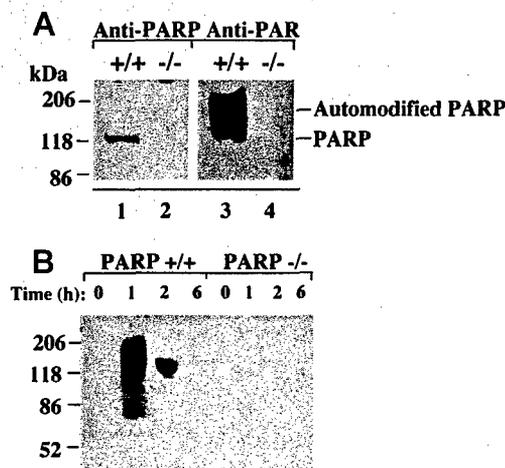
FIG. 8. **Effects of anti-Fas and cycloheximide on poly(ADP-ribosyl)ation of nuclear proteins in immortalized fibroblasts from wild-type and PARP knockout mice.** *A*, extracts of fibroblasts derived from PARP knockout and mice (PARP −/−) (*lanes 2* and *4*) from wild-type mice (PARP +/+) (*lanes 1* and *3*) were subjected to immunoblot analysis with antibodies to PARP (*lanes 1* and *2*) or to PAR (*lanes 3* and *4*). *B*, PARP +/+ and PARP −/− fibroblasts were exposed to anti-Fas (100 ng/ml) and cycloheximide (10 µg/ml) for the indicated times, after which cell extracts (30 µg) were subjected to immunoblot analysis with monoclonal antibodies to PAR.

A

B
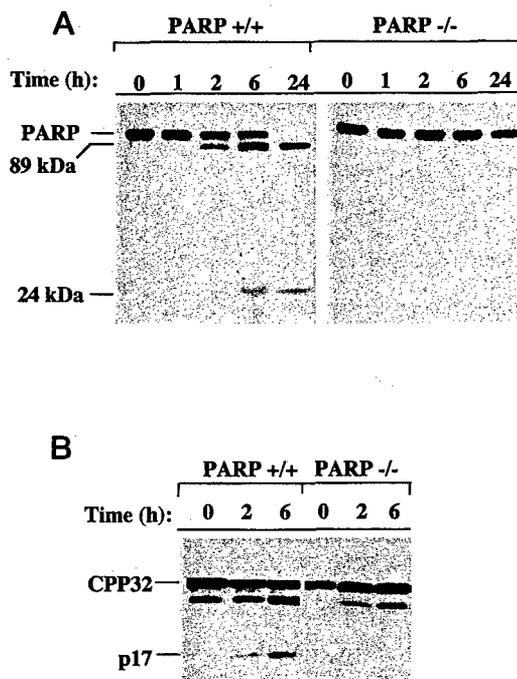
FIG. 9. **Effects of anti-Fas and cycloheximide on caspase-3-like activity (*A*) and proteolytic processing of CPP32 (*B*) in immortalized fibroblasts from PARP knockout and wild-type mice.** *A*, PARP +/+ and PARP −/− fibroblasts were incubated with anti-Fas (100 ng/ml) and cycloheximide (10 µg/ml) for the indicated times, after which cytosolic extracts were assayed for *in vitro* PARP-cleavage activity with [35S]PARP as substrate. *B*, cytosolic extracts from cells treated as in *A* were also subjected to immunoblot analysis with a monoclonal antibody to the p17 subunit of caspase-3.

than 80% of mock-transfected cells that had been preincubated in the absence or presence of dexamethasone, as well as antisense cells preincubated without dexamethasone, showed either chromatin condensation or nuclear fragmentation after 24-h treatment with anti-Fas. However, consistent with the results obtained with the 3T3-L1 antisense cells, no such

Time after induction (h)	PARP +/+	PARP -/-
0		
24		

FIG. 10. **Effects of anti-Fas and cycloheximide on nuclear morphology of immortalized fibroblasts from PARP knockout and wild-type mice.** PARP +/+ (*left panels*) and PARP -/- (*right panels*) fibroblasts were exposed to anti-Fas (100 ng/ml) and cycloheximide (10 μg/ml) for 0 h (*upper panels*) or 24 h (*lower panels*). Cells were fixed, stained with Hoechst stain, and observed under a fluorescence microscope for nuclear morphological changes associated with apoptosis. Original magnification, 40×.
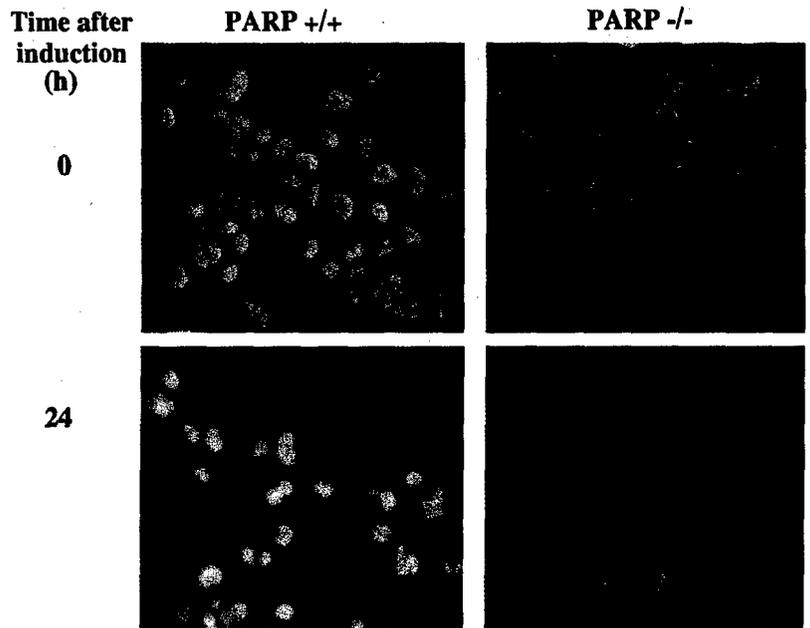
changes were evident in PARP-depleted Jurkat antisense cells exposed to anti-Fas (Fig. 7C).

Transient Poly(ADP-ribosyl)ation of Nuclear Proteins Also Occurs Early during Fas-mediated Apoptosis in PARP +/+ Fibroblasts but Not in PARP -/- Cells—To investigate whether prevention of the early burst of PAR synthesis by gene disruption could likewise affect the induction of biochemical or morphological markers of apoptosis when these cells are exposed to apoptosis inducers, fibroblasts derived from wild-type (PARP +/+) and PARP knockout mice (PARP -/-) (12), immortalized by the standard 3T3 protocol (28), were utilized. PARP -/- cells were confirmed devoid of PARP and PAR by immunoblot analysis with the corresponding antibodies (Fig. 8A). As with the other cell lines, these cells also exhibited a transient burst of poly(ADP-ribosyl)ation of nuclear proteins as early as 1 h after exposure to anti-Fas and cycloheximide (Fig. 8B), and PAR synthesis markedly declined thereafter, presumably by a combination of caspase-3-like mediated PARP cleavage and PAR-glycohydrolase activity. As anticipated, no burst of poly(ADP-ribosyl)ation was observed in PARP -/- fibroblasts after exposure to inducers of apoptosis for up to 6 h (Fig. 8B).

Immortalized Fibroblasts Derived from PARP Knockout Mice Do Not Exhibit Morphological and Biochemical Markers Characteristic of Apoptosis—Anti-Fas and cycloheximide induced a marked increase in caspase-3-like activity in PARP +/+ cells; this effect was maximal 24 h after induction of apoptosis, as indicated by the complete cleavage of PARP into 89- and 24-kDa fragments (Fig. 9A). In contrast, no such increase in caspase-3-like activity was evident in PARP -/- cells after exposure to anti-Fas and cycloheximide for up to 24 h.

To verify that CPP32 is proteolytically activated to caspase-3 during induction of apoptosis in these cells, extracts of cells that had been exposed to anti-Fas and cycloheximide for various times were subjected to immunoblot analysis with antibodies to CPP32. Whereas CPP32 was proteolytically processed to p17 in PARP +/+ fibroblasts exposed to anti-Fas and cycloheximide, no such effect was evident in the PARP -/- cells (Fig. 9B). The band migrating slightly faster than CPP32 corresponds to a protein that reacts nonspecifically with the antibodies to CPP32.

PARP +/+ cells showed substantial nuclear fragmentation and chromatin condensation 24 h after induction of Fas-mediated apoptosis (Fig. 10); ~97% of nuclei exhibited apoptotic

morphology by this time. In contrast, no substantial changes in nuclear morphology were apparent in the PARP -/- fibroblasts even after exposure to anti-Fas and cycloheximide for 24 h (Fig. 10) or 48 h (data not shown).

Transfection of PARP -/- Fibroblasts with Wild-type PARP Sensitizes These Cells to Fas-mediated Apoptosis—PARP -/- fibroblasts were stably transfected with pcD-12, a plasmid expressing wild-type PARP (17). Immunoblot analysis showed that three different cell clones (1, 2, and 3) and pooled clones (P) expressed PARP protein similar to the PARP +/+ cells, whereas PARP -/- cells and the clone transfected with the vector alone ("vec") did not (Fig. 11A). The ability of these clones to express PARP was also confirmed by *in vitro* PARP activity assays (data not shown).

These cells were induced to undergo apoptosis by exposure to anti-Fas and cycloheximide for up to 48 h. *In vivo* caspase-3-like PARP-cleavage activity was monitored by immunoblot analysis with antisera to PARP that recognizes both the 116-kDa PARP and its 24-kDa cleavage fragment (F1-23, Biomol) (Fig. 11B). PARP +/+ cells as well as PARP -/- clones stably transfected with PARP (clones 2 and 3) exhibited significant caspase-3-like activity after 48 h; ~95% of the PARP protein was cleaved *in vivo* to the 24-kDa cleavage fragment by 48 h (Fig. 11B). As expected, PARP was not expressed in the PARP -/- fibroblasts nor in -/- cells transfected with vector alone. Consistently, whereas exposure to anti-Fas and cycloheximide induced marked internucleosomal DNA fragmentation in PARP +/+ fibroblasts and PARP -/- cells stably transfected with PARP (clone 2), no apoptotic DNA ladders were evident in the PARP -/- cells when similarly treated (Fig. 11C).

Furthermore, exposure to anti-Fas plus cycloheximide for 48 h induced apoptotic nuclear morphology in PARP -/- cells transfected with PARP (clone 2) (Fig. 11D), almost to the same extent as the PARP +/+ cells (Fig. 10). Whereas ~85% of PARP-transfected cells showed either chromatin condensation or nuclear fragmentation after treatment with anti-Fas for 48 h (Fig. 11D), no such changes were apparent in mock-transfected PARP -/- cells when exposed to these inducers for the same time. These results confirm that the inability of the PARP -/- cells to undergo Fas-mediated apoptosis is attributed to the lack of PARP due to disruption of the gene and not due to other genetic alterations resulting from immortalization or clonal differences between the PARP +/+ and -/- cells.

A

B

C

D
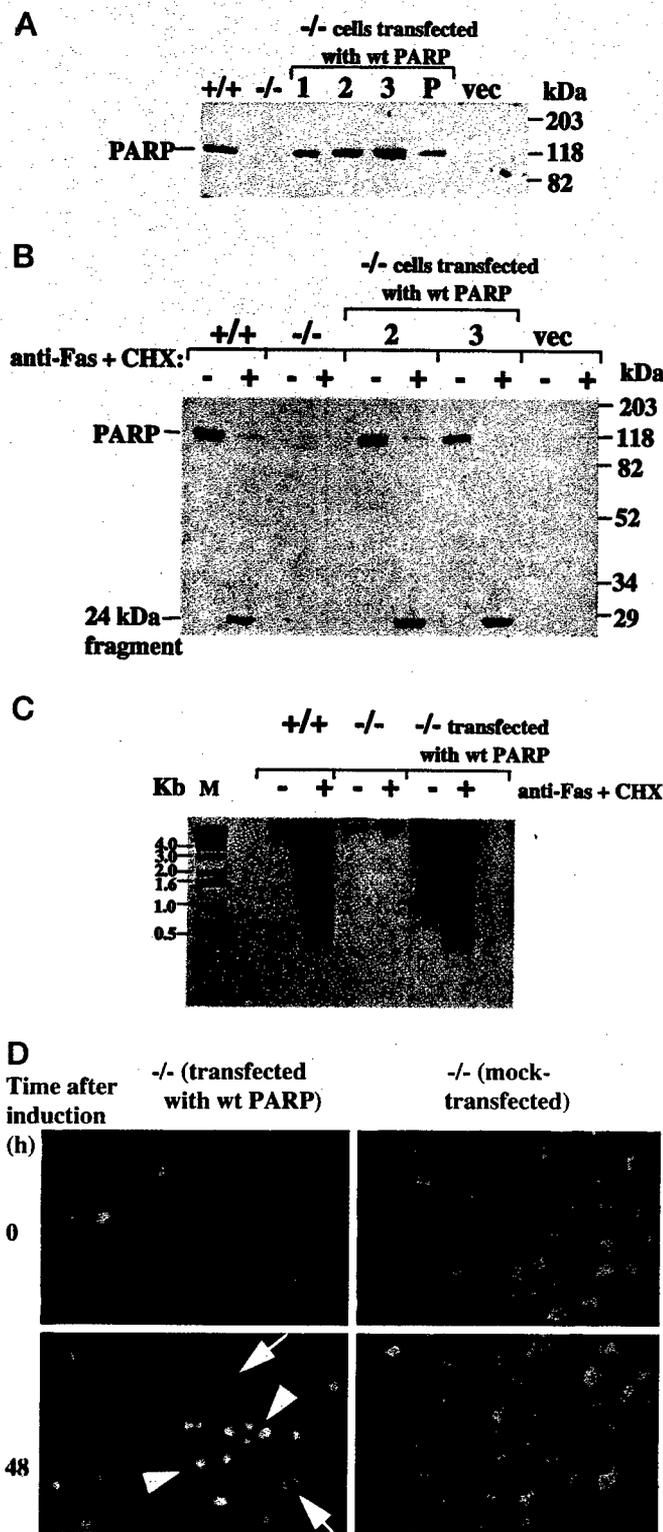
FIG. 11. **Effects of anti-Fas and cycloheximide (CHX) on caspase-3-like activity (B), internucleosomal DNA fragmentation (C), and nuclear morphology (D) in immortalized PARP +/+, PARP −/− fibroblasts, and PARP −/− fibroblasts stably transfected with wild-type (wt) PARP.** A, immunoblot analysis with anti-PARP was performed on cell extracts of PARP +/+ and PARP −/− fibroblasts as well as different cell clones (1, 2, and 3), and pooled clones (P) of PARP −/− cells that were stably transfected with wild-type PARP or with vector alone (vec). B, these cells were then exposed to a combination of anti-Fas (100 ng/ml) and cycloheximide (10 μg/ml) for 48 h. *In vivo* caspase-3-like PARP cleavage activity was monitored by immunoblot analysis of cell extracts utilizing antisera to PARP that recognizes both the 116-kDa PARP and its 24-kDa cleavage fragment (F1–23, Biomol). C, apoptosis was also monitored by extraction of total genomic DNA and detection of characteristic apoptotic internucleoso-

mal DNA ladders by agarose gel electrophoresis and ethidium bromide staining. Positions of DNA size standards (in kilobases) are indicated. D, cells were fixed, stained with Hoechst stain, and observed by fluorescence microscopy for development of apoptotic nuclear morphology. Original magnification, 40×.

DISCUSSION

To investigate, without the use of possibly nonspecific chemical inhibitors (30–32), the potential roles of PARP and poly-(ADP-ribosyl)ation in nuclear processes that require cleavage and rejoining of DNA strands, we have previously established and characterized several mammalian cell lines, including HeLa (16), keratinocytes (33), and 3T3-L1 preadipocytes (11), that are stably transfected with PARP antisense cDNA under the control of an inducible promoter. Establishment of conditions at which endogenous PARP protein and activity can be substantially depleted at specific times by expression of PARP antisense transcripts has enabled us to investigate the roles of PARP in DNA repair, recovery of cells from exposure to mutagenic agents (10, 33), gene amplification (10), and differentiation-linked DNA replication (11, 15, 63).

A role for PARP in apoptosis has been suggested by studies showing that the enzyme undergoes proteolytic cleavage into 89- and 24-kDa fragments during chemotherapy-induced (2) or spontaneous (4) apoptosis. PARP cleavage by caspase-3 has been shown to be necessary for apoptosis (4, 5); the cleavage and inactivation of PARP as well as subsequent apoptotic events are blocked by a peptide inhibitor of this protease. We recently showed by immunofluorescence microscopy that poly-(ADP-ribosyl)ation of nuclear proteins occurs early in apoptosis, prior to commitment to cell death, and is followed by cleavage and inactivation of PARP; only small amounts of PAR remained during the later stages of apoptosis, despite the presence of a large number of DNA strand breaks (9). We have now shown that the transient burst of poly(ADP-ribosyl)ation of nuclear proteins during the early stages of apoptosis occurs in several other cell systems as well. Furthermore, by depleting the normally abundant PARP from 3T3-L1 and Jurkat cells by antisense RNA expression prior to the induction of apoptosis, or with the use of immortalized fibroblasts derived from PARP knockout mice, we have demonstrated that prevention of this early activation of PARP blocks various biochemical and morphological changes associated with apoptosis, thus correlating the early poly(ADP-ribosyl)ation with later events in the Fas-mediated cell death cascade.

In contrast, it was recently shown that primary, nonimmortalized PARP −/− splenocytes and fibroblasts, from the same strain of PARP knockout mice from which the immortalized fibroblasts used in the present study were derived, undergo apparently normal apoptosis in response to anti-Fas, TNF-α, γ-irradiation, or dexamethasone (14). Although the concentration of anti-Fas used to induce apoptosis in these primary PARP −/− cells was substantially higher than that used in our study with immortalized fibroblasts, the apparent discrepancy between the responses of the primary and immortalized cells remains to be clarified. This difference between the two types of cells may be related to the process of immortalization. The immortalized fibroblasts used in the present study are essentially clonal in comparison, whereas the primary cultures used in previous studies (13, 14) contain cells at various stages of development. Although the physiological relevance of using immortalized cell lines requires further study, our results with PARP-antisense cell lines (both murine and human) are consistent with our data obtained with the immortalized PARP −/− fibroblasts.

In both 3T3-L1 and Jurkat PARP-antisense cells, endoge-

nous PARP protein was substantially depleted after incubation with 1 μM dexamethasone for 72 h, whereas PARP abundance was unaffected by dexamethasone treatment in control cells. With the use of an *in vitro* PARP-cleavage assay, marked induction of caspase-3-like activity was observed after exposure to anti-Fas and cycloheximide in control 3T3-L1 cells and immortalized PARP +/+ fibroblasts, as well as in control Jurkat cells treated with anti-Fas, and HL-60 cells exposed to camptothecin. These various treatments also induced a transient burst of poly(ADP-ribosyl)ation before the onset of biochemical events associated with apoptosis in these cells. In contrast, PARP-depleted 3T3-L1 or Jurkat antisense cells as well as immortalized PARP −/− fibroblasts did not undergo this early transient poly(ADP-ribosyl)ation nor did they show any increase in caspase-3-like activity, demonstrate internucleosomal DNA fragmentation, or exhibit morphological changes characteristic of apoptosis.

Proteolytic cleavage and processing of CPP32 into mature caspase-3 was also impaired in 3T3-L1 cells depleted of PARP by antisense RNA expression and in PARP −/− fibroblasts. Various lines of evidence indicate that caspase-3 is both necessary and sufficient to trigger apoptosis: (i) disruption of the caspase-3 gene in knockout mice results in excessive accumulation of neuronal cells due to a lack of apoptosis in the brain (34); (ii) multiple apoptotic signals, including serum withdrawal, Fas activation, ionizing radiation, and various pharmacological agents, activate caspase-3 by proteolytic cleavage of CPP32 (35–39); (iii) a tetrapeptide inhibitor of caspase-3 (AcDEVD-CHO) blocks initiation of the apoptotic program in response to various stimuli (4, 40); and (iv) addition of active caspase-3 to normal cytosol can activate the apoptotic program (41). Caspase-3 is responsible for the cleavage of various cellular substrates at the onset of apoptosis, including PARP, U1-70K, DNA-dependent protein kinase, the retinoblastoma, protein (Rb), fodrin, actin, lamin, gelsolin, and an inhibitor of a caspase-activated DNase (ICAD) (4, 5, 42–47); these proteins are implicated in DNA repair, mRNA splicing, regulation of the cell cycle, or in morphological changes and DNA fragmentation associated with apoptosis. However, it is still unclear whether cleavage of any one substrate is sufficient for a cell to be committed to apoptosis. The biological significance and biochemical consequences of PARP cleavage and its consequent inactivation also remain unclear.

The substantial extent of nuclear poly(ADP-ribosyl)ation apparent early during apoptosis in 3T3-L1, HL-60, Jurkat, and osteosarcoma cells as well as in immortalized PARP +/+ fibroblasts is consistent with the appearance of large (1 Mb) chromatin fragments at this reversible stage (6), given that the activity of PARP is absolutely dependent on DNA strand breaks. A marked decrease in NAD concentration, indicative of increased PAR synthesis, and a subsequent recovery in NAD levels prior to the appearance of internucleosomal DNA cleavage have also been previously observed (48). PARP activation has been detected during apoptosis induced by various DNA-damaging agents, including alkylating agents, topoisomerase inhibitors, Adriamycin, x-rays, ultraviolet radiation, mitomycin C, and cisplatin (49–53).

Whether this transient burst of PARP activity plays an important role or is simply a consequence of the presence of large 1-Mb DNA fragments at this early stage of apoptosis remains to be clarified. In the present study, several of the morphological and biochemical markers of apoptosis, such as development of nuclear apoptotic morphology, internucleosomal DNA fragmentation, proteolytic processing and activation of CPP32, and an increase in caspase-3-like activity, did not occur in cells when this early burst of poly(ADP-ribosyl)ation was prevented

by either gene disruption or by antisense RNA expression. The early activation of PARP was confirmed by immunofluorescence staining or immunoblot analysis in the various cell lines studied. Thus, PARP activation and poly(ADP-ribosyl)ation of relevant nuclear proteins during the early stages of apoptosis may be required for progression through the death program. Subsequent degradation of PARP may prevent the depletion of NAD and ATP needed for later steps in apoptosis (9).

Previous studies have suggested a correlation between poly-(ADP-ribosyl)ation of nuclear proteins and internucleosomal DNA fragmentation during apoptosis, as indicated by a suppressive effect of PARP inhibitors on DNA fragmentation (54, 55) or on nuclear fragmentation (56). However, the relevant target proteins for PARP during apoptosis remain to be identified. Poly(ADP-ribosyl)ation of histone H1, for example, during the early stages of apoptosis was suggested to facilitate internucleosomal DNA fragmentation by enhancing chromatin susceptibility to cellular endonucleases (53).

In preliminary studies (to be published elsewhere), we have obtained some potentially relevant targets for poly(ADP-ribosyl)ation during the burst of PAR synthesis at the early stages of apoptosis. These results show that induction of spontaneous apoptosis in osteosarcoma cells is associated with an increase in the intracellular abundance of p53. Immunoprecipitation and immunoblot analysis further indicate that extensive poly-(ADP-ribosyl)ation of p53 occurs concomitant with the burst of poly(ADP-ribosyl)ation and that subsequent degradation of PAR attached to p53 occurs concomitant with the increase in caspase-3-like activity. Thus, this posttranslational modification may play a role in the regulation of p53 function or, alternatively, in its degradation during p53-dependent apoptosis. These results are consistent with recent studies showing substantial poly(ADP-ribosyl)ation of p53, with polymer chain lengths from 4 to 30 residues, in cells undergoing apoptosis in response to DNA damage (57, 58). Electrophoretic mobility shift analysis further showed that ADP-ribose polymers attached to p53 blocked its sequence-specific binding to a 26-base pair oligonucleotide containing the palindromic p53 consensus binding sequence, suggesting that poly(ADP-ribosyl)ation of p53 may negatively regulate p53-mediated transcriptional activation of genes important in the cell cycle and apoptosis (59). Recently, primary fibroblasts from PARP −/− mice were further shown to have a 2-fold lower basal level of p53 and are defective in the induction of p53 in response to DNA damage (60).

Finally, the activity of Ca^{2+}, Mg^{2+}-dependent endonuclease is inhibited by poly(ADP-ribosyl)ation *in vitro* (61), and the enzyme is implicated in internucleosomal DNA cleavage during apoptosis; it is identical in size and kinetic properties to DNase γ, which is thought to be responsible for DNA fragmentation during thymic apoptosis (62). This enzyme also seems to be a target of the early burst of poly(ADP-ribosyl)ation during spontaneous apoptosis in osteosarcoma and HL-60 cells (data not shown), suggesting a possible negative regulatory role for PARP in apoptosis, whereby inactivation by caspase-3-catalyzed cleavage may release specific nuclear proteins from poly-(ADP-ribosyl)ation-induced inhibition. These ongoing studies aim to clarify the apparently essential requirement, at least in the clonal immortalized mouse and human cells studied here, for the early and brief poly(ADP-ribosyl)ation that occurs during the initial stages of apoptosis.

REFERENCES

1. Berger, N. A., Sims, J. L., Catino, D. M., and Berger, S. J. (1983) in *ADP-ribosylation, DNA Repair and Cancer* (Miwa, M., Hayaishi, O., Shall, S., Smulson, M., and Sugimura, T., eds) pp. 219–226, Japan Scientific Society Press, Tokyo
2. Kaufmann, S. H., Desnoyers, S., Ottaviano, Y., Davidson, N. E., and Poirier, G. G. (1993) *Cancer Res.* **53,** 3976–3985
3. Whitacre, C. M., Hashimoto, H., Tsai, M.-L., Chatterjee, S., Berger, S. J., and Berger, N. A. (1995) *Cancer Res.* **55,** 3697–3701
4. Nicholson, D. W., Ali, A., Thornberry, N. A., Vaillancourt, J. P., Ding, C. K., Gallant, M., Gareau, Y., Griffin, P. R., Labelle, M., Lazebnik, Y. A., Munday, N. A., Raju, S. M., Smulson, M. E., Yamin, T. T., Yu, V. L., and Miller, D. K. (1995) *Nature* **376,** 37–43
5. Tewari, M., Quan, L. T., O'Rourke, K., Desnoyers, S., Zeng, Z., Beidler, D. R., Poirier, G. G., Salvesen, G. S., and Dixit, V. M. (1995) *Cell* **81,** 801–809
6. Neamati, N., Fernandez, A., Wright, S., Kiefer, J., and McConkey, D. J. (1995) *J. Immunol.* **154,** 3788–3795
7. Alnemri, E., Livingston, D., Nicholson, D., Salvesen, G., Thornberry, N., Wong, W., and Yuan, J. (1996) *Cell* **87,** 171
8. Yuan, J., Shaham, S., Ledoux, S., Ellis, H. M., and Horvitz, H. R. (1993) *Cell* **75,** 641–652
9. Rosenthal, D. S., Ding, R., Simbulan-Rosenthal, C. M. G., Vaillancourt, J. P., Nicholson, D. W., and Smulson, M. E. (1997) *Exp. Cell Res.* **232,** 313–321
10. Ding, R., and Smulson, M. (1994) *Cancer Res.* **54,** 4627–4634
11. Smulson, M. E., Kang, V. H., Ntambi, J. M., Rosenthal, D. S., Ding, R., and Simbulan, C. M. G. (1995) *J. Biol. Chem.* **270,** 119–127
12. Wang, Z. Q., Auer, B., Stingl, L., Berghammer, H., Haidacher, D., Schweiger, M., and Wagner, E. F. (1995) *Genes Dev.* **9,** 509–520
13. de Murcia, J., Niedergang, C., Trucco, C., Ricoul, M., Dutrillaux, B., Mark, M., Oliver, J., Masson, M., Dierich, A., LeMeur, M., Waltzinger, C., Chambon, P., and deMurcia, G. (1997) *Proc. Natl. Acad. Sci. U. S. A.* **94,** 7303–7307
14. Wang, Z., Stingl, L., Morrison, C., Jantsch, M., Los, M., Schulze-Osthoff, K., and Wagner, E. (1997) *Genes Dev.* **11,** 2347–2358
15. Simbulan-Rosenthal, C. M. G., Rosenthal, D. S., Hilz, H., Hickey, R., Malkas, L., Applegren, N., Wu, Y., Bers, G., and Smulson, M. (1996) *Biochemistry* **35,** 11622–11633
16. Ding, R., Pommier, Y., Kang, V. H., and Smulson, M. (1992) *J. Biol. Chem.* **267,** 12804–12812
17. Alkhatib, H. M., Chen, D. F., Cherney, B., Bhatia, K., Notario, V., Giri, C., Stein, G., Slattery, E., Roeder, R. G., and Smulson, M. E. (1987) *Proc. Natl. Acad. Sci. U. S. A.* **84,** 1224–1228
18. Kawamitsu, H., Hoshino, H., Okada, H., Miwa, M., Momoi, H., and Sugimura, T. (1984) *Biochemistry* **23,** 3771–3777
19. Ludwig, A., Behnke, B., Holtlund, J., and Hilz, H. (1988) *J. Biol. Chem.* **263,** 6993–6999
20. Cherney, B. W., Midura, R. J., and Caplan, A. J. (1985) *Dev. Biol.* **112,** 115–125
21. Kohlhuber, F., Hermeking, K., Graessmann, A., and Eick, D. (1995) *J. Biol. Chem.* **270,** 28797–28805
22. Wu, Y., Tewari, M., Cui, S., and Rubin, R. (1996) *J. Cell Physiol.* **168,** 499–509
23. Wright, S., Kumar, M., Tam, A., Shen, N., Varma, M., and Larrick, J. (1992) *J. Cell Biochem.* **48,** 344–355
24. Totpal, K., Singh, S., Lapushin, R., and Aggarwal, B. (1996) *J. Interferon Cytokine Res.* **16,** 259–267
25. Ogasawara, J., Suda, T., and Nagata, S. (1995) *J. Exp. Med.* **181,** 485–491
26. Natoli, G., Ianni, A., Costanzo, A., De Petrillo, G., Ilari, I., Chirillo, P., Balsano, C., and Levrero, M. (1995) *Oncogene* **11,** 1157–1164
27. Althaus, F. R. (1987) in *ADP-ribosylation of Proteins, Enzymology and Biological Significance* (Althaus, F. R., and Richter, C., eds) Vol. 37, pp. 1–126, Springer-Verlag, Berlin
28. Aaronson, S., and Todaro, G. (1968) *J. Cell Physiol.* **72,** 141–148
29. Chiba, T., Takahashi, S., Sato, N., Ishii, S., and Kikuchi, K. (1996) *Eur. J. Immunol.* **26,** 1164–1169
30. Milam, K. M., and Cleaver, J. E. (1984) *Science* **223,** 589–591
31. Cleaver, J. E., Borek, C., Milam, K., and Morgan, W. F. (1985) *Pharmacol.*

32. Hunting, D., Gowans, B., and Henderson, J. F. (1985) *Biochem. Pharmacol.* **34,** 3999–4003
33. Rosenthal, D. S., Shima, T. B., Celli, G., De Luca, L. M., and Smulson, M. E. (1995) *J. Invest. Dermatol.* **105,** 38–44
34. Kuida, K., Zheng, T., Na, S., Kuan, C., Yang, D., Karasuyama, H., Rakic, P., and Flavell, R. (1996) *Nature* **384,** 368–372
35. Darmon, A. J., Ley, T. J., Nicholson, D. W., and Bleackley, R. C. (1996) *J. Biol. Chem.* **271,** 21709–21712
36. Chinnaiyan, A. M., Orth, K., O'Rourke, K., Duan, H., Poirier, G. G., and Dixit, V. M. (1996) *J. Biol. Chem.* **271,** 4573–4576
37. Martin, S., Amarante-Mendes, G., Shi, L., Chuang, T., Casiano, C., O'Brien, G., Fitzgerald, T., Tan, E., Bokoch, G., Greenberg, A., and Green, D. (1996) *EMBO J.* **15,** 2407–2416
38. Schlegel, J., Peters, I., Orrenius, S., Miller, D. K., Thornberry, N. A., Yamin, T.-T., and Nicholson, D. W. (1996) *J. Biol. Chem.* **271,** 1841–1844
39. Erhardt, P., and Cooper, G. M. (1996) *J. Biol. Chem.* **271,** 17601–17604
40. Dubrez, L., Savoy, I., Hamman, A., and Solary, E. (1996) *EMBO J.* **15,** 5504–5512
41. Enari, M., Talanian, R., Wong, W., and Nagata, S. (1996) *Nature* **380,** 723–726
42. Janicke, R., Walker, P., Lin, X., and Porter, A. (1996) *EMBO J.* **15,** 6969–6978
43. Casciola-Rosen, L., Nicholson, D., Chong, T., Rowan, K., Thornberry, N., Miller, D., and Rosen, A. (1996) *J. Exp. Med.* **183,** 1957–1964
44. Song, Q., Lees-Miller, S., Kumar, S., Zhang, Z., Chan, D., Smith, G., Jackson, S., Alnemri, E., Litwack, G., Khanna, K., and Lavin, M. (1996) *EMBO J.* **15,** 3238–3246
45. Kothakota, S., Azuma, T., Reinhard, C., Klippel, A., Tang, J., Chu, K., McGarry, T., Kirschner, M., Koths, K., Kwiatkowski, D., and Williams, L. (1997) *Science* **278,** 294–298
46. Martin, S., and Green, D. (1995) *Cell* **82,** 349–352
47. Sakahira, H., Enari, M., and Nagata, S. (1998) *Nature* **391,** 96–99
48. Nosseri, C., Coppola, S., and Ghibelli, L. (1994) *Exp. Cell Res.* **212,** 367–373
49. Marks, D., and Fox, R. (1991) *Biochem. Pharmacol.* **42,** 1859–1867
50. Tanizawa, A., Kubota, M., Hashimoto, H., Shimizu, T., Takimoto, T., Kitoh, T., Akiyama, Y., and Mikawa, H. (1989) *Exp. Cell Res.* **185,** 237–246
51. Tanizawa, A., Kubota, M., Takimoto, T., Akiyama, Y., Seto, S., Kiriyama, Y., and Mikawa, H. (1987) *Biochem. Biophys. Res. Commun.* **144,** 1031–1036
52. Manome, Y., Datta, R., Taneja, N., Shafman, T., Bump, E., Hass, R., Weichselbaum, R., and Kufe, D. (1993) *Biochemistry* **32,** 10607–10613
53. Yoon, Y.-S., Kim, J. W., Kang, K. W., Kim, Y. S., Choi, K. H., and Joe, C. O. (1996) *J. Biol. Chem.* **271,** 9129–9134
54. Jones, D. P., McConkey, D. J., Nicotera, P., and Orrenius, S. (1989) *J. Biol. Chem.* **264,** 6398–6403
55. Bertrand, R., Solary, E., Jenkins, J., and Pommier, Y. (1993) *Exp. Cell Res.* **207,** 388–397
56. Shiokawa, D., Maruta, H., and Tanuma, S. (1997) *FEBS Lett.* **413,** 99–103
57. Kumari, S., Mendoza-Alvarez, H., and Alvarez-Gonzalez, R. (1997) in *The 12th International Symposium on ADP-ribosylation Reactions,* Cancun, Mexico
58. Nozaki, T., Masutani, M., Nishiyama, E., Shimokawa, T., Wkabayashi, K., and Sugimura, T. (1997) in *The 12th International Symposium on ADP-ribosylation Reactions,* Cancun, Mexico
59. Malanga, M., and Althaus, F. (1997) in *The 12th International Symposium on ADP-ribosylation Reactions,* Cancun, Mexico
60. Agarwal, M., Agarwal, A., Taylor, W., Wang, Z. Q., and Wagner, E. (1997) *Oncogene* **15,** 1035–1041
61. Tanaka, T., Yoshihara, K., Itaya, A., Kamiya, T., and Koide, S. S. (1984) *J. Biol. Chem.* **259,** 6579–6585
62. Shiokawa, D., Ohyama, H., Yamada, T., Takahashi, K., and Tanuma, S. (1994) *Eur. J. Biochem.* **226,** 23–30
63. Simbulan-Rosenthal, C., Rosenthal, D., Boulares, H., Hickey, R., Malkas, L., Coll, J., and Smulson, M. (1998) *Biochemistry,* in press
64. Eldadah, B., Yakovlev, A., and Faden, A. (1996) *Nucleic Acids Res.* **24,** 4092–4093

Ther. **31,** 269–293

Involvement of PARP and poly(ADP-ribosyl)ation in the early stages of apoptosis and DNA replication

Cynthia Marie Simbulan-Rosenthal, Dean S. Rosenthal, Sudha Iyer, Hamid Boulares and Mark E. Smulson
Department of Biochemistry and Molecular Biology, Georgetown University School of Medicine, Washington, DC, USA

Abstract

We have focused on the roles of PARP and poly(ADP-ribosyl)ation early in apoptosis, as well as during the early stages of differentiation-linked DNA replication. In both nuclear processes, a transient burst of PAR synthesis and PARP expression occurs early, prior to internucleosomal DNA cleavage before commitment to apoptosis as well as at the round of DNA replication prior to the onset of terminal differentiation. In intact human osteosarcoma cells undergoing spontaneous apoptosis, both PARP and PAR decreased after this early peak, concomitant with the inactivation and cleavage of PARP by caspase-3 and the onset of substantial DNA and nuclear fragmentation. Whereas 3T3-L1, osteosarcoma cells, and immortalized PARP +/+ fibroblasts exhibited this early burst of PAR synthesis during Fas-mediated apoptosis, neither PARP-depleted 3T3-L1 PARP-antisense cells nor PARP -/- fibroblasts showed this response. Consequently, whereas control cells progressed into apoptosis, as indicated by induction of caspase-3-like PARP-cleavage activity, PARP-antisense cells and PARP -/- fibroblasts did not, indicating a requirement for PARP and poly(ADP-ribosyl)ation of nuclear proteins at an early reversible stage of apoptosis. In parallel experiments, a transient increase in PARP expression and activity were also noted in 3T3-L1 preadipocytes 24 h after induction of differentiation, a stage at which ~95% of the cells were in S-phase, but not in PARP-depleted antisense cells, which were consequently unable to complete the round of DNA replication required for differentiation. PARP, a component of the multiprotein DNA replication complex (MRC) that catalyzes viral DNA replication *in vitro*, poly(ADP-ribosyl)ates 15 of ~40 MRC proteins, including DNA pol α, DNA topo I, and PCNA. Depletion of endogenous PARP by antisense RNA expression in 3T3-L1 cells results in MRCs devoid of any DNA pol α and DNA pol δ activities. Surprisingly, there was no new expression of PCNA and DNA pol α, as well as the transcription factor E2F-1 in PARP-antisense cells during entry into S-phase, suggesting that PARP may play a role in the expression of these proteins, perhaps by interacting with a site in the promoters for these genes. (Mol Cell Biochem **193**: 137–148, 1999)

Key words: PARP, poly(ADP-ribosyl)ation, apoptosis, DNA replication

Introduction

Poly(ADP-ribose) polymerase (PARP), which is catalytically activated by DNA strand breaks, plays an auxiliary role in nuclear processes, such as DNA repair [1–5] , DNA replication [6–11], cellular differentiation [10–15], and more recently in apoptosis. PARP catalyzes the poly(ADP-ribosyl)ation of various nuclear proteins, with NAD as substrate, and under-goes proteolytic cleavage into 89- and 24-kDa fragments that contain the active site and the DNA-binding domain of the enzyme, respectively, during drug-induced [16] and spontaneous apoptosis [17, 18]. More recently, PARP has been implicated in the induction of both p53 expression and apoptosis [19] , with the specific proteolysis of the enzyme thought to be a key apoptotic event [17, 20, 21]. Caspase-3, a member of the family of aspartate-specific cysteine pro-

138

teases, is composed of two subunits of 17 and 12-kDa derived from a common proenzyme (CPP32), plays a central role in the execution of the apoptotic program [22], and is responsible for the cleavage of PARP during cell death [17, 21, 23]. Human osteosarcoma cells that undergo confluence-associated apoptosis over a 10-day period, exhibit a peak of caspase-3 activity, measured with a specific [^{35}S] PARP-cleavage assay in vitro, 6–7 days after initiation of apoptosis, concomitant with the onset of internucleosornal DNA fragmentation [17].

We recently examined the time course of PARP activation and cleavage during apoptosis in intact osteosarcoma cells by immunofluorescence microscopy [18] as well as by immunoblot analysis with antibodies to PARP and to poly(ADP-ribose) (PAR). The results showed that poly(ADP-ribosyl)ation of relevant nuclear proteins may be required at an early reversible stage of apoptosis but that degradation of PARP may be necessary at a later stage, suggesting a negative regulatory role for PARP in apoptosis. We have now investigated this hypothesis utilizing well-characterized cell lines stably transfected with inducible PARP- antisense constructs [11, 24, 25] as well as with immortalized fibroblasts derived from PARP knockout mice [26]. Induction of PARP antisense RNA in these cells have consistently shown significant depletion of endogenous PARP protein and activity. Using these PARP-depleted antisense cells, we have shown that PARP and poly(ADP-ribosyl)ation facilitates the initial rate of DNA repair in HeLa cells [1] and keratinocytes [24]. Although the PARP knock out mice from which the PARP -/- fibroblasts used in our studies were derived from were viable, fibroblasts and thymocytes from these mice exhibited proliferation deficiencies following DNA damage [26]; primary PARP -/- splenocytes derived from other knockout mice also showed abnormal apoptosis implicating a role for PARP in the regulation of cell death [27].

PARP and poly(ADP-ribosyl)ation has also been implicated in cellular differentiation since PARP inhibitors (i.e. nicotinamide and benzamide) markedly inhibit differentiation of 3T3-L1 preadipocytes into adipocytes by preventing a transient increase in PARP activity that appears essential for entering the differentiation program [28]. Consistently, we have shown that inducible stably transfected 3T3-L1 cells expressing PARP antisense RNA do not exhibit the increase in PARP protein and activity normally apparent 24 h after exposure to differentiation inducers and they fail to differentiate into adipocytes [11] . The inability of the antisense cells to synthesize PARP and PAR during the early stages of differentiation correlates with their inability to undergo the round of DNA replication required for onset of terminal differentiation. We have now extended these studies to better clarify the role of PARP in differentiation-linked DNA replication and its putative roles as a component of multi-protein DNA replication complexes (known as MRC or the DNA synthesome) in cells [10].

Results

PARP and PAR are synthesized early during apoptosis of human osteosarcoma cells

Human osteosarcoma cells were induced to undergo confluence-associated apoptosis for 10 days, and examined by immunofluorescence staining for PAR synthesis with antibodies to PAR (left panel), and PARP (middle panel); the levels of DNA strand breaks in cells were also assessed by staining cells with biotinylated PARP DBD and Texas red-conjugated streptavidin (right panel; [29]. Representative samples from immediate (day 1), early (day 3), mid- (day 6), and late (day 10) stages of apoptosis are shown (Fig. 1). The synthesis of PAR from NAD increased early and peaked 3 days after initiation of apoptosis, prior to the appearance of internucleosomal DNA cleavage and before the cells became irreversibly committed to apoptosis. During the same early period, new expression of full-length PARP was detected. At 6 days, however, the amounts of both PAR and PARP decreased markedly, and PAR was not observed during days 8–10, despite the presence of abundant DNA strand breaks (right panel), potential activators of intact PARP, during this time. Significant intemucleosornal DNA fragmentation was also shown to occur at days 6–9 of apoptosis in these cells [17, 18]. Thus, a transient burst of PARP expression and poly(ADP-ribosyl)ation of nuclear proteins occurs early, prior to commitment to death, in osteosarcoma cells and is
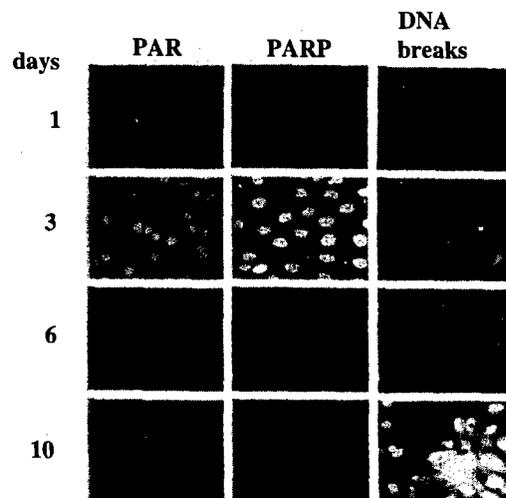
Fig. 1. Time courses of PAR synthesis, PARP expression, and the presence of DNA strand breaks during spontaneous apoptosis of human osteosarcoma cells. Cells were cultured without any changes in medium for 1–10 days, fixed, and subjected to immunofluorescence analysis with antibodies to PAR (left panel) and PARP (middle panel), as well as biotinylated recombinant PARP DBD which was used to detect DNA strand breaks (right panel).

followed by caspase-3 -mediated cleavage and inactivation of PARP.

Different cells undergo a transient burst of poly(ADP-ribosyl)ation of nuclear proteins early during apoptosis followed by a decline concomitant with the onset of PARP cleavage

In agreement with the immunofluorescence results shown in Fig. 1, immunoblot analysis with antibody to PAR of osteosarcoma cells at various stages of apoptosis also showed an early burst of poly(ADP-ribosyl)ation of nuclear proteins at day 4 of apoptosis, followed by a marked decline in poly(ADP-ribosyl)ation at later time points, coincident with the onset of PARP cleavage activity and internucleosomal DNA cleavage.

Consistently, other cell lines induced into Fas-mediated apoptosis (Figs. 2C and D) or by the topoisomerase inhibitor, camptothecin (Fig. 2B), also exhibited the same early burst of poly(ADP-ribosyl)ation of nuclear proteins during an early reversible stage of apoptosis, when the cells were still viable (as assessed by exclusion of trypan blue) and could still be replated. HL-60 cell extracts derived at early time points during camptothecin-induced apoptosis (Fig. 2B) as well as 3T3-L1 and PARP +/+ fibroblasts induced into apoptosis by a combination of antibody to Fas and cycloheximide (Fig. 2, C and D, respectively) all showed a similar transient peak of poly(ADP-ribosyl)ation of nuclear proteins 1–4 h after induction; PAR moieties that were bound to these proteins were degraded and no further modification was apparent thereafter, concomitant with the onset of caspase-3 catalyzed cleavage of PARP.

PARP-depleted 3T3-L1 antisense cells and immortalized PARP -/- fibroblasts do not exhibit the transient burst of PAR synthesis at the early stages of Fas-mediated apoptosis

To investigate the role(s) of PARP during the early stages of apoptosis, we examined PAR synthesis in PARP-depleted 3T3-L1 antisense and PARP -/- cells during this period. 3T3-L1 antisense cells that had been preincubated with dexamethasone (Dex) for 72 h to deplete endogenous PARP as well as fibroblasts derived from PARP knockout mice were exposed to anti-Fas and cycloheximide for various times and then subjected to immunofluorescence staining (data not shown) and immunoblot analysis with antibody to PAR. In control 3T3-L1 and PARP +/+ fibroblasts, PAR levels in the nucleus were significantly elevated at 4 and 1 h, respectively, after induction of apoptosis, a stage wherein all the cells were still viable and could be replated. This was followed by a
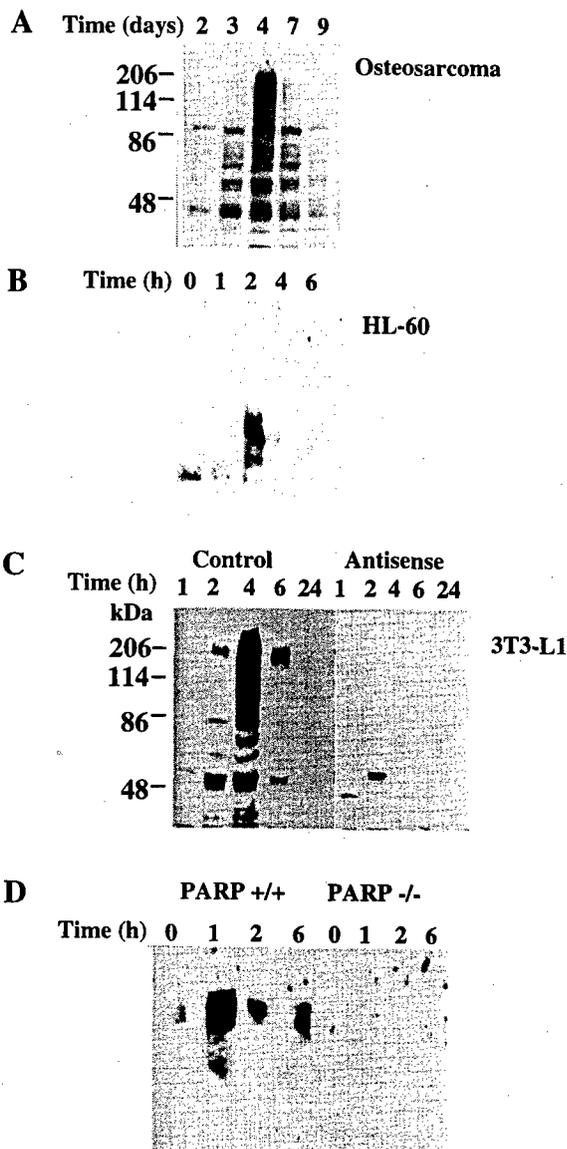

Fig. 2. Time course of poly(ADP-ribosyl)ation of nuclear proteins during apoptosis induced by various apoptotic stimuli. (A) Osteosarcoma cells were allowed to undergo confluence associated spontaneous apoptosis for 9 days; (B) HL-60 cells were induced into apoptosis with the topoisomerase inhibitor, camptothecin (10 μM); and (C) 3T3-L1 control and PARP-antisense fibroblasts as well as (D) immortalized PARP +/+ and PARP -/- fibroblasts were induced into apoptosis with a combination of anti-Fas (100 ng/ml) and cyclohexamide (10 μg/ml). 3T3-L1 control and antisense cells were preincubated with Dex for 72 h prior to apoptosis induction. At the indicated times, equal amounts of total cellular protein (30 μg) were subjected to immunoblot analysis with monoclonal antibody to PAR (1:250). The positions of the molecular size standards (in kilodaltons) are indicated.

marked decline in poly(ADP-ribosyl)ation at later time points, concomitant with the induction of PARP cleavage activity. In contrast, anti-Fas and cycloheximide did not induce this burst of poly(ADP-ribosyl)ation of nuclear

140

proteins during early apoptosis in PARP-depleted 3T3-L1 antisense cells (Fig. 2C) nor in PARP -/- cells (Fig. 2D), suggesting that the PARP and poly(ADP-ribosyl)ation may play a role at this early stage in Fas-mediated apoptosis in these cells.

Depletion of PARP by antisense RNA expression blocks progression of apoptosis in 3T3-L1 and Jurkat cells

PARP depletion induced by antisense RNA expression in 3T3-L1 cells under the present conditions were confirmed by immunoblot analysis with antibody to PARP (Fig. 3A). Whereas PARP levels in mock-transfected control 3T3-L1 cells were not affected by incubation with Dex for 72 h (Fig. 3A), Dex induced significant depletion of endogenous PARP
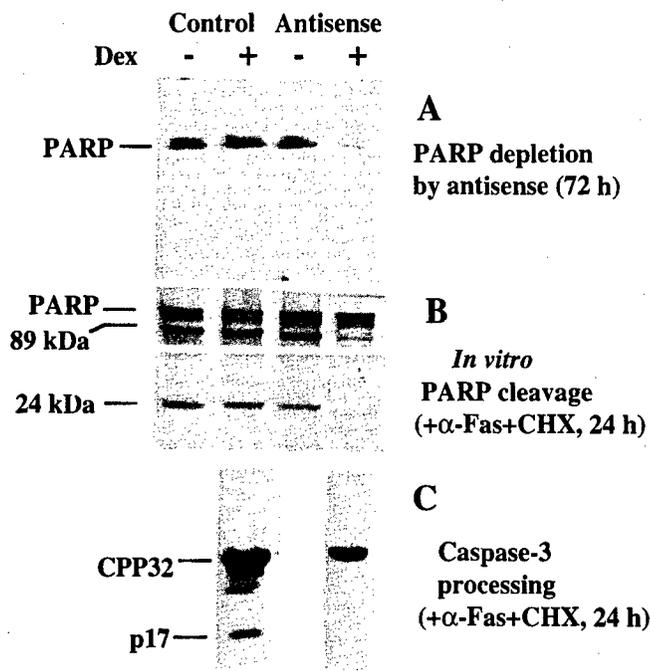
Fig. 3. PARP depletion by antisense RNA expression inhibits induction of anti-Fas mediated apoptosis in 3T3-L1 cells as monitored by induction of *in vitro* PARP cleavage activity and proteolytic processing of CPP32 to caspase-3. (A) Mock-transfected (control) and PARP-antisense 3T3-L1 cells were incubated in the absence or presence of 1 μM Dex for 72 h, after which equal amounts of total cellular protein (30 μg) were subjected to immunoblot analysis with antibody to full-length PARP. After preincubation in the absence or presence of 1 μM Dex, control and antisense cells were incubated with anti-Fas (100 ng/ml) and cycloheximide (10 μg/ml) for 24 h; equal amounts of cytosolic extracts were then assayed for *in vitro* PARP-cleavage activity with [³⁵S]PARP as substrate (B) or subjected to immunoblot analysis with a monoclonal antibody to the p17 subunit of caspase-3 (C). The positions of full length PARP and its 89- and 24-kDa cleavage products as well as those of CPP32 (32-kDa) and its active form (caspase-3, p17) are indicated.

in antisense cells, with only ~5% of the protein remaining after 72 h. Essentially equal protein loading and transfer among lanes was confirmed by Ponceau S staining for total protein on the same immunoblot (data not shown).

3T3-L1 control and antisense cells were then preincubated in the presence or absence of Dex for 72 h, and subsequently induced into apoptosis with a combination of antibody to Fas and cycloheximide for various times. Using an *in vitro* caspase-3 mediated PARP-cleavage assay [17], incubation of cells with anti-Fas and cycloheximide for 24 h were shown to result in a marked induction of caspase-3 activity (Fig. 3B), as indicated by generation of the 89- and 24-kDa cleavage fragments of PARP. There was no effect of anti-Fas by itself or cycloheximide alone on the induction of apoptosis in these cells [71]. Cycloheximide has been used to overcome resistance to Fas-mediated apoptosis in various cell lines [30–32], an effect which does not appear to be mediated by translational inhibition because resistant cells are sensitized to anti-Fas by subinhibitory concentrations.

Anti-Fas and cycloheximide induced a marked time-dependent increase in *in vitro* PARP-cleavage activity in control 3T3-L1 cells that had been preincubated either in the absence or presence of Dex (Fig. 3B), an effect which was maximal 24 h after induction of apoptosis. On the other hand, whereas PARP-antisense 3T3-L1 cells that were not exposed to Dex showed a similar increase in caspase-3 activity in response to anti-Fas and cycloheximide, no such increase in caspase-3 activity was apparent in PARP-antisense cells that had been depleted of PARP by preincubation with Dex and then induced for apoptosis (Fig. 3B).

Similar to other members of the caspase family, caspase 3 is expressed in cells as an inactive 32-kDa proenzyme (CPP32), which is activated during apoptosis by cleavage at specific Asp residues, with the mature active enzyme (caspase-3) consisting of a large 17-kDa subunit (p17), containing the catalytic domain, and a 12-kDa subunit (p12) [17]. Proteolytic processing of CPP32 to p17 during the course of apoptosis was then confirmed in 3T3-L1 cells by immunoblot analysis with a monoclonal antibody to the p17 subunit of caspase-3 (Fig. 3D). Whereas, in control cells, CPP32 was proteolytically processed to p17 (caspase-3) by 24 h, coinciding with the peak of *in vitro* PARP cleavage activity, proteolytic cleavage, processing, and activation of CPP32 to p17 was not apparent in the PARP-depleted antisense cells, again suggesting that PARP as well as presumably poly(ADP-ribosyl)ation plays a role in some early event in apoptosis, upstream of the proteolytic cascade mechanism for processing the caspase-3 precursor to its active form. Consistent with these results, whereas control 3T3-L1 cells as well as antisense cells preincubated in the absence of dexamethasone showed changes in nuclear morphology typical of apoptosis after exposure to anti-Fas and cyclo-

heximide i.e. chromatin condensation, nuclear and DNA fragmentation, antisense cells depleted of PARP by pre-incubation with Dex did not [71].

Essentially the same results were obtained with another cell line, Jurkat T cells, that were stably transfected with either the PARP antisense RNA construct or the empty vector. Immunoblot analysis confirmed that preincubation of Jurkat antisense cells for 72 h with Dex resulted in depletion of endogenous PARP by ~99% (Fig. 4A). Anti-Fas alone was used to induce apoptosis in these cells since Jurkat cells are Fas-sensitive and express high levels of the Fas antigen [30, 33]. After 4 h of exposure to anti-Fas, mock-transfected cells preincubated in the absence or presence of Dex as well as antisense cells in the absence of Dex showed a significant increase in caspase-3 activity, as indicated by the *in vitro* cleavage of exogenous PARP into 89- and 24-kDa fragments, however, caspase-3 activity remained negligible in PARP-depleted antisense cells treated with anti-Fas for up to 24 h (Fig. 4B). Furthermore, while anti-Fas induced changes in nuclear morphology consistent with apoptosis in control Jurkat cells preincubated with or without Dex as well as in antisense cells preincubated without Dex, no such changes were evident in PARP-depleted antisense cells treated with anti-Fas [71]. Depletion of PARP by antisense RNA expression

apparently blocks progression of Fas-mediated apoptosis in both 3T3-L1 and Jurkat cells.

Fibroblasts derived from PARP-knockout mice are resistant to Fas-mediated apoptosis

PARP knockout mice generated by disruption of the PARP gene by homologous recombination in embryonic stem cells [26] were used to derive immortalized fibroblasts by the 3T3 protocol, which were confirmed to be devoid of PARP (Fig. 5A) as evidenced by immunoblot analysis with antibody to PARP.

When immortalized PARP +/+ and PARP -/- fibroblasts were induced into apoptosis with a combination of anti-Fas
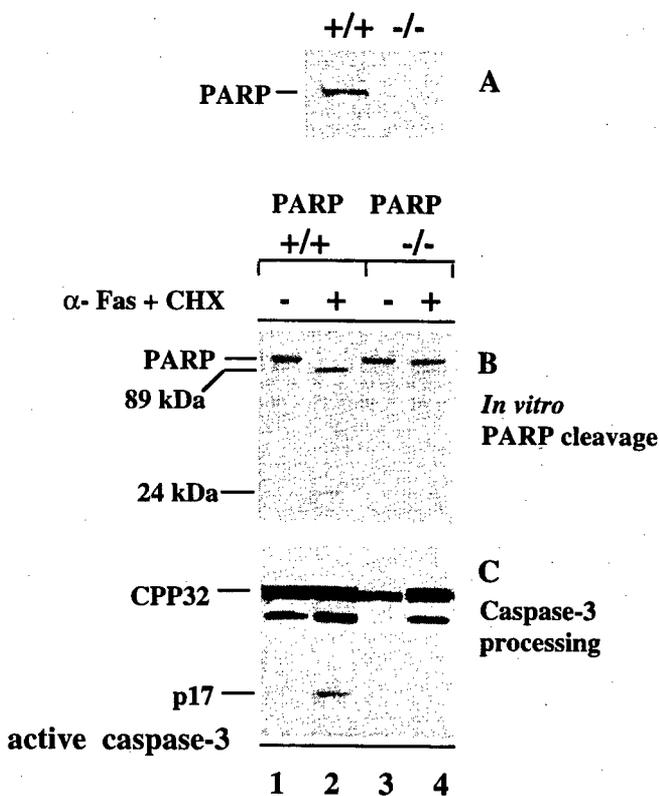

Fig. 4. PARP-depleted Jurkat antisense cells are unable to undergo Fas-mediated apoptosis as measured by caspase-3 activity assays. (A) Jurkat control and antisense cells were incubated in the absence or presence of 1 μM Dex for 72 h, after which equal amounts of total cellular protein (30 μg) were subjected to immunoblot analysis with anti-PARP. (B) Control and PARP antisense Jurkat cells were preincubated in the absence or presence of 1 μM Dex and then exposed to anti-Fas (50 ng/ml) for 24 h. Cytosolic extracts were prepared and equal amounts were assayed for PARP-cleavage activity with [^{35}S]PARP as substrate. The positions of full length PARP and its 89- and 24-kDa cleavage products are indicated.

Fig. 5. Fibroblasts derived from PARP knockout mice do not exhibit any increase in caspase-3 activity and proteolytic processing of CPP32 to caspase-3. (A) Immortalized fibroblasts (PARP -/-) derived from knockout mice as well as fibroblasts from wild type mice (PARP +/+) were subjected to immunoblot analysis with anti-PARP. (B) PARP +/+ and PARP -/- fibroblasts were incubated with anti-Fas (100 ng/ml) and cycloheximide (10 μg/ml) for 24 h, after which cytosolic extracts were assayed for *in vitro* PARP-cleavage activity with [^{35}S]PARP as substrate. (C) Cytosolic extracts in (B) were also subjected to immunoblot analysis with a monoclonal antibody to the p17 subunit of caspase-3. The positions of full length PARP and its 89- and 24-kDa cleavage products as well as those of CPP32 (32-kDa) and its active form (p17) are indicated.

and cycloheximide, PARP +/+ cells showed a rapid apoptotic response, as indicated by a marked increase in *in vitro* PARP-cleavage activity; the activity was maximal 24 h after induction as indicated by the complete cleavage of PARP in to 89 kDa- and 24 kDa cleavage fragments (Fig. 5B). In contrast, PARP -/- cells showed no such increase in caspase-3 mediated PARP cleavage after 24 h exposure to anti-Fas and cycloheximide. Immunoblot analysis with the antibody to the p17 subunit of caspase-3 further showed that CPP32 was proteolytically processed to p 17 in the PARP +/+ fibroblasts (Fig. 5C), but not in the PARP -/- cells exposed to anti-Fas. Furthermore, whereas PARP +/+ fibroblasts were ~99% apoptotic 24 h after induction as shown by development of nuclear apoptotic morphology, PARP -/- cells exhibited normal, non-apoptotic morphology even after 24 h of exposure to anti-Fas [71]. Altogether, these results confirm the earlier data obtained with the 3T3-L1 and Jurkat control and PARP antisense cells and provide further evidence for a role for PARP at an early event in apoptosis.

Poly(ADP-ribosyl)ation of p53 during the early stages of apoptosis in osteosarcoma cells

The apparent role for early PAR synthesis during apoptosis was further clarified by investigating a well-characterized apoptotic response to DNA strand breaks, the rapid accumulation of p53. Osteosarcoma cells were plated under conditions that result in spontaneous apoptosis over a 10-day period, with maximal caspase-3 mediated PARP-cleavage apparent around days 7–9 (Fig. 6C). Immunoblot analysis showed that the amount of p53 protein was markedly increased at days 4–7 and declined thereafter (Fig. 6A). Reprobing of the same immunoblot with antibodies to PAR revealed significant poly(ADP-ribosyl)ation of p53 at days 3–4 coincident with the burst of PAR synthesis during the early stages of apoptosis, and the extent of p53 modification declined thereafter at the onset of caspase-3 activity at days 7–9 (Fig. 6B and C). These experiments were not performed with Jurkat and HL-60 cells since these cells have been shown to be p53-null [34, 35].

A transient peak of PARP expression and poly(ADP-ribosyl)ation is also observed during the early stages of differentiation-linked DNA replication in control 3T3-Ll cells, but not in PARP depleted antisense cells

A transient peak of PARP expression occurs in postconfluent cultures of 3T3-L1 cells induced to differentiate to adipocytes for 7–8 days by exposure to insulin, Dex, and methyl-isobutylxanthine [11]. The time courses of PARP activity and % of cells in S-phase after exposure to inducers of differentia-
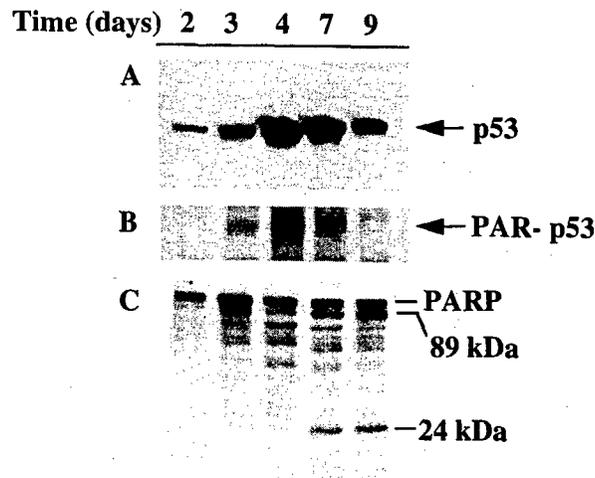

Time (days) 2 3 4 7 9

Fig. 6. Time courses of accumulation (A) and poly(ADP-ribosyl)ation (B) of p53 as well as caspase-3 mediated PARP-cleavage (C) during spontaneous apoptosis in osteosarcoma cells. Human osteosarcoma cells were induced to undergo spontaneous apoptosis for 9 days, and, at the indicated times, cytosolic extracts were derived and equal amounts of protein (30 μg) were subjected to immunoblot analysis with monoclonal antibody to p53 (A) or assayed for *in vitro* PARP-cleavage activity, using [^{35}S]PARP as a substrate (C). The positions of full length PARP and its 89- and 24-kDa cleavage products are indicated. The immunoblot in (A) was stripped with a buffer containing 100 mM 2-mercaptoethanol, 2% SDS, and 62.5 mM Tris-HCl pH 6.7 for 30 min at 50°C, blocked, and reprobed with monoclonal antibody to PAR (B).

tion were then compared in 3T3-L1 control cells and antisense cells (Fig. 7). FACS analysis was performed on control and antisense cells at various times after induction and the data quantitated. Prior to induction of differentiation (zero time), 70–80% of postconfluent control and antisense cells were in growth-arrest induced by contact inhibition. More than 95% of the control cells synchronously entered S phase by 24 h, coincident with the peak of poly(ADP-ribosyl)ation observed 24 h after induction of differentiation (Fig. 7). While the control cells progressed through one round of replication prior to the onset of terminal differentiation, the antisense cells did not show the burst of PAR synthesis apparent in the control cells and did not enter S phase. When the transient peak of PARP expression and poly(ADP-ribosl)ation is prevented in the antisense cells, these cells are unable to enter S-phase and undergo the round of DNA replication at the early stages of differentiation, and consequently, these cells do not differentiate, as confirmed by their inability to synthesize and accumulate cytoplasmic triglyceride [10, 11]. PARP is apparently required for a round of DNA replication that occurs within the first 24 h of differentiation and is necessary for differentiation in these cells.

Confocal microscopy further revealed that, during this early stage of differentiation, when essentially all control cells
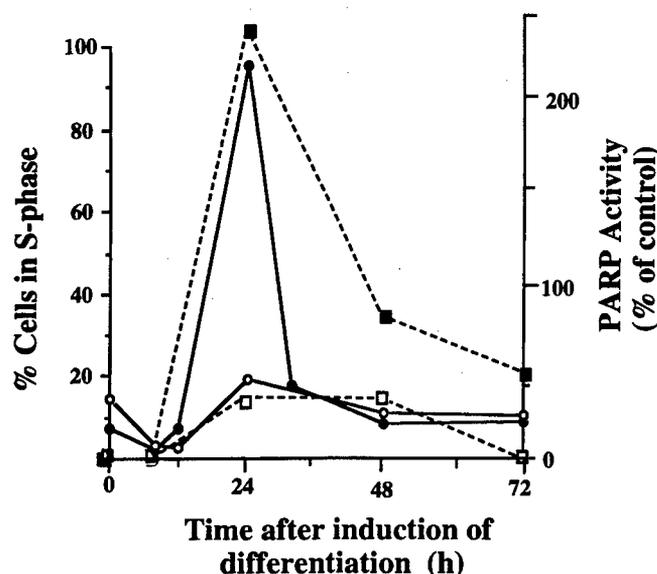
% Cells in S-phase

PARP Activity (% of control)

Time after induction of differentiation (h)

Fig. 7. PARP depleted- 3T3-L1 antisense cells do not undergo a peak of PAR synthesis and are unable to enter S-phase during the round of DNA replication at the early stages of differentiation. Control (solid symbols) and antisense (open symbols) cells were exposed to inducers of differentiation and harvested at the indicated times. Duplicate cell pellets were assayed for either PARP activity (dotted lines) or % cells in S-phase (solid lines). Cells were assayed for PARP activity by measuring [^{32}P]NAD incorporation into acid-insoluble acceptors at 25°C for 1 min, with 20 μg of protein per determination and triplicate determinations per time point. [^{32}P]NAD, incorporation of uninduced control 3T3-L1 cells was taken as baseline, and PARP activity values were calculated and plotted based on this control value. % of control and PARP antisense cells in S phase phase of the cell cycle was quantitated from flow cytometric (FACS) data of nuclei stained with propidium iodide (0.42 mg/ml).

have entered the S phase of the cell cycle, PARP is localized within distinct intranuclear granular foci that are associated with replication centers [10]. Consistently, we recently showed that PARP is a component of the multiprotein DNA replication complexes (MRC) or DNA synthesomes that catalyze replication of viral DNA *in vitro,* and contain replicative enzymes such as DNA polymerases α and δ (pol α and pol δ), DNA primase, DNA helicase, DNA ligase, and topoisomerase I and II, as well as accessory proteins such as proliferating-cell nuclear antigen (PCNA), RFC, and RPA. PARP catalyzes the poly(ADP-ribosyl)ation of about 15 of the ~40 MRC proteins, including pol α, DNA topoisomerase I, and PCNA [10]. To further clarify the involvement of PARP within the DNA synthesome during the round of DNA replication in the early stages of differentiation in 3T3-L1 cells, we have now purified and characterized replicative complexes from control cells that had entered S phase after induction of differentiation and from cells depleted of PARP by expression of PARP antisense RNA [72].

PARP regulates the expression of components of the DNA synthesome during entry into S-phase at the early stages of differentiation-linked DNA replication

The roles of PARP in modulating the composition and enzyme activities of the DNA synthesome were further investigated by characterizing the complex purified from 3T3-L1 cells before and 24 h after induction of a round of DNA replication required for differentiation of these cells; at the latter time point, ~95% of the cells are in S phase and exhibit a transient peak of PARP activity (Fig. 7). The MRC fraction was also purified from similarly treated 3T3-L1 cells depleted of PARP by expression of antisense RNA; these cells do not undergo DNA replication or terminal differentiation. Both PARP protein and activity and essentially all of the pol α and pol δ activities exclusively cosedimented with the MRC fractions from S phase control cells, and were not detected in the MRC fractions from PARP-antisense or uninduced control cells [72].

SDS-polyacrylamide gel electrophoresis and silver staining of MRC fractions prepared from control and PARP-antisense cells, before or 24 h after induction of differentiation, revealed that the most prominent difference was the presence of a 116-kDa protein, corresponding to the size of intact PARP, in the fraction from control cells in S phase but not in those from antisense cells or uninduced control cells. Consistent with these observations and with the PARP activity data, immunoblot analysis with polyclonal antibodies to PARP showed that PARP protein was present exclusively in the MRC fraction from control 3T3-L1 cells in S phase, and not in the MRC fractions nor total cell extracts from PARP-antisense cells or nonreplicating control cells ([72], Fig. 8).

We next investigated the effects of PARP depletion on the composition of the MRC by immunoblot analysis with antibodies to specific MRC components. Immunoblot analysis of cell extracts revealed that while the amount of PCNA was markedly increased in control cells upon exposure to inducers of differentiation, there was no new expression in the PARP antisense cells. Although PCNA was also present in the antisense cells and uninduced control cells (Fig. 8), PCNA as well as topoisomerase I appeared to be present in antisense cells and uninduced control cells only in the free, uncomplexed form, because they were detected in the MRC fraction only from replicating control cells, indicating that PARP may play a role in their recruitment into the DNA synthesome [72].

Immunoblot analysis of total cell extracts and MRC fractions with antibody to pol α further revealed induction of expression of this replicative enzyme during early S-phase in control cells and its absence from PARP-antisense cells (Fig. 8). These results indicate that PARP may play a role in the expression of pol α and PCNA during early S phase. We thus investigated the effect of PARP depletion on the abun-
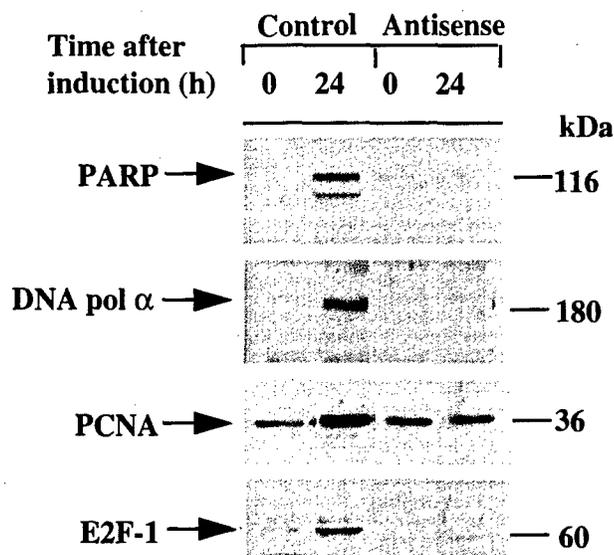
144

Time after induction (h)

Control		Antisense	
0	24	0	24

kDa

PARP → —116

DNA pol α → —180

PCNA → —36

E2F-1 → —60

Fig. 8. PARP depleted-3T3-L1 antisense cells do not exhibit new expression of PARP, pol α, PCNA, and E2F-1 during early S-phase. Total cell extracts from 3T3-L1 control and PARP antisense cells were prepare before and 24 h after induction of differentiation and equal amounts of total protein (30 µg) were subjected to immunoblot analysis with antibodies to PARP (1:2000 dilution), pol α (1:200), PCNA (1:250), and E2F-1 (1:1000). Arrows indicate the positions of the various proteins, and their molecular sizes (in kilodaltons) are indicated on the right.

dance of E2F-1, a transcription factor that positively regulates the expression of the pol α and PCNA genes during entry of cells into S phase. Immunoblot analysis of total cell extracts revealed that, whereas control cells exhibited a marked increase in the expression of E2F-1, PARP-depleted antisense cells contained negligible amounts of E2F-1 during the 24 h exposure to inducers of differentiation (Fig. 8). PARP may therefore play a role in the expression of pol α and PCNA by indirectly regulating the expression of E2F-1.

Discussion

PARP and poly(ADP-ribosyl)ation in the early stages of apoptosis

We have previously established and characterized several mammalian cell lines, including HeLa cells [25], keratinocytes [24], and 3T3-L1 fibroblasts [11] that are stably transfected with PARP antisense cDNA under the control of a Dex-inducible promoter in order to assess, without the use of possibly nonspecific chemical inhibitors [36–38], the potential roles of PARP and poly(ADP-ribosyl)ation in a variety of nuclear processes. Depletion of endogenous PARP protein and activity at specific times by PARP antisense RNA

expression has enabled us to investigate the roles of PARP in DNA repair, recovery of cells from exposure to mutagenic agents [24, 25], gene amplification [39], and differentiation-linked DNA replication [10, 11, 72].

Recently, PARP cleavage by caspase-3 has been shown to be necessary for apoptosis [17, 21] since the cleavage and inactivation of PARP as well as apoptotic events are inhibited by a peptide inhibitor of this protease, suggesting a negative regulatory role for PARP in apoptosis. Aside from Fas activation, multiple apoptotic signals can activate caspase-3 by proteolytic cleavage of CPP32, including serum withdrawal, ionizing radiation, and various pharmacological agents [40–44]. The peptide inhibitor of caspase-3 (AcDEVD-CHO) blocks the apoptotic program in response to various stimuli [17, 45], and addition of active caspase-3 to normal cytosol activates the apoptotic program [46].

We now show that poly(ADP-ribosyl)ation of nuclear proteins occurs early in the course of apoptosis induced by different apoptotic signals, including Fas activation (3T3-L1, PARP +/+, and Jurkat cells), pharmacological agents such as camptothecin (HL-60 cells), as well as serum depletion (osteosarcoma cells). This burst of PAR synthesis occurs prior to commitment to death, and is followed by cleavage and inactivation of PARP; only small amounts of PAR remain during the later stages of apoptosis, despite the presence of a large number of DNA strand breaks. By depleting the normally abundant PARP from 3T3-L1 and Jurkat cells by antisense RNA expression prior to the induction of apoptosis, or with the use of immortalized fibroblasts derived from PARP knockout mice, we further demonstrate that, whereas PARP cleavage is required in the later stages of apoptosis, the transient burst of poly(ADP-ribosyl)ation of relevant nuclear proteins appears to also play a role during the early stages of the death program. PARP-depleted 3T3-L1 and Jurkat PARP antisense cells as well as in PARP -/- fibroblasts did not undergo the burst of PAR synthesis early in apoptosis and progression into apoptosis was prevented in these cells, as assessed by the lack of *in vitro* PARP cleavage activity, proteolytic processing and activation of CPP32 to caspase-3, development of nuclear apoptotic morphology and internucleosomal DNA fragmentation [71].

A potential role for PAR synthesis at an early reversible stage in apoptosis is suggested by the substantial extent of nuclear poly(ADP-ribosyl)ation apparent at this time in 3T3-L1, HL60, and osteosarcoma cells and is consistent with the presence of large (1 Mb) chromatin fragments at this reversible stage [20] since the activity of PARP is dependent on DNA strand breaks. This stage of apoptosis may correspond to a stage described previously during which the initial events of nuclear breakdown occur and in which poly(ADP-ribosyl)ation may play an accessory role [20]; exposure of cells to chemical inhibitors of PARP at this time, but not later, prevents cell death [47]. A drop in NAD concentration,

indicative of increased PAR synthesis, followed by a recovery in NAD levels has also been previously noted to occur prior to the onset of internucleosomal DNA cleavage [47]. Furthermore, previous studies have suggested a correlation between poly(ADP-ribosyl)ation of nuclear proteins and internucleosomal DNA fragmentation during apoptosis, since PARP inhibitors have a suppressive effect on DNA fragmentation [48, 49]. However, the relevant target proteins for PARP during apoptosis have yet to be identified. During the early stages of apoptosis, poly(ADP-ribosyl)ation of histone H1, for example, was shown to facilitate internucleosomal DNA fragmentation by enhancing chromatin susceptibility to cellular endonucleases [50]. Although the concomitant loss of poly(ADP-ribosyl)ation of target proteins resulting from PARP cleavage and inactivation are consistent with the later stages of apoptosis during which cells become irreversibly committed to death, the biological significance and the biochemical consequences of PARP cleavage and its consequent inactivation remain unclear.

We showed that extensive poly(ADP-ribosyl)ation of p53 is apparent early during spontaneous apoptosis in osteosarcoma cells, and that degradation of PAR attached to these apoptosis-related proteins occurred concomitant with caspase-3 catalyzed PARP cleavage (Fig. 6). These results are consistent with recent studies showing substantial poly(ADP-ribosyl)ation of p53, with polymer chain lengths from 4–30 residues, in cells undergoing apoptosis in response to DNA damage [51, 52]. Electrophoretic mobility-shift analysis further showed that ADP-ribose polymers attached to p53 blocked its sequence specific binding to a 26-bp oligonucleotide containing the palindromic p53 consensus binding sequence, suggesting that poly(ADP-ribosyl)ation of p53 may negatively regulate p53-mediated transcriptional activation of genes important in the cell cycle and apoptosis [53]. Induction of spontaneous apoptosis in osteosarcoma cells is associated with an increase in the intracellular levels of p53 (Fig. 6). It remains to be determined whether this accumulation of p53 is due to induced expression of the protein or stabilization by reduced degradation as a result of posttranslational modification. Nevertheless, the extensive poly(ADP-ribosyl)ation of p53 that occurs early in apoptosis and the subsequent degradation of PAR attached to p53 concomitant with caspase-3 activity suggest that this post-translational modification may play a role in the regulation of p53 function or, alternatively, its degradation. The stabilization and accumulation of p53 has recently been shown to play a key role in apoptosis induced by proteasome inhibitors [54]. Poly(ADP-ribosyl)ation as well as caspase-3-catalyzed PARP cleavage and inactivation may contribute to the regulation of proteasome-mediated degradation of p53, by promoting p53 stabilization and accumulation at a stage when it is required in the apoptotic program.

PARP expression and poly(ADP-ribosyl)ation in the early stages of differentiation-linked DNA replication

We had previously shown that PARP depletion by antisense RNA expression inhibits the differentiation of 3T3-L1 preadipocytes, including the differentiation-linked round of DNA replication [11]. The differentiation of 3T3-LI preadipocytes as well as Friend erythroleukemia cells [55] is prevented by blocking this round of DNA replication at the early stages of differentiation. The failure of PARP-depleted 3T3-L1 cells to undergo terminal differentiation into adipocytes is thus correlated to their inability to undergo replication in the early stages of this process, indicating that PARP plays a role in this replication. We have also shown that PARP is tightly associated with the core proteins of MRC purified from HeLa and FM3A cells [10] that have been shown to support viral DNA replication *in vitro* and migrate as discrete, high molecular weight complexes on native polyacrylamide gel electrophoresis [56]. PARP has been thought to play a regulatory role within these complexes because it is capable of modulating the catalytic activity of some of the replicative enzymes or factors by physical association [pol α [9] or by catalyzing their poly(ADP-ribosyl)ation [pol α [57], DNA topoisomerase I and II [58–60], and RPA [61]. Consistently, we showed that 15 of the ~ 40 polypeptides of the MRC including pol α, topoisomerase I, and PCNA, are poly(ADP-ribosyl)ated by immunoprecipitation and immunoblot analysis with antibodies to PAR and these replication proteins [10].

To further clarify the role of PARP and the significance of the early burst of PAR synthesis during differentiation-linked DNA replication, we purified the MRC from 3T3 -L1 cells harvested prior to and 24 h after exposure to inducers of differentiation-linked DNA replication; at the latter time point, ~95% of control cells are in S phase and exhibit a transient peak of PARP activity (Fig. 7). DNA pol α and pol δ catalyze the synthesis of lagging and leading strands of DNA, and PCNA is required for pol δ-mediated synthesis of the leading strand [62]. Interestingly, only the MRC fraction from S phase control cells, not those from uninduced control cells nor from PARP-antisense cells, contained PARP protein and activity as well as pol α and pol δ activities. Thus, PARP depletion results in a replicative complex deficient in these two replicative enzyme activities. These results are consistent with our earlier data showing that *in vivo* DNA replication, as assessed by incorporation of bromodeoxyuridine or [³H]-thymidine into newly synthesized DNA, occurred only in replicating 3T3-L1 control cells, but not in the PARP-depleted antisense cells. We next tried to determine whether this effect was attributed to present, but inactive enzymes or due to absence of these enzymes in the MRC or in the cells.

Immunoblot analysis revealed that PCNA and DNA topoisomerase I were present in the MRC fraction only from S phase control cells, although they were both detected in total

146

cell extracts from control and PARP-antisense cells, indicating that PARP may play a role in the recruitment of these replicative proteins into the DNA synthesome during entry into S phase [72]. The absence of PCNA in the antisense MRC may account in part for the lack of any significant DNA pol δ activity in these MRCs. Immunoblot analysis with anti-PARP showed that, consistent with the PARP activity assays (Fig. 7), PARP protein was present exclusively in the MRC fractions from control 3T3-L 1 cells at S phase, but was essentially depleted in MRC from nonreplicating control cells or from the PARP-antisense cells [72]. Furthermore, pol α was absent from total cell extracts from PARP-antisense cells, suggesting that PARP may be also play a role in the expression of the pol α gene during entry of cells into S phase. Surprisingly, depletion of PARP by antisense RNA expression also down-regulated the expression of E2F-1 during the early stage of differentiation in 3T3-L1 cells. In mammalian cells, the transcription factor E2F-1 binds to a specific recognition site (5′-TTTCGCGC) and thereby activates the promoters of several genes that regulate S phase entry, such as c-myc [63], cyclin D, and cyclin E [64], and genes required for DNA synthesis, such as dihydrofolate reductase [65], thymidine kinase [66], pol α, and PCNA [64, 67]. Transcription of the E2F-1 gene, in turn, is also regulated during the cell cycle by E2F-DNA binding sites within its own promoter [68]. PARP has recently been shown to enhance activator-dependent transcription probably by interacting with RNA polymerase II-associated factors [69] and a basal eukaryotic transcription factor, THIIF, was reported to be a highly specific substrate for poly(ADP-ribosyl)ation [70]. Experiments are now underway to determine whether PARP plays a role in the transcription of the pol α, PCNA, and E2F-1 genes during entry into S-phase.

Acknowledgements

References

1. Ding R, Stevnsner T, Bohr V, Smulson M: Preferential gene repair and HN2 damage: Depletion of PADPRP by antisense RNA expression. Proceedings of the 1993 Medical Defense Bioscience Review, 1: 217–226, 1993

2. Molinete M, Vermeulen W, Burkle A, de Murcia JM, Kupper J, Hoeijmakers J, de Murcia G: Overproduction of the poly(ADP-ribose) polymerase DNA-binding domain blocks alkylation-induced DNA repair synthesis in mammalian cells. EMBO J 12: 2109–2117, 1993

3. Satoh M, Lindahl T: Role of poly(ADP-ribose) formation in DNA repair. Nature 356: 356–358, 1992

4. Satoh M, Poirier G, Lindahl T: NAD$^+$-dependent repair of damaged DNA by human cell extracts. J Biol Chem 268: 5480–5487, 1993

5. Smulson M, Istock N, Ding R, Cherney B: Deletion mutants of poly(ADP-ribose) polymerase support a model of cyclic association and dissociation of enzyme from DNA ends during DNA repair. Biochemistry 33: 6186–6191, 1994

6. Burzio L, Koide S: Activation of the template activity of isolated rat liver nuclei for DNA synthesis and its inhibition by NAD. Biochem Biophys Res Commun 53: 572–579, 1973

7. Anachkova B, Russev G, Poirier G: DNA replication and poly(ADP-ribosyl)ation of chromatin. Cytobios 58: 19–28, 1989

8. Cesarone C, Scarabelli L, Giannini P, Orunesu M: Differential assay and biological significance of poly (ADP-ribose) polymerase activity in isolated liver nuclei. Mutat Res 245: 157–63, 1990

9. Simbulan C, Suzuki M, Izuta S, Sakurai T, Savoysky E, Kojima K, Miyahara K, Shizuta Y, Yoshida S: Poly (ADP-ribose) polymerase stimulates DNA polymerase α. J Biol Chem 268: 93–99, 1993

10. Simbulan-Rosenthal CMG, Rosenthal D, Hilz H, Hickey R, Malkas L, Applegren N, Wu Y, Bers G, Smulson M: The expression of poly(ADP-ribose) polymerase during differentiation-linked DNA replication reveals that this enzyme is a component of the multiprotein DNA replication complex. Biochemistry 35: 11622–11633, 1996

11. Smulson M, Kang V, Ntambi J, Rosenthal D, Ding R, Simbulan CMG: Requirement for the expression of poly(ADP-ribose) polymerase during the early stages of differentiation of 3T3-L1 preadipocytes, as studied by antisense RNA induction. J Biol Chem 270: 119–127, 1995

12. Farzaneh F, Meldrum R, Shall S: Transient formation of DNA strand breaks during the induced differentiation of a human promyelocytic leukemic cell line, HL-60. Nucleic Acids Res 15: 3493–3502, 1987

13. Bhatia K, Pommier Y, Giri C, Fornace A, Imaizumi M, Breitman T, Chemey B, Smulson M: Expression of the poly(ADP-ribose) polymerase gene following natural and induced DNA strand breakage and effect of hyperexpression on DNA repair. Carcinogenesis 11: 123–128, 1990

14. Suzuki H, Uchida K, Shima H, Sato T, Okamoto T, Kimura T, Sugimura T, Miwa M: Molecular cloning of cDNA for human placental poly(ADP-ribose) polymerase and decreased expression of its gene during retinoic acid-induced granulocytic differentiation of HL-60 cells. In: M.K. Jacobson, E.L. Jacobson, (eds), ADP-Ribose Tranfer Reactions: Mechanisms and Biological Significance, New York: SpringerVerlag, 1989, pp. 511–514

15. Caplan A, Rosenberg M: Interrelationship between poly(ADP-rib) synthesis, intracellular NAD levels, and muscle or cartilage differentiation from mesodermal cells of embryonic chick limb. Proc Nacl Acad Sci 72: 1852–1857, 1975

16. Kaufmann S, Desnoyers S, Ottaviano Y, Davidson N, Poirier G: Specific proteolytic cleavage of poly(ADP-ribose)polymerase: An early marker of chemotherapyinduced apoptosis. Cancer Res 53: 3976–3985, 1993

17. Nicholson D, Ali A, Thomberry N, Vaillancourt J, Ding C, Gallant M, Gareau Y, Griffin P, Labelle M, Lazebnik Y, Munday N, Raju S, Smulson M, Yamin T, Yu V, Miller D: Identification and inhibition of the ICE/CED-3 protease necessary for mammalian apoptosis. Nature 376: 37–43, 1995

18. Rosenthal D, Ding R, Simbulan-Rosenthal CM, Vaillancourt J, Nicholson D, Smulson M: Intact cell evidence fo the early snthesis, and subsequent late apopainmediated suppression, of poly(ADP-ribose) during apoptosis. Exp Cell Res 232: 313–321, 1997

19. Whitacre C, Hashimoto H, Tsai ML, Chatterjee S, Berger S, Berger N: Involvement of NAD-poly(ADP-ribose) metabolism in p53 regulation and its consequences. Cancer Res 55: 3697–3701, 1995

20. Neamati N, Fernandez A, Wright S, Kiefer J, McConkey D: Degradation of lamin B1 precedes oligonucleosomal DNA fragmentation in apoptotic thymocytes and isolated thymocyte nuclei. J Immunology 154: 3788–3795, 1995

21. Tewari M, Quan L, O'Rourke K, Desnoyers S, Zeng Z, Beidler D, Poirier G, Salvesen G, Dixit V: Yarna/CPP32b, a mammalian homolog of CED-3, is a crmA-inhibitable protease that cleaves the death substrate poly(ADP-ribose) polymerase. Cell 81: 801–809, 1995

22. Alnenmi E, Livingston D, Nicholson D, Salvesen G, Thornberry N, Wong W, Ytian J: Human ICE/CED-3 protease nomenclature [letter]. Cell 87: 171, 1996

23. Ytian J, Shaham S, Ledoux S, Ellis H, Horvitz H: The C. elegans death gene ced-3 encodes a protein similar to mammalian interleukin-1-b-converting enzyme. Cell 75: 641–652, 1993

24. Rosenthal D, Shima T, Celli G, De Luca L, Smulson M: An engineered human skin model using poly(ADP-ribose) polymerase antisense expression shows a reduced response to DNA damage. J Invest Dermatol 105: 38–44, 1995

25. Ding R, Pommier Y, Kang V, Smulson M: Depletion of poly(ADP-ribose) polymerase by antisense RNA expression results in a delay in DNA strand break rejoining. J Biol Chem 267: 12804–12812, 1992

26. Wang ZQ, Auer B, Stingl L, Berghammer H, Haidacher D, Schweiger M, Wagner E: Mice lacking ADPRT and poly(ADP-ribosyl)ation develop normally but are susceptible to skin disease. Genes Dev 9: 509–520, 1995

27. de Murcia G, Masson M, Trucco C, Dantzer F, Oliver, Flatter E, Niedergang C, Ricoul M, Dutrillaux B, Dierich A, LeMeur M, Waltzinger C, Chambon P, de Murcia J: Poly(ADP-ribose) polymerase interacts with base excision repair enzymes and is required in recovery from DNA damage in mice and cells. The 12th International Symposium on ADP-ribosylation reactions, 1997

28. Lewis J, Shimizu Y, Shimizu N: Nicotinamide inhibits adipocyte differentiation of 3T3-L1 cells. FEBS Lett 146: 37–41, 1982

29. Rosenthal D, Ding R, Simbulan-Rosenthal CM, Cherney B, Vanek P, Smulson M: Detection of DNA breaks in apoptotic cells utilizing the DNA binding domain of poly(ADP-ribose) polymerase with fluorescence microscopy. Nucleic Acids Res 25: 1437–1441, 1997

30. Totpal K, Singh S, Lapushin R, Aggarwal B: Qualitative and quantitative differences in the cellular responses mediated through Fas antigen and TNFR. J Interferon Cytokine Res 16: 259–267, 1996

31. Ogasawara J, Suda T, Nagata S: Selective apoptosis of CD4+CD8+ thymocytes by the anti-Fas antibody. J Exp Med 181: 485–491, 1995

32. Natoli G, Ianni A, Costanzo A, De Petrillo G, Ilari I, Chirillo P, Balsano C, Levrero M: Resistance to Fas-mediated apoptosis in human hepatoma cells. Oncogene 11: 1157–1164, 1995

33. Chiba T, Takahashi S, Sato N, Ishii S, Kikuchi K: Fas-mediated apoptosis is modulated by intracellular glutathione in human T cells. Eur J Immunol 26: 1164–1169, 1996

34. Ronen D, Schwartz D, Teitz Y, Goldfinger N, Rotter V: Induction of HL-60 cells to undergo apoptosis is determined by high levels of wild-type p53 protein whereas differentiation of cells is mediated by lower p53 levels. Cell Growth Diff 7: 21–30, 1996

35. Yamato K, Yamamoto M, Hirano Y, Tsuchida N: A human temperature-sensitive p53 mutant p53Val-138: Modulation of the cell cycle, viability, and expression of p53-responsive genes. Oncogene 11: 1–6, 1995

36. Cleaver J, Borek C, Milam K, Morgan W: The role of poly(ADP-ribose) synthesis in toxicity and repair of DNA damage. Pharmacol Ther 31: 269–293, 1985

37. Hunting D, Gowans B, Henderson J: Effects of 6-aminonicotinamide on cell growth, poly(ADP-ribose) synthesis and nucleotide metabolism. Biochem Pharmacol 34: 3999–4003, 1985

38. Milam K, Cleaver J: Inhibitors of poly (adenosine diphosphate-ribose) synthesis: Effect on other metabolic processes. Science 223: 589–591, 1984

39. Ding R, Smulson M: Depletion of nuclear poly(ADP-ribose) polymerase by antisense RNA expression: Influences on genomic stability, chromatin organization and carcinogen cytotoxicity. Cancer Res 54: 4627–4634, 1994

40. Chinnaiyan A, Orth K, O'Rourke K, Duan H, Poirier G, Dixit V: Molecular ordering of the cell death pathway. Bcl-2 and Bcl-xL function upstream of the CED-3-like apoptotic proteases. J Biol Chem 271: 4573–4576, 1996

41. Darmon A, Ley T, Nicholson D, Bleackley R: Cleavage of CPP32 by granzyme B represents a critical role for granzyme B in the induction of target cell DNA fragmentation. J Biol Chem 271: 21709–21712, 1996

42. Erhardt P, Cooper G: Activation of CPP32 apoptostic protease byu distinct signalling pathways with differential sensitivity to Bcl-xL. J Biol Chem 271: 17601–17604, 1996

43. Martin S, Amarante-Mendes G, Shi L, Chuang T, Casiano C, O'Brien G, Fitzgerald P, Tan E, Bokoch G, Greenberg A, Green D: The cytotoxic cell protease granzyme B initiates apoptosis in a cell-free system by proteolytic processing and activation of the ICE/CED-3 family protease, CPP32, via a novel two-step mechanism. EMBO J 15: 2407–2416, 1996

44. Schlegel J, Peters I, Orrenius S, Miller D, Thornberry N, Yamin T, Nicholson D: CPP32/apopain is a key interleukin 1 beta converting enzyme-like protease involved in Fas-mediated apoptosis. J Biol Chem 271: 1841–1844, 1996

45. Dubrez L, Savoy I, Hamman A, Solary E: Pivotal role of a DEVD-sensitive step in etoposide-induced and Fas-mediated apoptosis. EMBO J 15: 5504–5512, 1996

46. Enari M, Talanian R, Wong W, Nagata S: Sequential activation of ICE-like and CPP32-like proteases during Fas-mediated apoptosis. Nature 380: 723–726, 1996

47. Nosseri C, Coppola S, Ghibelli L: Possible involvement of poly(ADP-ribosyl) polymerase in triggering stress-induced apoptosis. Exp Cell Res 212: 367–373, 1994

48. Jones D, McConkey D, Nicotera P, Orrenius S: Calcium-activated DNA fragmentation in rat liver nuclei. J Biol Chem 264: 6398–6403, 1989

49. Bertrand R, Solary E, Jenkins J, Pommier Y: Apoptosis and its modulation in human promyelocytic HL-60 cells treated with DNA topoisomerase I and II inhibitors. Exp Cell Res 207: 388–397, 1993

50. Yoon Y, Kim J, Kang K, Kim Y, Choi K, Joe C: Poly(ADP-ribosyl)ation of histone H1 correlates with intemucleosomal DNA fragmentation during apoptosis. J Biol Chem 271: 9129–9134, 1996

51. Kumari S, Mendoza-Alvarez H, Alvarez-Gortzalez R: Poly(ADP-ribosyl)ation of p53 in apoptotic cells following DNA damage. The 12th International Symposium on ADP-ribosylation reactions, 1997

52. Nozaki T, Masutani M, Nishiyarna E, Shimokawa T, Wkabayashi K, Sugimura T: Interactions between poly(ADP-ribose) polymerase and p53. The 12th International Symposium on ADP-ribosylation reactions, 1997

53. Malanga M, Pleschke J, Kleczkowska H, Althaus F: Poly(ADP-ribose) binds to specific domains of p53 and alters its DNA binding functions. J Biol Chem 273: 11839–11843, 1998

54. Lopes U, Erhardt P, Yao R, Cooper G: p53-dependent induction of apoptosis by proteosome inhibitors. J Biol Chem 272: 12893–12896, 1997

55. Spriggs L, Hill S, Jeter J: Proliferation is required for induction of terminal differentiation of Friend erythroleuken-iia cells. Biochem and Cell Biol 70: 1992

56. Tom T, Malkas L, Hickey R: Identification of multiprotein compexes containing DNA replication factors by native immunoblotting of HeLa cell protein preparations with T-antigen-dependent SV40 DNA replication activity. J Cell Biochem 63: 259, 1996

148

57. Yoshihara K, Itaya A, Tanaka Y, Ohashi Y, Ito K, Teraoka H, Tsukada K, Matsukage A, Kamiya T: Inhibition of DNA polymerase α, DNA polymerase β, terminal nucleotidyltransferase and DNA ligase II by poly (ADP-ribosyl)ation reaction *in vitro*. Biochem Biophys Res Commun 128: 61–67, 1985

58. Kasid U, Halligan B, Liu L, Dritschilo A, Smulson M: Poly(ADP-ribose)-mediated post-translational modification of chromatin-associated human topoisomerase I. Inhibitory effects on catalytic activity. J Biol Chem 264: 18687–18692, 1989

59. Ferro A, Olivera B: Poly (ADP-ribosylation) of DNA topoisomerase I from calf thymus. J Biol Chem 259: 547–554, 1984

60. Darby M, Schmitt B, Jongstra B, Vosberg H: Inhibition of calf thymus type II DNA topoisomerase by poly(ADP-ribosylation). EMBO J 4: 2129–2134, 1985

61. Eki T, Hurwitz J: Influence of poly(ADP-ribose) polymerase on the enzymatic synthesis of SV40 DNA. J Biol Chem 266: 3087–3100, 1991

62. Tsurimoto T, Stillman B: Replication factors required for SV40 DNA replication *in vitro*. I. DNA structure-specific recognition of a primer-template junction by eukaryotic DNA polymerase and their accessory proteins. J Biol Chem 266: 1950, 1991

63. Hiebert S, Lipp M, Nevins J: E1A-dependent transactivation of the human MYC promoter is mediated by the E2F factor. Proc Natl Acad Sci USA 86: 3594–3598, 1989

64. DeGregori J, Leoni G, Miron A, Jakoi L, Nevins J: Distinct roles for E2F proteins in cell growth control and apoptosis. Proc Nacl Acad Sci USA 94: 7245–7250, 1997

65. Blake M, Azizkhan J: Transcription factor E2F is required for efficient expression of hamster dihydrofolate-reductase gene *in vitro* and *in vivo*. Mol Cell Biol 9: 4994–5002, 1989

66. Ogris E, Rotheneder H, Mudrak I, Pichler A, Wintersberger E: A binding site for transcription factor E2F is a target for transactivation of murine thymidine kinase by polyoma large T antigen and plays an important role in growth regulation of the gene. J Virol 67: 1765–1771, 1993

67. Pearson B, Nasheuer H, Wang T: Human DNA polymerase α gene: Sequences controlling expression in cycling and serum-stimulated cells. Mol Cell Biol 11: 2081–2095, 1991

68. Neuman E, Flemington E, Sellers W, Kaelin W: Transcription of the E2F-1 gene is rendered cell cycle dependent by E2F DNA-binding sites within its promoter. Mol Cell Biol 15: 4660, 1995

69. Meisterernst M, Stelzer G, Roeder R: Poly(ADP-ribose) polymerase enhances activator-dependent transcription *in vitro*. Proc Natl Acad Sci USA 94: 2261–2265, 1997

70. Rawling J, Alvarez-Gonzalez R: TEIF, a basal eukaryotic transcription factor, is a substrate for poly(ADP-ribosyl)ation. Biochem J 324: 249–253, 1997

71. Simbulan-Rosenthal C, Rosenthal D, Iyer S, Boulares H, Smulson M: Transient poly(ADP-ribosylation) of nuclear proteins and role of poly(ADP-ribose) polymerase in the early stages of apoptosis. J Biol Chem 273: 13703–13712, 1998

72. Simbulan-Rosenthal C, Rosenthal D, Boulares H, Hickey R, Malkas L, Coll J, Smulson M.: Regulation of the expression or recruitment of components of the DNA synthesome by poly(ADP-ribose) polymerase. Biochemistry 37: 9363–9370, 1998

Poly(ADP-ribose) polymerase upregulates E2F-1 promoter activity and DNA pol α expression during early S phase

Cynthia M Simbulan-Rosenthal[1], Dean S Rosenthal[1], RuiBai Luo[1] and Mark E Smulson*[1]

[1]Department of Biochemistry and Molecular Biology, Georgetown University School of Medicine, Basic Science Building, Room 351, 3900 Reservoir Road NW, Washington DC 20007, USA

E2F-1, a transcription factor implicated in the activation of genes required for S phase such as DNA pol α, is regulated by interactions with Rb and by cell-cycle dependent alterations in E2F-1 abundance. We have shown that depletion of poly(ADP-ribose) polymerase (PARP) by antisense RNA expression downregulates pol α and E2F-1 expression during early S phase. To examine the role of PARP in the regulation of pol α and E2F-1 gene expression, we utilized immortalized mouse fibroblasts derived from wild-type and PARP knockout (PARP−/−) mice as well as PARP−/− cells stably transfected with PARP cDNA [PARP−/−(+PARP)]. After release from serum deprivation, wild-type and PARP−/−(+PARP) cells, but not PARP−/− cells, exhibited a peak of cells in S phase by 16 h and had progressed through the cell cycle by 22 h. Whereas [³H]thymidine incorporation remained negligible in PARP−/− cells, in vivo DNA replication maximized after 18 h in wild-type and PARP−/−(+PARP) cells. To investigate the effect of PARP on E2F-1 promoter activity, a construct containing the E2F-1 gene promoter fused to a luciferase reporter gene was transiently transfected into these cells. E2F-1 promoter activity in control and PARP−/−(+PARP) cells increased eight-fold after 9 h, but not in PARP−/− cells. PARP−/− cells did not show the marked induction of E2F-1 expression during early S phase apparent in control and PARP−/−(+PARP) cells. RT–PCR analysis and pol α activity assays revealed the presence of pol α transcripts and a sixfold increase in activity in both wild-type and PARP−/−(+PARP) cells after 20 h, but not in PARP−/− cells. These results suggest that PARP plays a role in the induction of E2F-1 promoter activity, which then positively regulates both E2F-1 and pol α expression, when quiescent cells reenter the cell cycle upon recovery from aphidicolin exposure or removal of serum.

Keywords: PARP; E2F-1; DNA polymerase α; DNA replication; promoter activity; gene expression

Introduction

Depletion of PARP from cells by expression of antisense RNA or by gene knockout has shown that the enzyme plays important roles in various nuclear processes that involve rejoining of DNA strand breaks. PARP depletion by antisense RNA expression results in a decrease in the initial rate of DNA repair in HeLa cells (Ding et al., 1992) and keratinocytes (Rosenthal et al., 1995), a reduction in the survival of cells exposed to mutagenic agents, alterations in chromatin structure, an increase in gene amplification (Ding and Smulson, 1994), and inhibition of the biochemical and morphological changes associated with apoptosis (Simbulan-Rosenthal et al., 1998b). Fibroblasts derived from PARP knockout mice exhibit proliferation deficiencies in culture, and thymocytes from these animals show a delayed recovery after exposure to γ-radiation (Wang et al., 1995). Other PARP knockout mice exhibit extreme sensitivity to ionizing radiation, and splenocytes derived from these animals undergo abnormal apoptosis (de Murcia et al., 1997).

We have shown that PARP-depleted 3T3-L1 cells expressing PARP antisense RNA fail to differentiate and to undergo DNA replication that normally precedes differentiation (Simbulan-Rosenthal et al., 1996; Smulson et al., 1995), indicating that PARP appears to be required for differentiation-linked DNA replication in these cells. PARP is a component of a multiprotein DNA replication complex (MRC or DNA synthesome) that catalyzes replication of viral DNA in vitro and contains pol α, pol δ, DNA primase, DNA helicase, DNA ligase, and topoisomerases I and II, as well as accessory proteins such as proliferating-cell nuclear antigen (PCNA), RFC, and RPA. PARP poly(ADP-ribosyl)ates 15 of the ~40 MRC component proteins, including pol α, topoisomerase I, and PCNA (Simbulan-Rosenthal et al., 1996).

We recently showed that PARP plays a role in regulation of the expression of several of the tightly associated proteins of the MRC, including pol α, DNA primase, and RPA (Simbulan-Rosenthal et al., 1998a). Depletion of PARP by antisense RNA expression also prevented induction of expression of the transcription factor E2F-1, which positively regulates transcription of genes encoding pol α, PCNA, and other S phase proteins, indicating that PARP may play a role in the expression of these genes during entry into S phase. E2F-1 is implicated in the regulation of cell cycle progression by activating expression of genes important for the execution of the S phase. This activity is regulated during the cell cycle by the binding of E2F-1 to the dephosphorylated form of the tumor suppressor protein Rb; phosphorylation of Rb by cyclin dependent kinases during entry into S phase releases E2F-1, consequently activating gene expression (Weinberg, 1995). Perturbation of these control pathways by inactivation of Rb and accumulation of E2F-1

transcription factor activity is suggested to result in the loss of cell growth control that underlie the development of human cancers. Indeed, overexpression of E2F-1 causes oncogenesis (Johnson et al., 1994a) and is sufficient to drive serum-starved fibroblasts through S phase and into the cell cycle (Johnson et al., 1993). Deregulated expression of E2F-1 in quiescent cells has also been shown to lead to S phase entry followed by p53-mediated apoptosis (Qin et al., 1994).

To clarify the role of PARP in regulation of the expression of pol α and E2F-1 genes associated with induction of proliferation in quiescent cells, we have now utilized mouse fibroblasts derived from wild-type (control) and PARP knockout (PARP−/−) mice as well as PARP−/− cells stably transfected with wild-type PARP cDNA (PARP−/−(+PARP)). Consistent with our previous results of PARP depletion by antisense RNA expression, our present data indicate that PARP plays an essential role in both differentiation-linked- as well as DNA replication associated with progression through the cell cycle. Furthermore, we demonstrate for the first time that PARP may regulate the expression of the E2F-1 and DNA pol α genes during early S phase by stimulating E2F-1 promoter activity. PARP appears essential for induction of promoter activity of the E2F-1 gene, which in turn, positively regulates transcription of the E2F-1 and pol α genes during early S phase.

Results

Wild-type and PARP−/−(+PARP) cells, but not PARP−/− cells, progress through the cell cycle after release from aphidicolin block.

We have previously shown that 3T3-L1 cells depleted of PARP by antisense RNA expression fail to undergo differentiation-linked DNA replication (Simbulan-Rosenthal et al., 1996); control cells progress through a round of replication prior to the onset of terminal differentiation. Thus, under these conditions, quiescent control cells are induced to proliferate and go through a round of the cell cycle, but not the PARP-depleted antisense cells. To determine whether depletion of PARP by gene disruption similarly blocks reentry of cells into S phase, we studied immortalized fibroblasts that were derived from wild-type (control) and PARP knockout (PARP−/−) mice (Wang et al., 1995). These PARP−/− cells were previously confirmed to be devoid of detectable PARP and poly(ADP-ribose) by immunoblot analysis with the corresponding antibodies (Simbulan-Rosenthal et al., 1998b). Although the presence of a novel activity capable of synthesizing ADP-ribose polymers has been shown recently in PARP−/− cells, this activity, which is induced by treatment with MNNG, is considerably less than that in wild-type cells and may not fully compensate for PARP depletion (Shieh et al., 1998). Consistent with our results with the PARP antisense cells, flow cytometric analysis revealed that, although there were no significant differences between the DNA histograms of asynchronously growing wild-type and PARP−/− cells, wild-type cells progressed through one round of the cell cycle 5 h after release from aphidicolin-induced block at the G1-S transition, while PARP−/− cells

did not. More than 65% of wild-type cells had synchronously entered S phase by 3 h, whereas the number of PARP−/− cells in S phase (~20%) did not increase substantially during the same time period (Figure 1).

Wild-type and PARP−/−(+PARP) cells, but not PARP−/− cells, reenter the cell cycle after release from serum deprivation

Wild-type and PARP−/− cells were also synchronized by serum deprivation for 45 h, and the quiescent cells were then stimulated to proliferate by the addition of serum. Although both wild-type and PARP−/− cells were effectively blocked at G_1/S by serum deprivation (~87% of the cells were in G_1), only the wild-type cells exhibited a peak of S phase at 16 h and had progressed through a round of the cell cycle by 24 h after addition of serum (Figure 2a). Thus, whereas >83% of the control cells were in S phase by 16 h, there was no apparent increase in the number of PARP−/− cells in S phase for up to 24 h after serum addition. FACS analysis further revealed a third small peak in the DNA histogram of PARP−/− cells which corresponds to the G_2/M peak of a genomically unstable tetraploid cell population. The results with fibroblasts from PARP−/− mice confirm a requirement for PARP during entry into S phase. The enzyme thus appears to play an essential role in DNA replication associated with either differentiation or reentry into and progression through the cell cycle after recovery from exposure to aphidicolin or serum deprivation.

Time after release from aphidicolin (h)
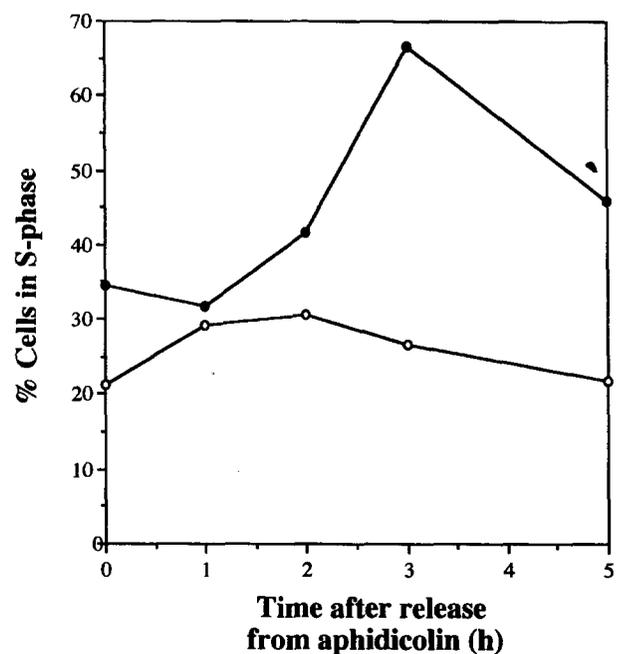
Figure 1 Flow cytometric analysis of wild-type and PARP−/− mouse fibroblasts at various times after release from aphidicolin block. Cells were harvested at the indicated times after release from aphidicolin-induced block at the G1/S transition. Nuclei were prepared by treatment of cells with detergent and trypsin and were stained with propidium iodide for flow cytometric analysis. DNA histograms were derived at various times after release from aphidicolin block and the cell cycle phase distribution was quantified and summarized in a figure showing per cent of wild-type (closed circles) and PARP−/− (open circles) cells in S phase of the cell cycle

PARP−/− fibroblasts were stably transfected with pCD12, a plasmid encoding wild-type PARP, and grown in selective medium. A stable clone was selected for further study on the basis of its ability to express PARP protein as revealed by immunoblot analysis with antibodies to PARP as well as by PARP activity assays (Simbulan-Rosenthal et al., 1998b). These PARP−/−(+PARP) cells were synchronized by serum deprivation, released into the cell cycle by addition of serum, and analysed by flow cytometry. Similar to the wild-type cells, PARP−/−(+PARP) cells synchronously entered S phase by 14 h (>60% of the PARP−/−(+PARP) cells were in S phase by this time), and had progressed through a round of the cell cycle by 22 h (Figure 2b). Thus, stable transfection of PARP−/− fibroblasts with wild-type PARP cDNA restored the ability of these cells to reenter the cell cycle after release from serum deprivation. The differences in cell cycling noted between the wild-type and PARP−/− cells can thus be attributed to PARP, and are not simply due to clonal differences. Interestingly, the tetraploid cell population (the third peak in the DNA histograms of PARP−/− cells) was no longer observed in PARP−/−(+PARP) cells after several generations suggesting that the presence of PARP may stabilize the genome and select against this unstable tetraploid population.

Incorporation of [³H]thymidine into nascent DNA was measured to confirm whether in vivo DNA replication was occurring under the conditions in these experiments where quiescent cells are stimulated to reenter the cell cycle by addition of serum. Consistent with the flow cytometric data, in vivo DNA replication was maximal 20 h after release of wild-type and PARP−/−(+PARP) cells into S phase, whereas negligible [³H]thymidine incorporation was apparent in PARP−/− during the same time period (data not shown). These results are also consistent with our previous data showing that in vivo DNA replication, as assessed by incorporation of bromodeoxyuridine or [³H]thymidine into newly synthesized DNA, was apparent only in 3T3-L1 control cells 24 h after induction of differentiation-linked DNA replication, but was not detected in PARP-depleted antisense cells (Simbulan-Rosenthal et al., 1996).

Wild-type and PARP−/−(+PARP) cells, but not PARP−/− cells, show induction of pol α transcripts and activity after release from serum deprivation

We have previously shown that PARP depletion by antisense RNA expression in 3T3-L1 cells results in downregulation of expression of pol α, DNA primase, and the transcription factor E2F-1, thus, implicating PARP in the expression of these proteins during early S phase (Simbulan-Rosenthal et al., 1998a). To investigate whether PARP depletion by gene knockout could exert a similar effect on the expression of the pol α gene at the level of transcription during early S phase, we compared the abundance of pol α mRNA by RT−PCR analysis in wild-type, PARP−/− and PARP−/−(+PARP) cells at either 0 or 20 h after addition of serum to serum-deprived cells. Pol α transcripts were detected in all three cell types in unsynchronized cultures, although their levels were higher in wild-type cells than in PARP−/− or the

PARP−/−(+PARP) cells (Figure 3b). Whereas pol α RNA was not detected in any of the three cell types when blocked at G1/S by serum deprivation, both the wild-type and PARP−/−(+PARP) cells exhibited a marked induction of pol α transcripts 20 h after serum addition. In contrast, no pol α RNA was detected in the PARP−/− cells at this time (Figure 3a).

We also examined the time course of pol α activity in the three cell types after release from serum deprivation. Consistent with the results of the RT−PCR analysis, wild-type and PARP−/−(+PARP) cells, but not the PARP−/− cells, exhibited a sixfold increase in pol α activity, relative to basal levels, 20 h after serum addition (Figure 4). We have also previously shown that depletion of PARP by antisense RNA expression results in a replicative complex devoid of any significant pol α activity (Simbulan-Rosenthal et al., 1998a). The significant increase in pol α catalytic activity correlates with the marked induction of pol α transcripts in the wild-type and PARP−/−(+PARP) cells 20 h after serum addition. These results indicate that PARP plays a role in the upregulation of pol α expression at the level of transcription in quiescent cells induced to reenter the cell cycle after release from serum deprivation.

*PARP−/− cells do not show the marked induction of E2F-1 expression during early S phase apparent in control and PARP−/−(+PARP) cells*

To investigate further the mechanism by which PARP contributes to regulation of pol α gene transcription during early S phase, we examined the effect of PARP depletion by gene knockout on the abundance of E2F-1, a transcription factor that positively regulates the transcription of several genes whose products are required for DNA replication and cell growth; these genes include those encoding pol α, PCNA, dihydrofolate reductase, thymidine kinase, c-MYC, c-MYB, cyclin D, cyclin E, and E2F-1 itself (Blake and Azizkhan, 1989; DeGregori et al., 1995; Nevins, 1992; Pearson et al., 1991; Slansky et al., 1993). We previously demonstrated that PARP depletion by antisense RNA expression in 3T3-L1 cells prevents induction of E2F-1 expression during the early stages of differentiation-linked DNA replication (Simbulan-Rosenthal et al., 1998a). Consistent with these results and with the fact that the E2F-1 gene is an early-response gene (Johnson et al., 1994b), immunoblot analysis with antibodies to E2F-1 revealed that both wild-type and PARP−/−(+PARP) cells exhibited a marked increase in E2F-1 abundance soon after release from serum starvation; E2F-1 protein levels remained high for 16 h in these cells and declined thereafter (Figure 5a). In contrast, PARP−/− cells contained negligible amounts of E2F-1 for up to 20 h after serum addition. The expression of PCNA did not differ among the three cell types during the same time period (Figure 5b), indicating that the lack of pol α and E2F-1 expression in the PARP−/− cells was not attributable to a general inability to undergo protein or RNA synthesis. Thus, PARP may regulate expression of the pol α gene at the level of transcription during early S phase by increasing the expression of E2F-1.

PARP−/− cells do not exhibit induction of E2F-1 promoter activity during early S phase

We next investigated whether PARP upregulates the expression of pol α as well as E2F-1 at the level of transcription during early S phase by stimulating the activity of the E2F-1 gene promoter. Wild-type, PARP−/−, and PARP−/−(+PARP) cells were transiently transfected with a construct containing the E2F-1 promoter sequence fused to a luciferase reporter gene (pGL2) and with pSV2-CAT. Cells were then synchronized by serum deprivation, and at various times after release into S phase, luciferase assays were performed as a measure of E2F-1 promoter activity; CAT activity was also assayed in order to correct for differences in transfection efficiency. E2F-1 promoter-luciferase activity, normalized by either CAT activity (Figure 6a) or protein (Figure 6b), increased after serum addition in both control and PARP−/−(+PARP) cells; the increase was maximal (eightfold higher than basal levels) at 9 h after serum addition. In contrast, E2F-1 promoter activity in PARP−/− cells showed no increase after serum addition. Thus, when quiescent cells are induced to proliferate by serum addition, PARP may upregulate pol α and E2F-1 expression during S phase by stimulating the activity of the E2F-1 gene promoter.

A

Wild-type   **PARP-/-**   **Time after addition of serum (h)**

Cell Number

Relative Fluorescence
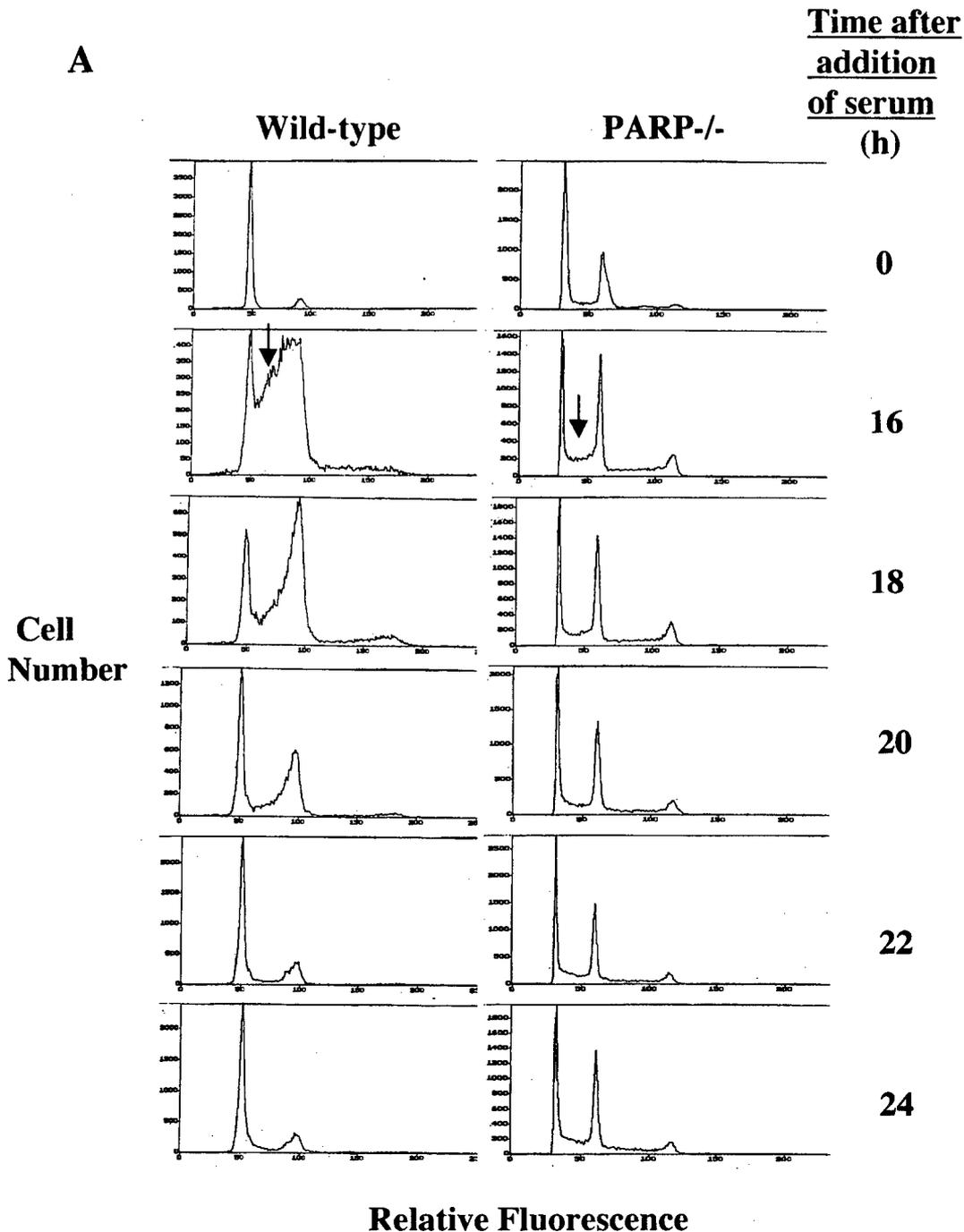
Discussion

We have demonstrated that PARP is tightly associated with the core proteins of the purified MRC (Simbulan-Rosenthal *et al.*, 1996) that support viral DNA replication *in vitro* and migrates as discrete, high molecular weight complexes on native polyacrylamide gel electrophoresis (Tom *et al.*, 1996). PARP is thought to play a regulatory role in these complexes because 15 of the ~40 polypeptides of the MRC, including pol α, topoisomerase I and PCNA, undergo poly(ADP-ribosyl)ation by PARP (Simbulan-Rosenthal *et al.*,

B

**PARP -/-
(+ PARP)**

**Time after
addition
of serum
(h)**

**Cell
Number**

0

14

16

18

20

22

**Relative
Fluorescence**
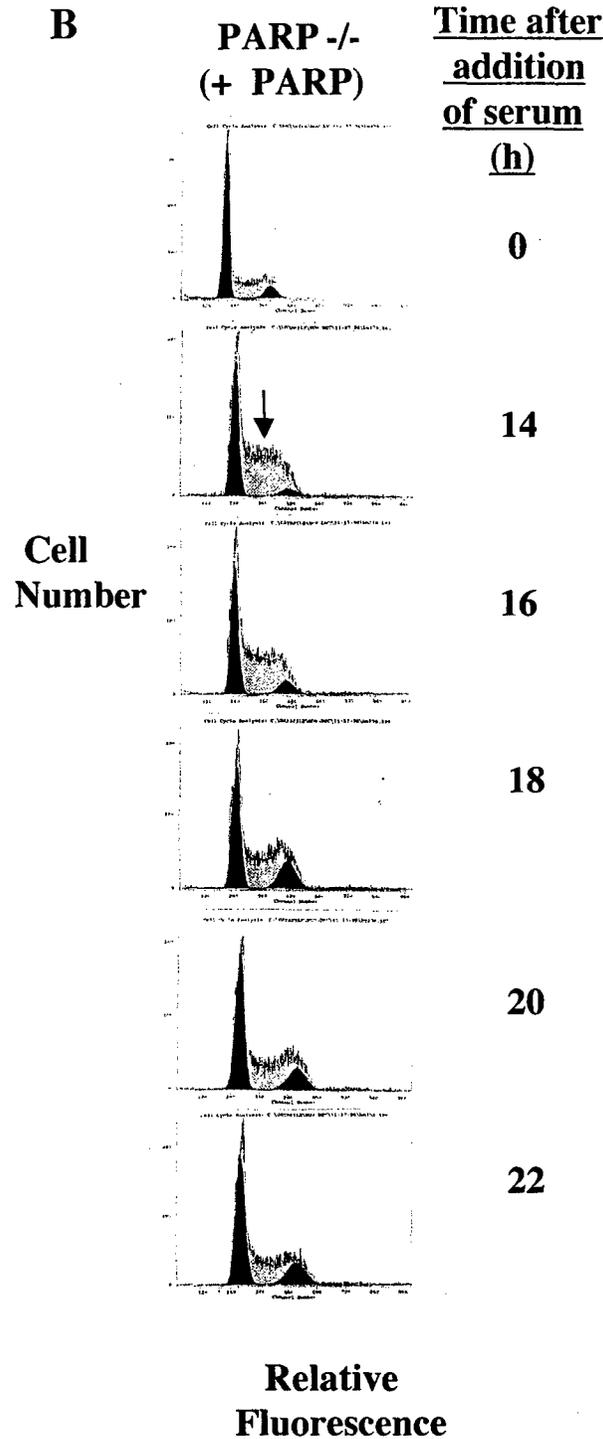
Figure 2   Flow cytometric analysis of wild-type and PARP−/− mouse fibroblasts (a) and PARP−/−(+PARP) cells (b) at various times after release from serum deprivation. Quiescent cells were released from serum deprivation and harvested at the indicated times after addition of serum. Nuclei were prepared and stained with propidium iodide for flow cytometric analysis. (a) DNA histograms of wild-type cells (left panels) at various times after addition of serum show a major peak of nuclei at G0/G1 at 0 h, a major peak of nuclei in S phase (arrow) at 16 h, and two major peaks of nuclei at G0/G1 and G2/M phases of the cell cycle at 18–20 h. DNA histograms of PARP−/− cells (right panels) show two major peaks of nuclei at G0/G1 and G2/M, as well as a third small peak corresponding to a tetraploid cell population, at all times after addition of serum. (b) Similar to wild-type cells, DNA histograms of PARP−/−(+PARP) cells show a major peak of nuclei at G0/G1 at 0 h, a peak of nuclei in S phase at 14 h, and 2 major peaks of nuclei at G₀/G₁ and G₂/M phases of the cell cycle by 18–22 h

5020

A

Time (h):

B
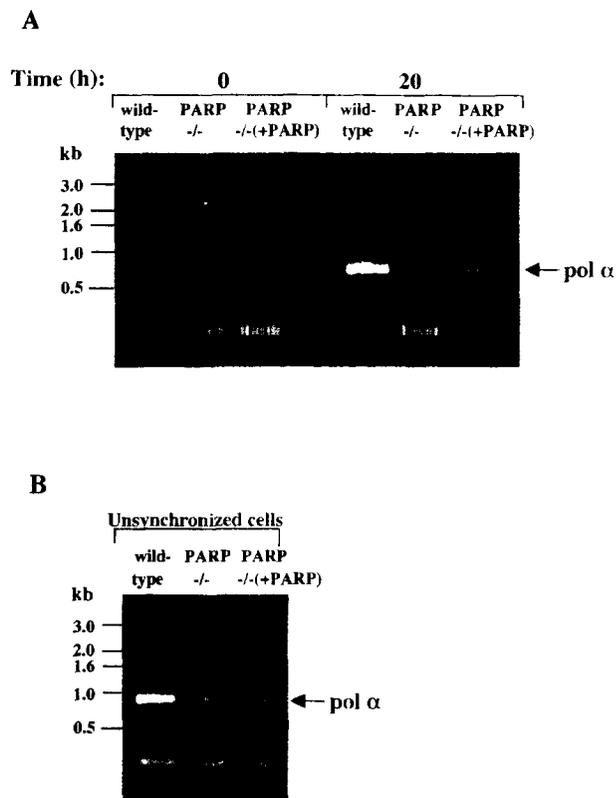
Figure 3 RT-PCR analysis of wild-type. PARP-/-, and PARP-/-(+PARP) cells prior to and 20 h after release from serum deprivation. Wild-type. PARP-/-, and PARP-/-(+PARP) were subjected to serum deprivation and harvested at 0 and 20 h after serum addition (a). Unsynchronized cells were also harvested for comparison of basal levels of pol α transcripts (b). Total RNA was purified from cell pellets and subjected to RT-PCR with pol α-specific primers. PCR products were separated on a 1.5% agarose gel and visualized by ethidium bromide staining. The positions of the specific pol α product (arrows) and of DNA size standards (in kilobases) are indicated

Figure 4 Time course of induction of pol α activity in wild-type, PARP-/- and PARP-/-(+PARP) cells after release from serum deprivation. Synchronized wild-type (closed circles). PARP-/- (open circles), and PARP-/-(+PARP) (closed squares) cells were harvested at the indicated times after release into S phase, and equal amounts of protein were assayed for pol α activity in vitro by measuring the incorporation of [³H]TTP into newly synthesized DNA for 1 h at 37°C with activated calf thymus DNA as template. Data are means of duplicate determinations and essentially identical results were obtained in two independent experiments

1996). The MRC purified from control 3T3-L1 cells in S phase, but not that from PARP antisense cells, contains both PARP and pol α activities (Simbulan-Rosenthal et al., 1998a). Furthermore, our observation that the expression of pol α, DNA primase, and E2F-1 is not induced during early S phase in PARP-depleted antisense cells implicated PARP in the induction of expression of the corresponding genes that occurs at this time.

Insight into the biological roles of PARP can also be obtained by gene disruption. While certain strains of PARP knockout mice are viable and fertile, primary fibroblasts derived from these animals exhibit proliferation deficiencies in culture (de Murcia et al., 1997; Wang et al., 1995). Thus, although both DNA replication and differentiation occur in these animals in the absence of PARP, isolated cell systems may show more profound effects of the lack of this enzyme that are not apparent in the animals. In the present study, we have therefore used immortalized fibroblasts derived from wild-type and PARP-/- mice to examine further the role of PARP in the regulation of pol α and E2F-1 expression during early S phase.

Consistent with our previous results with PARP antisense cells (Simbulan-Rosenthal et al., 1998a), we
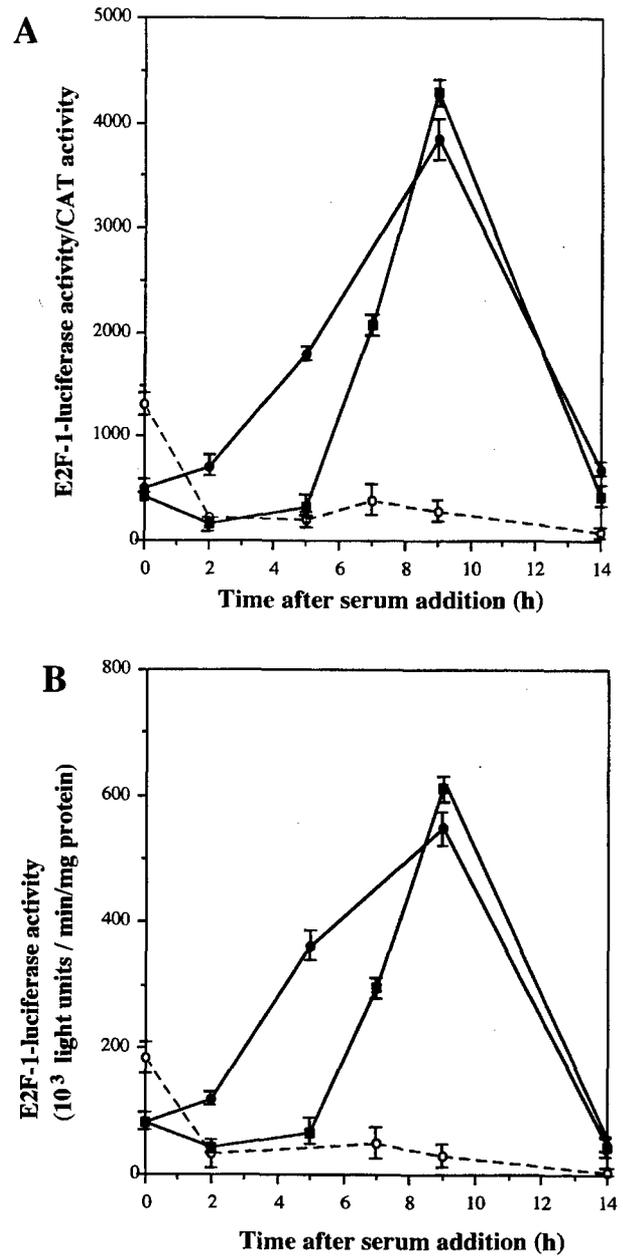
have now shown that depletion of PARP by gene disruption blocks quiescent cells from reentering the cell cycle after recovery from serum deprivation. PARP depletion also prevents the induction of pol α and E2F-1 gene expression that normally occurs during early S phase under these conditions. After release from either aphidicolin block or serum deprivation, wild-type cells synchronously reentered the cell cycle and exhibited a peak of in vivo DNA replication, whereas PARP-/- cells did not. Moreover, stable transfection of PARP-/- cells with PARP cDNA restored the ability of these cells to reenter the cell cycle and proliferate after release from serum starvation. Furthermore, wild-type and PARP-/-(+PARP) cells, but not PARP-/- cells, exhibited a substantial increase in in vitro pol α activity at the peak of S phase. These results indicate that PARP plays a role in DNA replication associated with reentry into the cell cycle after release from serum deprivation, in addition to its role in differentiation-linked DNA replication. The data obtained with the PARP-/- cells stably transfected with PARP cDNA also indicate that the differences apparent between the wild-type and PARP-/- cells are not due to differences in clonality but rather to PARP.

Pol α, together with its associated DNA primase, catalyzes the synthesis RNA primers and Okazaki fragments required for initiation of DNA replication and for lagging-strand DNA synthesis (Waga and Stillman, 1994). The pol α-DNA primase complex comprises four subunits the largest of which
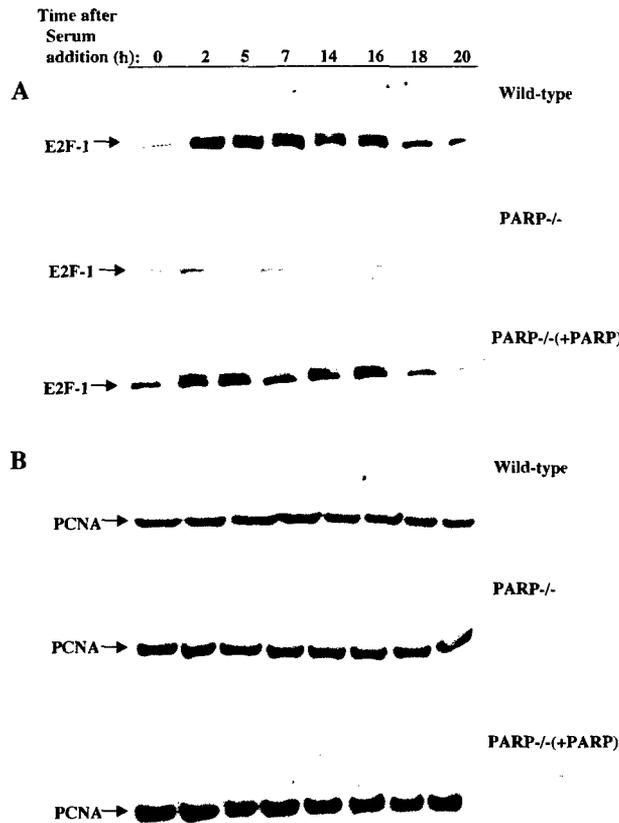
Figure 5 Time course of E2F-1 (a) and PCNA (b) expression in wild-type, PARP−/−, and PARP−/−(+PARP) cells after release from serum deprivation. Quiescent wild-type (upper panels), PARP−/− (middle panels), and PARP−/−(+PARP) (lower panels) cells were harvested at the indicated times after addition of serum. Cell extracts were prepared and equal amounts of protein (30 μg) were subjected to immunoblot analysis with antibodies to E2F-1 (a) or to PCNA (b). The positions of E2F-1 and PCNA are indicated on the left (arrows)

Figure 6 Time course of induction of E2F-1 promoter activity after release from serum deprivation in wild-type, PARP−/− and PARP−/−(+PARP) cells. Synchronized quiescent wild-type (closed circles), PARP−/− (open circles) and PARP−/−(+PARP) (closed squares) cells were harvested at the indicated times after addition of serum. To measure E2F-1-luciferase promoter activity, cell extracts were prepared and assayed for luciferase and CAT activities. The luciferase activity (light units/min) was then normalized against transfection efficiencies by CAT activity (a) or total protein (mg) (b). Data are means of triplicate determinations, and essentially identical results were obtained in two independent experiments

(∼180 kDa) is the catalytic subunit of pol α (Wong et al., 1986), and the two smallest subunits of which (∼58- and ∼48 kDa) constitute the DNA primase (Bambara and Jessee, 1991). Stimulation of quiescent cells to proliferate results in simultaneous increases in abundance of mRNAs encoding each of these four subunits prior to the onset of DNA synthesis, suggesting that the transcription of the genes for pol α and DNA primase is likely regulated by a common mechanism (Miyazawa et al., 1993). In response to growth stimulation, the expression of genes whose products are involved in DNA replication, including those for pol α and DNA primase, increases dramatically at late G1 (Baserga, 1991; Miyazawa et al., 1993). The cell cycle-regulatory transcription factor E2F-1, which binds to the specific recognition site 5′-TTTCGCGC, activates the promoters of the pol α gene and other genes that encode proteins required for DNA replication and cell growth, including those encoding dihydrofolate reductase, thymidine kinase, c-MYC, c-MYB, PCNA, cyclin D, and cyclin E (Blake and Azizkhan, 1989; DeGregori et al., 1995; Nevins, 1992; Pearson et al., 1991; Slansky et al., 1993). The E2F-1 gene promoter also contains E2F binding sites, and E2F-1 activates transcription of its own gene

during the cell cycle by binding to these sites (Neuman et al., 1994).

Depletion of PARP by gene knockout, similar to depletion of the protein by antisense RNA expression, prevented the increase in the abundance of E2F-1 associated with entry into S phase, an effect that appears attributable, at least in part, to the lack of induction of E2F-1 promoter activity in the PARP−/− cells. Together with the marked increase in pol α

transcripts and activity at the peak of S phase in wild-type and PARP−/−(+PARP) cells, but not in the PARP−/− cells, these data indicate that PARP plays a role in the induction of E2F-1 promoter activity, which then positively regulates pol α and E2F-1 expression during early S phase. The role of PARP in the regulation of transcription of the E2F-1 and pol α genes may be indirect, given that PARP has also been shown to enhance activator-dependent transcription by interacting with RNA polymerase II-associated factors (Meisterernst *et al.*, 1997). PARP also binds transcription enhancer factor 1 (TEF1) to enhance muscle-specific gene transcription (Butler and Ordahl, 1999) as well as the transcription factor AP-2 to coactivate AP-2-mediated transcription (Kannan *et al.*, 1999). The basal transcription factor TFIIF and TEF-1 are both highly specific substrates for poly(ADP-ribosyl)ation (Butler and Ordahl, 1999; Rawling and Alvarez-Gonzalez, 1997). Whether PARP modulates E2F-1-mediated transcription by binding to E2F-1 remains to be clarified. Alternatively, since PARP depletion by antisense RNA expression also results in significant changes in chromatin structure, effects of the lack of PARP on gene expression may be attributable, at least in part, to such changes. Experiments are now underway to determine whether PARP plays a more direct role in the transcription of pol α and E2F-1 genes by binding to the promoter sequences of the E2F-1 and/or pol α genes. Preliminary data from electrophoretic mobility shift assays indicate that purified recombinant PARP binds to both linear and circular constructs containing the E2F-1 promoter sequence, and that this binding is slightly inhibited in the presence of NAD, thus, suggesting that PARP may stimulate E2F-1 promoter activity directly (unpublished observations).

Materials and methods

Cells, vectors, and transfection

Wild-type and PARP−/− fibroblasts, immortalized by a standard 3T3 protocol, were kindly provided by ZQ Wang (International Agency for Research on Cancer, Lyon, France), grown in Dulbecco's modified Eagle's medium (DMEM) supplemented with 10% fetal bovine serum (FBS), penicillin (100 U/ml), and streptomycin (100 μg/ml), and subcultured every 4 days. PARP−/− fibroblasts were transfected with the use of lipofectamine (Life Technologies) with a plasmid encoding wild-type human PARP (pCD12; (Alkhatib *et al.*, 1987)) and the plasmid pTracer-CMV (Invitrogen), a zeocin-based vector system. This vector system was used because the PARP−/− fibroblasts express an endogenous neomycin resistance gene as a result of the procedure used to establish the original PARP knockout mice. Stable transfectants were selected in growth medium containing zeocin (500 μg/ml). Expression of PARP was confirmed by RNA, DNA, and immunoblot analysis of control and stably transfected cell lines; these cell lines were recently used in a study investigating the role of PARP in the early stages of apoptosis (Simbulan-Rosenthal *et al.*, 1998b).

The construct (pGl2) containing E2F-1 gene promoter fused to luciferase cDNA (Neuman *et al.*, 1994) was generously provided by Dr William Kaelin (Dana Farber Cancer Inst., Boston, MA, USA). Cells were transiently co-transfected with pGL2 (20 μg per plate) and pSV₂CAT (2 μg) (for normalization of transfection) using lipofectamine. The cells were allowed to recover overnight, supplied with fresh

medium, incubated for an additional 5 h, and then synchronized by serum deprivation for subsequent experiments.

Cell synchronization and release into S phase

Cells were plated at a density of 10^5 cells per plate 24 h prior to synchronization at the G1/S transition by either aphidicolin treatment or serum deprivation. For synchronization by aphidicolin block, the cells were incubated with 1.5 μM aphidicolin (Sigma) for 16–18 h as previously described for fibroblasts (Sukhorukov *et al.*, 1994). The cells were then washed twice with phosphate-buffered saline (PBS) and incubated in fresh medium for release into S phase. Because aphidicolin is a reversible inhibitor, most of the cells began DNA synthesis almost immediately after removal of the drug; they progressed through S phase and reached G2/M after an additional 5–6 h. For synchronization by serum deprivation, cells were washed twice with PBS and incubated for 30–45 h in DMEM supplemented with 0.5% FBS, after which the quiescent cells were stimulated to proliferate by incubation in DMEM containing 15% FBS.

Flow cytometry

Cells were harvested at various times after release into S phase, and nuclei were prepared for flow cytometric analysis as previously described (Vindelov *et al.*, 1983). Briefly, cells were exposed to trypsin in order to obtain a single-cell suspension, trypsin was neutralized by serum, and cells were then resuspended in 100 μl of a solution containing 250 mM sucrose, 40 mM sodium citrate (pH 7.6), and 5% dimethyl sulfoxide. They were then lysed by incubation for 10 min with trypsin (30 μg/ml) in a solution containing 3.4 mM sodium citrate, 0.1% NP-40, 1.5 mM spermine tetrahydrochloride, and 0.5 mM Tris-HCl (pH 7.6). After incubation for an additional 10 min with trypsin inhibitor and ribonuclease A (0.1 mg/ml) in the same solution, nuclei were stained for 15 min with propidium iodide (0.42 mg/ml) in the same solution, filtered through a 37-μm nylon mesh, and analysed with a dual-laser flow cytometer (FACScan).

Assays for pol α activity

At various times after release into S phase, cells were harvested, washed with ice-cold PBS, and subjected to assays for pol α activity *in vitro* or for DNA replication *in vivo*. *In vitro* pol α activity was assayed by measuring the incorporation of [³H]TTP into DNA during 1 h at 37°C, with activated calf thymus DNA as template, as previously described (Simbulan *et al.*, 1993).

Assay for E2F-1 promoter activity

At various times after release into S phase, cells were harvested and washed with ice-cold PBS, and cell extracts were assayed for luciferase activity according to standard procedures with a luciferase assay kit (Promega) and a luminometer. Luciferase activity was normalized by chloramphenicol acetyltransferase (CAT) activity, which was measured by incubating equal volumes of cell extracts with [³H]-acetyl-CoA and chloramphenicol.

Immunoblot analysis

SDS-polyacrylamide gel electrophoresis and transfer of separated proteins to a nitrocellulose membrane were performed according to standard procedures. After both staining with Ponceau S (0.1%) to confirm equal loading and transfer of samples and subsequent blocking of nonspecific sites, the membranes were incubated with monoclonal antibodies to either PCNA (1:1000 dilution; Calbiochem)

(detects the PCNA p36) or E2F-1 (1:1000 dilution: Santa Cruz Biotech) (detects E2F p60). Immune complexes were detected with appropriate horseradish peroxidase-labeled secondary antibodies (1:3000 dilution) and enhanced chemiluminescence (Pierce).

Reverse transcription-polymerase chain reaction (RT–PCR)

Unique oligonucleotide primer pairs were designed to 5' regions of the gene for the pol α catalytic subunit as follows: pol α 5' (bases 31-61, ATGCACGAAGAGGACTGTAA-ACTGGAGGCA) and pol α 3' (bases 830-801, TCTAC-CTTCTCTGTGTCCATGGACTCATCA) (Miyazawa *et al.*, 1993). The primer sets were prepared and diluted to a concentration of 50 pmoles/µl. Total cellular RNA was purified from cell pellets with the use of a total RNA extraction kit (Pharmacia Biotech) and was subjected to RT–PCR with the use of a Perkin Elmer Gene Amp EZ tTh RNA PCR kit. The reaction mix (50 µl) contained EZ buffer mix; 300 µM each of dGTP, dATP, dTTP, and dCTP; 2.5 µM Mn(Oac)2; 0.45 µM of each primer; 1 µg of total RNA; and 5 U of rTth DNA polymerase. With an Amplitron II Thermolyne PCR machine, RNA was first transcribed at 65°C for 40 min. after which cDNA was amplified by an initial incubation at 95°C for 2 min, followed by 40 cycles of 95°C for 1 min and 63°C for 90 s, another incubation at 65°C for 8 min, and a final extension at 70°C for 12 min. The PCR products were then separated by electrophoresis in a 1.5% agarose gel and visualized by ethidium bromide staining.

Abbreviations

PARP, poly(ADP-ribose) polymerase; MRC, multiprotein DNA replication complex; pol, DNA polymerase; PCNA, proliferating cell nuclear antigen; DMEM, Dulbecco's modified Eagle's medium; FBS, fetal bovine serum; PBS, phosphate-buffered saline; CAT, chloramphenicol acetyl-transferase; RT–PCR, reverse transcription-polymerase chain reaction.

References

Alkhatib HM, Chen DF, Cherney B, Bhatia K, Notario V, Giri C, Stein G, Slattery E, Roeder RG and Smulson ME. (1987). *Proc. Natl. Acad. Sci. USA*, **84**, 1224–1228.

Bambara R and Jessee C. (1991). *Biochim. Biophys. Acta*, **1088**, 11.

Baserga R. (1991). *J. Cell Sci.*, **98**, 433–436.

Blake M and Azizkhan J. (1989). *Mol. Cell Biol.*, **9**, 4994–5002.

Butler A and Ordahl C. (1999). *Mol. Cell Biol.*, **19**, 296–306.

de Murcia J, Niedergang C, Trucco C, Ricoul M, Dutrillaux B, Mark M, Oliver J, Masson M, Dierich A, LeMeur M, Waltzinger C, Chambon P and deMurcia G. (1997). *Proc. Natl. Acad. Sci. USA*, **94**, 7303–7307.

DeGregori J, Kowalik T and Nevins J. (1995). *Mol. Cell Biol.*, **15**, 4215–4224.

Ding R, Pommier Y, Kang VH and Smulson M. (1992). *J. Biol. Chem.*, **267**, 12804–12812.

Ding R and Smulson M. (1994). *Cancer Res.*, **54**, 4627–4634.

Johnson D, Cress W, Jakoi L and Nevins J. (1994a). *Proc. Natl. Acad. Sci. USA*, **91**, 12823–12827.

Johnson D, Ohtani K and Nevins J. (1994b). *Genes Dev.*, **8**, 1514–1525.

Johnson D, Schwaz J, Cress W and Nevins J. (1993). *Nature*, **365**, 349–352.

Kannan P, Yu Y, Wankhade S and Tainsky M. (1999). *Nucl. Acids Res.*, **27**, 866–874.

Meisterernst M, Stelzer G and Roeder R. (1997). *Proc. Natl. Acad. Sci. USA*, **94**, 2261–2265.

Miyazawa H, Izumi M, Tada S, Takada R, Masutani M, Ui M and Hanaoka F. (1993). *J. Biol. Chem.*, **268**, 8111–8122.

Neuman E, Flemington E, Sellers W and Kaelin W. (1994). *Mol. Cell Biol.*, **14**, 6607–6615.

Nevins J. (1992). *Science*, **258**, 424–429.

Pearson B, Nasheuer H and Wang T. (1991). *Mol. Cell Biol.*, **11**, 2081–2095.

Qin X, Livingston D, Kaelin W and Adams P. (1994). *Proc. Natl. Acad. Sci. USA*, **91**, 10918–10922.

Rawling J and Alvarez-Gonzalez R. (1997). *Biochem J.*, **324**, 249–253.

Rosenthal DS, Shima TB, Celli G, De Luca LM and Smulson ME. (1995). *J. Invest. Dermatol.*, **105**, 38–44.

Shieh WM, Ame JC, Wilson M, Wang ZQ, Koh D, Jacobson M and Jacobson E. (1998). *J. Biol. Chem.*, **273**, 30069–30072.

Simbulan C, Suzuki M, Izuta S, Sakurai T, Savoysky E, Kojima K, Miyahara K, Shizuta Y and Yoshida S. (1993). *J. Biol. Chem.*, **268**, 93–99.

Simbulan-Rosenthal CM, Rosenthal DS, Boulares AH, Hickey RJ, Malkas LH, Coll JM and Smulson ME. (1998a). *Biochemistry*, **37**, 9363–9370.

Simbulan-Rosenthal CM, Rosenthal DS, Iyer S, Boulares AH and Smulson ME. (1998b). *J. Biol. Chem.*, **273**, 13703–13712.

Simbulan-Rosenthal CMG, Rosenthal DS, Hilz H, Hickey R, Malkas L, Applegren N, Wu Y, Bers G and Smulson M. (1996). *Biochemistry*, **35**, 11622–11633.

Slansky J, Li Y, Kaelin W and Farnham P. (1993). *Mol. Cell Biol.*, **13**, 1610–1618.

Smulson ME, Kang VH, Ntambi JM, Rosenthal DS, Ding R and Simbulan CMG. (1995). *J. Biol. Chem.*, **270**, 119–127.

Sukhorukov V, Djuzenova C, Arnold W and Zimmermann U. (1994). *J. Membrane Biol.*, **142**, 77–92.

Tom T, Hickey R and Malkas L. (1996). *J. Cell. Biochem.*, **63**, 259–267.

Vindelov LL, Christensen IJ and Nissen NI. (1983). *Cytometry*, **3**, 323–327.

Waga S and Stillman B. (1994). *Nature*, **369**, 207–212.

Wang ZQ, Auer B, Stingl L, Berghammer H, Haidacher D, Schweiger M and Wagner EF. (1995). *Genes Dev.*, **9**, 509–520.

Weinberg R. (1995). *Cell*, **81**, 323–330.

Wong S, Paborsky L, Fisher P, Wang TS-F and Korn D. (1986). *J. Biol. Chem.*, **261**, 7958–7968.

Poly(ADP-ribosyl)ation of p53 during Apoptosis in Human Osteosarcoma Cells[1]

Cynthia M. Simbulan-Rosenthal, Dean S. Rosenthal, RuiBai Luo, and Mark E. Smulson[2]

Department of Biochemistry and Molecular Biology, Georgetown University School of Medicine, Washington, DC 20007

ABSTRACT

Spontaneous apoptosis in human osteosarcoma cells was observed to be associated with a marked increase in the intracellular abundance of p53. Immunoprecipitation and immunoblot analysis revealed that, together with a variety of other nuclear proteins, p53 undergoes extensive poly-(ADP-ribosyl)ation early during the apoptotic program in these cells. Subsequent degradation of poly(ADP-ribose) (PAR), attached to p53 presumably by PAR glycohydrolase, the only reported enzyme to degrade PAR, was apparent concomitant with the onset of proteolytic processing and activation of caspase-3, caspase-3-mediated cleavage of poly(ADP-ribose) polymerase (PARP), and internucleosomal DNA fragmentation during the later stages of cell death. The decrease in PAR covalently bound to p53 also coincided with the marked induction of expression of the p53-responsive genes *bax* and *Fas*. These results suggest that poly-(ADP-ribosyl)ation may play a role in the regulation of p53 function and implies a regulatory role for PARP and/or PAR early in apoptosis.

INTRODUCTION

p53, a tumor suppressor nuclear phosphoprotein, reduces the occurrence of mutations by mediating cell cycle arrest in G_1 or G_2-M or inducing apoptosis in cells that have accumulated substantial DNA damage, thus, preventing progression of cells through S phase before DNA repair is complete (1–3). One of the earliest nuclear events that follows DNA strand breakage during DNA repair in response to agents such as γ-irradiation, carcinogens, or alkylating agents is the poly(ADP-ribosyl)ation of various proteins that are localized near DNA strand breaks. PARP[3] catalyzes the poly(ADP-ribosyl)ation of nuclear proteins only when bound to single- or double-stranded DNA ends (4–6) and cycles on and off the DNA ends during DNA repair *in vitro* (7–10). In addition to undergoing automodification, PARP catalyzes the poly(ADP-ribosyl)ation of such nuclear proteins as histones, topoisomerases I and II (11, 12), SV40 large T antigen (13), DNA polymerase α, proliferating cell nuclear antigen, and ~15 protein components of the DNA synthesome (12). The modification of nucleosomal proteins also alters the nucleosomal structure of the DNA containing strand breaks and promotes access of various replicative and repair enzymes to these sites (14, 15).

Additionally, depletion of PARP by antisense RNA expression has indicated that poly(ADP-ribosyl)ation plays an auxiliary role in the repair of DNA strand breaks (16, 17), in preferential gene repair (18), in the survival of cells after exposure to various alkylating agents, in gene amplification (19), in differentiation-linked DNA replication (12, 20, 40), and recently, in an early stage of apoptosis (21). Given that PARP is only catalytically active when bound to DNA strand breaks, when PARP undergoes caspase-3-mediated cleavage into M_r 89,000 and M_r 24,000 fragments during drug-induced (22) or spontaneous (23, 24) apoptosis,

separation of its DNA binding domain from its catalytic site essentially inactivates the enzyme. PARP has also been implicated in the induction of p53 expression during apoptosis (25). The specific proteolytic cleavage of PARP by caspase-3 is a key apoptotic event because PARP cleavage and inactivation as well as subsequent apoptotic events are blocked by a peptide inhibitor of this protease (23, 26).

We have shown recently that a transient poly(ADP-ribosyl)ation of nuclear proteins in intact human osteosarcoma cells occurs early in apoptosis, prior to commitment to cell death, and is subsequently followed by cleavage and inactivation of PARP (24). No PAR is synthesized at the later stages of apoptosis, despite the presence of a large number of DNA strand breaks at this time. By depleting 3T3-L1 and Jurkat T cells of PARP by antisense RNA expression, or with the use of immortalized fibroblasts derived from PARP knockout (PARP−/−) mice, we demonstrated that prevention of this early activation of PARP blocks various biochemical and morphological changes associated with apoptosis (21), thus correlating the early poly(ADP-ribosyl)ation with later events in the cell death cascade.

p53 is induced by a variety of apoptotic stimuli and is required for apoptosis in many cell systems (27); overexpression of p53 is sufficient to induce apoptosis in various cell types (28). Interestingly, p53 can use transcription activation of target genes and/or direct protein-protein interaction to initiate p53-dependent apoptosis. It was shown recently that p53 is poly(ADP-ribosyl)ated *in vitro* by purified PARP, and that binding of p53 to a specific p53 consensus sequence prevents its covalent modification (29). We now show for the first time that modification of p53 by poly(ADP-ribosyl)ation also occurs *in vivo*, and that it represents one of the early acceptors of poly(ADP-ribosyl)ation during apoptosis in human osteosarcoma cells. Given that the *in vivo* half-life of PAR chains on an acceptor has been estimated to be about 1–2 min, we have additionally explored how this posttranslational modification of p53 is altered at the onset of caspase-3-mediated cleavage and inactivation of PARP during the later stages of the death program.

MATERIALS AND METHODS

Cell Culture and Induction of Apoptosis. Human osteosarcoma cells (23, 24) were cultured in DMEM supplemented with 10% fetal bovine serum, penicillin (100 U/ml), and streptomycin (100 μg/ml). Cell cultures were maintained as exponentially growing cells in a humidified 5% CO_2 incubator. Spontaneous apoptosis was induced by allowing the cells to grow for 10 days without any medium changes, as described previously (23, 24).

Immunoprecipitation and Immunoblot Analysis. For immunoblot analysis, SDS-PAGE and transfer of proteins (30 μg/lane) to nitrocellulose membranes were performed according to standard procedures. The membranes were stained with Ponceau S (0.5%) to confirm equal loading and transfer. Membranes were then incubated with polyclonal antibodie ›CPP32 (1:5000 dilution; a gift from Dr. D. Nicholson, Merck), to PARP (1:5000 dilution; BioMol), to Fas (1:200 dilution; Santa Cruz Biotechnology), or to Bax (1:100 dilution; Calbiochem) and to mAbs to human p53 (Ab-5; 1:10 dilution; Calbiochem) or to PAR (1:250 dilution; Ref. 30). The anti-p53 antibody recognizes wild-type but not mutant p53. The membranes were subsequently probed with appropriate peroxidase-labeled antibodies (1:3000 dilution), and immune complexes were detected by enhanced chemiluminescence (Pierce).

Immunoprecipitation was performed with another monoclonal antibody to p53 (Ab-1; Calbiochem), according to procedures described previously (31). Briefly, equal amounts of cell extracts (10 μg) were precleared overnight at 4°C with 200 μl of EBC buffer [50 mM Tris-HCl (pH 8.0), 120 mM NaCl, 0.5% NP40, and 0.1 TIU/ml aprotinin] and 10 μl of protein A-Sepharose beads

(Pharmacia). After centrifugation, the supernatants were then incubated for 1 h with 0.5 ml of NET-N buffer [20 mM Tris-HCl (pH 8.0), 100 mM NaCl, 1 mM EDTA, and 0.5% NP40] containing the anti-p53 mAb (2 μg/ml). The samples were then incubated for an additional 20 min with 20 μl of a 1:1 suspension of protein A-Sepharose beads in Tris-buffered saline containing 10% BSA. The beads were washed five times with NET-N buffer, and the proteins bound to the beads were then separated by SDS-PAGE, transferred to nitrocellulose, and subjected to immunoblot analysis with the mAb to PAR or sheep poly-clonal antibodies to p53 (Calbiochem).

PARP-Cleavage Assay *in Vitro*. PARP-cleavage assays were performed as described previously (23, 24). Full-length PARP cDNA pCD-12 (32) was used to synthesize [^{35}S]methionine-labeled PARP by T7 RNA polymerase-mediated transcription and translation in a reticulocyte lysate system (Promega). Cytosolic extracts were prepared, and PARP-cleavage activity was measured in 25-μl reaction mixtures containing 5 μg of cytosolic protein, [^{35}S]PARP ($\sim$5 $\times$ 10^4 cpm), 50 mM PIPES-KOH (pH 6.5), 2 mM EDTA, 0.1% 3-[(3-cholamidopropyl)dimethylammonio]-1-propanesulfonate, and 5 mM DTT. After incubation for 1 h at 37°C, reactions were terminated by the addition of SDS sample buffer, and PARP-cleavage products were detected by SDS-PAGE and fluorography.

Detection of Apoptotic Internucleosomal DNA Fragmentation. Total genomic DNA was extracted by lysing cells in 7 M guanidine hydrochloride and purified using a Wizard Miniprep Purification Resin (Promega). Apoptotic internucleosomal DNA fragmentation was then detected by gel electrophoresis (1% agarose) and ethidium bromide staining, as described previously (33).

RESULTS

Induction of Biochemical Markers of Apoptosis during Spontaneous Apoptosis in Human Osteosarcoma Cells. A transient burst of poly(ADP-ribosyl)ation of nuclear proteins occurs early during apoptosis in a number of different cell lines (21, 24, 34). Because rapid accumulation of p53 also occurs early during apoptosis (28, 35), we wanted to investigate whether p53 is one of the poly(ADP-ribosyl)ated proteins during the early burst of PARP activity. Human osteosarcoma cells were plated under conditions that result in spontaneous apoptosis over a 10-day period (23, 24). Biochemical markers of apoptosis were initially observed at day 5 and maximized around days 7–9, including caspase-3-mediated *in vitro* PARP-cleavage activity (Fig. 1A), proteolytic processing of the caspase-3 proenzyme (CPP32) to its active form (p17; Fig. 1B), and internucleosomal DNA fragmentation (Fig. 1C). During apoptosis, PARP is primarily cleaved by caspase-3 (23, 26), a member of the caspase family of aspartate-specific cysteine proteases that play a central role in the execution of the death program (36).

p53 Accumulation, *in Vivo* PARP Cleavage, and Poly(ADP-ribosyl)ation of Nuclear Proteins during Spontaneous Apoptosis in Osteosarcoma Cells. Consistent with previous studies showing p53 accumulation during early apoptosis in different cell lines, im-munoblot analysis with anti-p53 mAbs of extracts of osteosarcoma cells at various stages of spontaneous apoptosis revealed that endog-enous levels of p53 protein were significantly increased as early as days 2–3, maximized at day 4, and declined thereafter (Figs. 2A and 3B). Immunoblot analysis with antibodies to PARP to monitor *in vivo* PARP cleavage during the same time frame showed that $\sim$ 50% of endogenous PARP was cleaved to its M_r 89,000 fragment by day 7, and complete cleavage of PARP was noted by day 9 (Fig. 2B).

When the same extracts were subjected to immunoblot analysis with antibodies to PAR, low levels of polymer were observed at day 2 of apoptosis (Fig. 2C), indicating the absence of DNA strand breaks, PARP activity, or both. However, poly(ADP-ribosyl)ation of nuclear proteins was markedly increased at day 3 and was maximal at day 4, a stage at which all of the cells were still viable and could be replated, prior to any evidence of internucleosomal DNA fragmentation. Subsequently, a marked decline in poly(ADP-ribosyl)ation of nuclear proteins was ob-served at later time points (days 7–9), concomitant with the onset of substantial DNA fragmentation, proteolytic activation of caspase-3, and
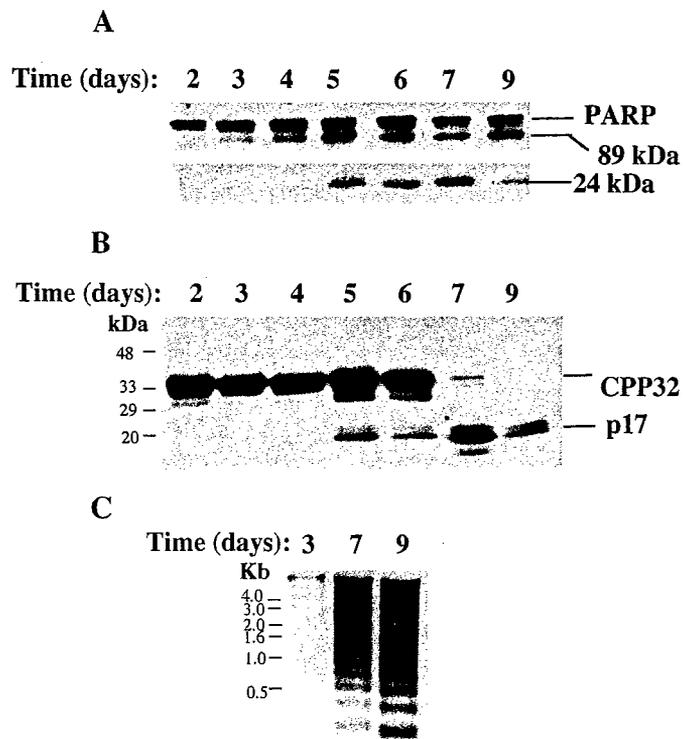

Fig. 1. Time courses of *in vitro* caspase-3 (PARP-cleavage) activity (A), proteolytic activation of CPP32 to its active form (p17; B), and internucleosomal DNA fragmentation (C) during spontaneous apoptosis in human osteosarcoma cells. At the indicated times during spontaneous apoptosis, cytosolic extracts were prepared and assayed for *in vitro* PARP-cleavage activity with [^{35}S]PARP as substrate (A) or subjected to immunoblot analysis with a mAb to the p17 subunit of caspase-3 (B). The positions of full-length PARP and of its M_r 89,000 and M_r 24,000 cleavage products as well as CPP32 and p17 are indicated. C, total genomic DNA was extracted, and internucleosomal DNA ladders characteristic of apoptosis were detected by agarose gel electrophoresis and ethidium bromide staining. The positions of the DNA size standards (in kilobases) are indicated.

caspase-3-mediated *in vitro* and *in vivo* cleavage of PARP. The specific-ity of the anti-PAR antibody used in these experiments has previously been confirmed biochemically in experiments showing that removal of PAR from immunoblots by phosphodiesterase treatment eliminates the polymer signal (12). PAR chains are cleaved from proteins by incubation of immunoblots with phosphodiesterase (37). When HeLa cell extracts were incubated *in vitro* in the presence or absence of NAD, poly(ADP-ribosyl)ated proteins were specifically detected only in the NAD-treated extracts after immunoblot analysis with the antibody to PAR; however, when duplicate lanes of the membrane were incubated with phosphodi-esterase, no immunoreactivity was detected when reprobed with anti-PAR, thus, verifying the specificity of this antibody (12).

Poly(ADP-ribosyl)ation of p53 during Spontaneous Apoptosis in Osteosarcoma Cells as Verified by Immunoprecipitation. Wild-type p53 can be modified by poly(ADP-ribosyl)ation *in vitro* using purified proteins (29). Poly(ADP-ribosyl)ation of nuclear proteins in response to DNA strand breaks is transient *in vivo* and is likely restricted mainly to the pool of potential target proteins located adjacent to DNA breaks (6). For example, <1% of the histone H1 pool is poly(ADP-ribosyl)ated both *in vivo* (38) and *in vitro* (5). Thus, detection of poly(ADP-ribosyl)ated p53 is likely to be difficult in most cell lines because only a small proportion of the available p53 is expected to be poly(ADP-ribosyl)ated *in vivo* at any one time, and the abundance of p53 in cells is normally low.

To confirm if p53 undergoes poly(ADP-ribosyl)ation *in vivo* during apoptosis in human osteosarcoma cells, cell extracts were derived at various times during spontaneous apoptosis and subjected to immuno-precipitation with an anti-p53 mAb. The immunoprecipitated proteins
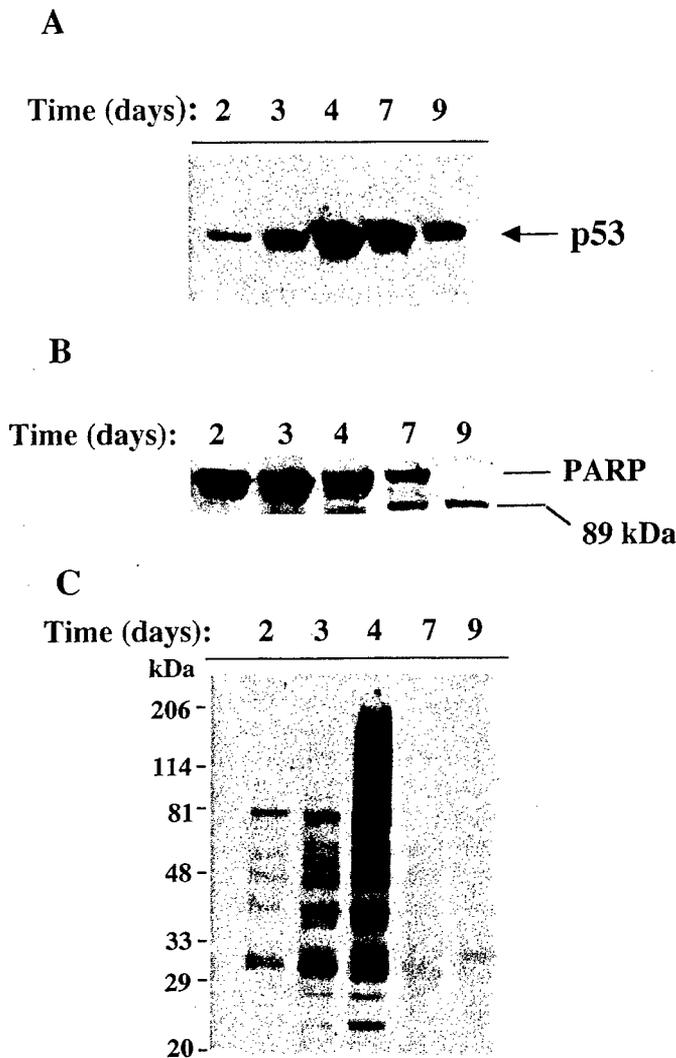
A

Time (days): 2 3 4 7 9

 ← p53

B

Time (days): 2 3 4 7 9

— PARP

89 kDa

C

Time (days): 2 3 4 7 9

kDa
206 –
114 –
81 –
48 –
33 –
29 –
20 –

Fig. 2. Time courses of p53 accumulation (*A*), *in vivo* PARP cleavage (*B*), and poly(ADP-ribosyl)ation of nuclear proteins (*C*) during apoptosis in osteosarcoma cells. At the indicated times of confluence-associated spontaneous apoptosis, cell extracts were prepared, and equal amounts of protein (30 μg) were subjected to immunoblot analysis with mAb to p53 (*A*); membranes were then stripped of antibodies and reprobed with mAbs to PARP (*B*) or to PAR (*C*). The positions of the molecular size standards are indicated in *C*.

(mainly p53 and its binding partners) were then subjected to immunoblot analysis with mAb to PAR. This approach revealed marked poly(ADP-ribosyl)ation of p53 at the early stages of apoptosis (days 3–4; Fig. 3*A*), coincident with the burst of PAR synthesis during this stage (Fig. 2*C*). The extent of poly(ADP-ribosyl)ation of p53 declined concomitant with the onset of both *in vitro* and *in vivo* caspase-3-mediated PARP cleavage (days 5–9; Figs. 1*A* and 2*B*). Reprobing of the blot with polyclonal antibodies to p53 confirmed that the modified protein was indeed p53 (Fig. 3*B*). On the other hand, no nonspecific binding of p53 was apparent when immunoprecipitation was performed with control antibodies (preimmune serum, Fig. 3, *Lanes C*) or with protein A-Sepharose beads alone (Fig. 3, *Lanes B*). The observation that p53 is specifically poly(ADP-ribosylated) during the early stages of spontaneous apoptosis in human osteosarcoma cells suggests that this posttranslational modification may play a role in regulating its function during the early phases of the cell death cascade.

Time Course of Induction of Bax and Fas Expression during Spontaneous Apoptosis in Osteosarcoma Cells. PARP can modulate the catalytic activity of a number of DNA-binding nuclear enzymes by catalyzing their poly(ADP-ribosyl)ation, including DNA polymerases α and

δ (39, 40) and DNA topoisomerases I and II (11, 41, 42). In most instances, poly(ADP-ribosyl)ation inhibits the activity of the modified protein, presumably because of a marked decrease in DNA-binding affinity caused by electrostatic repulsion between DNA and PAR. Thus, posttranslational modification of p53 may also alter DNA binding to specific DNA sequences in the promoters of target genes associated with the induction of p53-mediated apoptosis, such as those encoding Bax, IGF-BP3 (43), or Fas (44). The time course of accumulation and poly(ADP-ribosyl)ation of p53 during the early stages of apoptosis was thus correlated with the induction of expression of the p53-responsive genes *bax* and *Fas*. Immunoblot analysis of extracts of cells at various stages of apoptosis in osteosarcoma cells with antibodies to either Bax or Fas revealed that expression of both Bax and Fas (upper and middle panels, respectively) were negligible before and at the peak of p53 accumulation and poly(ADP-ribosyl)ation (days 3 and 4). Although p53 accumulation was already significantly elevated by day 2 (Fig. 3*B*), expression of Bax and Fas was markedly induced only at day 5 (Fig. 4), concomitant with a decline in PAR attached to p53 and the onset of caspase-3-mediated PARP cleavage and inactivation. The coincident decrease in PAR covalently bound to p53 and induction of Bax and Fas expression suggest that poly(ADP-ribosyl)ation may regulate p53 function early in apoptosis; caspase-3-mediated cleavage of PARP may release p53 from poly(ADP-ribosyl)ation-induced inhibition at the later stages of the apoptotic cascade.

DISCUSSION

Both PARP activity and p53 accumulation are induced by DNA damage, and both proteins have been implicated in the normal cellular
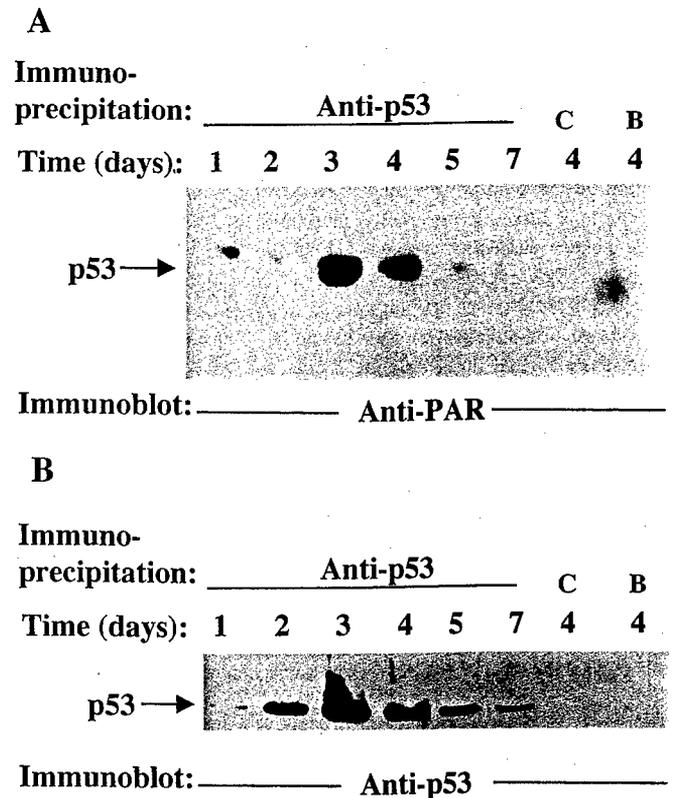
A

Immuno-
precipitation: Anti-p53   C   B
Time (days): 1 2 3 4 5 7 4 4

p53 →

Immunoblot: Anti-PAR

B

Immuno-
precipitation: Anti-p53   C   B
Time (days): 1 2 3 4 5 7 4 4

p53 →

Immunoblot: Anti-p53

Fig. 3. Poly(ADP-ribosyl)ation of p53 during apoptosis in osteosarcoma cells, as confirmed by immunoprecipitation with antibodies to p53. *A*, at the indicated times during spontaneous apoptosis, cell extracts were prepared, and equal amounts of total protein (100 μg) were subjected to immunoprecipitation with a mAb to p53. The immunoprecipitated proteins were then subjected to immunoblot analysis with a mAb to PAR. In control experiments with extracts derived from cells on day 4, immunoprecipitation was performed with control antibodies (*Lane C*, preimmune serum) or with protein A-Sepharose beads (*Lane B*) alone. *B*, the immunoblot shown in *A* was stripped of antibodies by incubation for 30 min at 50°C with a solution containing 100 mM 2-mercaptoethanol, 2% SDS, and 62.5 mM Tris-HCl (pH 6.7) and reprobed with sheep polyclonal antibodies to p53. The position of p53 is indicated.

responses to such damage. Whereas PAR synthesis increases within seconds after induction of DNA strand breaks (45), the amount of wild-type p53, which is usually low because of the short half-life (20 min) of the protein, increases 2–5 h after DNA damage as a result of reduced degradation (46, 47). A functional association of PARP and p53 has recently been suggested by coimmunoprecipitation of each protein *in vitro* by antibodies to the other (48, 49).

Exposure of human cell lines expressing wild-type p53 to various DNA-damaging agents that also stimulate PAR synthesis (including ionizing radiation, bleomycin, and DNA topoisomerase-targeting drugs) results in a rapid increase in the intracellular concentration of p53 (50). Chinese hamster cells that are unable to synthesize PAR because of unavailability of NAD show a marked decrease in baseline p53 concentration and activity, and they fail to exhibit a p53 response and to undergo apoptosis in response to DNA-damaging agents (25). Moreover, compared with wild-type cells, primary fibroblasts from PARP−/− mice express lower constitutive levels of p53 protein and exhibit a defective induction of p53 in response to DNA damage (51), indicating that PARP-dependent signaling may influence the synthesis or degradation of p53 in response to DNA damage.

In human osteosarcoma cells undergoing spontaneous apoptosis, a transient burst of poly(ADP-ribosyl)ation of nuclear proteins occurs early and is followed by caspase-3-mediated cleavage of PARP (24). Such an early burst of poly(ADP-ribosyl)ation was also observed in human HL-60 and Jurkat T cells, mouse 3T3-L1 cells, and immortalized fibroblasts derived from wild-type mice undergoing Fas-mediated or camptothecin-induced apoptosis (21). The substantial nuclear poly(ADP-ribosyl)ation early in the death program suggests a potential role for PAR synthesis at this reversible stage in apoptosis, and it is consistent with the presence of large (~1 Mb) chromatin fragments at this time (52), given that the catalytic activation of PARP is absolutely dependent on DNA strand breaks. We recently investigated the effects of preventing this early transient modification of nuclear proteins by depletion of PARP either by antisense RNA expression or by gene disruption on various morphological and biochemical markers of apoptosis (21). Whereas control mouse fibroblasts or Jurkat T cells exhibit proteolytic conversion of the CPP32 proenzyme to caspase-3, caspase-3 (PARP-cleavage) activity, internucleosomal DNA fragmentation, and characteristic nuclear morphological changes on induction of apoptosis, cells depleted of PARP by antisense RNA expression did not (21). Similar results were obtained with control and PARP-depleted human osteosarcoma antisense cells induced into apoptosis with staurosporine (data not shown).

Furthermore, whereas immortalized fibroblasts derived from wild-type (PARP+/+) mice show the early burst of poly(ADP-ribosyl)ation and a rapid apoptotic response when induced into Fas-mediated apoptosis,

fibroblasts derived from PARP−/− mice exhibit neither the early poly-(ADP-ribosyl)ation nor any of the biochemical or morphological changes characteristic of apoptosis when similarly treated (21). Stable transfection of PARP−/− fibroblasts with wild-type PARP cDNA sensitizes these cells to Fas-mediated apoptosis, suggesting that PARP and poly(ADP-ribosyl)ation may play an essential role in the early stages of apoptosis.

Accordingly, p53 may represent a potentially relevant target for poly-(ADP-ribosyl)ation during the burst of PAR synthesis at the early periods of apoptosis (Fig. 2C). Colocalization of PARP and p53 in the vicinity of large DNA breaks and their physical association (48, 49) suggest that poly(ADP-ribosyl)ation may regulate the DNA binding ability and, consequently, the function of p53. We have now shown that spontaneous apoptosis in osteosarcoma cells is associated with a marked increase in the intracellular p53 concentration early in the death program (Figs. 2A and 3B). This accumulation of p53 may be due to induced expression of the protein by the apoptotic stimuli or stabilization by inhibition of p53 degradation via modification of the protein. Furthermore, immunoprecipitation experiments revealed that p53 undergoes extensive poly(ADP-ribosyl)ation (Fig. 3) during the transient burst of PAR synthesis at the early stages of apoptosis; this occurs at a reversible stage when cells are still viable. This is the first report of poly(ADP-ribosyl)ation of p53 *in vivo* and suggests a negative regulatory role for PARP and/or PAR early in apoptosis. Subsequent degradation of PAR attached to p53 coincided with the increase in caspase-3 (PARP-cleavage) activity as well as the induction of expression of the p53-responsive genes *bax* and *Fas* at a stage when cells are irreversibly committed to death. Although the mechanism(s) of action of the Bax/Bcl$_2$ family of gene products during apoptosis remains to be clarified, induction of Bax expression may influence the decision to commit to apoptosis because homodimerization of Bax promotes cell death, and heterodimerization of Bax with Bcl$_2$ inhibits the antiapoptotic function of Bcl$_2$ (43). Wild-type p53, but not mutant p53, also up-regulates Fas expression during chemotherapy-induced apoptosis, and p53-responsive elements were identified recently within the first intron and the promoter of the *Fas* gene (44). Binding of Fas to Fas ligand recruits the adapter molecule FADD via shared protein motifs (death domains), resulting in subsequent activation of the caspase cascade leading to apoptosis.

Electrophoretic mobility-shift analysis has shown that PAR attached to p53 *in vitro* can block its sequence-specific binding to the palindromic p53 consensus sequence, suggesting that poly(ADP-ribosyl)ation of p53 may regulate p53-mediated transcriptional activation of genes important in the cell cycle and apoptosis (53). PARP cycles on and off DNA ends in the presence of NAD, and its automodification during DNA repair *in vitro* presumably allows access to DNA repair enzymes (7–9). Our results with *in vivo* poly(ADP-ribosyl)ation of p53 suggest that p53 may, similarly, cycle on and off its DNA consensus sequence, depending on its level of negative charge based on its poly(ADP-ribosyl)ation state. This may represent a mechanism for regulating transcriptional activation of *bax* and *Fas* by p53 during apoptosis. Alternatively, a polymer binding site in p53 has been localized near a proteolytic cleavage site (53), indicating that PAR binding could protect this sequence from proteolysis; similar protection has been noted after binding of monoclonal antibodies adjacent to this region (54). The significant poly(ADP-ribosyl)ation of p53 early in apoptosis, therefore, suggests that this posttranslational modification could also play a role in p53 up-regulation by protecting the protein from proteolytic degradation.

Time (days): 2 3 4 5 6 7 8 9

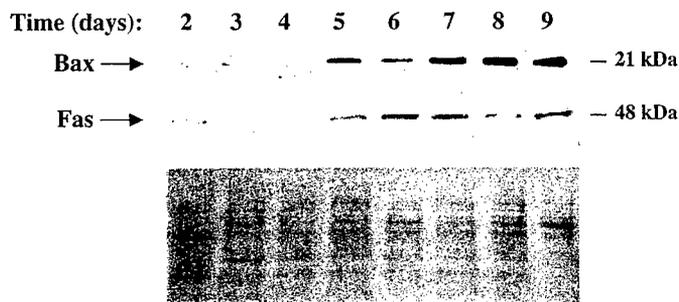Bax ⟶ — 21 kDa

Fas ⟶ — 48 kDa

Fig. 4. Time courses of Bax and Fas expression during spontaneous apoptosis in human osteosarcoma cells. At the indicated times during spontaneous apoptosis, cell extracts were prepared, and equal amounts of protein (30 μg) were subjected to immunoblot analysis with mAbs to Bax (*upper panel*). The immunoblot shown in the *upper panel* was stripped of antibodies and reprobed with antibodies to Fas (*middle panel*). The positions of Bax and Fas are indicated. Ponceau S staining of the same immunoblot was performed to confirm equal protein loading and transfer among the lanes (*lower panel*).

REFERENCES

1. Kastan. M. B.. Zhan. Q.. El-Delry. W. S.. Carrier. F.. Jacks. T.. Walsh. W. V.. Plunkett. B. S.. Vogelstein. B.. and Fornace. A. J. J. A mammalian cell cycle checkpoint pathway utilizing p53 and *GADD45* is defective in ataxia-telangiectasia. Cell. *71:* 587–597. 1992.

2. O'Connor. P. M.. Jackman. J.. Jondle. D.. Bhatia. K.. Magrath. I.. and Kohn. K. W. Role of the p53 tumor suppressor gene in cell cycle arrest and radiosensitivity of Burkitt's lymphoma cell lines. Cancer Res.. *53:* 4776–4780. 1993.

3. Levine. A. p53. the cellular gatekeeper for growth and division. Cell. *88:* 323–331. 1997.

4. Gradwohl. G.. Menissier de-Murcia. J. M.. Molinete. M.. Simonin. F.. Koken. M.. Hoeijmakers. J. H.. and de Murcia. G. The second zinc-finger domain of poly (ADP-ribose) polymerase determines specificity for single-stranded breaks in DNA. Proc. Natl. Acad. Sci. USA. *87:* 2990–2994. 1990.

5. Malik. N.. Miwa. M.. Sugimura. T.. Thraves. P.. and Smulson. M. Immunoaffinity fractionation of the poly(ADP-ribosyl)ated domains of chromatin. Proc. Natl. Acad. Sci. USA. *80:* 2554–2558. 1983.

6. Thraves. P. J.. Kasid. U.. and Smulson. M. E. Selective isolation of domains of chromatin proximal to both carcinogen-induced DNA damage and poly(ADP-ribosyl)ation. Cancer Res.. *45:* 386–391. 1985.

7. Satoh. M. S.. and Lindahl. T. Role of poly(ADP-ribose) formation in DNA repair. Nature (Lond.). *356:* 356–358. 1992.

8. Satoh. M. S.. Poirier. G. G.. and Lindahl. T. NAD$^+$-dependent repair of damaged DNA by human cell extracts. J. Biol. Chem.. *268:* 5480–5487. 1993.

9. Smulson. M.. Istock. N.. Ding. R.. and Cherney. B. Deletion mutants of poly(ADP-ribose) polymerase support a model of cyclic association and dissociation of enzyme from DNA ends during DNA repair. Biochemistry. *33:* 6186–6191. 1994.

10. Smulson. M. E.. Pang. D.. Jung. M.. Dimtchev. A.. Chasovskikh. S.. Spoonde. A.. Simbulan-Rosenthal. C.. Rosenthal. D.. Yakovlev. A.. and Dritschilo. A. Irreversible binding of poly(ADP-ribose) polymerase cleavage product to DNA ends revealed by atomic force microscopy: possible role in apoptosis. Cancer Res.. *58:* 3495–3498. 1998.

11. Kasid. U. N.. Halligan. B.. Liu. L. F.. Dritschilo. A.. and Smulson. M. Poly(ADP-ribose)-mediated post-translational modification of chromatin-associated human topoisomerase I. Inhibitory effects on catalytic activity. J. Biol. Chem.. *264:* 18687–18692. 1989.

12. Simbulan-Rosenthal. C. M. G.. Rosenthal. D. S.. Hilz. H.. Hickey. R.. Malkas. L.. Applegren. N.. Wu. Y.. Bers. G.. and Smulson. M. The expression of poly(ADP-ribose) polymerase during differentiation-linked DNA replication reveals that this enzyme is a component of the multiprotein DNA replication complex. Biochemistry. *35:* 11622–11633. 1996.

13. Baksi. K.. Alkhatib. H.. and Smulson. M. E. *In vivo* characterization of the poly (ADP-ribosyl)ation of SV40 chromatin and large T antigen by immunofractionation. Exp. Cell Res.. *172:* 110–123. 1987.

14. Poirier. G. G.. de Murcia. G.. Jongstra-Bilen. J.. Niedergang. C.. and Mandel. P. Poly(ADP-ribosyl)ation of polynucleosomes causes relaxation of chromatin structure. Proc. Natl. Acad. Sci. USA. *79:* 3423–3427. 1982.

15. Butt. T. R.. DeCoste. B.. Jump. D.. Nolan. N.. and Smulson. M. E. Characterization of a putative poly adenosine diphosphate ribose chromatin complex. Biochemistry. *19:* 5243–5249. 1980.

16. Ding. R.. Pommier. Y.. Kang. V. H.. and Smulson. M. Depletion of poly(ADP-ribose) polymerase by antisense RNA expression results in a delay in DNA strand break rejoining. J. Biol. Chem.. *267:* 12804–12812. 1992.

17. Rosenthal. D. S.. Shima. T. B.. Celli. G.. De Luca. L. M.. and Smulson. M. E. An engineered human skin model using poly(ADP-ribose) polymerase antisense expression shows a reduced response to DNA damage. J. Invest. Dermatol.. *105:* 38–44. 1995.

18. Stevnsner. T.. Ding. R.. Smulson. M.. and Bohr. V. A. Inhibition of gene-specific repair of alkylation damage in cells depleted of poly(ADP-ribose) polymerase. Nucleic Acids Res.. *22:* 4620–4624. 1994.

19. Ding. R.. and Smulson. M. Depletion of nuclear poly(ADP-ribose) polymerase by antisense RNA expression: influences on genomic stability. chromatin organization and carcinogen cytotoxicity. Cancer Res.. *54:* 4627–4634. 1994.

20. Smulson. M. E.. Kang. V. H.. Ntambi. J. M.. Rosenthal. D. S.. Ding. R.. and Simbulan. C. M. G. Requirement for the expression of poly(ADP-ribose) polymerase during the early stages of differentiation of 3T3-L1 preadipocytes. as studied by antisense RNA induction. J. Biol. Chem.. *270:* 119–127. 1995.

21. Simbulan-Rosenthal. C. M.. Rosenthal. D. S.. Iyer. S.. Boulares. A. H.. and Smulson. M. E. Transient poly(ADP-ribosyl)ation of nuclear proteins and role for poly(ADP-ribose) polymerase in the early stages of apoptosis. J. Biol. Chem.. *273:* 13703–13712. 1998.

22. Kaufmann. S. H.. Desnoyers. S.. Ottaviano. Y.. Davidson. N. E.. and Poirier. G. G. Specific proteolytic cleavage of poly(ADP-ribose)polymerase: an early marker of chemotherapy-induced apoptosis. Cancer Res.. *53:* 3976–3985. 1993.

23. Nicholson. D. W.. Ali. A.. Thornberry. N. A.. Vaillancourt. J. P.. Ding. C. K.. Gallant. M.. Gareau. Y.. Griffin. P. R.. Labelle. M.. Lazebnik. Y. A.. Munday. N. A.. Raju. S. M.. Smulson. M. E.. Yamin. T. T.. Yu. V. L.. and Miller. D. K. Identification and inhibition of the ICE/CED-3 protease necessary for mammalian apoptosis. Nature (Lond.). *376:* 37–43. 1995.

24. Rosenthal. D. S.. Ding. R.. Simbulan-Rosenthal. C. M. G.. Vaillancourt. J. P.. Nicholson. D. W.. and Smulson. M. E. Intact cell evidence for the early synthesis. and subsequent late apopain-mediated suppression. of poly(ADP-ribose) during apoptosis. Exp. Cell Res.. *232:* 313–321. 1997.

25. Whitacre. C. M.. Hashimoto. H.. Tsai. M-L.. Chatterjee. S.. Berger. S. J.. and Berger. N. A. Involvement of NAD-poly(ADP-ribose) metabolism in p53 regulation and its consequences. Cancer Res.. *55:* 3697–3701. 1995.

26. Tewari. M.. Quan. L. T.. O'Rourke. K.. Desnoyers. S.. Zeng. Z.. Beidler. D. R.. Poirier. G. G.. Salvesen. G. S.. and Dixit. V. M. Yama/CPP32b. a mammalian

27. homolog of CED-3. is a crmA-inhibitable protease that cleaves the death substrate poly(ADP-ribose) polymerase. Cell. *81:* 801–809. 1995.

27. Fisher. D. Apoptosis in cancer therapy: crossing the threshold. Cell. *78:* 539–542. 1994.

28. Yonish-Rouach. E.. Resnitzky. D.. Lotem. J.. Sachs. L.. Kimchi. A.. and Oren. M. Wild-type p53 induces apoptosis of myeloid leukaemic cells that is inhibited by interleukin-6. Nature (Lond.). *352:* 345–347. 1991.

29. Wesierska-Gadek. J.. Schmid. G.. and Cerni. C. ADP-ribosylation of wild-type p53 *in vitro*: binding of p53 protein to specific p53 consensus sequence prevents its modification. Biochem. Biophys. Res. Commun.. *224:* 96–102. 1996.

30. Kawamitsu. H.. Hoshino. H.. Okada. H.. Miwa. M.. Momoi. H.. and Sugimura. T. Monoclonal antibodies to poly(adenosine diphosphate ribose) recognize different structures. Biochemistry. *23:* 3771–3777. 1984.

31. Simbulan. C.. Suzuki. M.. Izuta. S.. Sakurai. T.. Savoysky. E.. Kojima. K.. Miyahara. K.. Shizuta. Y.. and Yoshida. S. Poly(ADP-ribose) polymerase stimulates DNA polymerase α. J. Biol. Chem.. *268:* 93–99. 1993.

32. Alkhatib. H. M.. Chen. D. F.. Cherney. B.. Bhatia. K.. Notario. V.. Giri. C.. Stein. G.. Slattery. E.. Roeder. R. G.. and Smulson. M. E. Cloning and expression of cDNA for human poly(ADP-ribose) polymerase. Proc. Natl. Acad. Sci. USA. *84:* 1224–1228. 1987.

33. Eldadah. B.. Yakovlev. A.. and Faden. A. A new approach for the electrophoretic detection of apoptosis. Nucleic Acids Res.. *24:* 4092–4093. 1996.

34. Simbulan-Rosenthal. C. M.. Rosenthal. D. S.. Iyer. S.. Boulares. H.. and Smulson. M. E. Involvement of PARP and poly(ADP-ribosyl)ation in the early stages of apoptosis and DNA replication. Mol. Cell. Biochem.. in press. 1999.

35. Lowe. S. W.. Ruley. H. E.. Jacks. T.. and Housman. D. E. p53-dependent apoptosis modulates the cytotoxicity of anticancer agents. Cell. *74:* 957–967. 1993.

36. Alnemri. E.. Livingston. D.. Nicholson. D.. Salvesen. G.. Thornberry. N.. Wong. W.. and Yuan. J. Human ICE/CED-3 protease nomenclature. Cell. *87:* 171. 1996.

37. Adamietz. P. Poly(ADP-ribose) synthase is the major endogenous nonhistone acceptor for poly(ADP-ribose) in alkylated rat hepatoma cells. Eur. J. Biochem.. *169:* 365–372. 1987.

38. Wong. M.. Miwa. M.. Sugimura. T.. and Smulson. M. Relationship between histone H1 poly(adenosine diphosphate ribosylation) and histone H1 phosphorylation using anti-poly(adenosine diphosphate ribose) antibody. Biochemistry. *22:* 2384–2389. 1983.

39. Yoshihara. K.. Itaya. A.. Tanaka. Y.. Ohashi. Y.. Ito. K.. Teraoka. H.. Tsukada. K.. Matsukage. A.. and Kamiya. T. Inhibition of DNA polymerase α. DNA polymerase β. terminal nucleotidyltransferase and DNA ligase II by poly (ADP-ribosyl)ation reaction *in vitro*. Biochem. Biophys. Res. Commun.. *128:* 61–67. 1985.

40. Simbulan-Rosenthal. C. M.. Rosenthal. D. S.. Boulares. A. H.. Hickey. R. J.. Malkas. L. H.. Coll. J. M.. and Smulson. M. E. Regulation of the expression or recruitment of components of the DNA synthesome by poly(ADP-ribose) polymerase. Biochemistry. *37:* 9363–9370. 1998.

41. Ferro. A. M.. and Olivera. B. M. Poly (ADP-ribosylation) of DNA topoisomerase I from calf thymus. J. Biol. Chem.. *259:* 547–554. 1984.

42. Darby. M. K.. Schmitt. B.. Jongstra. B. J.. and Vosberg. H. P. Inhibition of calf thymus type II DNA topoisomerase by poly(ADP-ribosylation). EMBO J.. *4:* 2129–2134. 1985.

43. Chinnaiyan. A.. Orth. K.. O'Rourke. K.. Duan. H.. Poirier. G.. and Dixit. V. Molecular ordering of the cell death pathway. Bcl-2 and Bcl-xL function upstream of the CED-3-like apoptotic proteases. J. Biol. Chem.. *271:* 4573–4576. 1996.

44. Muller. M.. Wilder. S.. Bannasch. D.. Israeli. D.. Lelbach. K.. Li-Weber. M.. Friedman. S.. Galle. P.. Stremmel. W.. Oren. M.. and Krammer. P. p53 activates the *CD95 (APO-1/Fas)* gene in response to DNA damage by anticancer agents. J. Exp. Med.. *188:* 2033–2045. 1998.

45. Berger. N. A.. and Petzold. S. J. Identification of the requirements of DNA for activation of poly (ADP-ribose) polymerase. Biochemistry. *24:* 4352–4355. 1985.

46. Fritsche. M.. Haessler. C.. and Brandner. G. Induction of nuclear accumulation of the tumor suppressor protein by p53 by DNA damaging agents. Oncogene. *8:* 307–318. 1993.

47. Kastan. M. B.. Onyekwere. O.. Sidransky. D.. Vogelstein. B.. and Craig. R. W. Participation of p53 protein in the cellular response to DNA damage. Cancer Res.. *51:* 6304–6311. 1991.

48. Vaziri. H.. West. M.. Allsop. R.. Davison. T.. Wu. Y.. Arrowsmith. C.. Poirier. G.. and Benchimol. S. ATM-dependent telomere loss in aging human diploid fibroblasts and DNA damage lead to the posttranslational activation of p53 protein involving poly(ADP-ribose) polymerase. EMBO J.. *16:* 6018–6033. 1997.

49. Wesierska-Gadek. J.. Bugajska-Schretter. A.. and Cerni. C. ADP-ribosylation of p53 tumor suppressor protein: mutant but not wild-type p53 is modified. J. Cell. Biochem.. *62:* 90–101. 1996.

50. Nelson. W. G.. and Kastan. M. B. DNA strand breaks: the DNA template alterations that trigger p53-dependent DNA damage response pathways. Mol. Cell. Biol.. *14:* 1815–1823. 1994.

51. Agarwal. M.. Agarwal. A.. Taylor. W.. Wang. Z. Q.. and Wagner. E. Defective induction but normal activation and function of p53 in mouse cells lacking PARP. Oncogene. *15:* 1035–1041. 1997.

52. Neamati. N.. Fernandez. A.. Wright. S.. Kiefer. J.. and McConkey. D. J. Degradation of lamin B1 precedes oligonucleosomal DNA fragmentation in apoptotic thymocytes and isolated thymocyte nuclei. J. Immunol.. *154:* 3788–3795. 1995.

53. Malanga. M.. Pleschke. J.. Kleczkowska. H.. and Althaus. F. Poly(ADP-ribose) binds to specific domains of p53 and alters its DNA binding functions. J. Biol. Chem.. *273:* 11839–11843. 1998.

54. Li. X.. and Coffino. P. Identification of a region of p53 that confers lability. J. Biol. Chem.. *271:* 4447–4451. 1996.

Chromosomal aberrations in PARP$^{-/-}$ mice: Genome stabilization in immortalized cells by reintroduction of poly(ADP-ribose) polymerase cDNA

Cynthia M. Simbulan-Rosenthal*†, Bassem R. Haddad†‡, Dean S. Rosenthal*†, Zoë Weaver§, Allen Coleman§, RuiBai Luo*, Hannah M. Young‡, Zhao-Qi Wang¶, Thomas Ried§, and Mark E. Smulson*‖

*Department of Biochemistry and Molecular Biology and the ‡Institute for Molecular and Human Genetics and Departments of Oncology and Obstetrics and Gynecology, Georgetown University School of Medicine, 3900 Reservoir Road NW, Washington, DC 20007; §National Cancer Institute, National Institutes of Health, Bethesda, MD 20892; and ¶International Agency for Research on Cancer, 69372 Lyon, France

Depletion of poly(ADP-ribose) polymerase (PARP) increases the frequency of recombination, gene amplification, sister chromatid exchanges, and micronuclei formation in cells exposed to genotoxic agents, implicating PARP in the maintenance of genomic stability. Flow cytometric analysis now has revealed an unstable tetraploid population in immortalized fibroblasts derived from PARP$^{-/-}$ mice. Comparative genomic hybridization detected partial chromosomal gains in 4C5-ter, 5F-ter, and 14A1-C1 in PARP$^{-/-}$ mice and immortalized PARP$^{-/-}$ fibroblasts. Neither the chromosomal gains nor the tetraploid population were apparent in PARP$^{-/-}$ cells stably transfected with PARP cDNA [PARP$^{-/-}$(+PARP)], indicating negative selection of cells with these genetic aberrations after reintroduction of PARP cDNA. Although the tumor suppressor p53 was not detectable in PARP$^{-/-}$ cells, p53 expression was partially restored in PARP$^{-/-}$(+PARP) cells. Loss of 14D3-ter that encompasses the tumor suppressor gene *Rb-1* in PARP$^{-/-}$ mice was associated with a reduction in retinoblastoma(Rb) expression; increased expression of the oncogene *Jun* was correlated with a gain in 4C5-ter that harbors this oncogene. These results further implicate PARP in the maintenance of genomic stability and suggest that altered expression of p53, Rb, and Jun, as well as undoubtedly many other proteins may be a result of genomic instability associated with PARP deficiency.

Poly(ADP-ribose) polymerase (PARP) is involved in nuclear processes involving cleavage and rejoining of DNA, such as DNA replication, differentiation, DNA repair and recombination, apoptosis, as well as maintenance of genomic stability (1, 2). Inhibition of PARP by either chemical inhibitors (3–5) or by dominant negative mutants (6, 7), or PARP depletion by antisense RNA expression (8, 9), results in an increased frequency of DNA strand breaks, recombination, gene amplification, micronuclei formation, and sister chromatid exchanges (SCE), all of which are markers of genomic instability, in cells exposed to DNA-damaging agents. PARP-deficient cell lines are hypersensitive to carcinogenic agents and also display increased SCE, implicating PARP as a guardian of the genome that facilitates DNA repair and protects against DNA recombination (10). We originally mapped the *PARP* gene to chromosome 1q41-q42 and *PARP*-like sequences to chromosomes 14q13-q32 and 13q34 (11); the latter pseudogene interrupts a *pol*-like element (12) and exhibits two-allele polymorphism (13) associated with predisposition to several cancers (14). Amplification of 1q41-q44 and increased PARP RNA expression are correlated with low genetic instability in human breast carcinomas (15).

PARP$^{-/-}$ mice with a disrupted *PARP* gene do not express any immunodetectable PARP (16, 17). Although a novel activity capable of synthesizing poly(ADP-ribose) (PAR) recently has been shown in PARP$^{-/-}$ mice and cells derived from them, this residual activity, which is induced by DNA strand breaks, is only 5–10% of that in wild-type cells and has not been shown to modify proteins aside from itself; thus, it may not fully compensate for PARP

depletion (18, 19). These mice are resistant to murine models of a number of human diseases, including focal cerebral ischemia (20), toxin-induced diabetes (21), 1-methyl-4-phenyl-1,2,3,6-tetrahydropyridine (MPTP)-induced Parkinsonism (22), and peroxynitrite-induced arthritis (23), suggesting that PARP activation, triggered by oxidative or nitrosative stress, plays a role in the pathophysiology of these diseases. Primary fibroblasts derived from PARP$^{-/-}$ mice show an elevated frequency of SCE and micronuclei in response to treatment with genotoxic agents (16, 24), further implicating PARP in the maintenance of genomic integrity. PARP$^{-/-}$ mice developed by another group exhibit extreme sensitivity to γ-irradiation and methylnitrosourea and increased genomic instability as revealed by a high level of SCE (17). Immortalized cells derived from these mice show retarded cell growth, G$_2$/M block, and chromosomal instability on exposure to DNA-alkylating agents, presumably because of a defect in DNA repair (25).

In the present study, flow cytometry revealed that immortalized fibroblasts derived from PARP$^{-/-}$ mice exhibit mixed ploidy, including a tetraploid cell population, which is also indicative of genomic instability. We characterized the genetic alterations associated with PARP depletion by comparative genomic hybridization (CGH) analysis (26, 27) of genomic DNA from both wild-type and PARP$^{-/-}$ mice as well as from immortalized fibroblasts derived from these animals. With a limit of detection of 5–10 Mb (28), this cytogenetic technique detects unbalanced chromosomal gains and losses in test DNA as a measure of genetic instability. Although CGH now is widely used as a powerful tool for generating maps of DNA copy number changes in human tumor genomes, only two studies to date have demonstrated its potential for evaluating genetic instability in transgenic mouse models (29, 30). CGH analysis revealed partial gains in chromosomes 4, 5, and 14, and partial loss of chromosome 14 in PARP$^{-/-}$ mice or immortalized PARP$^{-/-}$ fibroblasts. We further investigated the effect of stable transfection of PARP$^{-/-}$ cells with PARP cDNA on the genetic instability of these cells. Reintroduction of PARP cDNA into PARP$^{-/-}$ cells appeared to confer stability because the chromosomal gains as well as the unstable tetraploid population were no longer detected in these cells, further supporting an essential role for PARP in the maintenance of genomic stability.

CELL BIOLOGY

Materials and Methods

Cell Lines, Vectors, and Transfection. Homozygous PARP$^{-/-}$ mice that were generated by disrupting exon 2 of the *PARP* gene by homologous recombination (16) and wild-type (PARP$^{+/+}$) littermates (strain 129/Sv × C57BL/6; female) were used in the present study. Wild-type (PARP$^{+/+}$ clone A19) and PARP$^{-/-}$ (clone A1) fibroblasts were immortalized spontaneously by a standard 3T3 protocol (16) and cultured in DMEM supplemented with 10% FBS, penicillin (100 units/ml), and streptomycin (100 μg/ml). Immortalized PARP$^{-/-}$ fibroblasts were cotransfected by Lipofectamine (Life Technologies, Grand Island, NY) with human PARP (pCD12) cDNA (31) and the plasmid pTracer-CMV (a zeocin-based vector system; Invitrogen). This vector was used because the PARP$^{-/-}$ fibroblasts express a neomycin resistance gene that was introduced during establishment of the PARP knockout mice. Stable transfectants were selected in growth medium containing zeocin (500 μg/ml).

Immunoblot Analysis. SDS/PAGE and transfer of proteins to nitrocelluose membranes were performed according to standard procedures. Membranes were stained with Ponceau S (0.5%) to confirm equal loading and transfer of proteins. Membranes were incubated with antibodies to PARP (1:2,000 dilution; BioMol, Plymouth Meeting, PA), PAR (1:250; gift from M. Miwa, Japan), p53 (1:20 dilution; PAb421, Calbiochem), retinoblastoma (Rb) (1:20 dilution; clone IF8, Santa Cruz Biotechnology), glutamate dehydrogenase (1:1,000; Biodesign International, Kennebunkport, ME), Jun (1:1,000 dilution, Calbiochem), proliferating cell nuclear antigen (PCNA) (1:800; Calbiochem), or topoisomerase I (topo I) (1:2,500; TopoGen, Columbus, OH). After subsequent incubation with appropriate horseradish peroxidase-conjugated antibodies to mouse or rabbit IgG (1:3,000 dilution), immune complexes were detected by enhanced chemiluminescence (Pierce).

Flow Cytometry. Nuclei were prepared for flow cytometric analysis as described (33). Cells were exposed to trypsin and resuspended in 100 μl of a solution containing 250 mM sucrose, 40 mM sodium citrate (pH 7.6), and 5% (vol/vol) DMSO. The cells were lysed for 10 min in a solution containing 3.4 mM sodium citrate, 0.1% (vol/vol) NP-40, 1.5 mM spermine tetrahydrochloride, and 0.5 mM Tris·HCl (pH 7.6). After incubation of lysates for 10 min with ribonuclease A (0.1 mg/ml), nuclei were stained for 15 min with propidium iodide (0.42 mg/ml), filtered through a 37-μm nylon mesh, and analyzed with a dual-laser flow cytometer (FACScan, Becton Dickinson).

CGH. Normal DNA was extracted from spleen tissue of normal mice (FVB) and test DNA was prepared from liver tissue of wild-type and PARP$^{-/-}$ mice, as well as from immortalized PARP$^{-/-}$ and PARP$^{-/-}$(+PARP) fibroblasts according to standard protocols. Differences in the source of the DNA (spleen, liver, or cell lines) does not affect CGH results (26, 27). Normal metaphase chromosomes for CGH were prepared from a spleen culture of C57BL/6 mice as described (30). Labeling, hybridization, and detection of DNA were performed as described (30, 34). Normal DNA and test DNA were labeled in a nick-translation reaction in which dTTP was replaced by digoxigenin-11-dUTP (Boehringer Mannheim) (normal DNA) or biotin-16-dUTP (Boehringer Mannheim) (test DNA). A total of 500 ng each of labeled normal and test DNA was precipitated with ethanol in the presence of salmon sperm DNA (3 μg) and excess mouse Cot-1 DNA (50 μg) (GIBCO/BRL), and the precipitates were dried and resuspended in 15 μl of hybridization solution (50% formamide, 2× SSC, 10% dextran sulfate). The DNA was denatured at 80°C for 10 min and allowed to preanneal for 3 h at 37°C. Normal metaphase chromosomes were denatured at 80°C for 2 min in 2× SSC containing 70% formamide and then were dehydrated through an ethanol series (70%, 90%, and 100%).

The probe mixture was applied to the denatured metaphase chromosomes under a coverslip and sealed with rubber cement, and hybridization was performed for 4 days at 37°C. The biotin-labeled test DNA was visualized with FITC-conjugated avidin (Vector Laboratories), and the digoxigenin-labeled control DNA was detected with mouse anti-digoxigenin (Sigma) and tetramethylrhodamine isothiocyanate-conjugated goat antibodies to mouse IgG (Sigma). Chromosomes were counterstained with 4′,6-diamidino-2-phenylindole (DAPI) and embedded in antifading agent.

Microscopy and Digital Image Analysis. Gray scale images of FITC-labeled test DNA, the tetramethylrhodamine isothiocyanate-labeled control DNA, and the 4′,6-diamidino-2-phenylindole (DAPI) counterstain from at least eight metaphase spreads for each hybridization were acquired with a cooled charge-coupled device camera (CH250; Photometrics, Tucson, AZ) that was connected to a Leica DMRBE microscope equipped with fluorochrome-specific optical filters TR1, TR2, and TR3 (Chroma Technology, Brattleboro, VT). Quantitative evaluation of hybridization was performed with a custom computer program developed for analysis of mouse chromosomes that was based on a human CGH program (30, 35). Average ratio profiles were computed as the mean value of at least eight ratio images. Fluorescence ratio is defined as the ratio of the total test (green) to the total control (red) fluorescence at each position along the length of each chromosome; chromosomal regions with a fluorescence ratio of ≥ 1.25 were interpreted as a gain, whereas regions with a ratio of ≤ 0.75 were interpreted as a loss.

PCR and Reverse Transcription-PCR (RT-PCR). Unique oligonucleotide primer pairs for human and mouse *PARP*, *p53*, and *Rb-1* genes and mRNA were designed and prepared. Total RNA, purified from cell pellets or liver tissue with an RNA extraction kit (Amersham Pharmacia Biotech), was subjected to RT-PCR with a Perkin–Elmer Gene Amp EZ rtTh RNA PCR kit. The reaction mix (50 μl) contained 300 μM each of dGTP, dATP, dTTP, and dCTP, 0.45 μM of each primer, 1 μg of total RNA, and rTth DNA polymerase (5 units). With an Amplitron II PCR machine (Thermolyne, Dubuque, IA), RNA was transcribed at 65°C for 40 min, and DNA was amplified by an initial incubation at 95°C for 2 min, followed by 40 cycles of 95°C for 1 min, 60°C for 1.5 min, and 65°C for 0.5 min, and a final extension at 70°C for 22 min. For PCR, genomic DNA was prepared according to standard protocols and amplified as above. The PCR products then were separated by electrophoresis in a 1.5% agarose gel and visualized by ethidium bromide staining.

Results

An Unstable Tetraploid Population in Immortalized PARP$^{-/-}$ Cells. One marker of genomic instability in cells is the development of tetraploidy or aneuploidy, which is typical of many tumors and is associated with progression to malignancy or metastasis (36). Tetraploidy results when cells exit from mitosis in the absence of either chromosome segregation or cytokinesis; such cells are genetically unstable and become aneuploid at subsequent mitoses (37). Flow cytometric analysis of immortalized fibroblasts derived from PARP knockout mice (clone A1) revealed the existence of a tetraploid population of cells (Fig. 1). After cell synchronization and release from either aphidicolin block at the G$_1$-S transition or serum deprivation, DNA histograms of wild-type cells (clone A19) (Fig. 1*A*) showed a typical pattern characterized by two major peaks of nuclei at G$_0$-G$_1$ (haploid) and G$_2$-M (diploid) phases of the cell cycle. In contrast, in addition to these two major peaks, DNA histograms of PARP$^{-/-}$ cells (clone A1) (Fig. 1*B*) showed a third peak corresponding to the G$_2$-M peak of an unstable tetraploid cell population in these cells. Similar to those of wild-type cells, DNA histograms of PARP$^{-/-}$ cells stably transfected with PARP cDNA [PARP$^{-/-}$(+PARP)] (clone A3–2) and synchronized by serum deprivation exhibited only the two major peaks of nuclei at
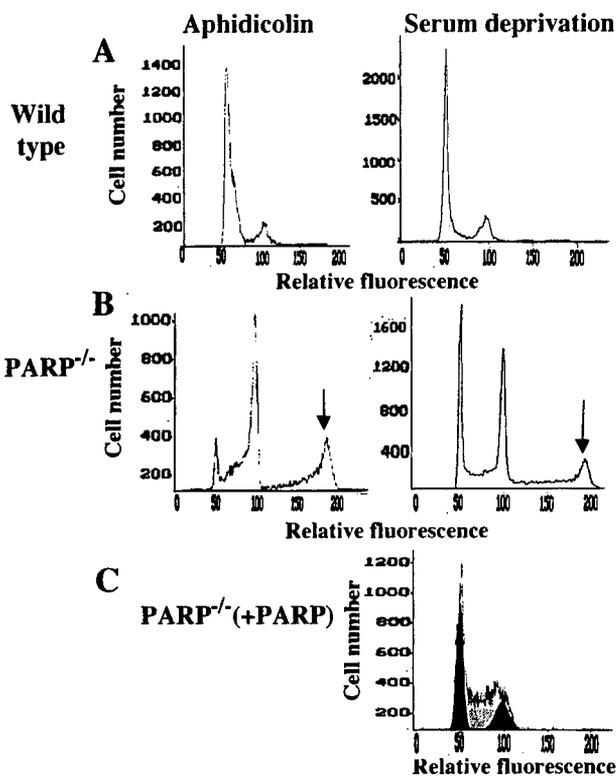
Fig. 1. Flow cytometric analysis of immortalized wild-type (A), PARP$^{-/-}$ (B), and PARP$^{-/-}$(+PARP) (C) fibroblasts. Cells were harvested 5 h after release from aphidicolin-induced G$_1$-S block (Left) or 18 h after release from serum deprivation (Right). Nuclei then were prepared and stained with propidium iodide for flow cytometric analysis. In addition to the two major peaks of nuclei at G$_0$-G$_1$ and G$_2$-M apparent in the DNA histograms of wild-type and PARP$^{-/-}$(+PARP) cells, the DNA histograms of PARP$^{-/-}$ cells exhibit a third peak corresponding to the G$_2$-M peak of an unstable tetraploid cell population (arrows).

G$_0$-G$_1$ and G$_2$-M (Fig. 1C). Thus, stable transfection of PARP$^{-/-}$ cells with PARP cDNA appeared to confer genomic stability to the PARP$^{-/-}$(+PARP) cells. Loss of PARP may allow the emergence and survival of cells with gross genetic abnormalities that normally would have been repaired.

Lack of p53 Protein Caused by PARP Deficiency in Immortalized PARP$^{-/-}$ Cells; Partial Restoration of p53 Expression by Reintroduction of PARP cDNA. Inactivation or loss of the tumor suppressor protein p53 in diploid cells results in the formation of unstable tetraploid cells predisposed to chromosome segregation abnormalities (38). We therefore investigated whether development of the unstable population of tetraploid cells in immortalized PARP$^{-/-}$ fibroblasts might be associated with loss of p53 expression. Immunoblot analysis with antibodies to PARP confirmed the lack of immunoreactive PARP in immortalized PARP$^{-/-}$ cells and its presence in wild-type and PARP$^{-/-}$(+PARP) cells (Fig. 2A). PARP$^{-/-}$ (+PARP) cells were stably transfected with human PARP cDNA; thus, RT-PCR analysis detected mouse or human PARP transcripts in wild-type and PARP$^{-/-}$(+PARP) cells, respectively, but not in PARP$^{-/-}$ cells. Reconstitution of PARP activity in PARP$^{-/-}$ (+PARP) cells was further verified by immunoblot analysis with antibodies to PAR. PARP expression also was confirmed in tissue extracts of wild-type, but not PARP$^{-/-}$, mice, by immunoblot analysis with anti-PARP; reprobing of the blot with anti-PAR revealed negligible poly(ADP-ribosyl)ation of nuclear proteins in PARP$^{-/-}$ tissue extracts (data not shown).

p53 was detected in lysates of wild-type cells, but not in PARP$^{-/-}$ cell extracts, by immunoblot analysis with antibodies to p53
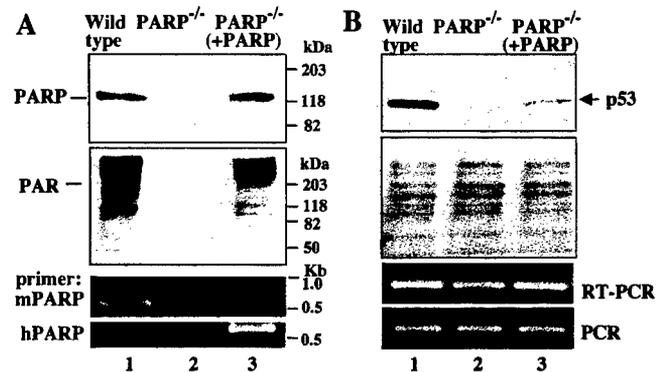

Fig. 2. PARP and p53 expression in immortalized wild-type, PARP$^{-/-}$, and PARP$^{-/-}$(+PARP) fibroblasts. (A) Cell extracts of wild-type, PARP$^{-/-}$, and PARP$^{-/-}$(+PARP) fibroblasts (30 μg protein) were subjected to immunoblot analysis with antibodies to PARP (Top) and to PAR (Middle). RT-PCR was performed with specific human (hPARP) and mouse (mPARP) PARP primers (Bottom). (B) Cell extracts were subjected to immunoblot analysis with mAb to p53 (PAb421) (Top). The blot was stained with Ponceau S to verify equal loading and transfer of proteins in both lanes (Middle). RT-PCR and PCR were performed with specific primers for p53 mRNA and gene (Bottom). The positions of PARP, PAR, p53, and PARP and p53 cDNA are indicated.

(PAb421) (Fig. 2B). Stable transfection with PARP cDNA partially restored p53 expression in the PARP$^{-/-}$(+PARP) cells. Consistent with other studies (39), the decrease in p53 expression in PARP$^{-/-}$ cells was not attributable to lower p53 transcript levels or a decrease in copy number, as revealed by RT-PCR analysis of RNA and PCR analysis of genomic DNA from these cells. This finding suggests that the lack of p53 in PARP$^{-/-}$ cells may be the result of reduced protein stability and that PARP may be involved in p53 stabilization and accumulation. Because the loss of p53 allows the survival of cells with severe DNA damage, thus, promoting tetraploidy (40), down-regulation of p53 expression in PARP$^{-/-}$ cells may contribute, at least in part, to the genomic instability and the development of tetraploidy in these cells.

CGH Analysis of Chromosomal Aberrations Associated with PARP Deficiency. CGH was used in the present study to map chromosomal gains and losses associated with PARP depletion. CGH analysis of DNA from liver tissue of PARP$^{-/-}$ mice revealed partial gains in chromosome 4 (4C5-ter), chromosome 5 (5F-ter), and chromosome 14 (14A1-C2), as well as a deletion that mapped to chromosome 14 (14D3-ter) (Fig. 3B). In contrast, CGH analysis detected no chromosomal abnormalities in wild-type (PARP$^{+/+}$) mice (Fig. 3A). These results indicate that the specific chromosomal changes detected in the PARP$^{-/-}$ mice are attributable to PARP deficiency.

To investigate the effects of reintroduction of PARP cDNA into PARP$^{-/-}$ cells, CGH analysis also was performed on genomic DNA from immortalized PARP$^{-/-}$ (clone A1) and PARP$^{-/-}$ (+PARP) (clone A3–2) fibroblasts that had been passaged for >10 generations. The partial chromosomal gains detected at 4C5-ter, 5F-ter, and 14A1-C2 in PARP$^{-/-}$ mice were also present in the immortalized PARP$^{-/-}$ fibroblasts (Fig. 4B). However, these gains were not detected in the average ratio profiles of genomic DNA from PARP$^{-/-}$(+PARP) cells (Fig. 4C). Only the partial loss of chromosome 14 was retained in these cells. Additional chromosomal aberrations were detected by CGH in both the immortalized PARP$^{-/-}$ and PARP$^{-/-}$(+PARP) cells, which are likely attributable to the immortalization process (data not shown).

Altered Expression of Tumor Suppressor Rb-1 and the Jun Oncogene in PARP$^{-/-}$ Mice. Deletions or gains of chromosomal regions detected by CGH may indicate the site of genes that promote further genomic instability through loss of tumor suppressor
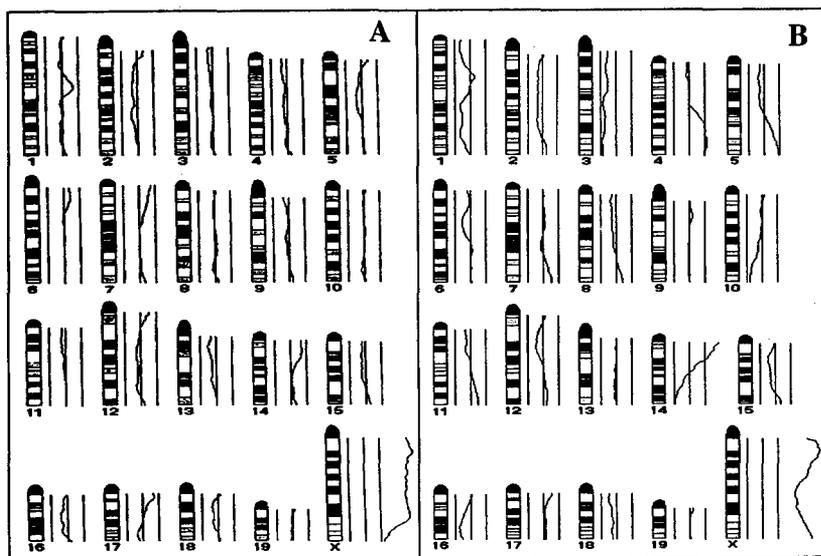
Fig. 3. CGH average ratio profiles of genomic DNA from liver tissue of wild-type (A) and PARP⁻/⁻ (B) mice. Average ratio profiles were computed for all chromosomes and used for the mapping of changes in copy number. The three vertical lines to the right of the chromosome ideograms represent values of 0.75, 1, and 1.25 (left to right, respectively) for the fluorescence ratio between the test DNA and the normal control DNA. The ratio profile (curve) was computed as a mean value of at least eight metaphase spreads. A ratio of ≥ 1.25 was regarded as a gain and a ratio of ≤ 0.75 as a loss.

genes or gains of oncogenes. It was therefore of interest to assess the expression of some key genes that map to regions of chromosomal gain or loss in the PARP⁻/⁻ mice, although clearly many other genes could have been chosen. The region of chromosome 14 that is deleted in PARP⁻/⁻ mice (14D3-ter) encompasses the tumor suppressor gene *Rb-1* (Fig. 5*A*) along with numerous other genes. Interestingly, immunoblot analysis of tissue extracts with antibodies to Rb revealed a marked reduction in constitutive expression of Rb in PARP⁻/⁻ mice relative to that in wild-type mice. Rb expression also was decreased in immortalized PARP⁻/⁻ fibroblasts compared with wild-type fibroblasts (data not shown). Similarly, the glutamate dehydrogenase (*Glud*) gene, a neighboring gene that also maps to 14D3, exhibits reduced expression in the PARP⁻/⁻ mice as shown by lower levels of the glutamate dehydrogenase protein in tissue extracts. In addition, the oncogene *Jun* is located (at 4C5-C7) in the region of chromosome 4 that exhibits a gain in PARP⁻/⁻ mice and cells. Immunoblot analysis of tissue extracts with antibodies to Jun confirmed that Jun expression is increased in PARP⁻/⁻ mice (Fig. 5*B*). In contrast, no difference in protein expression of the *Pcna* and *Top1* genes was detected in wild-type and PARP⁻/⁻ mice (Fig. 5*C*); these genes map to chromosome 2B-C and 2H, respectively, regions that show no gains or losses by CGH analysis.

A marked decrease in Rb transcript levels in PARP⁻/⁻ mice, as revealed by RT-PCR analysis, correlates with decreased abundance of Rb protein in these animals (Fig. 5*D*). In contrast, p53 transcript levels were similar in wild-type and PARP⁻/⁻ mice, in agreement with CGH results showing that the *Rb* gene, but not the *p53* gene (located in chromosome 11B2-C), is in a deleted chromosomal

region. PCR analysis of DNA from liver tissue further revealed that the Rb gene copy number also is reduced in PARP⁻/⁻ mice compared with wild-type mice, whereas the p53 gene copy number is unchanged (Fig. 5*D*). Thus, the decreases in Rb protein and transcript levels in PARP⁻/⁻ mice are consistent with the loss of the *Rb* gene.

Discussion

Although exhibiting varying phenotypes, two groups of PARP knockout mice developed by different laboratories both exhibit increased genomic instability as indicated by elevated frequencies of SCE and micronuclei formation after treatment with DNA-damaging agents, providing support for a role for PARP in the maintenance of genomic integrity (16, 17). We have now identified a population of tetraploid cells, another indication of genetic instability (37), among immortalized fibroblasts derived from PARP⁻/⁻ mice. This tetraploid cell population was no longer apparent in PARP⁻/⁻(+PARP) cells, suggesting that the reintroduction of PARP into PARP⁻/⁻ cells may have stabilized the genome and resulted in selection against this genomically unstable population.

CGH analysis revealed that PARP knockout mice and immortalized fibroblasts derived from these animals exhibit similar chromosomal aberrations, including gains in regions of chromosomes 4, 5, and 14. In contrast, the CGH profile of DNA from wild-type (PARP⁺/⁺) mice showed no DNA gains or losses, indicating that the chromosomal imbalances detected in the PARP⁻/⁻ genome are caused by PARP deficiency. Interestingly, the chromosomal gains in the PARP⁻/⁻ genome were no longer detected in the CGH profiles of DNA from PARP⁻/⁻(+PARP)
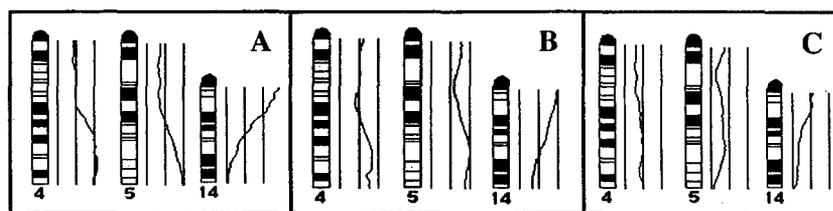
Fig. 4. Comparison of the CGH profiles of chromosomes 4, 5, and 14 among PARP⁻/⁻ mice (A) and immortalized PARP⁻/⁻ (B) and PARP⁻/⁻(+PARP) (C) fibroblasts. Average ratio profiles were computed for all chromosomes from at least eight metaphase spreads as described in Fig. 3, with only the results for chromosomes 4, 5, and 14 shown. PARP⁻/⁻(+PARP) fibroblasts did not show the gains at 4C5-ter, 5F-ter, or 14A1-C2 that were apparent in both PARP⁻/⁻ mice and immortalized PARP⁻/⁻ cells, although they retained the partial loss at 14D3-ter.
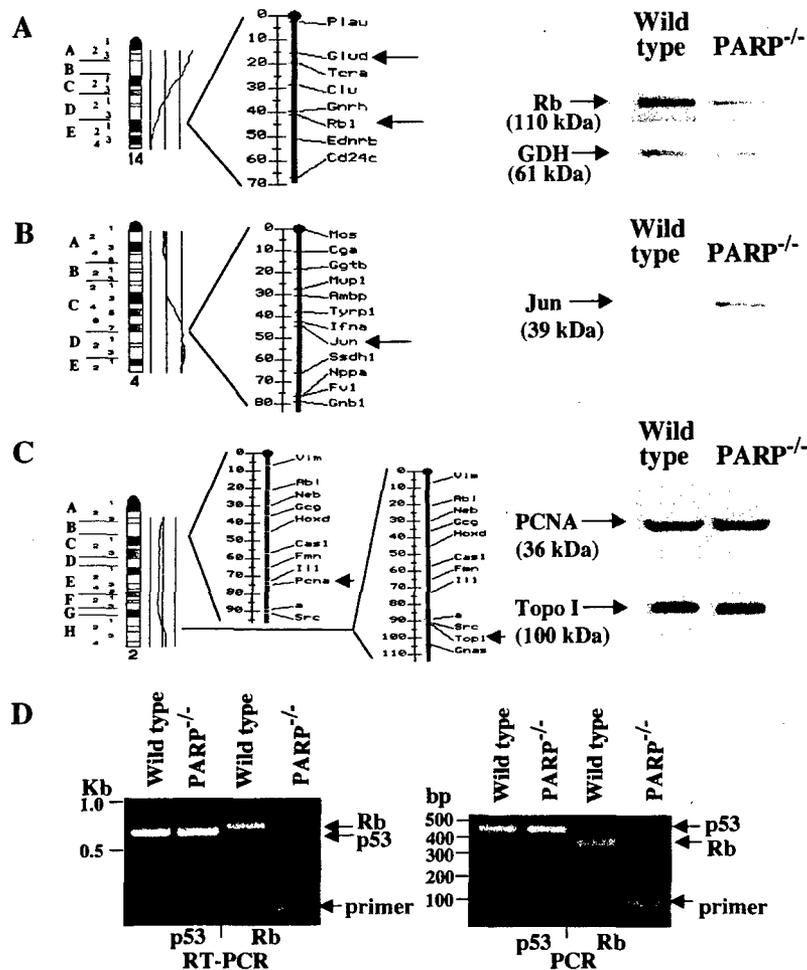
Fig. 5. Location of *Rb-1* and *Jun* in chromosomal regions with copy number changes in PARP^-/- mice and altered expression of Rb and Jun in these animals. (*A*) CGH profile of chromosome 14 of the PARP^-/- mice showing the loss of 14D3-ter, and the location of *Rb-1* and *Glud* (arrows) on 14D3. Immunoblot analysis with antibodies to Rb and glutamate dehydrogenase (GDH) of tissue extracts from wild-type and PARP^-/- mice. (*B*) CGH profile of chromosome 4 of PARP^-/- mice showing the partial gain of 4C5-ter and the location of *Jun* (arrow) on mouse chromosome 4C5. The immunoblot in *A* was reprobed with antibodies to Jun. (*C*) Balanced CGH profile of chromosome 2 of PARP^-/- mice and the location of *Pcna* and *TopI* genes (arrows) on 2B-C and 2H. The immunoblot in *A* was reprobed with antibodies to PCNA and to topo I. The positions of Rb (110 kDa), glutamate dehydrogenase (61 kDa), Jun (39 kDa), PCNA (36 kDa), and topo I (100 kDa) are indicated. (*D*) RT-PCR and PCR analysis of wild-type and PARP^-/- mice liver using p53 and Rb-specific primers. The positions of p53 and Rb cDNA (arrows) and of DNA size standards (in kb and bp) are indicated.

cells. The loss of 14D3-ter that encompasses the tumor suppressor gene *Rb-1* and presumably numerous other genes from the genome of PARP^-/- mice was associated with a marked reduction in Rb protein, transcript, and gene copy number in these animals. Furthermore, increased expression of the oncogene *Jun* in the PARP^-/- mice also was correlated with a gain in 4C5-ter that harbors the *Jun* oncogene. In contrast, there was no difference in expression of the *Pcna* and *Top1* genes in wild-type and PARP^-/- mice; these genes are considered unaffected by location within a region of chromosomal gain or loss. These results suggest that the gain or loss of large chromosomal regions, such as that encompassing *Rb-1* and numerous other genes, is caused by PARP deletion and concomitant genomic instability in the PARP^-/- mice.

The loss of tetraploidy and the chromosomal gains in the PARP^-/- cells after stable transfection of PARP cDNA provide further support for an apparent essential role of PARP in the maintenance of genomic stability. One mechanism by which PARP may confer genetic stability is via its putative role in p53 induction, accumulation, and stabilization. p53 is involved in the maintenance of diploidy as a component of the spindle checkpoint (41) and by regulating centrosome duplication (42). Given that the loss of p53 from diploid cells promotes the survival of cells with severe DNA damage and the development of tetraploidy (38, 40, 41), the presence of a tetraploid population among the immortalized PARP^-/- cells is consistent with the lack of immunoreactive p53 in these cells. Cells that are incapable of poly(ADP-ribosyl)ation because of unavailability of NAD (43) and primary fibroblasts from PARP^-/- mice (44) also

show reduced basal levels of p53 and defective p53 induction in response to DNA damage. Interestingly, the loss of the tetraploid population in the PARP^-/-(+PARP) cells further correlates with the partial restoration of p53 expression in these cells.

We recently showed that p53 is extensively poly(ADP-ribosyl)ated by PARP during early apoptosis and that degradation of the PAR attached to p53 coincides with expression of p53-responsive genes, suggesting that poly(ADP-ribosyl)ation may regulate p53-mediated transcriptional activation of these genes (45). The location of a PAR attachment site adjacent to a proteolytic cleavage site in p53 further suggests that PAR may protect p53 from proteolysis (46); similar protection has been noted after binding of mAbs adjacent to this region (47). The lack of regularly spliced wild-type p53 in PARP^-/- cells also has been attributed to decreased protein stability, not lower levels of p53 mRNA (39). Consistently, RT-PCR and PCR analysis of RNA and DNA from immortalized wild-type and PARP^-/- cells revealed that reduced expression of p53 in the PARP^-/- cells was not attributable to lower levels of p53 transcripts or a decrease in p53 gene copy number. Modification of p53 by PARP therefore is implicated in p53 accumulation and stabilization (45, 46, 48), which may explain the apparent lack of p53 in PARP^-/- cells. Lack of p53 in PARP^-/- cells may promote further genomic alterations via different mechanisms, including abnormal centrosome amplification, which is associated with lack of wild-type p53 and also generates numerical chromosome aberrations (49).

p53 monitors genomic integrity and reduces the occurrence of mutations either by mediating cell cycle arrest in G_1 or at G_2-M or by inducing apoptosis in cells that have accumulated substantial DNA damage (50, 51). Increased expression of the p53 homolog

CELL BIOLOGY

p73 may compensate for the lack of wild-type p53 in immortalized PARP$^{-/-}$ cells (39). Consistently, the region of chromosome 4 (4C5-ter) that shows a gain in PARP$^{-/-}$ mice harbors the *p73* gene. However, although p73, when overexpressed, can activate p53-responsive genes and induce apoptosis, it is unable to detect DNA lesions and, thus, is not induced by DNA damage (52). Both PARP activity and p53 accumulation are induced by DNA damage, and both proteins have been implicated as sensors of such damage. A functional association of PARP and p53 has been suggested by immunoprecipitation experiments (53). PARP cycles on and off the ends of DNA in the presence of NAD, and its automodification during DNA repair *in vitro* facilitates access to DNA repair enzymes (54, 55). Thus, both the increased sensitivity of PARP$^{-/-}$ mice and cells to DNA-damaging agents (17, 25) and their genetic instability are consistent with their deficiencies in PARP and p53. Our results suggest that some of the consequences of PARP deficiency in PARP$^{-/-}$ mice may be attributed, at least in part, to indirect effects resulting from changes in other DNA damage checkpoint proteins, such as p53.

We also have shown that, whereas immortalized wild-type fibroblasts exhibit an early activation of PARP and a rapid Fas-mediated apoptotic response, PARP$^{-/-}$ cells do not; stable transfection of PARP$^{-/-}$ cells with PARP cDNA renders the cells sensitive to Fas-mediated apoptosis, indicating a role for PARP and poly(ADP-ribosyl)ation in the early stages of this death program (32). Immortalized PARP$^{-/-}$ cells also show severe defects in base-excision DNA repair, as indicated by a delay in rejoining of DNA strand breaks after exposure to genotoxic agents (25). It is therefore conceivable that the loss of PARP and the lack of p53 expression in PARP$^{-/-}$ cells may allow the survival of cells with gross genetic abnormalities because of both an impaired ability to perform efficient DNA repair (25) and to undergo Fas-mediated apoptosis (32) in cells that have accumulated substantial DNA damage.

1. Althaus, F. R., Hilz, H. & Shall, S. (1985) *ADP-Ribosylation of Proteins* (Springer, Berlin).
2. Jacobson, M. K. & Jacobson, E. L. (1989) *ADP-Ribose Transfer Reactions: Mechanisms and Biological Significance* (Springer, New York).
3. Morgan, W. & Cleaver, J. (1982) *Mutat. Res.* **104**, 361–366.
4. Burkle, A., Heilbronn, R. & Zur, H. H. (1990) *Cancer Res.* **50**, 5756–5760.
5. Waldman, A. & Waldman, B. (1991) *Nucleic Acids Res.* **19**, 5943–5947.
6. Schreiber, V., Hunting, D., Trucco, C., Gowans, B., Grunwald, P., de Murcia, G. & de Murcia, J. (1995) *Proc. Natl. Acad. Sci. USA* **92**, 4753–4757.
7. Kupper, J., Muller, M. & Burkle, A. (1996) *Cancer Res.* **56**, 2715–2717.
8. Ding, R., Pommier, Y., Kang, V. H. & Smulson, M. (1992) *J. Biol. Chem.* **267**, 12804–12812.
9. Ding, R. & Smulson, M. (1994) *Cancer Res.* **54**, 4627–4634.
10. Chatterjee, S., Berger, S. & Berger, N. (1999) *Mol. Cell. Biochem.* **193**, 23–30.
11. Cherney, B. W., McBride, O. W., Chen, D. F., Alkhatib, H., Bhatia, K., Hensley, P. & Smulson, M. E. (1987) *Proc. Natl. Acad. Sci. USA* **84**, 8370–8374.
12. Lyn, D., Deaven, L., Istock, N. & Smulson, M. (1993) *Genomics* **18**, 206–211.
13. Lyn, D., Cherney, B., Lalande, M., Berenson, J., Lupold, S., Bhatia, K. & Smulson, M. E. (1993) *Am. J. Hum. Genet.* **52**, 124–134.
14. Bhatia, K. G., Cherney, B. W., Huppi, K., Magrath, I. T., Cossman, J., Sausville, E., Barriga, F., Johnson, B., Gause, B., Bonney, G., *et al.* (1990) *Cancer Res.* **50**, 5406–5413.
15. Bieche, I., de Murcia, G. & Lidereau, R. (1996) *Clin. Cancer Res.* **2**, 1163–1167.
16. Wang, Z. Q., Auer, B., Stingl, L., Berghammer, H., Haidacher, D., Schweiger, M. & Wagner, E. F. (1995) *Genes Dev.* **9**, 509–520.
17. de Murcia, J., Niedergang, C., Trucco, C., Ricoul, M., Dutrillaux, B., Mark, M., Oliver, J., Masson, M., Dierich, A., LeMeur, M., *et al.* (1997) *Proc. Natl. Acad. Sci. USA* **94**, 7303–7307.
18. Shieh, W. M., Ame, J. C., Wilson, M., Wang, Z. Q., Koh, D., Jacobson, M. & Jacobson, E. (1998) *J. Biol. Chem.* **273**, 30069–30072.
19. Ame, J., Rolli, V., Schreiber, V., Niedergang, C., Apiou, F., Decker, P., Muller, S., Hoger, T., de Murcia, J. & de Murcia, G. (1999) *J. Biol. Chem.* **274**, 17860–17868.
20. Eliasson, M., Sampei, K., Mandir, A., Hurn, P., Traystman, R., Bao, J., Pieper, A., Wang, Z. Q., Dawson, T., Snyder, S. & Dawson, V. (1997) *Nat. Med.* **3**, 1089–1095.
21. Pieper, A., Brat, D., Krug, D., Watkin, C., Gupta, S., Blackshaw, S., Verma, A., Wang, Z. Q. & Snyder, S. (1999) *Proc. Natl. Acad. Sci. USA* **96**, 3059–3064.
22. Mandir, S., Przedboeski, S., Jackson-Lewis, V., Wang, Z. Q., Simbulan-Rosenthal, C., Smulson, M., Hoffman, B., Guastella, D., Dawson, V. & Dawson, T. (1999) *Proc. Natl. Acad. Sci. USA* **96**, 5774–5779.
23. Szabo, C., Virag, L., Cuzzocrea, S., Scott, G., Hake, P., O'Connor, M., Zingarelli, B., Salzman, A. & Kun, E. (1998) *Proc. Natl. Acad. Sci. USA* **95**, 3867–3872.
24. Wang, Z., Stingl, L., Morrison, C., Jantsch, M., Los, M., Schulze-Osthoff, K. & Wagner, E. (1997) *Genes Dev.* **11**, 2347–2358.
25. Trucco, C., Oliver, F., de Murcia, G. & de Murcia, J. (1998) *Nucleic Acids Res.* **26**, 2644–2649.
26. Kallioniemi, A., Kallioniemi, O.-P., Sudar, D., Rutovitz, D., Gray, J., Waldman, F. & Pinkel, D. (1992) *Science* **258**, 818–821.
27. Du Manoir, S., Speicher, M., Joos, S., Schrock, E., Popp, S., Dohner, H., Kovacs, G., Robert-Nicoud, M., Lichter, P. & Cremer, T. (1993) *Hum. Genet.* **90**, 590–610.
28. Forozan, F., Karhu, K., Kononen, J., Kallionemi, A. & Kallionemi, O. (1997) *Trends Genet.* **13**, 405–409.
29. Shi, Y., Naik, P., Dietrich, W., Gray, J., Hanahan, D. & Pinkel, D. (1997) *Genes Chromosomes Cancer* **2**, 104–111.
30. Weaver, Z., McCormack, S., Liyanage, M., du Manoir, S., Coleman, A., Schrock, E., Dickson, R. & Ried, T. (1999) *Genes Chromosomes Cancer* **25**, 251–260.
31. Alkhatib, H. M., Chen, D. F., Cherney, B., Bhatia, K., Notario, V., Giri, C., Stein, G., Slattery, E., Roeder, R. G. & Smulson, M. E. (1987) *Proc. Natl. Acad. Sci. USA* **84**, 1224–1228.
32. Simbulan-Rosenthal, C. M., Rosenthal, D. S., Iyer, S., Boulares, A. H. & Smulson, M. E. (1998) *J. Biol. Chem.* **273**, 13703–13712.
33. Vindelov, L. L., Christensen, I. J., Jensen, G. & Nissen, N. I. (1983) *Cytometry* **3**, 332–339.
34. Figueiredo, B., Stratakis, C., Sandrini, R., DeLacerda, L., Pianovsky, M., Young, H. & Haddad, B. (1999) *J. Clin. Endocrinol. Metab.* **84**, 1116–1121.
35. du Manoir, S., Schrock, E., Bentz, M., Speicher, M., Joos, M., Ried, T., Lichter, P. & Cremer, T. (1995) *Cytometry* **19**, 24–41.
36. Robinson, J., Rademaker, A., Goolsby, C., Traczyk, T. & Zoladz, C. (1996) *Cancer* **77**, 284–291.
37. Andreassen, P., Martineau, S. & Margolis, R. (1996) *Mutat. Res.* **372**, 181–194.
38. Ramel, S., Sanchez, C., Schimke, M., Neshat, K., Cross, S., Raskind, W. & Reid, B. (1995) *Pancreas* **11**, 213–222.
39. Schmid, G., Wang, Z. Q. & Wesierska-Gadek, J. (1999) *Biochem. Biophys. Res. Commun.* **255**, 399–405.
40. Yin, X., Grove, L., Datta, N., Long, M. & Prochownik, E. (1999) *Oncogene* **18**, 1177–1184.
41. Cross, S., Sanchez, C., Morgan, C., Schimke, M., Ramel, S., Idzerda, R., Raskind, W. & Reid, B. (1995) *Science* **267**, 1353–1356.
42. Fukasawa, K., Choi, T., Kuriyama, R., Rulong, S. & Vande Woude, G. (1996) *Science* **271**, 1744–1747.
43. Whitacre, C. M., Hashimoto, H., Tsai, M.-L., Chatterjee, S., Berger, S. J. & Berger, N. A. (1995) *Cancer Res.* **55**, 3697–3701.
44. Agarwal, M., Agarwal, A., Taylor, W., Wang, Z. Q. & Wagner, E. (1997) *Oncogene* **15**, 1035–1041.
45. Simbulan-Rosenthal, C. M., Rosenthal, D. S. & Smulson, M. E. (1999) *Cancer Res.* **59**, 2190–2194.
46. Malanga, M., Pleschke, J., Kleczkowska, H. & Althaus, F. (1998) *J. Biol. Chem.* **273**, 11839–11843.
47. Li, X. & Coffino, P. (1996) *J. Biol. Chem.* **271**, 4447–4451.
48. Simbulan-Rosenthal, C. M., Rosenthal, D. S., Ding, R., Bhatia, K. & Smulson, M. E. (1998) *Biochem. Biophys. Res. Commun.* **253**, 864–868.
49. Weber, R., Bridger, J., Benner, A., Weisenberger, D., Ehemann, V., Reifenberger, B. & Lichter, P. (1998) *Cytogenet. Cell Genet.* **83**, 266–269.
50. Kastan, M. B., Onyekwere, O., Sidransky, D., Vogelstein, B. & Craig, R. W. (1991) *Cancer Res.* **51**, 6304–6311.
51. O'Connor, P. M., Jackman, J., Jondle, D., Bhatia, K., Magrath, I. & Kohn, K. W. (1993) *Cancer Res.* **53**, 4776–4780.
52. Kaghad, M., Bonnet, H., Yang, A., Creancier, L., Biscan, J., Valent, A., Minty, A., Chalon, P., Lelias, J., Dumont, M., *et al.* (1997) *Cell* **90**, 809–819.
53. Vaziri, H., West, M., Allsop, R., Davison, T., Wu, Y., Arrowsmith, C., Poirier, G. & Benchimol, S. (1997) *EMBO J.* **16**, 6018–6033.
54. Satoh, M. S. & Lindahl, T. (1992) *Nature (London)* **356**, 356–358.
55. Smulson, M., Istock, N., Ding, R. & Cherney, B. (1994) *Biochemistry* **33**, 6186–6191.

MCMR-RMI-S   (70-1y)   1 Apr 03

MEMORANDUM FOR Administrator, Defense Technical Information
Center (DTIC-OCA), 8725 John J. Kingman Road, Fort Belvoir,
VA   22060-6218

SUBJECT: Request Change in Distribution Statement

1. The U.S. Army Medical Research and Materiel Command has
reexamined the need for the limitation assigned to technical
reports written for this Command. Request the limited
distribution statement for the enclosed accession document
numbers be changed to "Approved for public release; distribution
unlimited." Copies of these reports should be released to the
National Technical Information Service.

2. Point of contact for this request is Ms. Judy Pawlus at
DSN 343-7322 or by e-mail at judy.pawlus@det.amedd.army.mil.

FOR THE COMMANDER:

Encl   PHYLIS M. RINEHART
                                  Deputy Chief of Staff for
                                      Information Management

ADB277986
ADB263450
ADB267669
ADB277564
ADB261754
ADB257280
ADB283722
ADB249627
ADB282841
ADB266235
ADB283529
ADB283519
ADB256683
ADB262564
ADB271045
ADB283537
ADB257204
ADB283513
ADB281571
ADB262777
ADB270818
ADB283748
ADB274588
ADB283788
ADB259015
ADB266031